

**Role of Terminal Sialic Acid of GABA  
Transporter 1 in GABA uptake  
& Purification and Characterization of this  
Transporter for Structural Analysis**



Dissertation  
zur Erlangung der Doktorwürde  
am Fachbereich Biologie, Chemie, Pharmazie  
der Freien Universität Berlin

Vorgelegt von  
**Jing Hu**  
aus Wuxi, V.R. China

Berlin 2010

**Charité-Universitätsmedizin Berlin**  
**Campus Benjamin Franklin**  
**Institut für Biochemie und Molekularbiologie**  
**Arnimallee 22**  
**14195 Berlin-Dahlem**

**The work was done under the supervision of P.D. Dr. Hua Fan. The experimental work was performed during the period from June 2006 to December 2010 at the Institute of Biochemistry and Molecular Biology (AG Reutter / AG Fan) in Berlin**

**Part of the work has already been published:**

Hu J, Fei J, Reutter W, Fan H. (2011) Involvement of Sialic Acid in the Regulation of GABA Uptake Activity of GABA Transporter 1. *Glycobiology*. 21(3):329-39  
(<http://glycob.oxfordjournals.org/content/21/3/329.full>)

- 1. Gutachter: Frau P.D. Dr. Hua Fan**
- 2. Gutachter: Herr Prof. Dr. Gerd Multhaup**

**Disputation am: 17.03.2011**

天行健，君子以自强不息；

地势坤，君子以厚德载物。

——“易经”

*As heaven maintains vigor through movements,  
a superior man should constantly strive for self-perfection;*

*As earth's condition is receptive devotion,  
a superior man should hold the outer world with broad mind.*

——‘I Ching’

*For My Devoted Jian Yin  
and Zichen Yin*

**Acknowledgements**

Firstly, I would like to give my deepest respect and most valuable credit to my supervisor P.D. Dr. Hua Fan and Professor Dr. Werner Reutter! Thank you for the patient guidance and the introduction to the mysteries of science. I have been really impressed by your contagious enthusiasm for science and serious attitude as a scientist. I enjoyed a lot of the open discussions with you. Your insightful thinking makes it possible for me to fly on a giant's shoulders. Surely, I will miss that amazing and wonderful time spent in the lab!!!

I am so grateful that Prof. Dr. Gerd Multhaupt for agreeing to be my thesis reviewer.

I would like to specially appreciate Dr. Felista Tansi, Dr. Kaya Bork and Dr. Maria Kontou. Thank you for your invaluable theoretical and technical helps all the time especially at the initial stage of my PhD study. Since you are always busy and I often have a lot of questions, I really appreciate your patience and spending so much time on discussion.

Sincere thanks are due all my coworkers at our group, who create such a friendly work environment. Cordially thanks Mrs. Susanne Thamm, Mrs. Christiane Kilian, Mrs. Sabine Stehling and Mrs. Melanie Leddermann for showing me techniques involved in cell and molecular biology. Thanks Mrs. Felicitas Kern for your kind helps not only in the official, but also in private matters. Many thanks go to Mrs. Yujing Yao and Mr. Duc Nguyen for your discussions and helps.

Thanks P.D. Dr. Christoph Böttcher (Forschungszentrum für Elektronenmikroskopie, Freie Universität Berlin) for lots of measurements of TEM measurement and discussion on the results. Thanks Dr. Christoph Weise (Institut für Chemie und Biochemie, Freie Universität Berlin) for his protein sequencing experiments and helpful discussion. Thanks for Dr. Faustin Kamena (Department of Biomolecular Systems, Max Planck Institute of Colloids and Interfaces) for providing the help of ultracentrifugation. Thanks Dr. Birte Fuchs (Octapharma R&D, Molecular Biochemistry Berlin) and Mr. Xiaoqiang Guo (MPI) for correcting part of my thesis. I am very grateful for many helps from Dr. Yijian Rao (Freie Universität Berlin) for the radio-isotope experiments.

I would like to thank all my friends in China and Germany for their precious friendship kept me moving forward.

Finally, there is a special note of appreciation to my parents and husband. They are always so supportive and considerate while I pursued what is important to me. And to my dearest baby girl who brings the most beautiful sunshine into my life.

# Contents

<b>Contents</b> .....	<b>i</b>
<b>1 Introduction</b> .....	<b>1</b>
<b>1.1 GABA and GABA transmission</b> .....	<b>1</b>
<b>1.2 GABA and Disease</b> .....	<b>3</b>
<b>1.3 The Family of Na<sup>+</sup>/Cl<sup>-</sup> GABA Transporters (GATs)</b> .....	<b>3</b>
1.3.1 History and characterization of GATs.....	4
1.3.2 Localization of GATs.....	5
1.3.3 GATs pharmacology .....	8
1.3.3.1 Pharmacological properties of GATs .....	8
1.3.3.2 Inhibitors of GATs .....	9
<b>1.4 GAT-1</b> .....	<b>12</b>
1.4.1 Mechanism .....	12
1.4.2 Topology.....	15
1.4.3 Structure and Function.....	17
1.4.3.1 Neurotransmitters binding site.....	18
1.4.3.2 Sodium binding site.....	20
1.4.3.3 Chloride binding site.....	22
1.4.4 Conformational changes.....	23
1.4.5 N-Glycosylation of GAT1 .....	27
<b>1.5 Sialic acids</b> .....	<b>28</b>
1.5.1 Structure and occurrence of sialic acids .....	28
1.5.2 Biological Functions of sialic acids .....	29
1.5.2.1 Adhesion and cell-cell-interaction.....	29
1.5.2.2 Sialic acids as recognition determinants for pathogens.....	31
1.5.2.3 Masking of antigenic determinants by sialic acids.....	32
1.5.2.4 Influence of sialic acids on structure and function of glycoconjugates and their carrier.....	33
1.5.2.5 Sialic acids and carcinoma .....	33
<b>2 Aim of this work</b> .....	<b>35</b>
<b>3 Results</b> .....	<b>37</b>
<b>3.1 The role of terminal sialic acid of GAT1 in GABA uptake activity</b> .....	<b>37</b>
3.1.1 The expression and characterization of GAT1/GFP in CHO, CHO Lec3 and Hek293 cells.....	37
3.1.2 Effect of deficiency of terminal sialic acid on GABA uptake activity of GAT1/GFP.....	40
3.1.2.1 Determination of sialic acid concentration in CHO and CHO Lec3 cells.....	40
3.1.2.2 Quantification of the influence of deficiency of terminal sialic acid on the GABA uptake activity of GAT1/GFP.....	41
3.1.2.3 Influence of ManNAc and ManNProp on GABA uptake activity of GAT1 in CHO Lec3 cells ..	43
3.1.3 Effect of removal of terminal sialic acid on GABA uptake activity of GAT1/GFP.....	44

3.1.3.1	Reduction of GABA transport activity of GAT1/GFP by sialidase treatment .....	44
3.1.3.2	Quantification of influence of removal of terminal sialic acid on GABA uptake activity of GAT1/GFP .....	45
3.1.4	Effect of oxidation of terminal sialic acid on GABA uptake activity of GAT1/GFP.....	47
3.1.5	Kinetic analysis of GABA uptake activity of GAT1/GFP protein .....	48
3.1.5.1	Deficiency, removal or oxidation of terminal sialic acid did not change the $K_m$ GABA values of GAT1.....	49
3.1.5.2	Deficiency and removal of terminal sialic acid increased $K_mNa^+$ values of GAT1 .....	51
3.1.5.3	Oxidation of terminal sialic acid did not change the $K_mNa^+$ value of GAT1 .....	53
<b>3.2</b>	<b>Influence of natural occurring and chemical synthetic compounds on GABA uptake activity of GAT1 .....</b>	<b>54</b>
3.2.1	Effect of hexosamines on GABA uptake activity.....	54
3.2.2	Effect of natural occurring on GABA uptake activity.....	59
<b>3.3</b>	<b>Expression, characterization and purification of GAT1/GFP fusion protein .....</b>	<b>62</b>
3.3.1	Purification of GAT1/GFP fusion protein in Hek293 cells .....	62
3.3.1.1	Isolation of GAT1/GFP fusion protein in Hek293 cells by ion-exchange chromatography.....	62
3.3.1.2	Isolation of GAT1/GFP fusion protein in Hek293 cells by lectin-affinity chromatography .....	63
3.3.1.3	Purification of GAT1/GFP fusion protein in Hek293 cells by immunoaffinity chromatography and size exclusion-fast liquid chromatography (SE-FPLC).....	64
3.3.1.3.1	Purification of anti-GFP antibody.....	64
3.3.1.3.2	Purification of GAT1/GFP fusion protein in Hek293 cells by immunoaffinity chromatography and SE-FPLC .....	65
3.3.2	Expression, characterization and purification of GAT1/GFP fusion protein with BAC-TO-BAC <sup>®</sup> -Baculovirus system .....	68
3.3.2.1	Cloning, Preparation and analysis of GAT1-recombinant baculovirus .....	68
3.3.2.2	Expression and characterization of GAT1/GFP fusion protein in insect cells .....	68
3.3.2.3	Isolation of GAT1/GFP fusion protein in insect cells by ion-exchange chromatography .....	72
3.3.2.4	Purification of GAT1/GFP fusion protein in insect cells by immunoaffinity chromatography and SE-FPLC .....	74
3.3.2.5	Transmission electron microscopy (TEM) analysis.....	78
<b>4</b>	<b>Discussion.....</b>	<b>87</b>
<b>4.1</b>	<b>Role of terminal sialic acid in the GABA uptake activity of GAT1 .....</b>	<b>87</b>
4.1.1	Terminal sialic acid is essential for GABA uptake activity of GAT1 .....	87
4.1.2	Terminal sialic acid affects kinetics of transport cycle.....	91
4.1.3	Terminal sialic acid in altering access transport model .....	93
<b>4.2</b>	<b>Influence of synthetic <i>N</i>-acyl hexosamines on GABA uptake activity of GAT1 ..</b>	<b>94</b>
<b>4.3</b>	<b>Potent inhibitors on GABA uptake activity of GAT1 from naturally occurring compounds.....</b>	<b>95</b>

<b>4.4 Expression, characterization and purification of GAT1/GFP recombinant protein</b>	<b>96</b>
<b>5 Future perspectives</b>	<b>100</b>
<b>6 Summary</b>	<b>101</b>
<b>7 Zusammenfassung</b>	<b>103</b>
<b>8 Materials and methods</b>	<b>105</b>
<b>8.1 Materials</b>	<b>105</b>
8.1.1 Chemicals	105
8.1.2 Cells and bacteria	105
8.1.3 Cell culture materials and mediums	106
8.1.4 Vectors	107
8.1.5 Primers	107
8.1.6 Markers and Enzymes	107
8.1.7 Antibodies	107
8.1.8 Lectins	108
8.1.9 Kits	108
8.1.10 Laboratory equipments and instruments	108
<b>8.2 Methods</b>	<b>110</b>
8.2.1 Molecular biological methods	110
8.2.1.1 Generation of competent <i>E.coli</i> cells	110
8.2.1.2 Transformation of <i>E.coli</i> competent cells	110
8.2.1.3 Preparation of plasmid-DNA from <i>E.coli</i>	111
8.2.1.4 Determination of DNA concentration	112
8.2.1.5 Digestion with restriction endonucleases	112
8.2.1.6 Agarose gel electrophoresis	113
8.2.1.7 DNA sequencing	113
8.2.1.8 Polymerase Chain Reaction (PCR)	114
8.2.1.9 Expression of recombinant proteins in Baculovirus system	115
8.2.1.9.1 Cultivation of insect cells	116
8.2.1.9.2 Generation of recombinant Bacmid DNA	117
8.2.1.9.3 Analysis of Bacmid DNA	117
8.2.1.9.4 Generation of recombinant virus	117
8.2.1.9.5 Amplification of virus	118
8.2.1.9.6 Plaque Assay	118
8.2.1.9.7 Expression of recombinant protein in insect cells	119
8.2.2 Cell biological methods	119
8.2.2.1 General cultivation conditions	119
8.2.2.2 Stable transfection of GAT1/GFP in CHO and CHO Lec3 cells	120
8.2.2.3 Stable transfection of GAT1/GFP in Hek293 cells	120



8.2.2.4 Selection of stable transfected cells by cloning	121
8.2.2.5 FACS and Fluorescence microscopy analysis	121
8.2.2.6 Cell counting	121
8.2.3 Protein biochemical and immunological methods	121
8.2.3.1 Immunoprecipitation	121
8.2.3.2 Biotinylation	122
8.2.3.3 Sialidase treatment	122
8.2.3.4 Sodium periodate treatment	123
8.2.3.5 Mild sodium borohydride treatment	123
8.2.3.6 Alamar Blue Assay	123
8.2.3.7 Determination of protein concentration	123
8.2.3.7.1 Bradford assay	123
8.2.3.7.2 BCA methods	124
8.2.3.8 Endoglycosidase H treatment	124
8.2.3.9 SDS-polyacrylamide gel electrophoresis (SDS-PAGE)	125
8.2.3.10 Silver staining	126
8.2.3.11 Coomassie blue staining	127
8.2.3.12 Analysis and identification of protein by MALDI-TOF-MS	127
8.2.3.13 Western blot	129
8.2.3.14 Glycan staining	130
8.2.3.15 GABA uptake assay	131
8.2.3.16 Sialic acid concentration assay	131
8.2.3.17 Cell surface sialic acid analysis by flow cytometry	132
8.2.3.18 Membrane preparation and solubilization	132
8.2.3.19 Ion exchange chromatography	133
8.2.3.20 Lectin affinity chromatography	134
8.2.3.21 Immuno-affinity chromatography	134
8.2.3.21.1 Purification of the GFP-specific antiserum	134
8.2.3.21.2 Preparation of immunoaffinity column	135
8.2.3.21.3 Isolation of GAT1/GFP by immunoaffinity column	135
8.2.3.22 Size exclusion chromatography	136
8.2.3.23 Transmission electron microscopy (TEM) analysis	136
8.2.3.23.1 Negative staining preparation	136
8.2.3.23.2 Cryo-TEM preparation	136
8.2.3.23.3 Cryo-TEM	137
<b>9 References</b>	<b>138</b>
<b>Appendix</b>	<b>155</b>
Abbreviations	155
Restriction Map and Multiple Cloning Site (MCS) of pEGFP-N1 Vector	157

*Contents*

---

Restriction Map and Multiple Cloning Site (MCS) of pFASTBAC™ 1-Vector .....	158
Curriculum Vitae .....	159
Publications .....	160

## 1 Introduction

### 1.1 GABA and GABA transmission

Activity in the vertebrate brain depends on a yin and yang balance between excitatory and inhibitory neurotransmission. A deficit of excitatory neurotransmission will lead to unconsciousness; a deficit of inhibitory neurotransmission will lead to epileptic seizures. The most abundant inhibitory neurotransmitter in vertebrates and invertebrates is  $\gamma$ -Aminobutyric acid (GABA), also called as 4-aminobutyric acid. GABA plays a fundamental role in controlling neuronal information processing (Wilson *et al.* 1994, Krnjevic, 1997), neuronal plasticity (Sur and Leamey 2001), and network synchronization (Blatow *et al.* 2003). In vertebrates, GABA acts at inhibitory synapses in the brain. In contrast, GABA exhibits excitatory actions in insects, mediating muscle activation at synapses between nerves and muscle cells, and also the stimulation of certain glands. Studies with laser ablation of the single or multiple neurons revealed that GABA acts as both an inhibitory and excitatory neurotransmitter in *Caenorhabditis elegans* (*C. elegans*) (Schuske *et al.* 2004). GABA is primarily acting at neuromuscular junctions; in vertebrates, GABA acts in the central nervous system (CNS). GABA neurons comprise 10% of the nervous system; in vertebrates, 30–40% of synapses in the brain are GABAergic (Docherty *et al.* 1985).

GABAergic neurotransmission is the most abundant part of inhibitory neurotransmission in CNS. As Fig. 1.1 shown, GABA is synthesized in the cytoplasm of the neuron by glutamic acid decarboxylase (GAD), which is encoded by gene *unc-25* (Jin *et al.* 1999), and then is packaged into synaptic vesicles. Afterwards, it is released by the fusion of the vesicles with the synaptic plasma membrane. Following its diffusion across the synaptic cleft, it binds to one of two types of receptor: GABA<sub>A</sub> receptors and GABA<sub>B</sub> receptors: respectively. GABA<sub>A</sub> receptors are ligand-gated ion channels that hyperpolarize the neuron by increasing inward chloride conductance and have a rapid inhibitory effect (Mohler 2009). GABA<sub>B</sub> receptors are G protein-linked receptors that hyperpolarize the neuron by increasing potassium conductance. GABA<sub>B</sub> receptors decrease calcium entry and have a slow inhibitory effect. Then the GABA neurotransmission is efficiently terminated by re-uptake mediated by the membrane GABA transporters (GATs) into the presynaptic nerve ending or surrounding astrocytes via quickly removing the rest of GABA from the synaptic cleft. Uptake into the GABAergic neuron allows reuse of GABA by vesicular uptake from the cytosol of the neuron. When transported into surrounding glia cells, GABA is metabolized via GABA transaminase and subsequent oxidation to

succinate, and it may be either fully oxidized or converted to glutamine which can reenter the neuron and ultimately regenerate GABA (Waagepetersen *et al.* 2003). However, it is believed that the major fraction of the glial pathway leads to degradation of GABA instead of reuse (Schousboe *et al.* 2004).

The activity of GABA transporters on the plasma membrane was proved by rescuing *unc-25/GAD* function: addition of exogenous GABA can restore GABA to the GABAergic neurons (AVL and DVB) and can restore the normal neuronal behaviour (McIntire *et al.* 1993). While the GABA transporters are blocked by nipecotic acid, the drug blocks the transport of GABA and rescue of the *unc-25* mutant (Schuske *et al.* 2004).

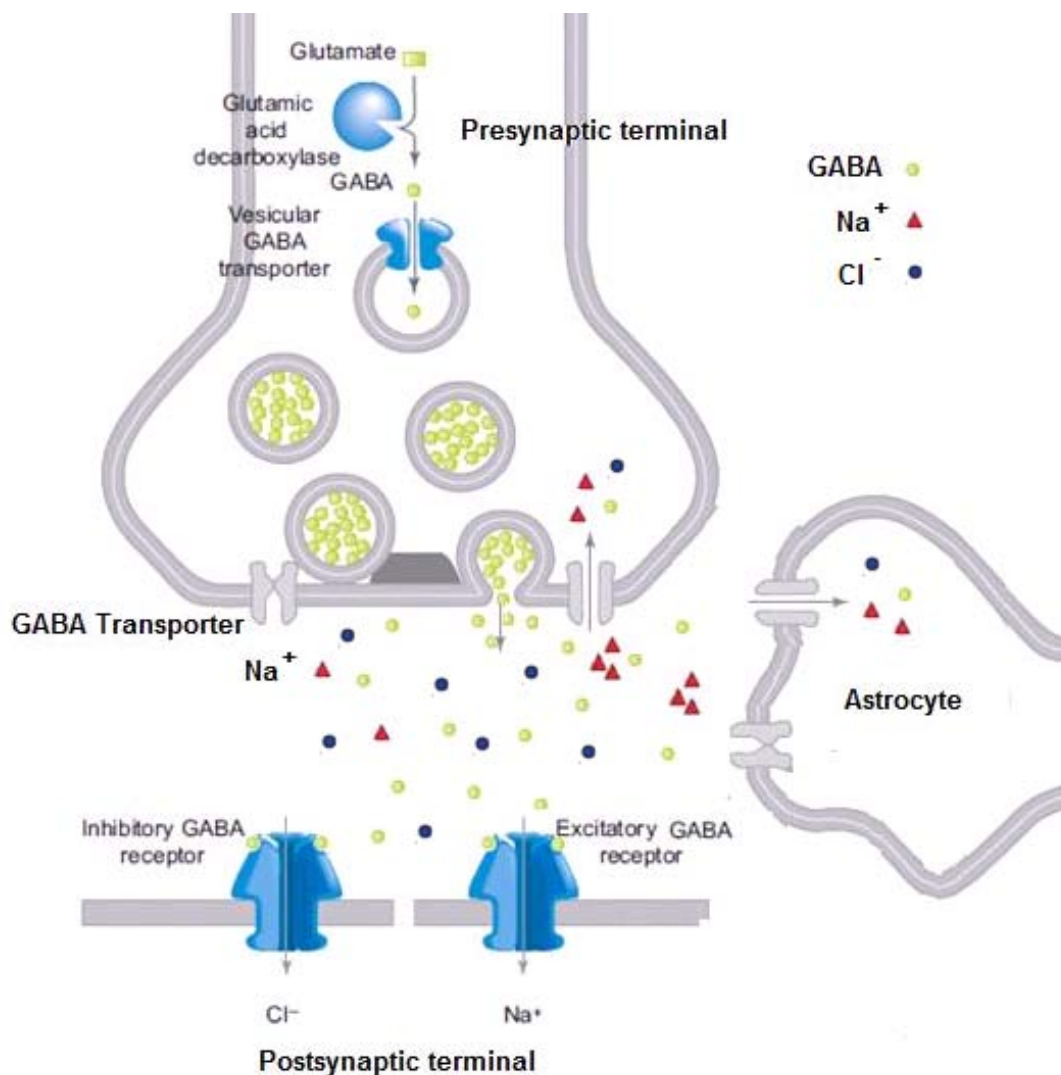


Figure 1.1 A representation of GABAergic neurotransmission at a neuronal synapse. Modified from (Schuske *et al.* 2004)

## **1.2 GABA and Diseases**

GABAergic system has been implicated in many diseases of the CNS, such as epilepsy (Treiman 2001; Cope *et al.* 2009), depression (Krystal *et al.* 2002; Liu *et al.* 2007), various pain states (Otsuka and Yanagisawa 1990; Jasmin *et al.* 2004), and Alzheimer's disease (Lanctot *et al.* 2004; Garcia-Alloza *et al.* 2006), as well, GABA has also been found to play an essential role in controlling cardiovascular function by the CNS (Roberts and Krause 1982; DeFeudis 1983). For instance, epilepsy is a heterogeneous neurological disorder characterized by the onset of spontaneous convulsive and non-convulsive seizures. A number of experimental and clinical studies found that abnormalities of GABAergic function have been observed in genetic and acquired animal models of epilepsy (Ribak *et al.* 1979; King and LaMotte 1988). A number of studies of human epileptic brain tissue have shown reductions in GABA concentrations or GABA-receptor densities in human epileptic tissue (During and Spencer 1993; During *et al.* 1995).

Since the attenuation of GABA removal will prolong the effect of this inhibitory transmitter, the regulation of GABA activity is of considerable medical interest. Blockade of GABA transporters increases the synaptic availability of GABA and constitutes an attractive approach to increase overall GABA neurotransmission, suggesting GABA transporters as promising drug targets (Schousboe *et al.* 2004; Madsen *et al.* 2009; Thoeringer *et al.* 2009).

## **1.3 The Family of Na<sup>+</sup>/Cl<sup>-</sup> GABA Transporters**

There are four distinct families of neurotransmitter transporters that function on the membranes: (a) general amino acid transport systems that are responsible for regulating the availability of neurotransmitters outside the cells (McGivan and Pastor-Anglada, 1994); (b) Na<sup>+</sup>- and Cl<sup>-</sup>-dependent (Na<sup>+</sup>/Cl<sup>-</sup>) transporters that function on the plasma membrane of neuronal and glia cells, such as GABA transporters (Schloss *et al.*, 1992; Uhl, 1992; Amara and Kuhar, 1993), termed SLC6 (solute carrier 6) or NSS (neurotransmitter: sodium symporters); (c) Na<sup>+</sup>/K<sup>+</sup>-dependent transporters that operate on the plasma membranes, specially for glutamate uptake (Kanner, 1993), termed SLC1; and (d) vesicular transporters that transport neurotransmitters into synaptic vesicles and granules (Schuldiner, 1994).

In mammals, the SLC6 transporters are divided into five subfamilies: GABA transporters, monoamine transporters, amino acid (which are not neurotransmitters) transporters, orphan transporters and bacterial transporters (Nelson 1998).

### 1.3.1 History and Characterization of GABA transporters (GATs)

The existence of high affinity GATs in neurons and astrocytes was first proved by Iversen and Neal (1968). GATs are normally located in the plasma membranes of neurons and glia with high density. They are present in those areas of the cell membrane that face the synapse. They serve to keep the neurotransmitter concentrations in the synaptic cleft sufficiently low, so that neuronal signalling from the presynaptic nerve cells can be detected in the form of exocytotically released transmitters by the postsynaptic receptors. GATs are key elements in the termination of the synaptic actions of GABA. Moreover, they serve to keep the extracellular transmitter concentrations below neurotoxic levels.

A GABA transporter was firstly purified and identified in a functional form from rat brain by a reconstitution system as the first neurotransmitter transporter (Radian and Kanner 1985; Radian *et al.* 1986). Furthermore, a cDNA encoding this GABA transporter of 599 amino acids in rat brain and in human brain was the first to be cloned, sequenced and expressed, which is designated as GAT1 (Guastella *et al.* 1990; Nelson *et al.* 1990). Combined with the protein sequence information of a noradrenaline transporter obtained by expression cloning subsequently (Pacholczyk *et al.* 1991), numerous other members of this neurotransmitter transporters SLC6 superfamily were rapidly cloned (Uhl 1992; Amara and Kuhar 1993).

The evidence of GAT heterogeneity was firstly provided by determination of the inhibition of a series of GABA analogues on GABA uptake activity in neuronal and astroglial cells (Krogsgaard-Larsen *et al.* 1987). The complexity of GATs has been revealed with the application of molecular biology. So far, four cDNAs encoding highly homologous rat and human GATs have been cloned: GAT-1, BGT-1 (for Betaine/GABA Transporter), GAT-2 and GAT-3. An analogous nomenclature, is originally suggested by Liu *et al.*. From the mouse brain, four GATs have been cloned and named GAT1, GAT2, GAT3 and GAT4 encoding pztroteins of 598, 614, 602, and 627 amino acids, respectively with a  $K_m$  for GABA of 7, 79, 18, and 0.7  $\mu\text{M}$ , respectively. Whereas mGAT1 is the homologue of r/hGAT-1, mGAT2, mGAT3, and mGAT4 appear to be the homologous to BGT-1, r/hGAT-2 and r/hGAT3, respectively. Table 1.1 summarizes the GAT nomenclature categorized in columns for species homology.

Mouse GAT2 also shows affinity for betaine with a  $K_m$  of 398  $\mu\text{M}$  (Liu *et al.* 1992; Liu *et al.* 1993). BGT-1 is homologous to mouse GAT-2, encoding proteins of 614 amino acids for canine and human and 628 amino acids for rat, and like mouse GAT-2 they show a greater affinity for GABA than for betaine (Yamauchi *et al.* 1992; Borden *et al.* 1995;

Burnham *et al.* 1996). The rat GAT-2 and GAT-3 consist of 602 and 627 amino acids, respectively with a  $K_m$  for GABA of 8 and 12  $\mu$ M. They also transport  $\beta$ -alanine suggesting a greater similarity to glial GAT (Borden *et al.* 1992; Christiansen *et al.* 2007). The human GAT-2 and GAT-3 consist 602 and 632 amino acids, respectively (Borden *et al.* 1994; Christiansen *et al.* 2007).

**Table 1.1 GABA transporter nomenclature across species**

<i>Species</i>	<i>Nomenclature</i>			
<i>SLC6 gene</i>	<i>SLC6a1</i>	<i>SLC6a12</i>	<i>SLC6a13</i>	<i>SLC6a11</i>
<b>Rat</b>	GAT-1 <sup>a</sup>	BGT-1 <sup>b</sup>	GAT-2 <sup>c</sup>	GAT-3 <sup>c</sup>
<b>Human</b>	GAT-1 <sup>d</sup>	BGT-1 <sup>e</sup>	GAT-2 <sup>f</sup>	GAT-3 <sup>g</sup>
<b>Mouse</b>	GAT1 <sup>h</sup>	GAT2 <sup>h</sup>	GAT3 <sup>h</sup>	GAT4 <sup>h</sup>
<b>HUGO</b>	GAT1	BGT1	GAT2	GAT3

<sup>a</sup> (Guastella *et al.* 1990); <sup>b</sup> (Yamauchi *et al.* 1992); <sup>c</sup> (Borden *et al.* 1992); <sup>d</sup> (Nelson *et al.* 1990); <sup>e</sup> (Borden *et al.* 1995); <sup>f</sup> (Christiansen *et al.* 2007); <sup>g</sup> (Borden *et al.* 1994); <sup>h</sup> (Liu *et al.* 1993).

They share similar structures and amino acid sequences, which encode highly hydrophobic proteins of about 67-70 kDa, but differ in their expression, distribution and pharmacological properties. GAT2, GAT3 and GAT4 exhibit >60% identity in their amino acid sequences, while they are =50% identical to GAT1 and =40% identical to members of the other subfamilies. In heterologous cell systems, GATs exhibit different substrate specificities and inhibitor sensitivities (Borden 1996; Grossman and Nelson 2003). It seems that GAT1 behaves as the neuronal GAT whereas GAT2 and GAT3 resemble the astrocytic GAT when transport of GABA is inhibited with diamino butyric acid (DABA) and  $\beta$ -alanine, respectively. In addition, both their kinetics and density at synapse are affected by regulatory mechanisms, which are coupled to factors controlling transmitter release (Quick *et al.* 1997; Deken *et al.* 2003) and hormone levels, and may display regional selectivity (Herbison *et al.* 1995). Regulatory mechanisms may exert differential, or even opposite effects on different GATs. For instance, pH alterations affect GAT3 more than that of GAT1 (Grossman and Nelson 2002). The details will be described in the following sections.

### 1.3.2 Localization of GATs

It was reported that there were a multitude of  $\text{Na}^+$ -dependent GABA uptake systems with  $K_m$  values ranging from 1  $\mu$ M to 4 mM (Krogsgaard-Larsen *et al.* 1987). Generally, the uptake systems were divided into two groups of neuronal and glial transporters according

to their sensitivity to nipecotic acid or  $\beta$ -alanine (Guastella *et al.* 1990). Further distribution studies of GAT just reveal a more complicated picture, suggesting that more GATs are localized in specific parts of the brain (Kanner and Bendahan 1990) (Fig. 1.2). It will also help to define the roles of these transporters in GABAergic transmission. Moreover, different types of GATs could be present not only in different brain areas, but also in different stages during nervous system development thus to fulfill the neurological function required for each developmental stage (Oland *et al.*; Jursky and Nelson 1999; Minelli *et al.* 2003; Conti *et al.* 2004).

GAT1 and GAT3 are abundantly but restrictedly expressed through the rat, mouse, and human central nervous system (Borden *et al.* 1992; Liu *et al.* 1993; Jursky *et al.* 1994; Borden 1996; Conti *et al.* 2004), which makes these two subtypes as potential drug targets. GAT-1 is the most copiously expressed GAT in the cerebral cortex. The distribution studies are by *in situ* hybridization mapping in conjunction with immunocytochemistry. *In situ* hybridization studies in rat neocortex demonstrated that GAT-1 is localized to both neurons and some astroglia (Minelli *et al.* 1995). Moreover, immunocytochemical studies showed laminar patterns of GAT-1+ puncta resembling axon terminals and fibers in the neocortex of rats, monkeys, and humans indicating that the expression pattern of GAT-1 is cortical type related (Minelli *et al.* 1995; Conti *et al.* 1998).

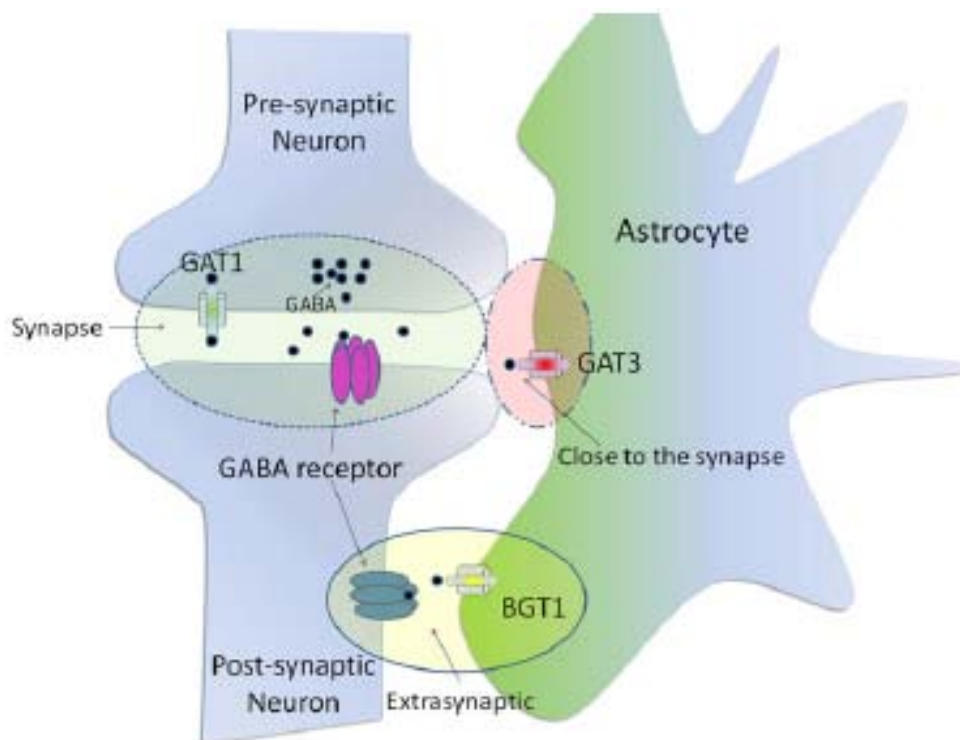


**Figure 1.2** A graphical representation of the primary subcellular localization of GAT1, BGT1 and GAT3. GAT1 is primary located presynaptically. GAT3 is primary located on distal astrocytic process in



close proximity to the synapse. BGT1 is located in the extrasynaptic region. (Madsen *et al.*)

GABA uptake in the developing cortex transiently exceeds adult levels (Coyle and Enna 1976; Ramsay *et al.* 1980; Blakely *et al.* 1991) and  $V_{\max}$  of transport exhibits a similar trend but  $K_m$  remains constant (Coyle and Enna 1976). Correspondingly, GAT-1 transiently over-expresses and reaches the peak above adult levels in neuronal and astrocytic cell bodies at intermediate and late phases of cortical maturation (Yang *et al.* 1997; Hachiya and Takashima 2001; Minelli *et al.* 2003).

The localization of GAT3 is more restricted when compared to GAT1 showing strong intensity in retina, olfactory bulb, brainstem, diencephalon and low levels in hippocampus and cortex. GAT-3 is localized to distal astrocytic processes, which were found in the neuropil and adjacent to axon terminals having either symmetric or asymmetric specializations (Minelli *et al.* 1996), as well as to neurons and their processes. A similar localization of GAT-3 in human and rat cortex is indicated (Melone *et al.* 2003; Conti *et al.* 2004).

GAT-2 is present not only in brain and retina, but also the peripheral tissues such as liver and kidney, in which the homologue mouse GAT3 mRNA is especially abundant (Lopez-Corcuera *et al.* 1992; Liu *et al.* 1993; Jursky *et al.* 1994). The expression of mouse GAT3 mRNA in mouse brain is developmentally regulated, and its mRNA is abundant in neonatal brain, but not in adult brain. Early studies showed that GAT-2 was exclusively expressed in leptomeningeal and ependymal cells (Ikegaki *et al.* 1994; Durkin *et al.* 1995), while it is also found to be present in the cortical parenchyma. Ultrastructural studies showed that GAT-2 is present in both neuronal and non-neuronal cortical cells, in astrocytic processes, and in leptomeningeal cells and their processes (Conti *et al.* 1999). In the rodent brain, the maturation of GAT-2 expression pattern is at the end of the second postnatal week (Minelli *et al.* 2003).

Mouse, rat, and human BGT-1 is found in both brain and periphery (Lopez-Corcuera *et al.* 1992; Borden *et al.* 1995; Rasola *et al.* 1995; Burnham *et al.* 1996) and believed to be involved in osmoregulation (Chen *et al.* 2004) but has recently also been suggested to play a role in the control of epilepsy (Schousboe *et al.* 2004).

### 1.3.3 Pharmacology of GATs

#### 1.3.3.1 Pharmacological properties of GATs

The accumulation of GABA in neurons and astrocytes can be blocked by the GABA analogue DABA, 3-aminocyclohexanecarboxylic acid (ACHC) and  $\beta$ -alanine, respectively, reflecting difference pharmacological properties of at least two different GABA transport systems, neuronal and astrocytic GATs (Iversen and Neal 1968; Iversen and Kelly 1975; Neal and Bowery 1977). As shown in Table 1.2,  $\beta$ -alanine and 4,5,6,7-tetrahydroisoxazolo[4,5-c]pyridin-3-ol (THPO) are about two-fold more potent for astrocytic GAT compared to neuronal GAT. A hypothesis arises that selective inhibition of astrocytic GABA transport could possess superior anticonvulsant properties compared to inhibition of neuronal GABA transport since DABA has been shown to be proconvulsant and GABA taken up in astrocytes is metabolized and lost (Schousboe 2000; White *et al.* 2002).

A series of conformational restricted GABA analogues were tested as GABA transport blockers to determine the pharmacological properties of the cloned GATs (Table 1.2). For example,  $\beta$ -alanine, a selective ligand selective for glial GAT (Kanner and Bendahan 1990), inhibited GABA uptake by GAT2 and GAT3, and to much lesser extent by GAT1 and BGT-1 (Lopez-Corcuera *et al.* 1992; Liu *et al.* 1993; Borden 1996). In contrast, guvacine and nipecotic acid interact well with all subtypes except BGT-1. GAT2 and GAT3 can be distinguished by l-DABA which displays higher affinity for GAT2 than for GAT3. It has been difficult to use the subtype pharmacological profiles to explain the neuronal vs glial specificity of the compounds.

$\beta$ -Alanine and THPO display a two-fold selectivity for astrocytic GAT compared to neuronal GAT (Table 1.2). However, the conversion of the isoxazolol group of THPO to the carboxyl group resulted in the generation of two compounds, nipecotic acid and guvacine which are very potent inhibitors but with a concomitant loss of selectivity for astrocytic GAT (Schousboe *et al.*, 1979, 1981). Nipecotic acid and guvacine have subsequently been used as lead structures in the efforts to synthesize potent GAT inhibitors. The glial selectivity of THPO prompted the synthesis of a series of compounds where the secondary amino group of THPO was moved to an exocyclic position becoming a primary amino group (exo-THPO) (Fig. 1). The pharmacological action of selected GAT inhibitors from this series is summarized in Table 1. Of special interest is its monomethylated derivative (N-methyl-exo-THPO) which is the most selective inhibitor for astrocytic versus neuronal GAT (Falch *et al.*, 1999).

Table 1.2. Inhibition of GABA uptake by selected GABA analogues (IC<sub>50</sub> or K<sub>m/i</sub>, μM)

	<i>Neurons</i>	<i>Astrocytes</i>	<i>GAT1</i>	<i>GAT2</i>	<i>GAT3</i>	<i>GAT4</i>
GABA	8	32	17 <sup>a</sup>	51 <sup>a</sup>	15 <sup>a</sup>	17 <sup>a</sup>
Nipecotic acid	12	16	24	2350	113	159
Guvacine	32	29	39	1420	228	372
DABA	1000	>5000	128	528 <sup>c</sup>	300	710
ACHC	200	700	132	1070 <sup>c</sup>	>1000	>10,000
β-Alanine	1666	843	2920	1100 <sup>c</sup>	66	110
THPO	501	262	1300	3000	800	5000
<i>exo</i> -THPO	883	208	1000	3000	>3000	>3000
<i>N</i> -Me- <i>exo</i> -THPO	423	28	450	>3000	>3000	>3000
Tiagabine	0.45	0.18	0.11	300	>300	800
SNAP-5114	-	-	>30 <sup>b</sup>	22 <sup>b</sup>	20 <sup>b</sup>	6.6 <sup>b</sup>
NNC 05-2090	-	-	19 <sup>b</sup>	1.4 <sup>b</sup>	41 <sup>b</sup>	15 <sup>b</sup>
EF-1502	2	2	7	26	>300	>300
( <i>R</i> )-EF-1502			4	22	>150	>150
( <i>S</i> )-EF-1502	>100	>100	120	34	>150	>150

<sup>a</sup> K<sub>m</sub>, <sup>b</sup> K<sub>i</sub>, <sup>c</sup> hBGT-1

Sources: Data from (Schousboe 1979; Larsson *et al.* 1983; Suzdak *et al.* 1992; Borden *et al.* 1995; Thomsen *et al.* 1997; Bolvig *et al.* 1999; Falch *et al.* 1999; White *et al.* 2002; Clausen *et al.* 2005)

### 1.3.3.2 Inhibitors of GATs

The inhibitors of GABA transporters can be divided into two groups: (1) small substrate-related analogs of GABA and β-alanine (Fig. 1.3) and (2) GABA and β-alanine analogs containing aromatic lipophilic side chains (Fig. 1.4) (Clausen *et al.* 2006).

The small-sized GABA analogs have been important pharmacological tools rather than therapeutic candidates since they are substrates and do not readily penetrate the blood–brain barrier (BBB) by passive diffusion due to the high polarity at physiological pH. The initial characterization of GATs has to a large extent been made possible due to a naturally occurring compound from the fly agaric mushroom, muscimol (Fig. 1.3). Muscimol is a potent GABA<sub>A</sub> receptor agonist with weak inhibitory effect on GAT. The pharmacological profile of muscimol was separated into the rigid GABA analogue, 4,5,6,7-tetrahydroisoxazolo[5,4-c]pyridin-3-ol (THIP) which is a selective extrasynaptic GABA<sub>A</sub> receptor agonist (Wafford and Ebert 2006) and the rigid β-alanine analogue THPO which retained GAT activity (Krogsgaard-Larsen *et al.* 1975; Krogsgaard-Larsen *et al.* 2000).

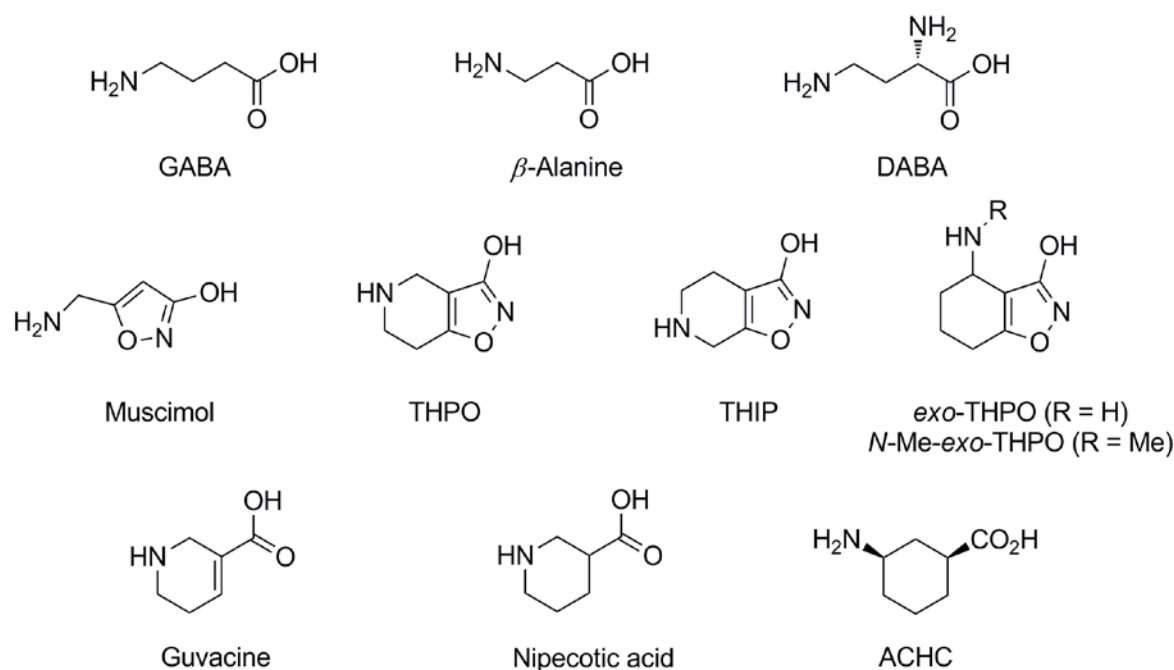


**Figure 1.3** Substrate-related GAT inhibitors

Nipepicotic acid and guvacine have been important lead structures for the development of a large number of GABA uptake inhibitors. The development was initiated by the discovery that introduction of the lipophilic diaromatic side chain 4,4-diphenylbut-3-en-1-yl (DPB) at these compounds gave very potent GABA uptake inhibitors. The ability to penetrate the BBB of these lipophilic aromatic analogs provides the possibility of therapeutic application of GABA uptake inhibition. For instance, *N*-4,4-diphenylbut-3-en-1-yl-nipepicotic acid (SKF89976A) and *N*-4,4-diphenylbut-3-en-1-yl-guvacine (SKF100330A) are orally active (Yunger *et al.* 1984; Ali *et al.* 1985). Moreover, they are no longer substrates for GABA transporters; although they act as competitive inhibitors (Larsson *et al.* 1988). Many of the very potent uptake inhibitors are highly GAT1-selective (Borden *et al.* 1994), which may be due to a high expression of GAT1. A large number of analogs have been synthesized by extensive variation in the lipophilic aromatic side chain, of which are modestly selective. Among these analogs, Tiagabine and 1-(2-(((diphenylmethylene)amino)oxy)ethyl)-1,2,5,6-tetrahydro-3-pyridinecarboxylic (NNC-711) are highly GAT1 selective compounds, while (*S*)-1-[2-[tris(4-methoxyphenyl)methoxy]ethyl]-3-piperidinecarboxylic acid (SNAP-5114) is a modestly mGAT4 selective inhibitor (Dhar *et al.* 1994). 1-(3-(9H-carbazol-9-yl)-1-propyl)-4-(2-methoxyphenyl)-4-piperidinol (NNC 05-2090), which is devoid of an acidic moiety, is reported to be a GAT2/BGT-1 selective compound with affinity for mGAT3 and mGAT4 as well (Thomsen *et al.* 1997). A novel mGAT2/BGT-1 selective inhibitor (*S*)-4-[*N*-[1,1-

bis(3-methyl-2-thienyl)but-1-en-4-yl]-N-methylamino]-4,5,6,7-tetrahydrobenzo[d]isoxazol-3-ol ((S)-EF1502) has been developed based on *N*-Me-*exo*-THPO substituted with the side chain from Tiagabine (Clausen *et al.* 2005). The combination of EF 1502 with tiagabine or SNAP-5114 produces a synergistic anticonvulsant effect, indicating a role for BGT-1 in the control of seizure activity (White *et al.* 2005; Madsen *et al.* 2009). It is possible that simultaneous inhibition of GATs would produce a synergistic therapeutic effect and a reduced side effect, for which the development of selective non-GAT1 inhibitors is required.

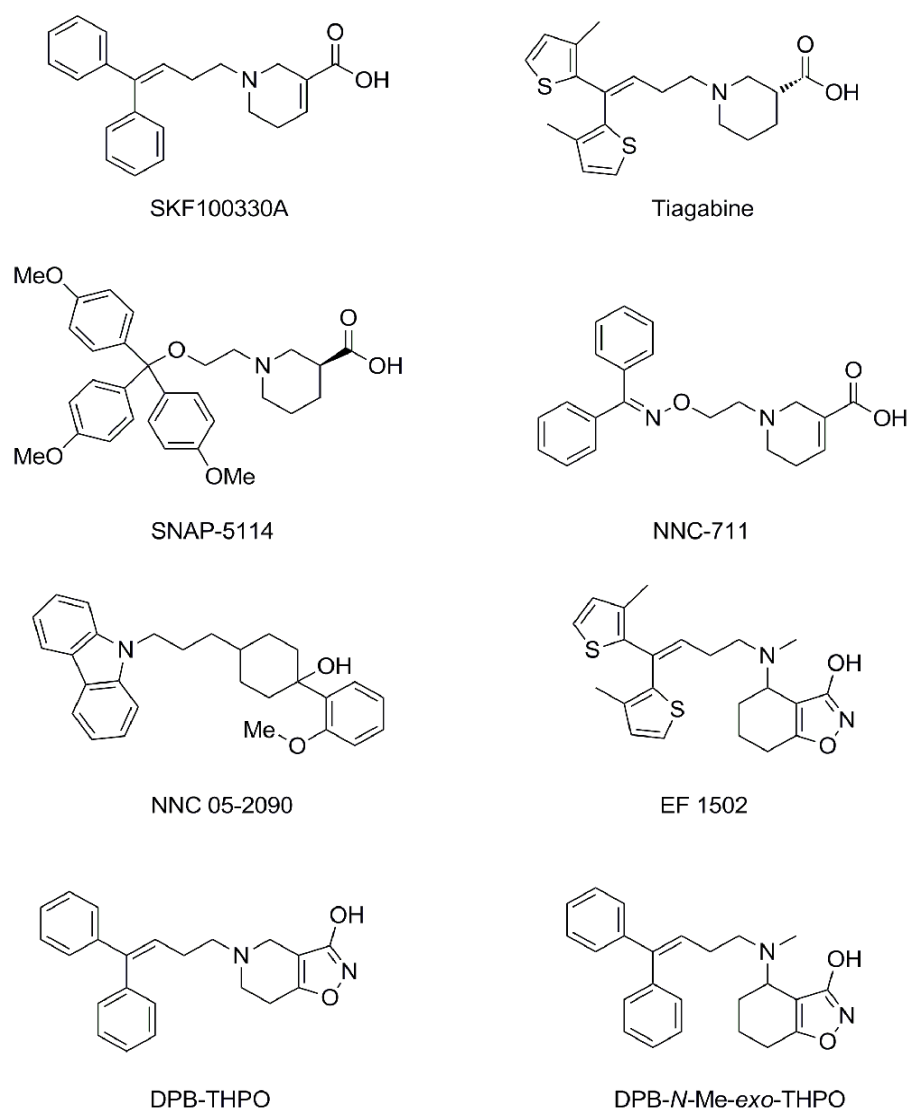


Figure 1.4 Lipophilic aromatic GAT inhibitors

## 1.4 GAT-1

The first neurotransmitter transporter to be cloned was a GABA transporter, termed GAT-1 (Guastella *et al.* 1990). And it is also the only neurotransmitter transporter that was cloned based on its amino acid sequence. Most of the other members of this transporter family were cloned based on the initial sequence information obtained from the GABA and noradrenaline transporters. The predominant GAT in GABAergic nerve endings is GAT-1 (Iversen and Kelly, 1975).

### 1.4.1 Mechanism

A widely accepted theory of the transport process mediated by neurotransmitter transporters across membrane is thought to be an alternating access mechanism. The allosteric model suggest that a central binding site of transporters connect both sides of the membrane by exposure alternately to either side of membrane with conformational changes, only one of which is accessible at a time. Concomitantly, different affinities of transporter for their substrate caused by conformational changes result in catching up the substrates on one side and releasing them on the other (Jardetzky 1966). In order to explain how the ions and substrate move together through an ion-coupled transporter at the molecular level, the complete transport cycle is proposed in four steps:

Step 1. The outward-facing transporter binds one or more sodium ions together with the neurotransmitter through open external gate. In this way, the movement of substrate is driven by ion gradient energy.

Step 2. As a consequence, the external gate closes, which is coupled to the opening of the internal gate. The coupling is critical that two gates can't open simultaneously to keep energy stored in the sodium gradient.

Step 3. After sodium and the neurotransmitter have been released to the inside of the cell, the internal gate closes.

Step 4. This closure is coupled to the opening of the external gate. The last two steps are referred to as the "return of the unloaded (or empty) transporter" (Kanner and Zomot 2008). Hilgemann *et al.* developed an alternating access transport model in *Xenopus* oocyte membranes, assuming two predominantly states of GAT-1,  $E_{in}$  and  $E_{out}$  (Hilgemann and Lu 1999). The crystal structures of bacterial homologue LeuT<sub>Aa</sub> and rabbit skeletal muscle Ca<sup>2+</sup>-ATPase, which show a closure of the active site in the transporters from the aqueous phase on either or both sides of the membrane, provide strong evidence for this suggestion (Yamashita *et al.* 2005; Olesen *et al.* 2007). With the aid of Modeller

software, a detailed structural model of the cytoplasm-facing state of LeuT is constructed to support the alternating access mechanism (Forrest *et al.* 2008).

GAT-1 cotransports GABA with two sodium ions and one chloride ion in an electrogenic process with thermodynamic and kinetic measurements (Radian and Kanner 1983; Keynan and Kanner 1988). The transport process can be measured for the stoichiometry study by radioactive flux assay in various experimental systems, such as brain plasma membrane vesicles (Kanner and Sharon 1978), liposomes inlaid with the detergent-solubilized transporter (Keynan and Kanner 1988), and *Xenopus* oocytes (Loo *et al.* 2000). The other measurement is electrophysiological approaches (Kavanaugh *et al.* 1992; Mager *et al.* 1993). The stoichiometry of other SLC6 members is not the same. The bacterial homologue LeuT<sub>Aa</sub>, a leucine transporter from *Aquifex aeolicus*, mediates sodium-dependent but chloride-independent transport.

GAT-1, as well as many members of the SLC6 family has an additional ionic requirement in that the transport activity of these carriers also depends on chloride ions. However, one study with charge ratio determination in oocytes suggests that for GAT-1, uptake of each GABA molecule is accompanied with two Na<sup>+</sup>, while they indicate an internal with external chloride exchange mechanism during the transport cycle, thus there is no net transport of chloride per transport cycle. (Loo *et al.*, 2000). Some dispute arises on the involvement of chloride. The fluxes measurements demonstrate direct sodium- and GABA-dependent transport of radioactive chloride in a reconstituted system of liposomes into a partially purified GABA transporter preparation (Keynan and Kanner 1988). Moreover, the reversal potentials defined with specific GAT-1 inhibitors also indicate a coupling of the fluxes of sodium, chloride and GABA (Lu & Hilgemann, 1999b). On the other hand, at very negative potentials the dependence of the GABA-induced currents on extracellular chloride is not absolute. The possible explanation is that another ion, such as hydroxyl replaces the role of chloride under such conditions. However, all three substrates, sodium, GABA, and chloride appear essential on the cytoplasm side for the outward GAT-1 current (“reverse transport mode”). Inward GAT-1 current remains bulky in the nominal absence of chloride (Lu & Hilgemann, 1999b; Mager *et al.*, 1993).

The current generated by the activity of most members of SLC6 family, consists of three components, termed transport current (Sonders and Amara, 1996), transmitter-gated current (Galli *et al.*, 1997), and transmitter-independent leak current (Sonders and Amara, 1996). The transport current is caused by translocation of net charges attributed to cotransport of Na<sup>+</sup> and Cl<sup>-</sup> ions along with the substrate at a fixed stoichiometry. The

binding of the neurotransmitter to the transporter but not their translocation is necessary for the transmitter-gated current. The third component, the transmitter-independent leak current, can be detected in the absence of transmitter and is supposed to be carried by alkali ions (Sonders and Amara, 1996), the example is the GAT1 expressed in human embryonic kidney cells (Cammack and Schwartz, 1996). One study demonstrated that the GABA-induced current in *X.laavis* oocytes can be separated into a transport current, which is coupled with GABA uptake and a chloride-independent GABA-gated current mediated by a sodium-conductance pathway. The transport current is generated from a fixed stoichiometry directly determined by radioactive tracer reflux measurements. A specific GAT-1 inhibitor is characterized as an effective tool to separate these two components. Besides steady-state transport currents, a sodium-dependent transient current, which can be detected in the absence of GABA, is blocked by GABA analogues since only binding of the analogues to the transporter but no translocation occurs (Mager *et al.*, 1993). These transients are due to a charge moving conformational change after sodium binding. A saturating internal chloride concentration can disable the charge moving reactions. It is thought that in most models that cytoplasmic chloride and external sodium bind to the transporter in a mutually exclusive manner, providing strong evidence for an alternating access mode of GABA uptake of GAT-1 (Lu & Hilgemann, 1999b; Hilgemann & Lu, 1999). The external chloride is associated to increase the affinity for external sodium (Mager *et al.*, 1996).

Two reports from separate groups illuminate the basis for the chloride dependence by identifying structural elements crucial for the binding of chloride (details described in section 1.3.3.3) (Forrest *et al.* 2007; Zomot *et al.* 2007). Although different transporters and approaches are utilized, similar findings of the role of chloride during the transport cycle are obtained that the negative charge contributed either by a chloride ion or by the transporter itself is necessary for sodium binding and translocation of the neurotransmitter (Amara 2007).

Recently, a same core architecture was identified based on several crystal structures of sodium symporters of different families, which strongly support this alternating access mechanism as a common transport mechanism (Yamashita *et al.* 2005; Faham *et al.* 2008; Weyand *et al.* 2008; Abramson and Wright 2009; Ressler *et al.* 2009). A transport model for sodium-substrate symport containing six-state is further developed as shown in Fig. 1.5. The direction of transport is dependent upon the ligand concentrations on each side of the membrane and the membrane potential.



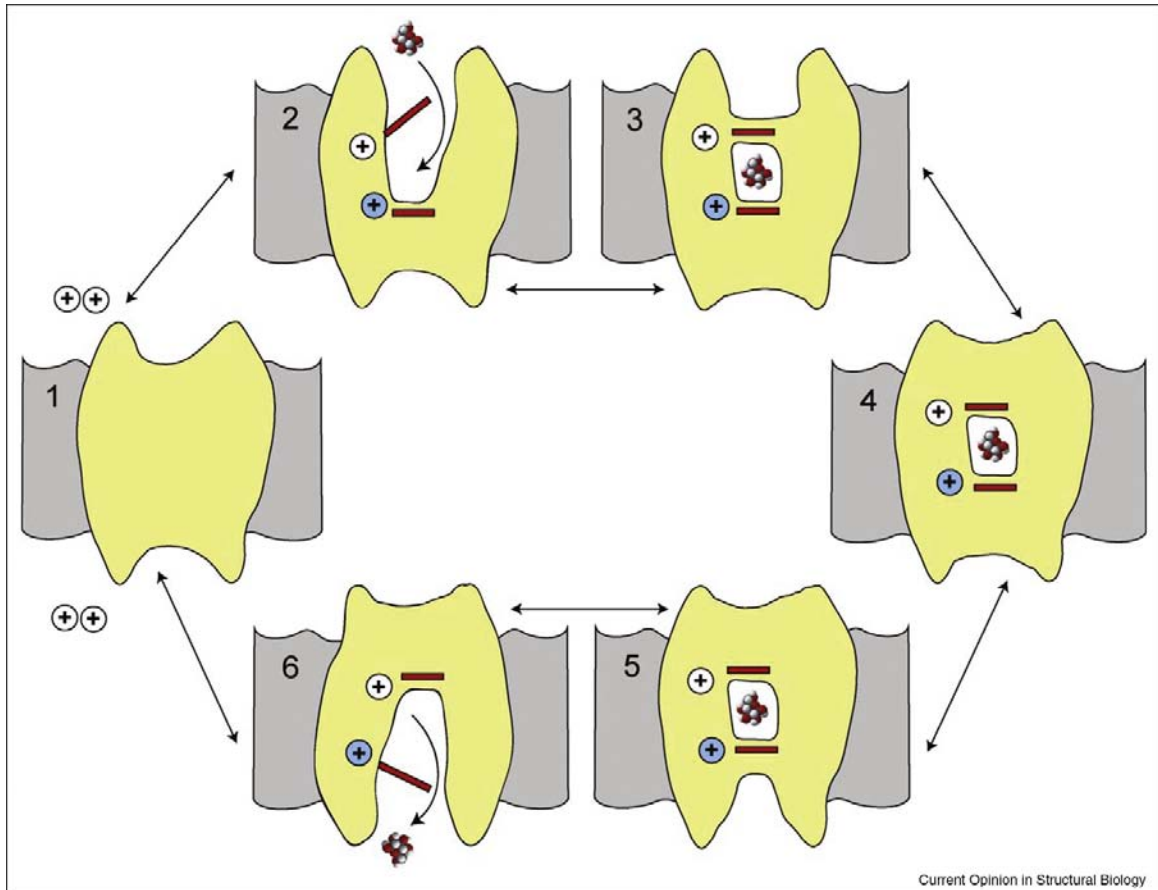


**Figure 1.5 A simple six-state model for sodium-substrate symport.** In this model: State 1. The starting point is with no bound ligands. State 2. In the presence of extracellular sodium, one (or two)  $\text{Na}^+$  ions bind to open the external gates to the substrate-binding site. State 3. External substrate then binds to its binding site and the external gate is closed. State 4. The external vestibule is closed. State 5. The internal vestibule opens. State 6. Substrate and sodium ion(s) dissociate and exit into the intracellular side of membrane. The cycle is completed by the closure of the internal vestibule and the return to State 1. (Abramson and Wright 2009)

### 1.4.2 Topology

GAT-1 cDNA has a predicted open reading frame of 1797 nucleotides which could encode a protein containing 599 amino acids with a molecular weight of 67 kDa, which is consistent with the molecular weight of the deglycosylated, purified GABA transporter protein (Kanner *et al.* 1989).

The transmembrane topology of GAT-1 has been predicted and analyzed by hydropathy plots (Guastella *et al.* 1990; Clark 1997) and has been further developed by *N*-glycosylation scanning mutagenesis (Bennett and Kanner 1997). The theoretical model, as shown in Fig. 1.6, predicts twelve transmembrane domains (TM), which are  $\alpha$ -helical stretch, connected by hydrophilic loops. Both carboxyl and amino termini are located in the cytoplasm; the latter localization is based on the lack of a recognizable signal sequence.

It is deduced that GAT-1 protein contains four potential glycosylation sites. Three of four consensus *N*-glycosylation sites (Asn176, Asn181 and Asn184) are located on the large extracellular loop between transmembrane domains 3 and 4 and are indicated as branched lines (Y-shaped symbols), while the remaining putative glycosylation site is located within transmembrane domain 9 and is not shown. This prediction is consistent with the observed neuraminidase sensitivity of GABA uptake by synaptosomes (Zaleska and Erecinska 1987). Three putative protein kinase C phosphorylation sites (Ser24, Thr46, and Ser562) are located on both N- and C-terminal sites. The remaining four protein kinase C sites and the single protein kinase A site are located externally or within membrane segments and are not illustrated.

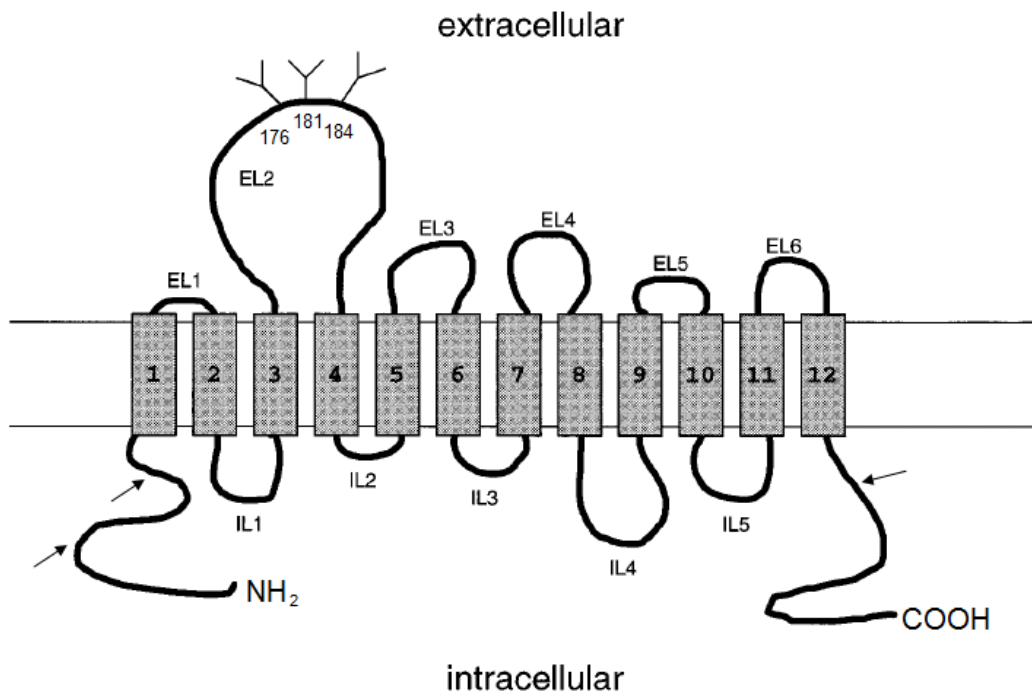


**Figure 1.6 Theoretical membrane topology of GAT1.** The hydrophilic loops and tails into which the N-linked glycosylation consensus sites have been inserted are designated EL (extracellular loops) and IL (intracellular loops) and are numbered. The three consensus *N*-glycosylation sites present in GAT-1 are located in EL2 and are indicated (Y-shaped symbols). Three putative protein kinase C phosphorylation sites are marked with arrows. Modified from (Bennett and Kanner 1997).

The topological model presented here is relevant not only for GAT-1, but also for all other members of the superfamily. Studies on the serotonin transporter SERT by site-directed chemical labeling (Chen *et al.* 1998) and the glycine transporter GLYT1 by introducing *N*-glycosylation sites provide evidence to support the revised model.

The topological model is also in agreement with the high-resolution crystal structure of LeuT<sub>Aa</sub> (Fig. 1.7), a homologue of the SLC/NSS transporters from the bacterium *Aquifex aeolicus* (Yamashita *et al.* 2005). The LeuT<sub>Aa</sub> structure represents a good model for the study of GAT-1 and other SLC6 members. The resolution of the LeuT<sub>Aa</sub> structure is remarkably high for a membrane protein (1.6 Å) and the structure reveals several topological features that could not have been predicted. The first one is that there is an internal inverted structural repeat of two structural units (TM1-TM5 and TM6-TM10) can be pseudosymmetrical superimposed with respect to the plane of the membrane. The interface of these two repeats might form the binding site of the transporter with two alternative permeation pathways connecting both sides of the membrane (Yamashita *et al.*, 2005). The second feature is the unwinding of the transmembrane domains for efficient coordination geometry, which was first observed in the calcium pump (Toyoshima *et al.*, 2000).

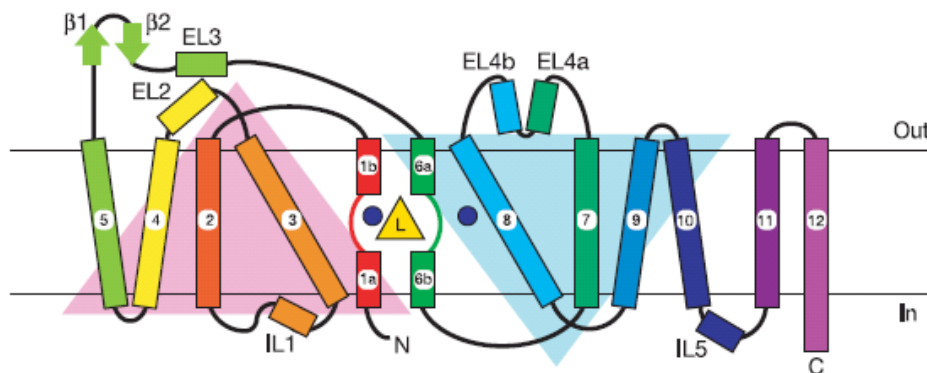


**Figure 1.7 Topology of the leucine transporter.** The internal inverted units TM1-TM5 and TM6-TM10 are shown as pink and blue triangles. The position of leucine and the two sodium ions are depicted as a yellow triangle and blue circles. (Yamashita *et al.*, 2005)

### 1.4.3 Structure and Function

The crystal structure of the LeuT<sub>Aa</sub> demonstrates not only a completely new protein fold but also an extremely clear portrait of the binding pocket for substrate and two sodium ions. In LeuT<sub>Aa</sub>, TM1 and TM6 have breaks in their helical structure approximately halfway across the membrane bilayer, which enable main-chain carbonyl oxygen and nitrogen atoms to expose for hydrogen bonding and ion binding (Fig. 1.7). Residues on TM3, TM7 and TM8 also contribute to the binding of sodium and substrate (Yamashita *et al.*, 2005). Some of the residues have already been implicated in ion and/or substrate binding by functional studies of mutants of several of the neurotransmitter transporters. It appears that

the LeuT<sub>Aa</sub> structure is a physiologically relevant conformation of the transporter, which provides a good model for the study of GAT-1 and other SLC6 members.

Even though LeuT crystallized as a dimer, each monomer had its own binding pocket, indicating that the monomer is the functional unit (Yamashita *et al.* 2005). One study by freeze-fracture and electron microscopy showed that GAT1 expression in the plasma membrane led to the appearance of a distinct population of 9-nm freeze-fracture particles which represented GAT1 dimers (Gonzales *et al.* 2007). Another structural and functional approach with rGAT1 suggests that despite oligomer formation in the plasma membrane, each monomer functions independently (Soragna *et al.* 2005). Also, because of the conservation of key residues of the LeuT-binding pocket throughout the entire SLC6 family, it is also likely that in the neurotransmitter transporters the monomer is the functional unit.

#### 1.4.3.1 Neurotransmitters binding site

In the LeuT<sub>Aa</sub> structure, as shown in Fig. 1.8, the substrate molecule is coordinated by the sodium ion bound at the Na1 site, main-chain carbonyl oxygens from amino acid residues from the unwound regions of TMs 1 and 6, main-chain amide nitrogens from TM6, and side-chain atoms of amino acid residues from TMs 3, 6, and 8 (Yamashita *et al.* 2005).

The structure of the unwound region in TM6 is stabilized by Glu-62, which interacts with the amide nitrogen of Gly-258 directly and with the amide nitrogens of Gly-260, Ala-261 and Ile-262 through a water molecule (Fig. 1.8) (Yamashita *et al.* 2005). This glutamate is conserved and the replacement of Glu-101, the equivalent residue in GAT1 by aspartate, abolishes the transporter activity (Keshet *et al.* 1995).

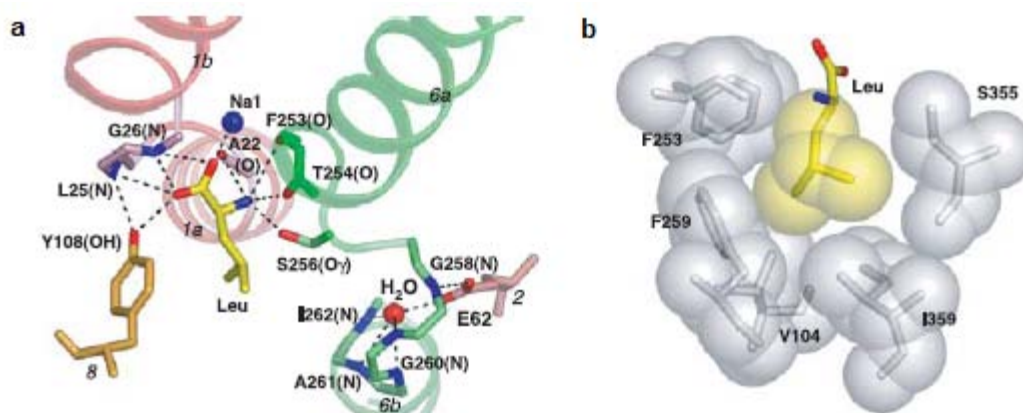


**Figure 1.8** Substrate binding site in LeuT<sub>Aa</sub>. a. Hydrogen bonds and ionic interaction in the leucine binding pocket depicted as dashed lines. b. Hydrophobic interactions between the leucine and the transporter. Van

der Waals surfaces for the leucine side chain and interacting residues shown as spheres. Tyr-108 and Ser-256 are omitted from the picture for clarity. (Yamashita *et al.* 2005)

The amino group of leucine is coordinated by main-chain carbonyl oxygens from Ala-22 in TM1, Phe-253 and Thr-254 in TM6, and by a side-chain hydroxyl from Ser-256 in TM6 (Fig. 1.8) (Yamashita *et al.* 2005). Ser-256 is not conserved in GATs due to the amino group at the  $\gamma$  position which may interact with its own carboxy group in a “cyclic” conformation (Kanner and Zomot 2008).

The carboxy group interacts directly with Na1, amide nitrogens from Leu-25 and Gly-26 in TM1, and the only side-chain hydroxyl from Tyr-108 in TM3 (Fig. 1.8) (Yamashita *et al.* 2005). This tyrosine is strictly conserved among all NSS family members and has been implicated in substrate binding and transport in GAT-1 (Bismuth *et al.* 1997), serotonin transporter (SERT) (Chen *et al.* 1997), and the glycine transporter GlyT2a (Ponce *et al.* 2000). The equivalent of Tyr-108 in GAT-1 is Tyr-140, of which the replacement by phenylalanine or tryptophane results in abolished transport activity. Sodium binding is unimpaired since both mutants still exhibit the sodium-dependent transient currents. However, these transients cannot be suppressed by GABA or its non-transportable analogues as wild-type GAT-1, which suggests that Tyr-140 is involved in the binding of GABA (Bismuth *et al.* 1997). It is likely that the hydroxyl side chain of the conserved tyrosine coordinates the carboxy group of all of the NSS transporters of amino acids.

The substrates of biogenic amine transporters, such as SERT, do not possess a carboxy group to contribute to the binding of sodium. A key difference of amino acid sequence is that, at TM1 position 24 of LeuT, all amino acid transporters have a glycine, whereas the biogenic amine transporters have an aspartate (Torres *et al.* 2003). In GAT-1, Gly-24 in LeuT is equivalent to Gly-63, which is critical for GAT-1 function (Kanner 2003). Modeling of an aspartate instead Gly-24 of LeuT<sub>Aa</sub> shows that the  $\beta$ -carboxyl group of the aspartate can be positioned to within 1 Å of the substrate leucine and within 3 Å of the sodium ion at Na1 (Yamashita *et al.* 2005). This indicates that in the biogenic amine transporters the carboxy group of the aspartyl residue may replace the carboxy group of amino acid substrates and coordinate a sodium ion (Yamashita *et al.* 2005). The lithium leak currents remain intact; however, no GABA transport can be measured in GAT-1 mutants at position 63. The membrane-impermeant sulfhydryl reagent inhibits these currents of the cysteine but not of the serine mutant, indicating that this position at the binding pocket can be reached from the external aqueous medium (Kanner 2003).

Mutations at Tyr-60 result in the reduction of the apparent affinity for sodium (Kanner 2003). In LeuT<sub>Aa</sub> Asn-21 is equivalent to this tyrosine. It is close but not at hydrogen bonding distance from the substrate and the sodium ions (Yamashita *et al.* 2005). The observed effects of mutations at this position in GATs may be due to a smaller distance in one of the other conformations or indirect effects.

Recently, several crystal structures of sodium symporters, such as LeuT<sub>Aa</sub>, the Na<sup>+</sup>-galactose symporter (vSGLT), nucleobase (Mnp1) and the glycine-betaine/proline-betaine (BetP)-symporters were solved and found to share the same core architecture, which implies a common transport mechanism (Yamashita *et al.* 2005; Faham *et al.* 2008; Weyand *et al.* 2008; Abramson and Wright 2009; Ressler *et al.* 2009).

#### **1.4.3.2 Sodium binding sites**

In the LeuT<sub>Aa</sub> structure two sodium ion binding sites, Na1 and Na2, were identified, which have key roles in stabilizing the LeuT<sub>Aa</sub> core, the unwound structures of TM1 and TM6, and the bound substrate molecule (Yamashita *et al.* 2005).

As Fig. 1.9 shown, Na1 is coordinated by the carboxy oxygen of the bound leucine, two main-chain carbonyl oxygens of Ala-22 (TM1) and Thr-254 (TM6), and three side-chain oxygens from Asn-27 (TM1), Asn-286 (TM7), and Thr-254 (TM6) (Yamashita *et al.* 2005). The equivalents of the latter three residues in GAT-1 are Asn-66, Asn-327, and Ser-295. And they are conserved or conservatively substituted in the NSS family. This conservation suggests that this family shares a similar Na1 site. Na2 is coordinated by three main-chain carbonyl oxygens from Gly-20 and Val-23 (TM1) and Ala-351 (TM8), as well as by two side-chain hydroxyl oxygens from Thr-354 and Ser-355 (TM8) (Yamashita *et al.* 2005). Thr-354 is not conserved and equivalent to Asp-395 in GAT-1, whereas Ser-355 is almost fully conserved throughout, with conservative substitutions (to Thr) only in the two glycine transporters. Functional analysis of mutations of these residues in GAT-1 confirmed these conservations and suggested that these same residues may be involved in the coordination of sodium in the neurotransmitter transporters of this family (Zhou *et al.* 2006).

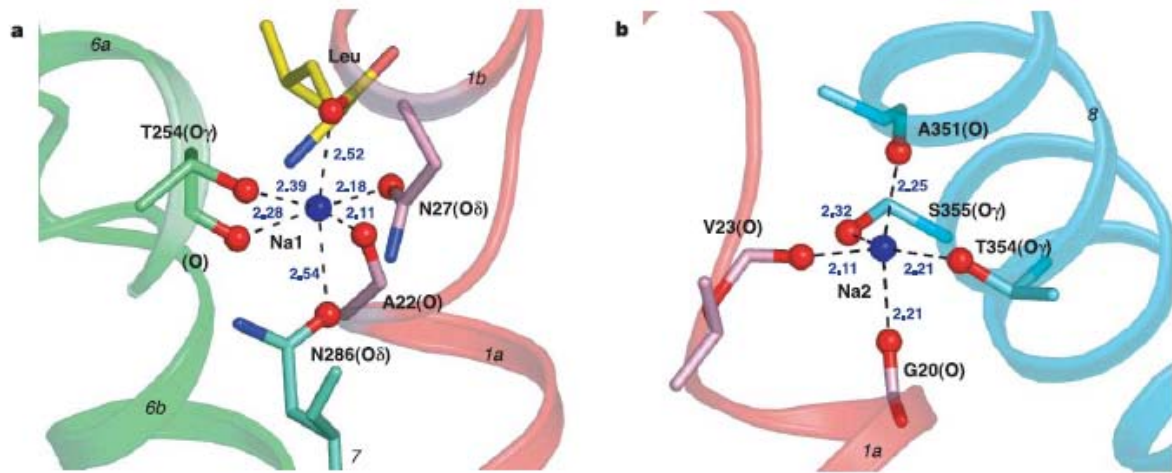


**Figure 1.9 Sodium ion binding sites in LeuT<sub>Aa</sub>.** a. Na1 is liganded by by amino acid residues from TM1a, TM1b, TM6a and TM7 together with the carboxy group of bound leucine. b. Na2 is liganded by residues from TM1a and TM8. Distances (Å) are in blue letters. (Yamashita *et al.* 2005)

Even though lithium by itself does not support GABA transport (Bennett *et al.* 2000; MacAulay *et al.* 2002), it has been proposed that lithium can replace sodium at one of the binding sites but not at the other (MacAulay *et al.* 2002). In GAT-1, only Asp-395 (TM8), one of the five residues corresponding to those whose side chains participate in the two sodium-binding sites of LeuT<sub>Aa</sub> (Thr-354), is not well conserved. At varying extracellular sodium concentrations, lithium stimulates sodium-dependent transport currents as well as [<sup>3</sup>H]-GABA uptake in wild-type GAT-1, and the extent of this stimulation is dependent upon the GABA concentration (Zhou *et al.* 2006). In mutants where Asp-395 is replaced by threonine or serine, the stimulation of transport by lithium is abolished (Zhou *et al.* 2006). Moreover, these mutants are unable to mediate the lithium leak currents. Even though their transport properties are severely impacted, this phenotype is not observed in mutants at the four other positions. Thus, at saturating GABA, the site corresponding to Na2 behaves as a low-affinity sodium-binding site, where lithium can replace sodium. Probably GABA participates in the other sodium binding site, just like leucine does in the Na1 site, and at limiting GABA concentrations this site determines the apparent sodium affinity of transport (Zhou *et al.* 2006)

For the SLC6 neurotransmitter transporters, several of these transporters have a different sodium/substrate stoichiometry. For instance, the norepinephrine transporter (NET) and SERT both transport Na<sup>+</sup> and their respective substrate in a ratio of 1:1 (Rudnick 2002), the sodium-to-substrate ratio in GAT1 and GlyT1b is 2:1, and in GlyT2a it is 3:1 (Kavanaugh *et al.* 1992; Roux and Supplisson 2000). It is suggested that the Na1 site is a

common binding site for the co-transported sodium ion in all NSS members and since the Na2 site may not be functional in some transporters, there may exist a third yet unknown sodium binding site. The LeuT<sub>Aa</sub> structure still appears to be a good model for the SLC6 neurotransmitter transporters.

#### 1.4.3.3 Chloride binding site

LeuT<sub>Aa</sub> mediates a sodium-dependent transport in a chloride-independent manner (Yamashita *et al.* 2005). However, the co-transport of GAT-1, as well as many NSS transporters is also chloride-dependent (Keynan and Kanner 1988; Krause and Schwarz 2005). The mechanism of chloride dependence is not very clear. Two reports from two separate groups identify the chloride-binding site for NSS transporters and suggest that the chloride charge facilitates sodium binding and substrate transport. The crystal structure of LeuT<sub>Aa</sub> provides a useful scaffold for these new studies, even though the only Cl<sup>-</sup> ion identified in the LeuT structure interacts with non-conserved residues in external loops at a site far away from the binding pocket (Yamashita *et al.* 2005).

One of the studies predicted Glu-290 (TM7) in LeuT<sub>Aa</sub>, which is close to the Na1 site, in TMs 2, 6, 7, as the Cl<sup>-</sup> binding site by calculations of pK<sub>AS</sub> (Forrest *et al.* 2007). On the structural basis of LeuT<sub>Aa</sub>, the mammalian SERT was generated by homology modeling (Forrest *et al.* 2007). Mutation of Ser-372 (equivalent to Glu-290 in LeuT<sub>Aa</sub>) to a Glu or Asp makes transport by SERT chloride-independent (Forrest *et al.* 2007). The data suggest that the acidic residues could replace the negative charge provided by the bound chloride in chloride-dependent transporters. In NSS transporters, serine occupies this position and is highly conserved, which provides strong evidence for this idea.

The crystal structure of a chloride/proton antiporter (Accardi and Miller 2004) reveals that the chloride ions are coordinated by main-chain NH groups and side-chain hydroxyls from serine and tyrosine residues (Dutzler *et al.* 2002; Dutzler *et al.* 2003). The other study of chloride-independent GAT1 mutants showed that introduction of a negatively charged at position 331 (Ser), which is equivalent to Glu-290 of LeuT, led to chloride-independent transport (Zomot *et al.* 2007). Moreover, introduction of residues (Ala and Gly) with a smaller side chain than Ser at position 331 of GAT-1 creates more space at the chloride site and thus potentiates the ability of anions larger than chloride to stimulate transport (Zomot *et al.* 2007). A low rate of chloride-independent GABA transport by S331E is still 5–10-fold that of this transport by wild type GAT-1 (Zomot *et al.* 2007). In S331E transporter, the fixed negative charge of the introduced glutamate residue remains where



the chloride is released to the cytoplasm in the wild type, thus could potentially limit the reorientation step of the empty transporter and slow transport. In contrast to wild-type GAT-1, a marked stimulation of the rate of net flux, but not of exchange, was observed when the internal pH was lowered, which is expected to neutralize the negative charge (Zomot *et al.* 2007), indicating that either a mobile (chloride) or a fixed negative charge is required during the sodium-coupled substrate translocation step.

In their studies the identification of the chloride-binding site for this family of symporter and its close proximity to the Na1 sites explains the tight coupling of the two ions during the inward movement of GABA and the two sodium ions, which stabilize the binding of the co-transported sodium ions by counterbalancing the charge. The elucidation of the binding site for chloride may reveal more information on additional anion movements during the transport cycle.

#### **1.4.4 Conformational changes**

Recently, several crystal structures of sodium symporters, such as LeuT<sub>Aa</sub>, the Na<sup>+</sup>-galactose symporter (vSGLT), nucleobase (Mnp1) and the glycine-betaine/proline-betaine (BetP)-symporters were solved and found to share the same core architecture, which implies a common transport mechanism (Yamashita *et al.* 2005; Faham *et al.* 2008; Weyand *et al.* 2008; Abramson and Wright 2009; Ressler *et al.* 2009). Conformational differences of these different transporters with the same core structure provide an insight into the structural basis of the conformational changes underlying the transport mechanism. According to the alternating access mechanism, the transporter must undergo several separated conformational transitions during the transport cycle so that the transporter is sequentially accessible to the outside and the inside of the membrane. The conformation of LeuT<sub>Aa</sub> with leucine and two sodium ions occluded in the binding pocket represents the substrate-loaded transition state of the transporter (Yamashita *et al.* 2005). It was proposed that the extracellular and cytoplasmic segments, TM1b-TM6a and TM1a-TM6b, respectively, may move relative to TM3 and TM8, which controls the opening and closing of the extra- and intracellular gates (Fig. 1.10). Future elucidation of structures of outward- and inward-facing conformations of LeuT or a related transporter will be required for more insights into the transport mechanism.

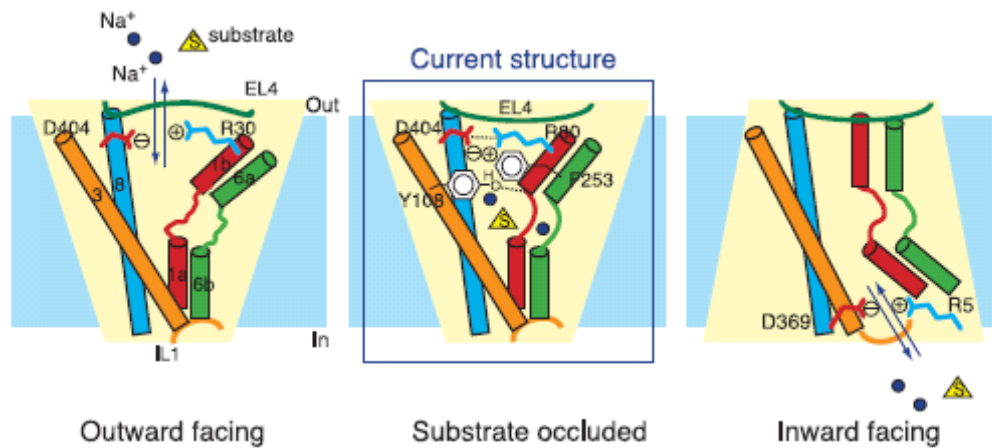


**Figure 1.10 Speculative conformational change upon substrate/sodium ion transport.** The left panel shows the outward-facing state. TM1a and TM6b assume the closed arrangement, whereas TM1b and TM6a adopt the open one. The middle panel shows the substrate-occluded state, which corresponds to the current crystal structure. TM1a and TM6b assume the closed arrangement, whereas TM1b and TM6a adopt a partially open one with some residues blocking the permeation pathway. The right panel shows the inward-facing state. TM1b and TM6a assume the closed arrangement, whereas TM1a and TM6b adopt the closed one, to open the pathway to the cytoplasm. (Yamashita *et al.* 2005)

In the extracellular gate of LeuT<sub>Aa</sub>, the leucine and sodium binding sites are primarily obstructed by the highly conserved Tyr-108 (TM3) and Phe-253 (TM6) (Fig. 1.10). There is a conserved charged pair composed of Arg-30 (TM1) and Asp-404 (TM10), which interact via a pair of water molecules, above these residues. Arg-30 interacts also with Phe-253 and Gln-250 (TM6) (Yamashita *et al.* 2005). The binding site of tricyclic antidepressants (TCAs) in LeuT<sub>Aa</sub> was identified to be at the bottom of the extracellular vestibule, about 11 Å above the substrate and directly above the extracellular gating residues Arg-30/Asp-404. In the TCA-containing structure, the water molecules between Arg-30 and Asp-404 are replaced by a direct salt bridge for stabilizing the extracellular gate in a closed conformation (Singh *et al.* 2007; Zhou *et al.* 2007). The equivalent residues of Arg-30 and Gln-250 in GAT-1 (Arg-69 and Gln-291, respectively) are absolutely essential for GABA transport (Pantanowitz *et al.* 1993; Kanner 2003; Mari *et al.* 2004). These residues together suggest part of the extracellular gate in the neurotransmitter transporters similar to that in LeuT<sub>Aa</sub>.

The intracellular gate of LeuT<sub>Aa</sub> is far more substantial compared to the extracellular one. TM1a, TM6b and TM8 together block cytoplasmic access to the leucine and sodium binding sites. Arg-5 and Trp-8 (TM1), Asp-369 (TM8), Tyr-265, Ser-267 and Tyr-268 (TM6) are strictly conserved residues and all participate in the formation of the

intracellular gate of LeuT<sub>Aa</sub> (Yamashita *et al.* 2005). Mutations of residues equivalent to Arg-5 or Trp-8 in the GAT-1 disrupt net transport, reflecting a similar internal gate as in LeuT<sub>Aa</sub>, while it remain sodium dependent exchange of GABA, suggesting the residues impair the coupling between the two gates only when the transporter is empty thus control the return of the unloaded transporter (Bennett *et al.* 2000). In one recent study, a single-molecule fluorescence resonance energy transfer (smFRET) method has been developed and combined with functional and computational studies of the prokaryotic NSS homologue LeuT<sub>Aa</sub> to investigate the conformational changes regulated by substrates and inhibitors, as well as by functionally related mutations (Zhao *et al.*, 2010). The data reveal molecular details of the modulation of intracellular gating of LeuT by substrates and inhibitors, as well as by mutations that alter binding, transport or both. The direct observations of single-molecule transitions indicating the relatively slow conformational switching events of the intracellular region of LeuT<sub>Aa</sub>, provide an explanation of the allosteric nature of the transport mechanism.

Studies on GAT-1 also provide a few evidences for the existence of conformational changes. The accessibility of engineered cysteines of GAT-1 has been inferred from the functional impact on the activity of these cysteine mutants in the presence of sodium, GABA or nontransportable GABA analogues by membrane-impermeant sulfhydryl reagents. Mutations in different structural domains include extracellular loop 4 (Zomot and Kanner 2003), TM1 (Zhou *et al.* 2004), and TM8 (Golovanevsky and Kanner 1999). Some residues far away from the substrate-binding site, according to the LeuT<sub>Aa</sub> structure (Yamashita *et al.* 2005), still result in changes in activities, indicating conformational changes but not direct involvement in substrate or ion binding. For example, Ala-364 in the fourth extracellular loop which connects TM7 with TM8 is conformationally sensitive (Zomot and Kanner 2003). Inhibition of GABA transport by the A364C/C74A double mutant, where the introduced cysteine becomes the only externally accessible residue, is enabled by the presence of sodium and chloride, whereas is protected by GABA even at 4°C. The non-transportable substrate analogue SKF100330A can protect or potentiate the inhibition of transport of A364C/C74A by impermeant reagents, in the presence or absence of sodium, respectively. This blocker may bind to the GAT-1 under both conditions, indicating a different conformation of GAT-1 (Zomot and Kanner 2003). On the other hand, accessibility studies on some residues close to the binding sites are also found to be involved conformational changes. One example is the endogenous cysteine at position 399 on the intracellular loop connecting TM8 with TM9. It is near the Na<sub>2</sub> site as defined by

the LeuT<sub>Aa</sub> structure (Yamashita *et al.* 2005) and its accessibility is also conformational sensitive (Golovanovsky and Kanner 1999).

The structural units that permit flexible structure of GAT-1 are necessary for its multiple conformational changes. Glycines can provide considerable flexibility to proteins, there are two good examples, a glycine residue acts as a hinge in potassium channels (Jiang *et al.* 2002) and engineered glycine residues in the proton-coupled lactose transporter of *Escherichia coli* introduces conformational flexibility (Weinglass *et al.* 2001). A conserved Gly-80 at the top of TM2 of GAT-1 has been determined to play a role in the conformational changes during transport (Zhou and Kanner 2005).

Replacement of Gly-80 by cysteine results in complete abolished GABA uptake activity, but oocytes expressing this mutant exhibit the sodium-dependent transient currents. In contrast to the wild type, the transients by G80C do not recover, when sodium is removed and subsequently added back. Remarkably, the transients by G80C, as well as by the wild type, can be restored after exposure of the oocytes to either GABA or a depolarizing prepulse. For the Gly-80 mutants, not like in the wild type, lithium-leak currents can be observed only when GABA is added or the oocytes are subjected to a depolarizing prepulse but not after prior sodium depletion. Thus, Gly-80 appears to be essential for conformational transitions in GAT-1. When this residue is mutated, removal of sodium results in “freezing” the transporter in one conformation from which it can only exit by compensatory changes induced by GABA or depolarization. These results can be interpreted by a model invoking two outward-facing states of the empty transporter and a defective transition between these states in the Gly-80 mutants  $\beta$ er binds (or releases) sodium (Mager *et al.* 1993; Mager *et al.* 1996; Lu and Hilgemann 1999; Kanner 2003). Sometimes the leak currents can be ascribed to a particular conformation of the transporter. In GAT-1, a leak mode, observed in the absence of sodium and in the presence of lithium (Mager *et al.* 1996), represents a distinct conformation of the transporter (MacAulay *et al.* 2001). Moreover, the lithium leak currents are inhibited in the presence of low concentrations of sodium due to the the transition from the leak mode to the coupled mode of the transporter mediated by sodium (MacAulay *et al.* 2002; Kanner 2003). Mutation of Asp-395 at the Na<sub>2</sub> site of GAT-1 to uncharged residues abolishes both the stimulating ability of lithium to GABA transport and the lithium-leak currents (Zhou *et al.* 2006), indicating that the Na<sub>2</sub> site is also used for ion permeation in the leak mode. A biochemical evidence for such conformational transitions is that the proteolytic cleavage of

GAT-1 can be protected against by GABA in the presence of sodium and chloride ions (Mabjeesh and Kanner 1993).

#### **1.4.5 N-Glycosylation of GAT1**

*N*-Glycosylation is a major post-translational modification in eukaryotic cells. Recent results suggest that *N*-glycosylation may influence many of the physicochemical and biological properties of proteins, such as protein folding, stability, targeting, dynamics and ligand binding, as well as cell-matrix and cell-cell interactions (Varki 1993; Schauer 2000; Hedlund *et al.* 2008). It has also been suggested that *N*-glycosylation is involved in surface expression of neurotransmitter transporters and the regulation of the transport activity. Functional expression of GAT is abolished by tunicamycin, a potent inhibitor of *N*-glycosylation. Experiments with HeLa transfectants showed that removal of one or two *N*-glycosylation sites by site-directed mutagenesis had little effect on the expression of GABA uptake activity (Keynan *et al.* 1992). Liu *et al.* demonstrated that in *Xenopus oocytes* mutations of two of the three *N*-glycosylation sites led to a reduction in turnover rates and complex changes in the interaction of external Na<sup>+</sup> with the transport protein as measured by voltage clamping (Liu *et al.* 1998).

Previously, our group had studied the biological significance of *N*-glycosylation and *N*-glycan of membrane glycoproteins and demonstrated that deficiency of *N*-glycosylation by site-directed mutagenesis resulted in reduction of protein stability, intracellular trafficking and correct folding of dipeptidyl peptidase IV (DPPIV) (Fan *et al.* 1997), as well as GAT1. However, inhibition of *N*-glycosylation processing by 1-deoxymannojirimycin (dMM) resulting in a mannose rich type of *N*-glycans did not affect either the protein stability or intracellular trafficking of GAT1 (Cai *et al.* 2005). This finding suggests that the co-translational *N*-glycosylation, but not the terminal trimming of *N*-glycans is involved in the regulation of the stability and trafficking of GAT1. However, dMM reduced markedly the GABA-uptake activity of GAT1 indicating an involvement of the terminal part of *N*-glycans in the regulation of the GABA uptake activity of GAT1 (Cai *et al.* 2005). Kinetic analysis demonstrated that deficient *N*-glycan trimming decreased the  $V_{max}$  values of GABA uptake by GAT1, while the  $K_m$  GABA values were not affected (Cai *et al.* 2005). It is indicated that the turnover rate of the transporter is affected, but not the substrate binding process. Voltage-clamp experiments revealed that the deficiency of *N*-glycans leads to the reduction of the affinity of GAT1 to Na<sup>+</sup> (Liu *et al.* 1998; Cai *et al.* 2005). In this event the *N*-glycans, in particular terminal structures of *N*-glycans play a role in the

regulation of GABA uptake activity of GAT1 by affecting the affinity to sodium ions (Cai *et al.* 2005).

## **1.5 Sialic acids**

### **1.5.1 Structure and occurrence of sialic acids**

Sialic acids comprise a family of acidic sugars whose basic structure consists of nine carbon atoms. The original isolation of sialic acids was accomplished in 1935 from glycolipids of brain or in 1936 from submaxillary mucin (Klenk, 1935; Blix, 1936). There is a carboxylate group at the C-1 position which is ionized at physiological pH; and an amino group at C-5 position. The amino group is usually acetylated, leading to *N*-acetylneuraminic acid (Neu5Ac), the most common biosynthetic precursor for most of the 50 naturally occurring sialic acids. Neuraminic acid with an unsubstituted group occurs extremely rare in nature (Manzi *et al.* 1990). The high structural diversity of sialic acids arises from the combination of a variety of linkages to the underlying sugar chain from the C-2 and various types of substitutions at the C-4, C-5, C-7, C-8 and C-9 (Angata and Varki 2002). Acetyl, lactoyl, sulfonyl, phosphonyl, or methyl groups have been identified as substitutions at the hydroxyl group, while substitutions at the amino group have been described as acetyl and glycolyl groups (Varki 1992); Schauer *et al.*, 1995). The sialic acids found so far in mammalian glycoconjugates are only  $\alpha$ -configured. An exception is the nucleotide-activated sugar of sialic acid, CMP-Neu5Ac, which occurs in anomeric  $\beta$ -configuration (Kolter and Sandhoff 1997).

Sialic acids are essential components of glycoconjugates in deuterostomes (vertebrates, echinoderms and ascidians) and it is an exception for them to be found in other life forms (Corfield, 1982). The deuterostomes line shows all types of the *O*-modification (Angata and Varki 2002), but sialic acids in vertebrates are usually only *O*-acetylation and occasional *O*-lactylation. The diversity of sialic acids differs from species, development and tissue organization (Varki 1993). Thus 14 different sialic acids in bovine submandibular gland were identified (Reuter *et al.* 1983). In human tissue, there are only 3 different types of sialic acids, the Neu5Ac, the 9-*O*-acetylated Neu5Ac and the 9-*O*-lactosylated Neu5Ac. The absence of the *N*-glycolylneuraminic acid (Neu5Gc) in human tissue based on a mutation in CMP-Neu5Ac hydroxylase gene (Irie *et al.* 1998) is the only presently known molecular difference between humans and chimpanzees (Gagneux *et al.* 2005). The occurrence of the individual sialic acid is determined by the activities of numerous specific sialyltransferases (Paulson *et al.* 1989); Basu *et al.*, 1995).

## **1.5.2 Biological functions of sialic acids**

The group of sialic acids contributes significantly to the structural diversity of glycoconjugates. Therefore many biological functions are associated with sialic acids. Due to their physical properties, such as negative charge and spatial distribution, sialic acids directly affect their immediate environment of glycoconjugates. Thus their functions can be divided into two main groups that explain many phenomena. Sialic acids act as a biological mask to shield recognition sites (Kelm and Schauer 1997; Schauer 2009). On the other hand, the structural diversity of the sialic acids makes them serve as recognition determinants by the specific binding with a great variety of molecules (Lasky 1995). The following shows several examples of the biological functions of sialic acids.

### **1.5.2.1 Adhesion and cell-cell-interaction**

Cell-cell adhesion and cell-matrix adhesion are fundamental process for direct cell migration and tissue formation during development and organogenesis, as well as for inflammatory reactions, malignant cell growth or metastasis (Edelman and Crossin 1991; Hynes and Lander 1992). As terminal components of glycoconjugates, sialic acids are exposed to the cellular environment which leads to the specific recognition by cell adhesion molecules in many adhesion processes. There are two most famous families of sialic acid-binding lectins, the selectins and siglecs (sialic acid-binding immunoglobulin superfamily lectins).

The selectins (lectin-EGF-complement binding-cell adhesion molecules, LEC-CAMs) are a family of receptors that are expressed on leukocytes, endothelial cells and platelets. They play a crucial role in processes such as the innate, nonspecific immune response, haemostasis and acute and chronic inflammation (Varki 2007). The selectins mediate the interaction so-called "rolling" which initiates the migration of activated leukocytes on vascular endothelium (Lasky 1995). The selectins which is bound in a calcium-dependent manner possess a tetrasaccharide motif sialyl Lewis<sup>x</sup> (Neu5Ac $\alpha$ 2-3Gal $\beta$ 1-4(Fuc $\alpha$ 1-3)GlcNAc $\beta$ 1-3Gal) or sialyl Lewis<sup>a</sup> (Neu5Ac $\alpha$ 2-3 Gal $\beta$ 1-3(Fuc $\alpha$ 1-4) GlcNAc $\beta$ 1-3Gal). So far there are three known selectins. L-selectin is constitutively expressed on many types of leukocyte. E- and P-Selectin is not constitutively expressed of endothelial cells. For an optimal binding of L-selectin, 6'-sulfo-sialyl Lewis<sup>x</sup> structures are necessary (Varki 2007). The subsequent invasion of leukocytes into the epithelium is mediated by integrins and molecules of the immunoglobulin superfamily. The intensity of adhesion is modulated by the sialic acid content of binding partners; the adhesion is stronger with less sialylated structures (Takeda 1987).

Siglecs (sialic-acid-binding immunoglobulin-like lectins) constitute the largest family of sialic acid-binding lectins in mammals. In humans, 13 different Siglecs have been found so far (Fig. 1.11), what are responsible for the innate and adaptive immune response (Crocker *et al.* 2007). Siglecs are type-I membrane proteins with an extracellular region containing a homologous N-terminal V-set Ig-like domain that mediates sialic acid recognition following by a varying number (1-16) of C2-set Ig-like domain (Fig. 1.11). Of all Siglecs apart from sialoadhesin, the transmembrane part is with a cytoplasmic tail (Crocker and Varki 2001). Siglecs 1/sialoadhesin expresses heterogeneously and exclusively on macrophages and regulates the interaction with other cells of the immune system by binding to  $\alpha$ 2, 3-linked sialic acids (Hartnell *et al.* 2001). Siglec2/CD22, in contrast, only binds to  $\alpha$ 2, 6-linked sialic acids (Tedder *et al.* 1997). It is a negative modulator of signal transduction of B-cell receptor and is also involved in the homotypic interaction of B cells (Poe *et al.* 2004). Siglec-4a/myelin-associated glycoprotein (MAG), the most highly conserved Siglec, is presented on neuroglia cells and serves to maintain the intact structure of myelin sheath (Schachner and Bartsch 2000).

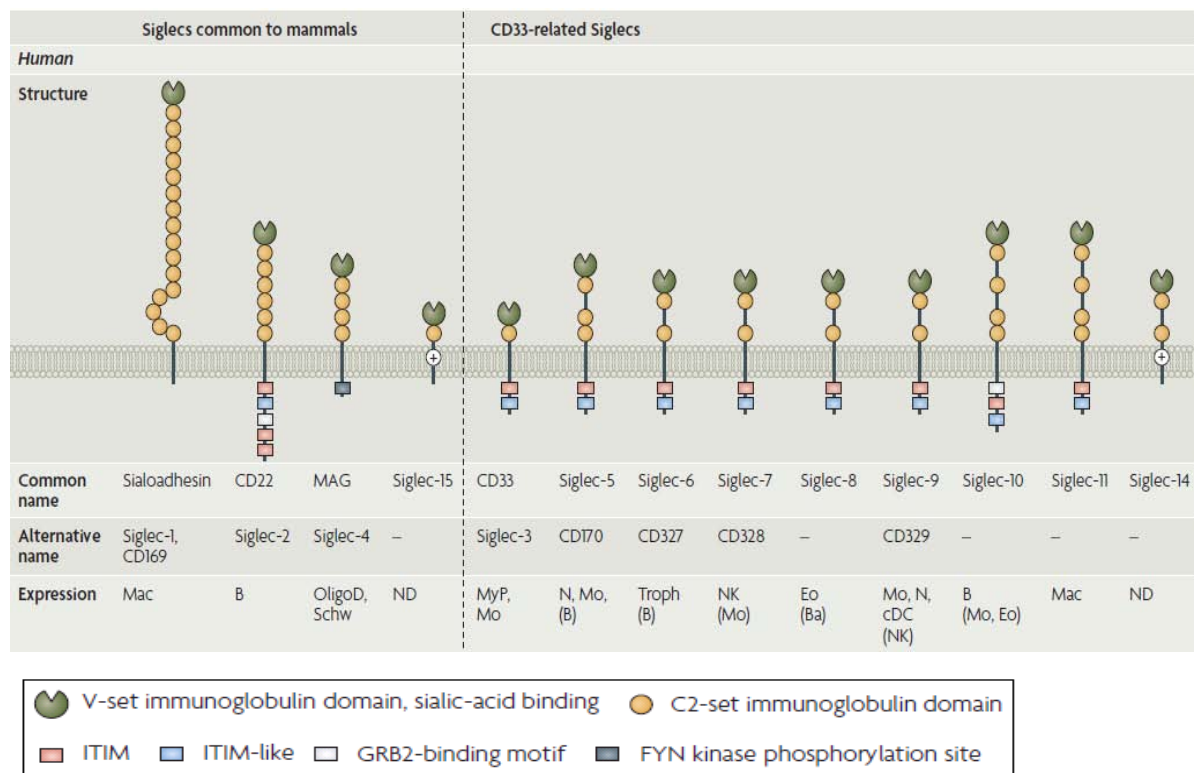


**Figure 1.11 Siglec-family proteins in humans.** Sialic-acid-binding immunoglobulins superfamily lectins (Siglecs) are type 1 membrane proteins containing an amino-terminal V-set immunoglobulin domain and varying numbers of C2-set immunoglobulin domains.



The neural cell adhesion molecule NCAM mediates homotypic and heterotypic cell-cell interactions. The adhesion behaviour of NCAM is modulated directly by sialic acid content (Cremer *et al.* 1994). In embryonic cells, many NCAM molecules are polysialylated. Because of their negative charge and large composition and size, the polysialic acid chains maintain only weak interactions between the cells. During development NCAM express polysialic acid with a progressive loss, so that the adhesion between nerve cells is increased (Bruses and Rutishauser 2001). Studies on a new mouse model which combine polySia-deficiency with normal NCAM expression clarify distinct functions of NCAM and polySia and indicate a vital role of polySia as a specific control element of NCAM-mediated interactions (Hildebrandt *et al.* 2007).

#### **1.5.2.2 Sialic acids as recognition determinants for pathogens**

Sialic acids are essential components of highly specific binding receptors for pathogens such as viruses, bacteria, parasites and toxins (Schauer, 1985; (Varki 1992; Karlsson 1995). The hemagglutinin of influenza A virus, a sialic acid-binding lectin, is involved in the mediation of the agglutination of erythrocytes and mediates virus entry into the host cell. The hemagglutinins of influenza A virus recognize and bind to Neu5Ac  $\alpha$ 2, 6Gal structures, while Neu5Ac  $\alpha$ 2, 3gal structures are for influenza B viruses. A 9-O-acetylation of the Neu5Ac prevents the binding of influenza A and B to their target cell (Varki and Varki 2007). The hemagglutinin of influenza C virus can bind specifically to Neu5, 9Ac2 structures (Zimmer *et al.* 1994), and then deacetylate the sialic acids on the host cells by an additional 9-O-acetyl-esterase (Herrler *et al.* 1985).

Experiments showed that the binding of viruses to their receptors on the host cells surface can be affected by the metabolically modified *N*-acetyl side chain *N*-acetylneuraminic acid (Keppler *et al.* 1995). The hemagglutinin of influenza A virus specifically binds the *N*-acetyl group of sialic acids. Influenza A virus infection are greatly reduced by the modification of the *N*-Acyl side chain of sialic acids in host cells (Keppler *et al.* 1998). The same inhibitions exist also with B-lymphotropic Papovavirus (Keppler *et al.* 1995) and murine polyomavirus (Herrmann *et al.* 1997). The virus-receptor interaction may also be affected by the hydrophobic interactions from certain sialic acids. The modified *N*-acyl side chain of the sialic acids of the target cells affects the invasion of human polyomavirus BK by the increased expression of *N*-propanoylneuraminic acid and *N*-butanoylneuraminic acid on the cell surface. On the other hand the infection was inhibited by longer side chains (Keppler *et al.* 1995). The specificity of influenza viruses to recognize different sialic acid

types depends on the host cells (human, chicken or pork) (Suzuki *et al.* 2000). Cross-infection of influenza A viruses occurs in different host cells because of the close proximity between animals and people or animals. The avian influenza strain H5N1 can permanently skip the species barrier and infect humans. A new strain of virus can develop between virus species within the host cell and combines features of both tribes by horizontal gene transfer. These viruses are then adapted to the sialylation type of human cells and thus lead to seasonal epidemics (Ito *et al.* 1998).

The sialic acid-binding lectins of pathogenic bacteria are called as adhesins and mediate the binding of the microorganisms to host cells (Ofek and Sharon 1990). The expression of the adhesins is strain-specific and regulates the infection of certain tissue. *Helicobacter pylori* expresses two adhesins that bind selectively to glycoproteins or gangliosides (Miller-Podraza *et al.* 1997), while the adhesion possessed by *E. coli* K99 binds specifically to Neu5Gc, which is particularly strong expressed in the host cells in the intestines of pigs (Yuyama *et al.* 1993). Occasionally, the toxins of microorganisms can also bind to sialic acid. The toxins of cholera, botulinum and tetanus bind to the specific sialylated gangliosides of their hosts and then the receptor-mediated endocytosis is performed (Richards *et al.* 1979; Schengrund *et al.* 1991).

### **1.5.2.3 Masking of antigenic determinants by sialic acids**

Sialic acids can mask antigenic determinants and thus prevent the detection by the immune system. *Trypanosoma cruzi*, the causative agent of Chagas' disease, binds to sialic acids of glycoconjugates on the surface of host cells. The trans-sialidase of the pathogen, which express both sialidase and sialyltransferase activity, can transfer sialic acids from the parasite to the host's and then mask its antigenic structures (Colli 1993; Tomlinson *et al.* 1994).

Embryonic cells also mask its antigenicity by sialic acids and thus are protected from the maternal immune system (Schauer, 1985). Once the protective zona pellucida of blastocysts are removed which contain sialic acid, antigenic determinants are recognized by the complement system within short time, which initiates the lysis of the blastocyst. Early embryonic stem cells (ES cells) are low sialylated. During differentiation the sialic acid content is increased and ES cells are less sensitive to complement-mediated lysis (Kircheis *et al.* 1996). Sialic acids can also control immune responses. For example, blood group antigens, which are characterized by a specific sialyl structure, lose their antigenicity after sialidase treatment (Pilatte *et al.* 1993).

#### **1.5.2.4 Influence of sialic acids on structure and function of glycoconjugates and their carrier**

The structures and biological functions of some glycoproteins are determined by sialic acids. The desialylated somatostatin receptor leads to a conformational change and exhibits a weak affinity for agonists (Rens-Domiano and Reisine 1991). After desialylation the function of nucleoporins p62, which mediates macromolecules transport between nucleus and cytoplasm, is significantly reduced (Emig *et al.* 1995).

In many cases, sialic acids protect proteins, such as acetylcholine receptor, from degradation of proteolytic activities presumably by steric hindrance (Olden *et al.* 1982). Sialic acid is involved in the regulation of the lifetime of serum glycoproteins and blood cells. After the loss of sialic acids or sialic acid-containing structures, the red cells and platelets can be recognized and phagocytosed by macrophages (Schlepper-Schafer *et al.* 1980; Kluge *et al.* 1992). The desialylated serum glycoproteins are endocytosed and degraded by recognition of the sialic acid-less glycoconjugates with the asialoglycoprotein of liver (Ashwell and Harford 1982). Recent work shows that there is a lack of asialoglycoprotein accumulation in the blood of asialoglycoprotein receptor-deficient mice. The asialoglycoprotein receptor helps to regulate the relative concentration of serum glycoproteins bearing  $\alpha$ 2, 6-linked sialic acid (Park *et al.* 2005). Erythropoietin (EPO) is an important growth factor for erythropoiesis, maintaining the body's red blood cell mass at an optimum level, especially in cancer patients. The decreased *in vivo* activity of desialylated EPO with a reduced half-life time in blood is due to the clearance by the asialoglycoprotein receptor (Wasley *et al.* 1991; Egrie and Browne 2001). The proliferation of cells can be affected by sialic acids of ganglioside GM<sub>3</sub>. GM<sub>3</sub> inhibits cell growth by reducing tyrosine phosphorylation of the epidermal growth factor receptor (Bremer *et al.* 1986), while de-acetylation at the sialic acid moiety of GM<sub>3</sub> makes the inhibition reversed (Hanai *et al.* 1988).

#### **1.5.2.5 Sialic acids and carcinoma**

The high sialic acid concentration on the cell surface in numerous tumors is associated with increased malignancy. In many cases, a linear relationship between the metastatic potential of tumours and sialic acid concentration were observed (Fogel *et al.* 1983; Hakomori 1989; Bresalier *et al.* 1990; Bhavanandan 1991; Sawada *et al.* 1994). Many cancer cells mask their antigenic determinants with sialic acids, as well as pathogens, and then evade the immune surveillance (Dennis and Laferte 1985). Only after removal of

sialic acids by sialidase treatment, they can be recognized and lysed by natural killer cells (Ahrens and Ankel 1987).

The gangliosides show a quantitative and qualitative change in sialic acid content in different types of tumors. For example, it was reported that the gangliosides in melanoma, GD2 and GD3, have significantly higher concentration of Neu5, 9Ac2 (Thurin *et al.* 1985; Sjoberg *et al.* 1992), while the ganglioside in colon and lung carcinomas GM3 contains Neu5Gc content (Higashi, 1990). Ganglioside GM3, a simple monosialoganglioside modulates cell adhesion, proliferation, and differentiation (Manfredi *et al.* 1999; Mitsuzuka *et al.* 2005). Recent results show that GM3 is an endogenous suppressor of angiogenesis due to its inhibitory effect on vascular endothelial growth factor (VEGF) (Mukherjee *et al.* 2008). In contrast to GM3, complex gangliosides like GM2, GM1, GD1a, GD1b, GT1b, and GD3, which contain longer oligosaccharide chains than that of GM3, enhance tumor cell proliferation, invasion, and metastasis (Alessandri *et al.* 1987; Hakomori 1996; Mitsuzuka *et al.* 2005).

The tumor-specific sialyl structure can be used as marker for tumor diagnosis (Bhavanandan 1991; Dreyfuss *et al.* 1992; David *et al.* 1993; Yamashita *et al.* 1995; Brockhausen 2006). For example, Neu5, 9Ac2 structures serve as a marker for melanoma (Fahr and Schauer 2001). In many malignancies, since increased levels of serum total sialic acid and/or sialic acid on glycolipids have been observed (Sillanaukee *et al.* 1999), the cancerous states can be determined by measuring the sialic acid concentration in serum in clinic (Fischer and Egg 1990).

## **2 Aim of this work**

### **2.1 Investigation of the role of terminal sialic acid of GAT1 in the GABA transport process**

It has been suggested the *N*-glycosylation is involved in surface expression of neurotransmitter transporters and the regulation of the transport activity. Previous studies in this group showed that *N*-glycans, especially their terminal structures are involved in the GABA uptake process of GAT1. Deficient *N*-glycosylation as well as inhibition of the terminal trimming of *N*-glycans reduced the transport activity of GAT1, which can be partially attributed to a reduced apparent affinity to extracellular Na<sup>+</sup> ions and slowed down kinetics of the transport cycle. The negatively charged sialic acid is the terminal sugar of the oligosaccharides of cell surface or serum glycoconjugates determining many biological functions. The aim of my work is: (1) to study whether the terminal sialic acid residues on *N*-glycans of GAT1 are involved in GABA uptake activity; (2) if so, to clarify which properties of sialic acid contribute to this process; (3) to further reveal the molecular mechanisms of the role of terminal sialic acid in GABA uptake of GAT1.

### **2.2 Investigation of the influence of chemical synthetic and naturally occurring compounds on GABA uptake activity of GAT1**

GAT1 is an interesting drug target due to its ability to regulate GABA concentration in GABAergic transmission.

#### **2.2.1 Investigation of the influence of hexosamines on GABA uptake activity of GAT1**

Since *N*-glycosylation was involved in GABA uptake activity of GAT1, and also we found that terminal sialic acid is crucial in the GAT1 activity, in my work, the influence of chemical synthetic analogues of hexosamines on GAT1 activity is determined to search potent inhibitors of GAT1, as well as the inhibitors of *N*-glycosylation or biosynthesis of sialic acid.

#### **2.2.2 Investigation of the influence of natural extracts on GABA uptake activity of GAT1**

In this work, in order to search for agonists of GAT1, the influence of several natural extracts from traditional Chinese medicine (TCM) on GABA uptake of GAT1 should be determined. The functional mechanisms of these samples will be further studied.

### **2.3 Expression, characterization, purification of homogenous GAT1**

The 3-dimensional structure of GAT1 remains unclear. Another aim of this work is the expression and purification of high amounts of the GAT1 protein for structural analysis.

2.3.1 Expression and purification of GAT1 protein from GAT1 stably transfected mammalian cells

2.3.2 Expression and purification of GAT1 protein from GAT1-expressed *Sf9* cells using BAC-TO-BAC<sup>TM</sup>- Baculovirus expression system.

2.3.3 Analysis of the purified GAT1 by transmission electron microscopy (TEM).

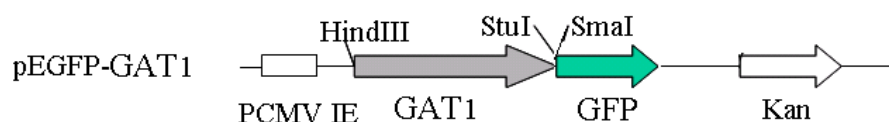
### 3 Results

#### 3.1 The role of terminal sialic acid of GAT1 in GABA uptake activity

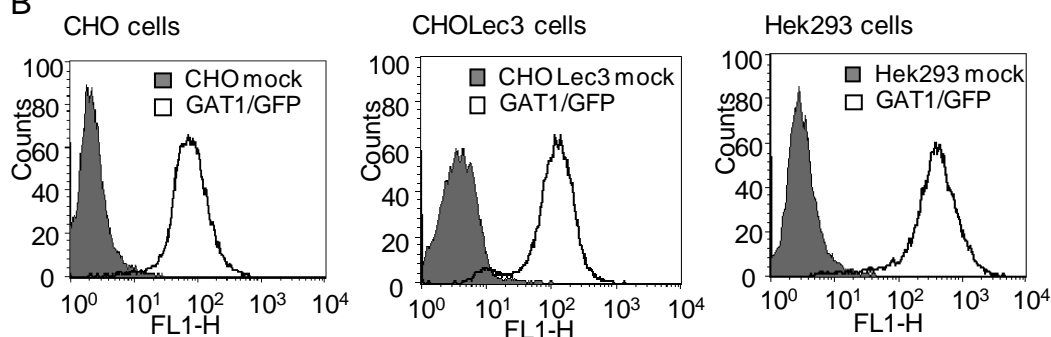
##### 3.1.1 The expression and characterization of GAT1/GFP in CHO, CHO Lec3 and Hek293 cells

The mouse GAT1 cDNA was cloned in the Hind III and Sma I site of the pEGFP-N1 vector which enables expression of GAT1 protein with a carboxyl-terminal GFP fusion tag in mammalian cell lines (Fig. 3.1 A). Then the GAT1/GFP recombinant protein was expressed in CHO, CHO Lec3 and Hek293 cells by stable transfection, all of them do not express endogenous GAT1 and GFP, respectively. After selection with 600 mg/L geneticin (G418) for 2-3 weeks, stable transfectant clones were then cultured in growth medium with 400 mg/L G418. Stable clones with green fluorescence were controlled by flow cytometry (Fig. 3.1 B) as well as fluorescence microscopy (Fig. 3.1 C).

A



B



C

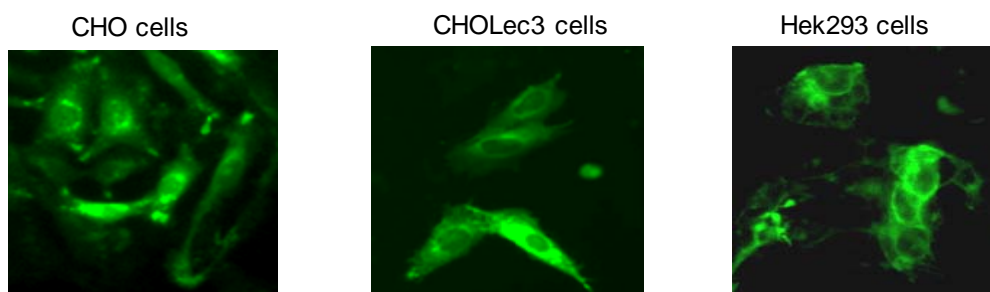
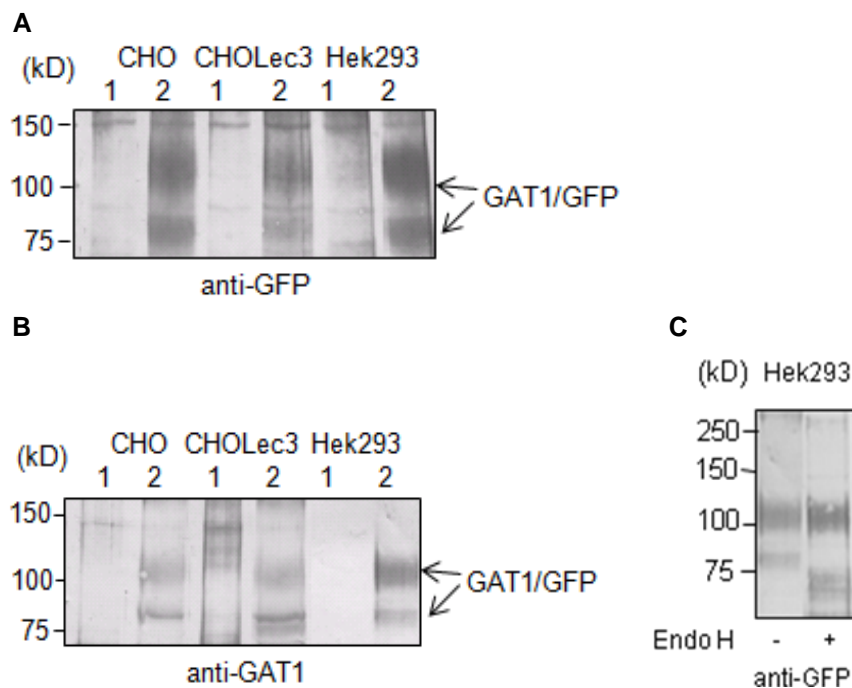


Figure 3.1 Flow cytometry and fluorescence microscopy of GFP-tagged GAT1 in transfected CHO,

**CHO Lec3 and Hek293 cells.** (A) Schematic representation of the GAT1/GFP fusion protein construct. (B) Flow cytometry analysis of GFP-tagged GAT1 in CHO, CHO Lec3 and Hek293 cells. (C) Fluorescence microscopy of three different stable transfectants. The fluorescence of GFP in GAT1/GFP-fusion protein was detected.

The expression of GAT1/GFP fusion protein in these cell lines were determined by Western blotting with either anti-GAT1 pAb (Fig. 3.2 B) or anti-GFP pAb (Fig. 3.2 A, C) following immunoprecipitation with anti-GFP mAb. In transfected CHO cells, the GAT1/GFP fusion protein showed several bands in SDS/PAGE (7.5%), two monomeric forms running as a main band of about 110 kDa and a small band of about 90 kDa. In transfected CHO Lec3 and Hek293 cells, the GAT1/GFP fusion protein shows the same bands of same size (Fig. 3.2 A and B) as those in CHO cells. In transfected Hek293 cells, the 110 kDa polypeptide was resistant to Endo H digestion, while the 90 kDa polypeptide was converted into a polypeptide of 75 kDa after digestion with Endo H (Fig. 3.2 C). It indicated that the 110 kDa polypeptide contains mature *N*-glycans of the complex type, while the 90 kDa peptide contains only *N*-glycans of the oligomannosidic type.



**Figure 3.2 Protein expression and *N*-glycosylation processing of GFP-tagged GAT1 in CHO, CHO Lec3 and Hek293 cells.** The solubilized protein of different transfectants were subjected to immunoprecipitation with anti-GFP mAb IgG and aliquots of some immunoprecipitates were treated either with or without Endo H. The resulting mixture and the other aliquots of those immunoprecipitates were then analyzed by SDS/PAGE (7.5%) and immunoblotting. (A) and (B) Western-blotting analysis of GFP-tagged GAT1 from different transfectants with anti-GFP pAb (A) or anti-GAT1 pAb (B) following



immunoprecipitation. Two main GAT1/GFP protein bands are indicated with arrows. Host cells (lane 1); GAT1/GFP transfectants (lane 2). (C) Western-blotting analysis of GFP-tagged GAT1 in Hek293 cells with anti-GFP pAb after Endo H treatment.

Furthermore, in order to determine whether GAT1/GFP fusion protein correctly expressed with function, GABA uptake assay was performed with stable clones of CHO, CHO Lec3 and Hek293 cells compared to those mock cells, respectively. As showed in Fig. 3.3, in CHO, CHO Lec3 and Hek293 cells, GAT1/GFP stable transfected clones had significantly higher GABA uptake activity than that of mock cells. CHO Lec3 transfectants ( $0.066 \text{ pmol}/10^4 \text{ cells}$ ) have relatively low activity comparing to CHO transfectants ( $0.24 \text{ pmol}/10^4 \text{ cells}$ ), while Hek293 transfectants ( $0.64 \text{ pmol}/10^4 \text{ cells}$ ) have much higher activity due to their high expression. The results showed GAT1/GFP recombinant protein was functionally expressed in mammalian cells.

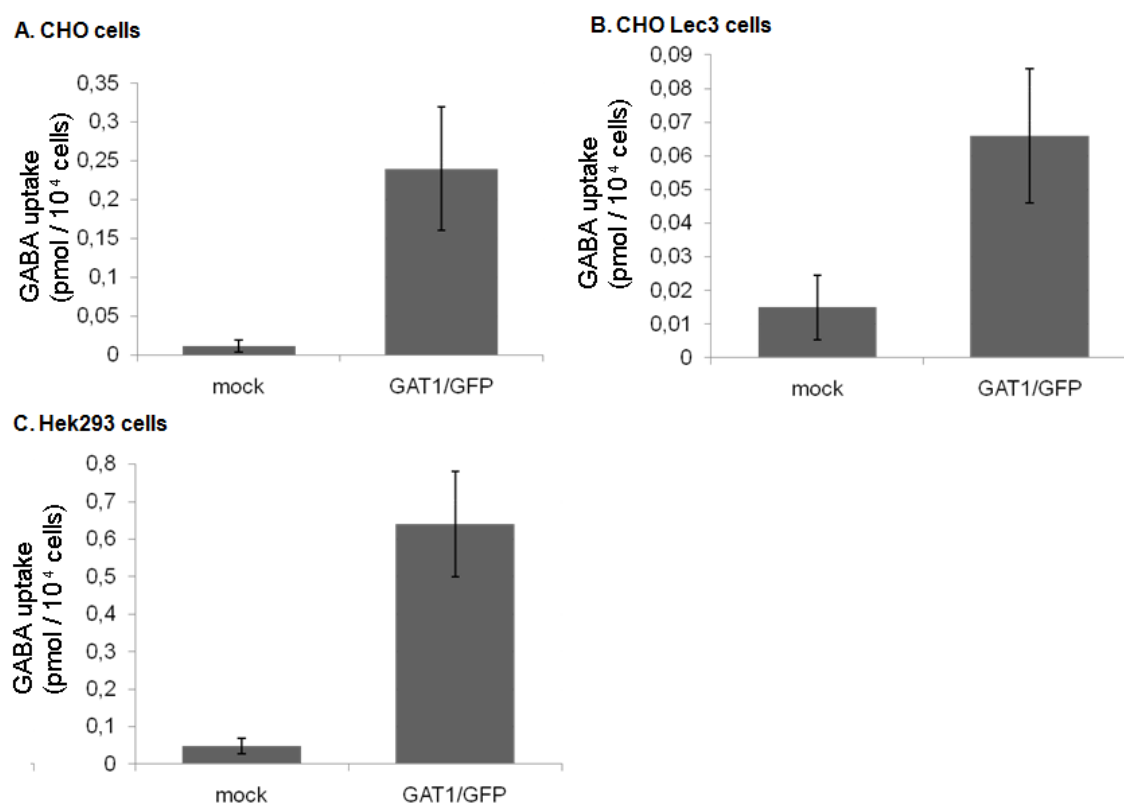


**Figure 3.3 Functional determination of GFP-tagged GAT1 in CHO (A), CHO Lec3 (B) and Hek293 (C) cells by GABA uptake assay.** The GABA uptake activities were normalized to the total cell number. The values represent the mean  $\pm$  SD of at least three separate experiments.

### 3.1.2 Effect of deficiency of terminal sialic acid on GABA uptake activity of GAT1/GFP

#### 3.1.2.1 Determination of sialic acid concentration in CHO and CHO Lec3 cells

CHO Lec3 cells are deficient in sialic acid residues on cell surface glycoconjugates due to mutations in the *gne* gene, which abolished UDP-*N*-acetylglucosamine 2-epimerase (UDP-GlcNAc 2-epimerase) activity (Hong and Stanley 2003). The total sialic acid concentration of CHO, CHO Lec3 and their transfected cells were quantified applying the resorcinol/periodic acid assay. As showed in Fig 3.4, compared to the CHO wild type cells (18.38 pmol/cell), the total sialic acid concentration of CHO Lec3 mutant cells was much lower (7.13 pmol/cell). And after stable transfection with GAT1/GFP, the total sialic acid concentration of CHO Lec3 transfectants was in the same range (7.75 pmol/cell) of CHO Lec3 cells, while the concentration of CHO transfectants increased to 38.63 pmol/cell. This showed that after the introduction of GAT1/GFP, the total sialic acid concentration remains low in CHO Lec3 mutant while increases in CHO cell lines.

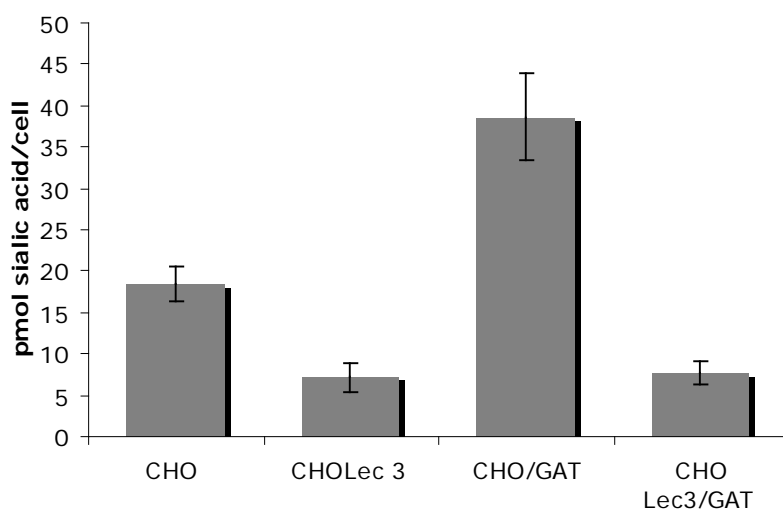


**Figure 3.4 Concentration of sialic acid in CHO, CHO Lec3 and their transfected clones.** Sialic acid concentration was measured using periodate/resorcinol method. Bars represent mean values  $\pm$  S.D. of three independent experiments carried in duplicates.

Furthermore, the cell surface sialylation in CHO and CHO Lec3 cells was analyzed by flow cytometry using fluorochrome-labeled sialic acid-sensitive lectins. As shown in Fig. 3.5, CHO Lec3 cells showed a marked decreased binding of the sialic acid-specific lectin LFA compared to CHO cells, indicating a much lower cell surface sialylation in CHO

Lec3 cells. This is consistent with the previous results of the total sialic acid content of these cells.

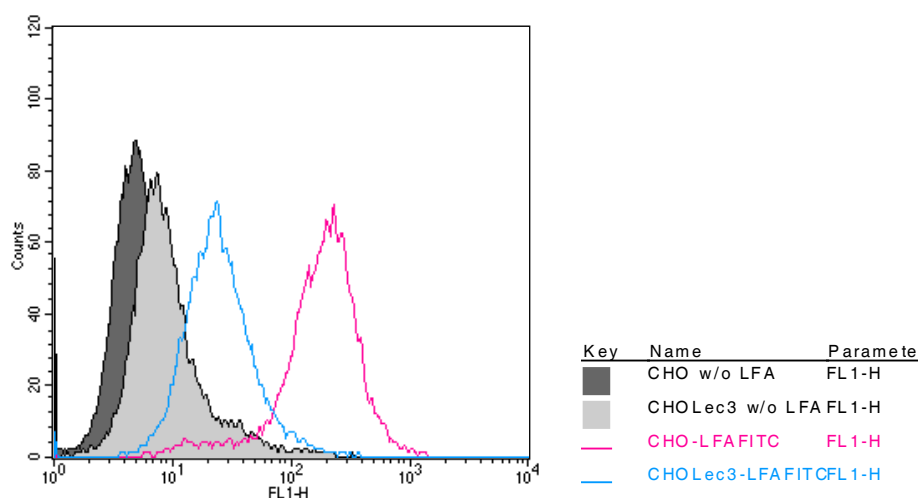


**Figure 3.5 Detection of cell surface sialylation by flow cytometry in CHO and CHO Lec3 cells.** Histograms illustrate the expression of sialic acids on the cell surface of CHO (red lines) and CHO Lec3 (blue lines) cells as determined by flow cytometry. The histograms for CHO cells (dark gray) and CHO Lec3 cells (light gray) without lectin staining are shown as references.

### 3.1.2.2 Quantification of the influence of deficiency of terminal sialic acid on the GABA uptake activity of GAT1/GFP

To study the role of terminal sialic acid of GAT1 in GABA uptake activity, quantitative measurement was first performed with CHO and CHO Lec3 transfectants. Aliquots of these two stable transfectants were used for determination of both GAT1 protein amounts and sialic acid concentrations of GAT1 and the other aliquots were used for the GABA uptake assay simultaneously. Fig. 3.6 A and B show that the total and plasma membrane GAT1/GFP protein expressed in CHO Lec3 cells as well as in CHO cells, which indicated that the deficiency of sialic acids in the mutants affects the GAT1/GFP protein expression slightly. The expression of the terminal sialic acids on GAT1/GFP was detected by lectin *maackia amurensis agglutinin* (MAA) and *sambucus nigra agglutinin* (SNA). In these cell lines, only  $\alpha$ 2,3-linked sialic acid could be detected by MAA, but using SNA  $\alpha$ 2,6-linked sialic acid was not detected (data not shown). Both sialic acid concentration and GABA uptake activity of GAT1/GFP were normalized to the amount of plasma membrane expressed GAT1/GFP protein. The concentration of terminal sialic acid of GAT1/GFP protein in CHO Lec3 cells was only  $35.2 \pm 13\%$  of that in CHO cells (Fig. 3.6 C, D). Remarkably, the GABA uptake activity of CHO Lec3 cells was also

reduced to  $33.8 \pm 5.7\%$  (Fig. 3.6 E), in comparison to that of CHO cells. These results suggest that a deficiency in the terminal sialic acid composition of GAT1/GFP results in a significant reduction of the GABA uptake activity.

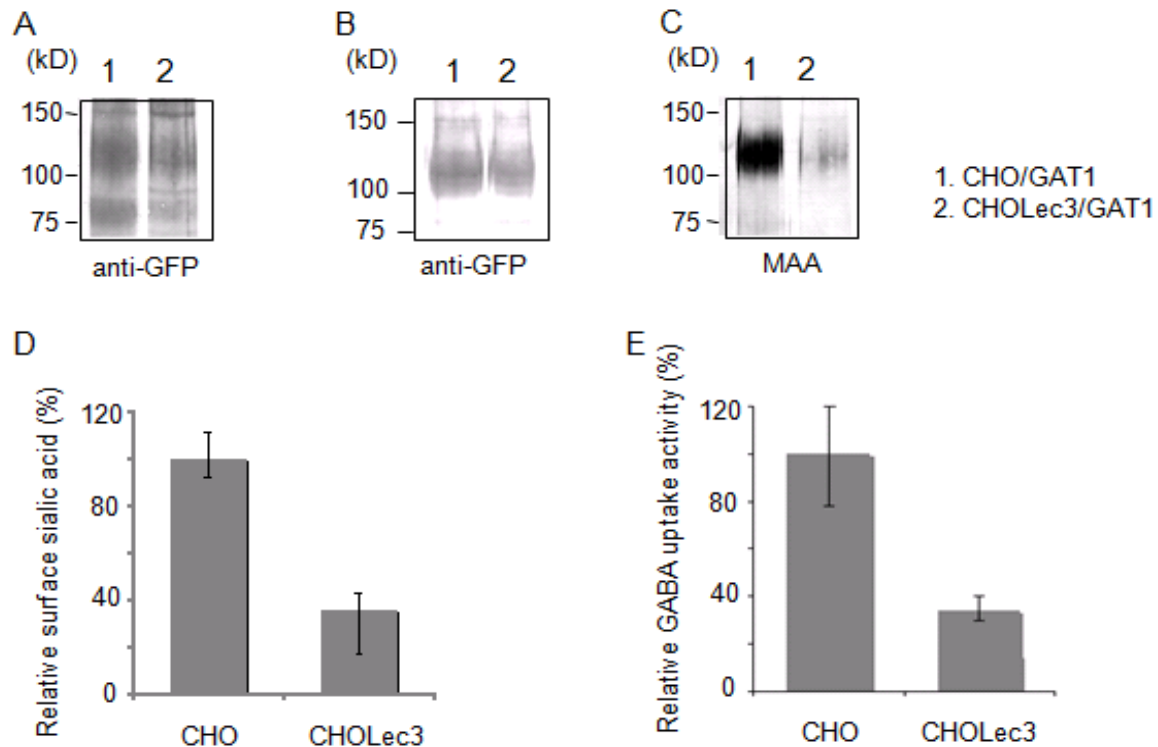


**Figure 3.6 Quantitative analysis of influence of terminal sialic acid of GAT1/GFP on GABA uptake activity in CHO and CHO Lec3 cells.** Transfected CHO and CHO Lec3 cells were separated in aliquots for immunoprecipitation with anti-GFP mAb Igs, cell surface biotinylation and GABA uptake assay. Aliquots of each immunoprecipitate and biotinylation probes were analyzed by SDS/PAGE (7.5%) and then transferred onto the nitrocellulose membrane for either immunostaining or lectin staining. (A) Total expressed GAT1/GFP protein. The aliquots of immunoprecipitate probes were immunoblotted with anti-GFP pAb. (B) Plasma membrane expressed GAT1/GFP protein. Biotinylation probes were immunoblotted with anti-GFP pAb. (C) Sialic acid concentrations of GAT1. The other aliquots of immunoprecipitate probes were stained with MAA (DIG Glycan Differentiation Kit) to detect  $\alpha$ 2,3-linked sialic acids on *N*-glycans of GAT1. GAT1/GFP in CHO cells (lane 1); GAT1/GFP in CHO Lec3 cells (lane 2). (D) Quantification of sialic acid concentrations of GAT1/GFP in CHO and CHO Lec3 cells. (E) Quantification of GABA uptake activities by GAT1/GFP fusion protein in CHO and CHO Lec3 cells. The total GAT1/GFP (A), plasma membrane GAT1/GFP (B) protein expression and sialic acid (C) were quantified with Quantity One software (Bio-Rad). Both sialic acid concentrations and GABA uptake activity values were normalized to the amount of plasma membrane GAT1 protein. And both values in CHO/GAT1 cells were set at 100%. All other values were expressed relative to these values. The values represent the mean  $\pm$  SD of three separate experiments.

### 3.1.2.3 Influence of ManNAc and ManNProp on GABA uptake activity of GAT1 in CHO Lec3 cells

*N*-Acetyl-D-mannosamine (ManNAc) is the physiological precursor of all sialic acids. ManNAc is formed from UDP-*N*-acetylglucosamine (UDP-GlcNAc) by epimerization of the hydroxyl-group in position 2 and cleavage of UDP by the UDP-*N*-acetylglucosamine 2-epimerase (Stasche *et al.* 1997). *N*-propanoyl-D-mannosamine (ManNProp) was reported to be taken up by cells and efficiently metabolized to *N*-propanoyl neuraminic acids (NeuProp) *in vitro* and *in vivo* (Kayser *et al.* 1992; Keppler *et al.* 2001). It has been reported that there was an increased sialylation in hyposialylated HL60-I and BJA-B K20 cells after treatment with ManNAc or ManNProp (Mantey *et al.* 2001). Similarly, CHO Lec3 cells cannot synthesize ManNAc and sialic acid *de novo* due to the mutation of UDP-GlcNAc 2-epimerase. Then the GABA uptake activity of GAT1 protein in CHO Lec3 cells was determined after 72 h incubation with ManNAc and ManNProp as shown in Fig. 3.7. In CHO transfectants, there was no clear effect of these two compounds on GABA uptake. However, both ManNAc- and ManNProp-treated CHO Lec3 transfectants showed a remarkably increased GABA uptake activity which should be due to an increased cell surface sialylation. Interestingly, ManNProp-treated cells (98%) exhibit much higher GABA uptake activity than ManNAc-treated cells (50%) probably because the cells can more easily take up and efficiently metabolize ManNProp. This finding suggests that the supplement of natural or unphysiological precursor of sialic acid biosynthesis can activate GABA uptake activity of GAT1 by increasing sialylation of unsialylated GAT1.

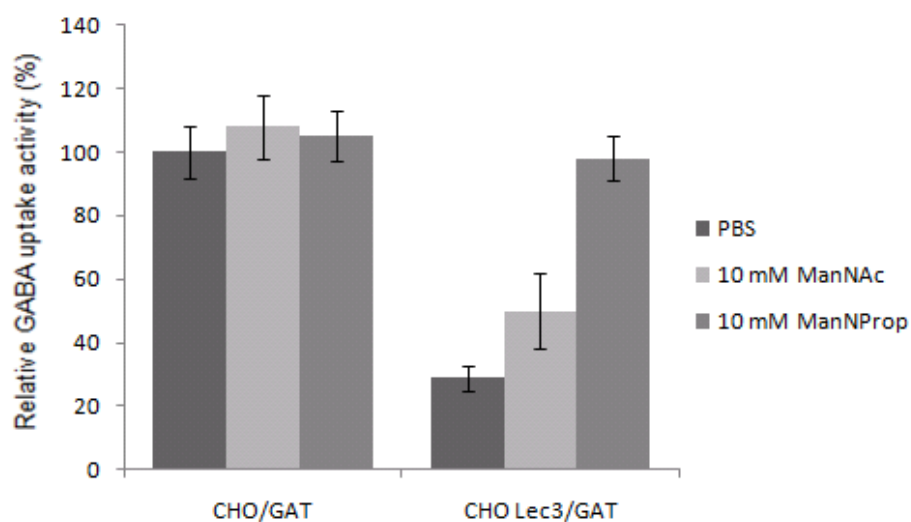


**Figure 3.7 Determination of GABA uptake activity of GAT1/GFP in CHO and CHO Lec3 cells after treatment of ManNAc and ManNProp.** Aliquots of transfected CHO and CHO Lec3 cells were cultured with the supplementation of culture medium with 10 mM ManNAc or ManNProp or PBS as control. GABA uptake assay was then performed. The values were normalized to the amount of total protein. And the value in CHO/GAT1 cells was set at 100%. All other values were expressed relative to these values. The values represent the mean  $\pm$  SD of three separate experiments.

### **3.1.3 Effect of removal of terminal sialic acid on GABA uptake activity of GAT1/GFP**

#### **3.1.3.1 Reduction of GABA transport activity of GAT1/GFP by sialidase treatment**

In order to verify that the reduced GABA uptake activity of GAT1 in CHO Lec3 cells does not result from other mutational effects of the CHO Lec3 cells, sialidase was used to remove the cell surface sialic acids from membrane glycoconjugates including the GAT1/GFP protein, and then the GABA uptake activity of GAT1/GFP was determined. Both GAT1/GFP transfected CHO and Hek293 cells were treated with sialidase at different doses. Sialidase works efficiently under weak acidic conditions; however, the cell growth was affected when the pH value is  $<5.0$ . At pH 5.5, sialidase maintained the enzymatic activity and the growth of the cells was hardly affected (data not shown). Further experiments were performed in a serum-free medium with pH 5.5. Fig. 3.8 A shows that in transfected CHO cells, after treatment of sialidase with 0.05, 0.2, 0.4, 0.6 and 0.8 U/ml in pH5.5 and serum free medium for 4 hours, the GABA uptake activities of GAT1 were reduced to 72%, 55%, 28%, 21% and 17%, respectively. Also, as seen in Fig. 3.8 B, it shows the same tendency in transfected Hek293 cells with sialidase treatment. After treated with 0.05, 0.2, 0.4, 0.6 and 0.8 U/ml sialidase under the same conditions, the GABA uptake activities in Hek293 cells were reduced to 89%, 70%, 61%, 48% and 34%, respectively. These results indicate that sialidase reduces GABA uptake activity in a dose dependent manner.

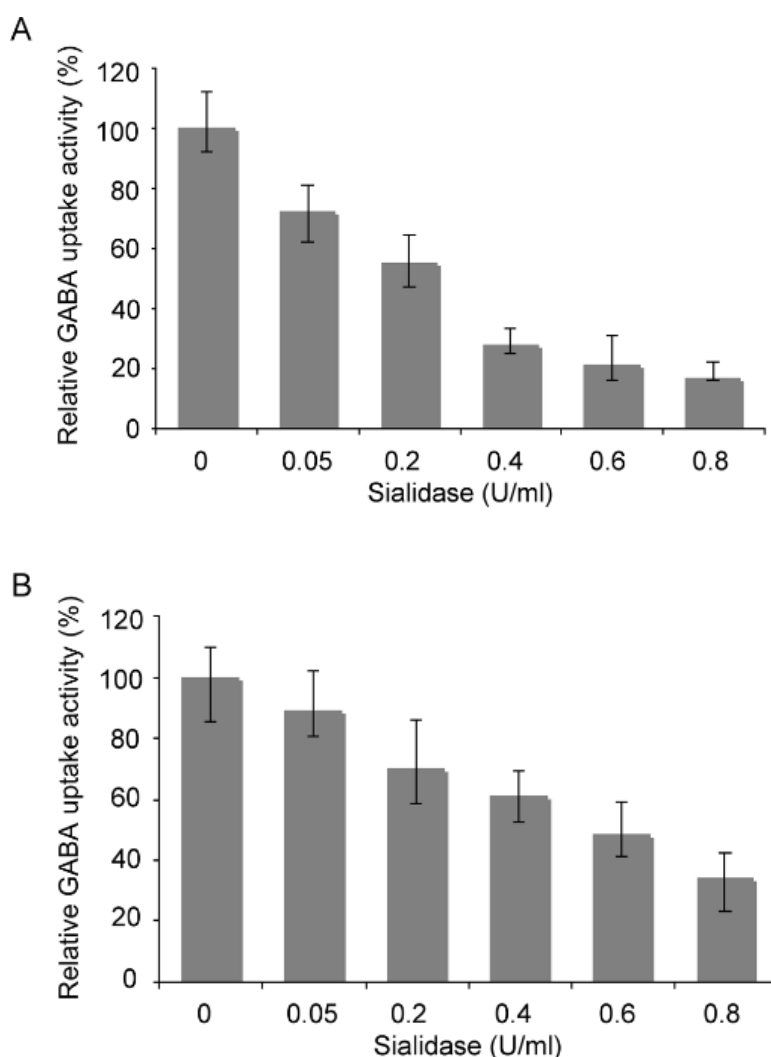


**Figure 3.8 Determination of GABA uptake activity of GAT1/GFP in CHO and Hek293 cells after treatment with sialidase.** Aliquots of the GAT1/GFP stable transfected CHO (A) and Hek293 (B) cells were incubated without or with 0.05, 0.2 0.4, 0.6 and 0.8 U/mL of sialidase in pH5.5 and serum-free medium for 4 h. The values of GABA uptake by transfected CHO and Hek293 cells without treatment of sialidase were set at 100%. All other values were expressed relative to this value. The values represent the mean  $\pm$  SD of three separate experiments.

### 3.1.3.2 Quantification of the influence of removal of terminal sialic acid on GABA uptake activity of GAT1/GFP

Since our results show that removal of sialic acid by sialidase has a direct influence on GAT1 activity, quantitative measurements were further performed with GAT1/GFP stably transfected Hek293 cells, in which GAT1/GFP protein expressed significantly higher than in CHO cells.

After incubation with 1 U/ml sialidase in serum free medium (pH5.5) for 4 h, the aliquots of cells were used to determine the amount of protein and sialic acids expression, while

the other aliquots were used to measure the GABA uptake activity by GAT1. Fig. 3.9 A and B show that after sialidase treatment, the amounts of total and plasma membrane GAT1/GFP protein of Hek293 cells were in the same range as those of cells without treatment of sialidase; while the amount of  $\alpha$ 2,3-linked sialic acid of GAT1 reduced significantly to  $13.8\pm 10.5\%$  (Fig. 3.9 C and D). As well, the GABA uptake activity was reduced to  $22.2\pm 11.5\%$  (Fig. 3.9 E), compared to that of cells without sialidase treatment. These results suggest that after sialidase treatment, the terminal sialic acids were removed without a significant influence on the protein expression and stability of GAT1. However, the reduction of sialic acid concentration leads to the marked decrease in the GABA uptake of GAT1. This indicates that terminal sialic acids on *N*-glycans are crucial for the GABA uptake activity of GAT1.

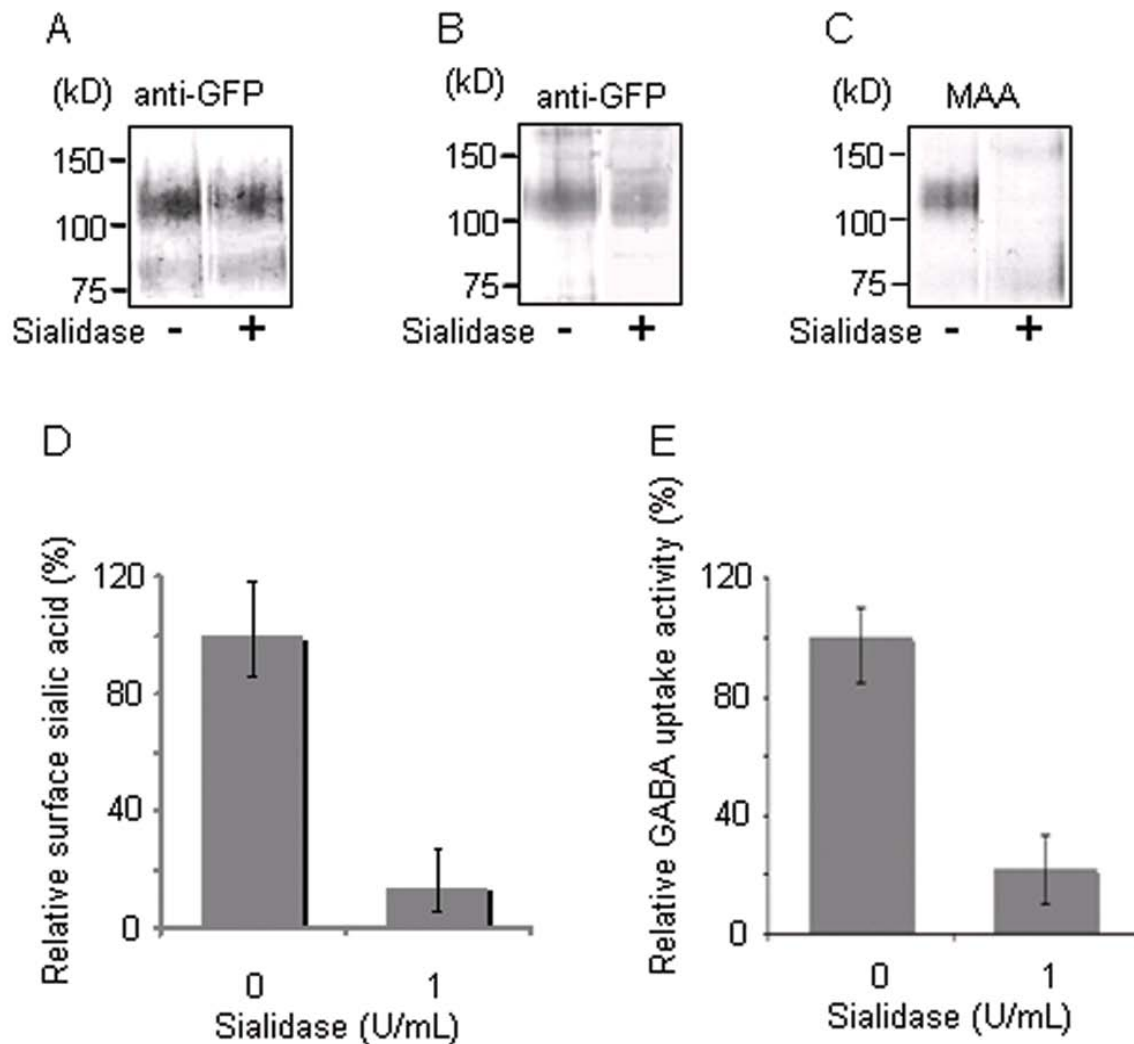


**Figure 3.9** Quantitative analysis of influence of terminal sialic acid of GAT1/GFP on GABA uptake activity in Hek293 cells after sialidase treatment. After sialidase treatment, GAT1/GFP stable transfected



Hek293 cells were separated in aliquots for immunoprecipitation with anti-GFP mAb IgG, cell surface biotinylation and GABA uptake assay. Aliquots of each immunoprecipitate and biotinylation probes were analyzed by SDS/PAGE (7.5%) and then western blotting. (A) Total expressed GAT1/GFP protein. The aliquots of immunoprecipitate probes were immunoblotted with anti-GFP pAb. (B) Plasma membrane expressed GAT1/GFP protein. Biotinylation probes are immunoblotted with anti-GFP pAb. (C) Sialic acid concentrations of GAT1. The other aliquots of immunoprecipitate probes were stained with MAA. (D) Quantification of the levels of sialic acids of GAT1/GFP in Hek293 transfectants with or without sialidase treatment. (E) Quantification of GABA uptake activity in Hek293 transfectants with or without sialidase treatment. The total GAT1/GFP (A), plasma membrane GAT1/GFP (B) protein expression and sialic acid levels (C) were quantified with Quantity One software (Bio-Rad). Both sialic acid levels and GABA uptake activity values were normalized to the amount of the plasma membrane GAT1 protein. And both the values of untreated Hek293/GAT1 cells were set at 100%. All other values were represented relative to these values. The values represent the mean  $\pm$  SD of three separate experiments.

#### **3.1.4 Effect of oxidation of terminal sialic acid on GABA uptake activity of GAT1/GFP**

Previous studies in this group showed that deficient *N*-glycosylation as well as inhibition of the terminal trimming of *N*-glycans reduced the transport activity of GAT1, which can be partially attributed to a reduced apparent affinity to extracellular Na<sup>+</sup> ions. Our results show that the deficiency and removal of terminal sialic acid of GAT1 also reduced GAT1 activity, indicating a reduced affinity to extracellular Na<sup>+</sup> ions due to the negative charge of terminal sialic acid (see also 3.1.5.2). In order to clarify whether the GABA uptake activity is dependent only on the acidic property of sialic acid of GAT1 protein, chemical oxidation of surface membrane-associated sialic acid residues was performed by using NaIO<sub>4</sub> (Perez *et al.* 1985). In order to prevent the formation of Schiff base from the formed aldehyde with available amino groups, aliquots of cells were further treated with sodium borohydride (NaBH<sub>4</sub>) to convert aldehyde to alcohol. After NaIO<sub>4</sub> treatment, the amounts of total and plasma membrane bound GAT1 protein of Hek293 transfectants were not affected compared to those of cells without treatment of NaIO<sub>4</sub> (Fig. 3.10 A, B), however, the amount of  $\alpha$ 2,3-linked sialic acid of GAT1 is reduced to 30.5 $\pm$ 10.5% (Fig. 3.10 C, D). Concomitantly, the GABA uptake activity was reduced to 25.2 $\pm$ 11.5% (Fig. 3.10 E), compared to that of cells without NaIO<sub>4</sub> treatment. Meanwhile, after further mild NaBH<sub>4</sub> reduction which converted aldehyde to alcohol, the reduced GABA uptake activity was not affected apparently (Fig. 3.10 E). These results provide further evidence that terminal sialic acids are necessary for the regulation of GABA uptake activity of GAT1.

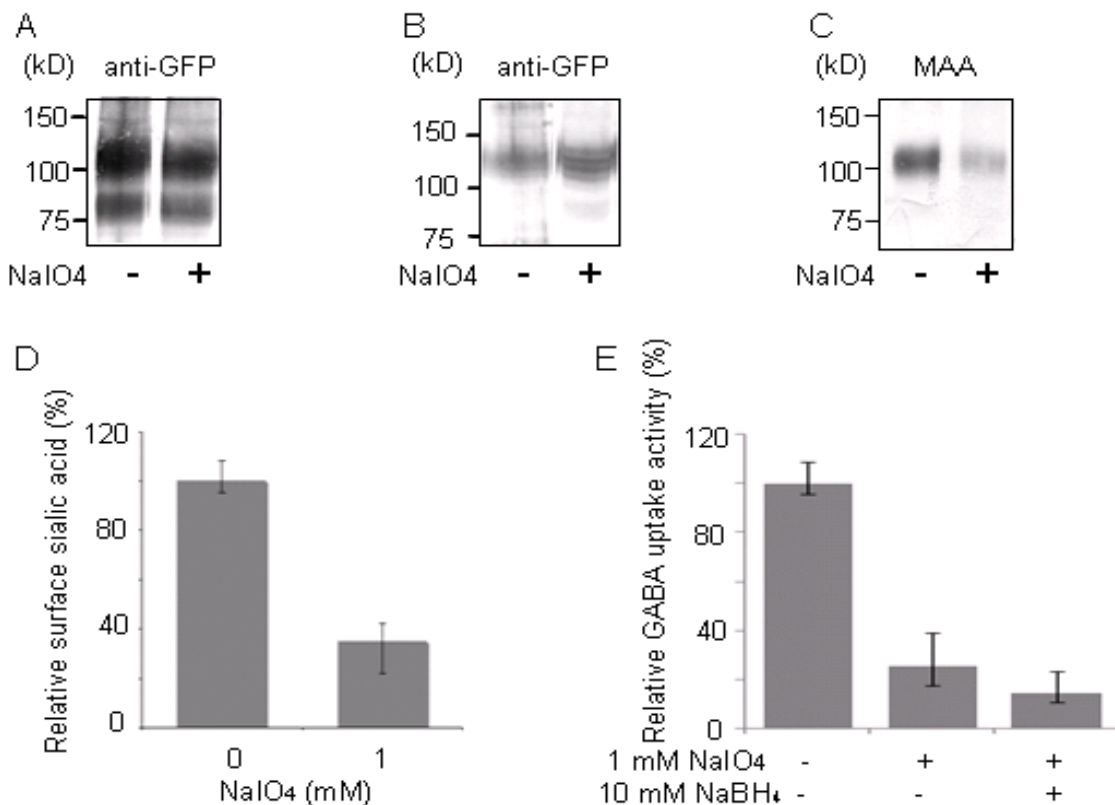


**Figure 3.10 Quantitative determination of GABA uptake activity of GAT1/GFP in Hek293 cells after treatment of NaIO<sub>4</sub>.** After NaIO<sub>4</sub> treatment, the cells were separated in aliquots for immunoprecipitation with anti-GFP mAb IgG, cell surface biotinylation and GABA uptake assay. (A) Total expressed GAT1/GFP protein. The aliquots of immunoprecipitate probes were immunoblotted with anti-GFP pAb. (B) Plasma membrane expressed GAT1/GFP protein. Biotinylation probes were immunoblotted with anti-GFP pAb. (C) Sialic acid concentrations of GAT1. The other aliquots of immunoprecipitate probes were stained with MAA. (D) Quantification of the levels of sialic acids of GAT1/GFP in Hek293 transfectants with or without NaIO<sub>4</sub> treatment. (E) Quantification of GABA uptake activity in Hek293 transfectants with or without NaIO<sub>4</sub> treatment. The total GAT1/GFP (A), plasma membrane GAT1/GFP (B) protein expression, and sialic acid levels (C) were quantified with Quantity One software (Bio-rad). Both sialic acid levels and GABA uptake activities values were normalized to the amount of plasma membrane GAT1 protein. And both values of untreated Hek293/GAT1 cells were set at 100%. All other values were expressed relative to these values. The values represent the mean  $\pm$  SD of three separate experiments.

### 3.1.5 Kinetic analysis of GABA uptake activity of GAT1/GFP protein

The above results demonstrate that a deficiency, removal and oxidation of terminal sialic acid residues all resulted in a remarkable reduction of the GABA uptake activity of GAT1. Kinetic analysis was performed to further study the molecular mechanisms of sialic acids of GAT1 in GABA transport.

### 3.1.5.1 Deficiency, removal and oxidation of terminal sialic acid did not change the $K_m$ GABA values of GAT1

We first determined whether the terminal sialic acids of GAT1 have influence the affinity of GAT1 for GABA. GABA concentration dependent uptake of GAT1 was analyzed on the basis of the Michaelis–Menten equation:

$$V = V_{\max} \text{GABA} \frac{[\text{GABA}]}{K_m \text{GABA} + [\text{GABA}]}$$

The GABA uptake activities of GAT1/GFP transfected CHO and CHO Lec3 cells, GAT1/GFP transfected Hek293 cells with and without treatment with sialidase or NaIO<sub>4</sub> were determined kinetically with different GABA concentrations. As depicted in Fig. 3.12 A, the  $V_{\max}$ GABA value of CHO Lec3/GAT1 was reduced significantly compared to CHO/GAT1 cells. The  $V_{\max}$ GABA value of CHO/GAT1 is 1.5 pmol·mg·protein<sup>-1</sup>·min<sup>-1</sup>, whereas the value for mutant CHO Lec3/GAT1 was only 0.31 pmol·μg protein<sup>-1</sup>·min<sup>-1</sup>. However, the  $K_m$  GABA values of CHO Lec3/GAT1 cells (4.4 μM) showed in the same range as that of CHO/GAT1 cells (4.2 μM). And the same tendency can be seen in Hek293/GAT1 cells after treatment of sialidase or NaIO<sub>4</sub>. Fig. 3.12 B shows that that the  $V_{\max}$  GABA values of untreated Hek293/GAT1 cells is 3.63 pmol·μg protein<sup>-1</sup>·min<sup>-1</sup>, whereas these values of the cells with sialidase and NaIO<sub>4</sub> treatment are strongly reduced to 1.22 and 1.02 pmol·μg protein<sup>-1</sup>·min<sup>-1</sup>, respectively. Although the deficiency of sialic acid reduced the  $V_{\max}$ GABA uptake markedly, however, either  $K_m$ GABA values of Hek293/GAT1 cells treated with sialidase or NaIO<sub>4</sub> (7.5 μM) did not increased comparing to that of untreated Hek293/GAT1 cells (7.6 μM). These results suggest that a deficiency, removal and oxidation of terminal sialic acids decrease the  $V_{\max}$  GABA values without affecting the binding affinity of GAT1 to GABA.

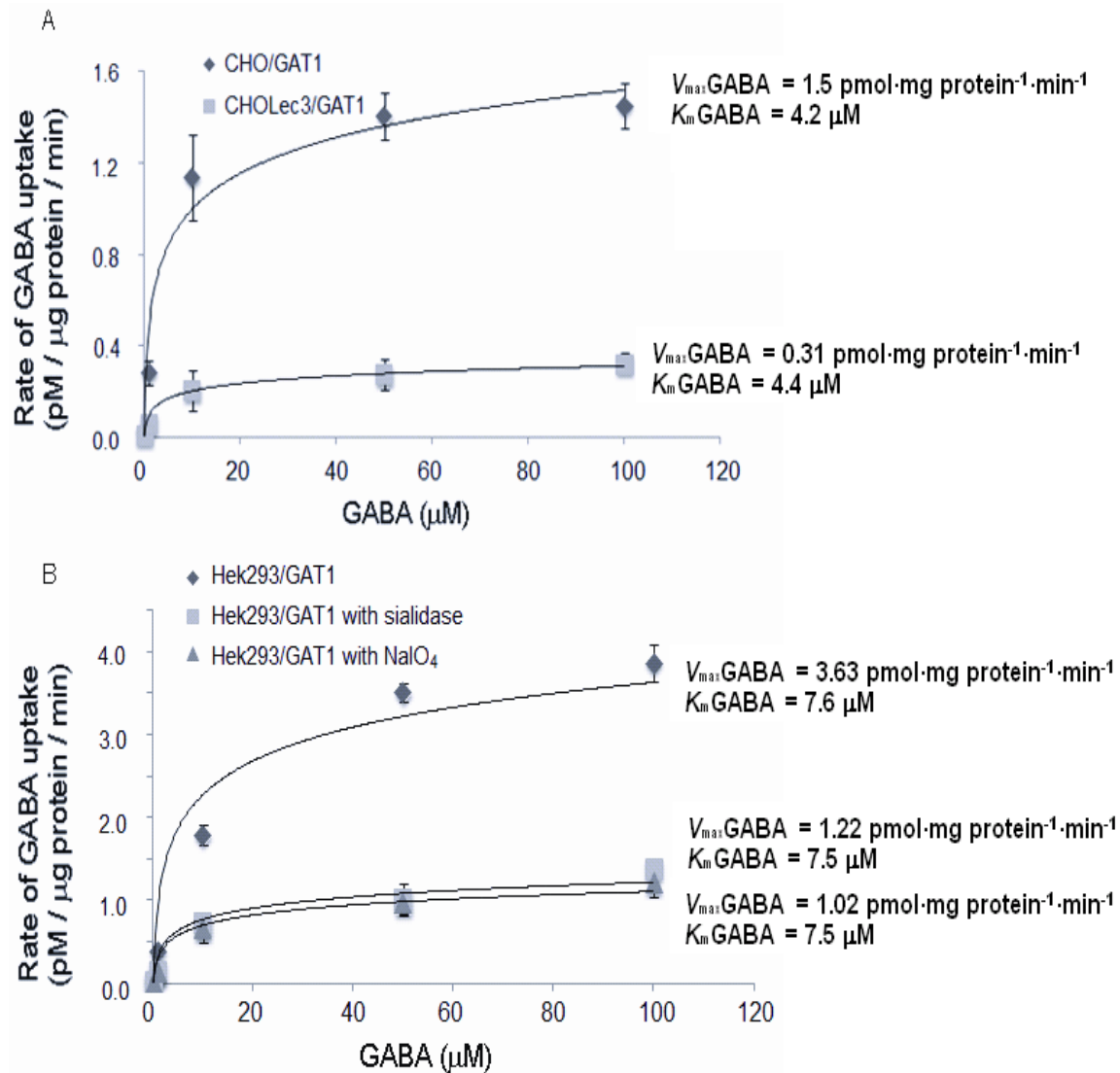


**Figure 3.12 Kinetic analysis of GABA uptake by GAT1/GFP in different cell lines with different GABA concentrations.** GABA uptake assays were performed with different GABA concentrations in CHO and CHO Lec3 transfectants, as well as Hek293 transfectants pre-incubated with and without sialidase (1U/mL) or NaIO<sub>4</sub> (1mM), respectively. All values presented were calculated after subtraction of the mock values. The data were fitted and calculated by a Michealis-Menten equation. (A) In transfected CHO and CHO Lec3 cells,  $K_m$  values in the same range of 4.2 and 4.4  $\mu\text{M}$ , and  $V_{max}$  values of 1.5 and 0.31  $\text{pmol} \cdot \mu\text{g protein}^{-1} \cdot \text{min}^{-1}$  were calculated, respectively. (B) In untreated, sialidase-treated and NaIO<sub>4</sub>-treated Hek293 transfectants,  $K_m$  values also in the same range of 7.6, 7.5, 7.5  $\mu\text{M}$ , and  $V_{max}$  values of 3.63, 1.22 and 1.02  $\text{pmol} \cdot \mu\text{g protein}^{-1} \cdot \text{min}^{-1}$  were calculated, respectively. The values represent the mean  $\pm$  SD of at least three separate experiments.

### **3.1.5.2 Deficiency and removal of terminal sialic acid increased $K_mNa^+$ values of GAT1**

Kinetic analysis was also performed by lowering sodium ion concentrations to further determine the influence of the terminal sialic acids of GAT1 on the affinity of GAT1 for  $Na^+$ . For solutions with reduced  $Na^+$ , the NaCl was replaced by KCl to create equal osmotic pressure. Sodium-dependent GABA uptake was thus measured at the different extracellular  $Na^+$  concentrations. Since the GAT1-dependent  $Na^+$  uptake is proportional to GABA uptake at the ratio 2:1,  $Na^+$  uptake rate can be determined with the value of GABA uptake rate. Fig. 3.13 shows the GABA uptake rate of GAT1 is dependent on the extracellular  $Na^+$  concentration. The kinetic constants were then calculated on the basis of the Michaelis-Menten equation by the double-reciprocal plot analysis.  $K_mNa^+$  values are 125 and 1000 mM for CHO/GAT1 and CHO Lec3//GAT1 cells, respectively. The deficiency of terminal sialic acids on *N*-glycans of GAT1 in CHO Lec3/GAT1 cells reduced the apparent affinity from  $8 M^{-1}$  in CHO/GAT1 cells to  $1 M^{-1}$  (Fig. 3.13 A). In Hek293 cells, the  $K_mNa^+$  value after removal of cell surface sialic acids by sialidase treatment increased from 205 mM to 1180 mM, resulting in the reduction in the apparent affinity of GAT1 to  $Na^+$  from  $4.9 M^{-1}$  to around  $0.85 M^{-1}$  (Fig. 3.13 B). This result suggests that the reduced GABA uptake activity can at least partially be attributed to a reduced apparent affinity of GAT1 for extracellular  $Na^+$  and slowed kinetics of the GABA transport cycle.

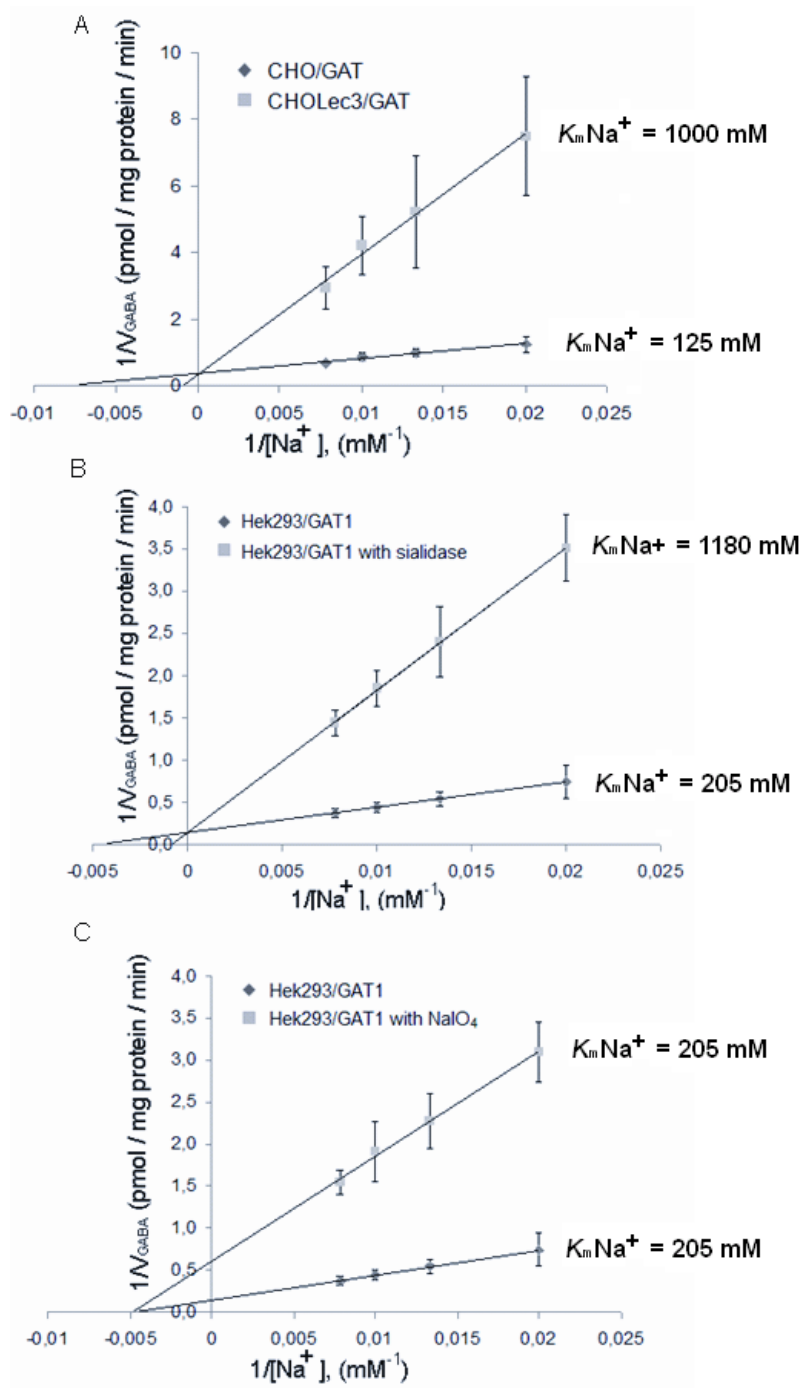


**Figure 3.13 Kinetic analysis of GABA uptake by GAT1/GFP in different cell lines with different  $\text{Na}^+$  concentrations.** GABA uptake assays were performed with different  $\text{Na}^+$  concentrations in CHO and CHO Lec3 transfectants, as well as Hek293 transfectants pre-incubated with and without sialidase (1U/mL) or  $\text{NaIO}_4$  (1mM), respectively. (A) The lines represent fits of a Michealis-Menten equation with  $K_m \text{Na}^+$  value of 125 mM and 1000 mM for CHO/GAT1 and CHO Lec3/GAT1 cells, respectively. (B) and (C) The data were fitted with a same  $K_m \text{Na}^+$  value of 205 mM for untreated and  $\text{NaIO}_4$  treated Hek293/GAT1 cells, while 1180 mM for sialidase treated Hek293/GAT1 cells. The values represent the mean  $\pm$  SD of at least three separate experiments.

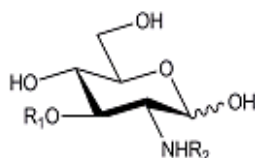
### **3.1.5.3 Oxidation of terminal sialic acid did not change the $K_m$ $\text{Na}^+$ value of GAT1**

Above experiments show that oxidation of terminal sialic acid of GAT1 reduced also significantly the GABA uptake activity of GAT1. However, kinetic analysis show that  $\text{NaIO}_4$  treatment did not change the  $K_m$  value for  $\text{Na}^+$  indicating that the affinity of GAT1 to sodium ion is related to the protein pair, since it is not affected by oxidation of sialic acids (Fig. 3.13 C). The modification with  $\text{NaIO}_4$  remained the negative charge, but removed two terminal exocyclic carbon atoms from membrane sialic acid. This suggests that not only the negative charge, but the structure of sialic acid itself is directly involved in the regulation of the GABA turnover rate of GAT1.

## 3.2 Influence of chemical synthetic compounds and natural occurring on GABA uptake activity of GAT1

### 3.2.1 Effect of *N*-acyl glucosamines on GABA uptake activity

It has been reported that *N*-propionylglucosamine (GlcNProp) and 3-*O*-methyl-*N*-acetylglucosamine (3-*O*-Met-GlcNAc) inhibits *N*-acetylmannosamine kinase *in vitro* (Grunholz *et al.* 1981; Reutter and Bauer 1985; Zeitler *et al.* 1992). Based on the above conclusion that the terminal sialic acids play a crucial role in GABA uptake activity of GAT1, the effect of a series of synthetic *N*-acyl glucosamines (Fig. 3.14) on GABA uptake activity were tested to determine whether they are involved in the sialic acid biosynthesis.



Name	Abbr	R1	R2
<i>N</i> -acetylglucosamine	GlcNAc	H	-CO-CH <sub>3</sub>
<i>N</i> -propionylglucosamine	GlcNProp	H	-CO-CH <sub>2</sub> -CH <sub>3</sub>
<i>N</i> -butanoylglucosamine	GlcNBut	H	-CO-CH <sub>2</sub> -CH <sub>2</sub> -CH <sub>3</sub>
<i>N</i> -hexanoylglucosamine	GlcNHex	H	-CO-CH <sub>2</sub> -CH <sub>2</sub> -CH <sub>2</sub> -CH <sub>2</sub> -CH <sub>3</sub>
<i>N</i> -cyclopropylglucosamine	GlcNCyclo	H	-CO-(CH-CH <sub>2</sub> -CH <sub>2</sub> )
<i>N</i> -glycolyl	GlcNGc	H	-CO-CH <sub>2</sub> -OH
<i>N</i> -formamidoacetylglucosamine	GlcNAc-Formamido	H	-CO-CH <sub>2</sub> -NH-CHO
<i>N</i> -acetamidoacetylglucosamine	GlcNAc-Acetamido	H	-CO-CH <sub>2</sub> -NH-CO-CH <sub>3</sub>
<i>N</i> -(2-benzoic acid)acetylglucosamine	GlcNAc-Benzoic acid	H	-CO-(2-COOH-C <sub>6</sub> H <sub>4</sub> )
3- <i>O</i> -methyl- <i>N</i> -acetylglucosamine	3- <i>O</i> -Met-GlcNAc	OMe	-CO-CH <sub>3</sub>
3- <i>O</i> -methyl- <i>N</i> -propionylglucosamine	3- <i>O</i> -Met-GlcNProp	OMe	-CO-CH <sub>2</sub> -CH <sub>3</sub>
3- <i>O</i> -methyl- <i>N</i> -cyclopropylglucosamine	3- <i>O</i> -Met-GlcNCyclo	OMe	-CO-(CH-CH <sub>2</sub> -CH <sub>2</sub> )

Figure 3.14 Structure of *N*-acyl glucosamines.

In order to determine the appropriate concentration of these sugar analogues (dissolved in PBS), which could not affect the cell growth, the proliferation rate was first measured for further GABA uptake assay. PBS was added and tested as control. ManNAc and ManNProp were tested as reference compounds since they do not change GAT1 activity. Fig. 3.15 A and B showed that GlcNProp, GlcNAc-Benzoic acid (10 mM), GlcNGc and 3-*O*-Met-GlcNProp (10 mM) inhibited cell proliferation slightly, while the other *N*-acyl glucosamines had almost no obvious effect on cell growth. The further GABA uptake assay were performed with the same incubation concentrations.



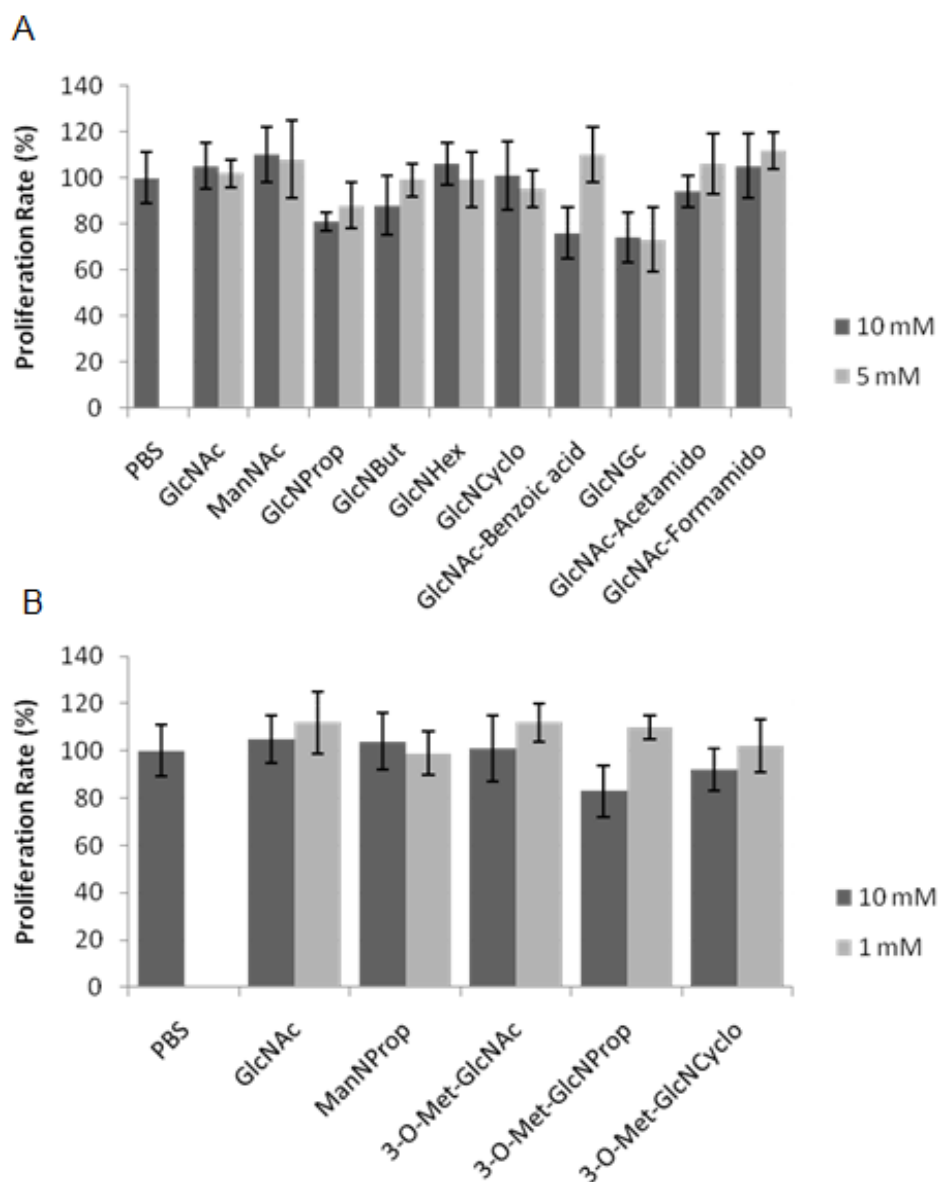


**Figure 3.15 Proliferation of GAT1/GFP transfected Hek293 cells after treatment with different hexosamines.** The Hek293/GAT1 cells were treated with different concentrations of GlcNAc, ManNAc, ManNProp, GlcNProp, GlcNBut, GlcNHex, GlcNCyclo, GlcNAc-Benzoic acid, GlcNGc, GlcNAc-Acetamido or GlcNAc-Formamido (10 and 5 mM, A), 3-O-Met-GlcNAc, 3-O-Met-GlcNProp or 3-O-Met-GlcNCyclo (10 and 1 mM, B) dissolved in PBS and PBS was used as control. After treatment for 72 h, proliferation rate were measured by Alamar Blue Assay. Results present means  $\pm$  SD of at least three separate experiments.

As shown in Fig. 3.16, GlcNAc, ManNProp, GlcNBut, GlcNAc-benzoic acid, 3-O-Met-GlcNProp and 3-O-Met-GlcNCyclo had no apparent effect on the GABA uptake activity of Hek293/GAT1 transfectants after treatment with these analogues. GlcNGc and

GlcNAc-formamido had also slightly influence on GABA uptake activity at a concentration of 10 mM, while the GABA uptake activities were increased to 156% and 135% at a concentration of 5 mM, respectively. At a concentration of 10 mM the GABA uptake activities were reduced to 54%, 63%, 63%, 67% and 53% by the treatment of GlcNProp, GlcNHex, GlcNCyclo, GlcNAc-acetamido and 3-*O*-Met-GlcNAc, respectively.

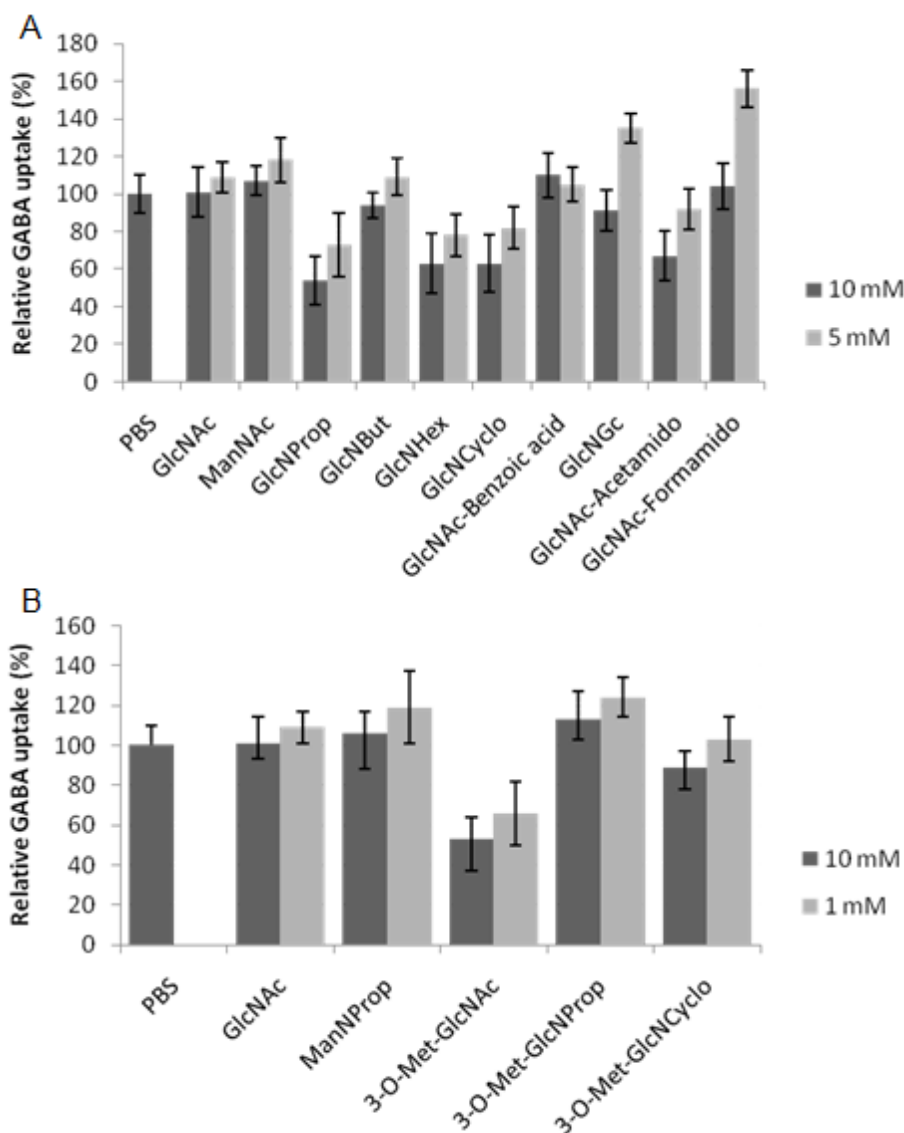


**Figure 3.16 Determination of GABA uptake activity of GAT1/GFP in CHO and Hek293 cells after treatment with different hexosamines.** The Hek293/GAT1 cells were treated with different concentrations of GlcNAc, ManNProp, GlcNProp, GlcNBut, GlcNHex, GlcNCyclo, GlcNAc-benzoic acid, GlcNGc, GlcNAc-acetamido, GlcNAc-formamido (10 and 5 mM, A), 3-*O*-Met-GlcNAc, 3-*O*-Met-GlcNProp or 3-*O*-Met-GlcNCyclo (10 and 1 mM, B) dissolved in PBS and PBS was used as control. After treatment for 72 h,

GABA uptake assay were then performed. GABA uptake activity values were normalized to the total protein amount. The value of GABA uptake by transfected Hek293 cells treated with PBS was set at 100%. All other values were expressed relative to this value. The values represent the mean  $\pm$  SD of at least three separate experiments.

In order to study the following mechanism, quantitative measurements were performed after treatment with different concentrations of GlcNProp, GlcNHex, GlcNCyclo, GlcNAc-Acetamido and 3-*O*-Met-GlcNAc for 72 h. Aliquots of treated Hek293 transfectants were used for determination of both GAT1 protein amounts and sialic acid concentrations. Fig. 3.17 shows that the expression of GAT1/GFP protein and the terminal  $\alpha$ 2,3-linked sialic acid of GAT1 after treatment of GlcNProp (A), GlcNCyclo (B), GlcNHex (C), 3-*O*-Met-GlcNAc (D) and GlcNAc-Acetamido (E). The GAT1/GFP protein bands were indicated with arrows. It can be seen in Fig. 3.17 A, B, C and E that after treatment with these *N*-acyl glucosamines, the GAT1/GFP protein was intended to form the molecules containing *N*-glycans of with different extents, meanwhile, the concentration of terminal sialic acid was reduced, indicating their effect on *N*-glycosylation process, especially terminal trimming of *N*-glycans including sialylation. However, both the size and amount of GAT1/GFP protein was not changed after treated with 3-*O*-Met-GlcNAc, while only the concentration of terminal sialic acid was reduced as shown in Fig. 3.17 D, suggesting that 3-*O*-Met-GlcNAc has an inhibitory effect on sialic acid biosynthesis or sialylation of glycoproteins. After normalized to the amount of GAT1/GFP protein, as depicted in Fig. 3.17 F, the concentration of terminal sialic acid of GAT1/GFP protein in Hek293 cells was reduced to 57% and 79% by 10 and 5 mM GlcNProp, 72% and 82% by 10 and 5 mM GlcNCyclo, 71% and 81% by 10 and 5 mM GlcNHex, 66.8% by 10 mM 3-*O*-Met-GlcNAc and 56% by 10 mM GlcNAc-Acetamido, respectively. In comparison with GlcNProp, the hexanoyl and cyclopropylcarbox groups hold less inhibitory effects on GABA uptake activity and *N*-glycan trimming, whereas the acetamidoacetyl group remained the inhibitory effect on GAT1 activity indicating an unknown mechanism of the interaction between this structure and its targets. It suggests that GlcNProp, GlcNCyclo, GlcNHex and GlcNAc-Acetamido could be inhibitors of terminal trimming of *N*-glycans including sialylation, while 3-*O*-Met-GlcNAc could be an inhibitor of sialic acid biosynthesis or sialylation of glycoproteins. These results demonstrate a correlation between the GABA uptake activity and the terminal sialic acid of GAT1/GFP, which confirmed our previous findings.

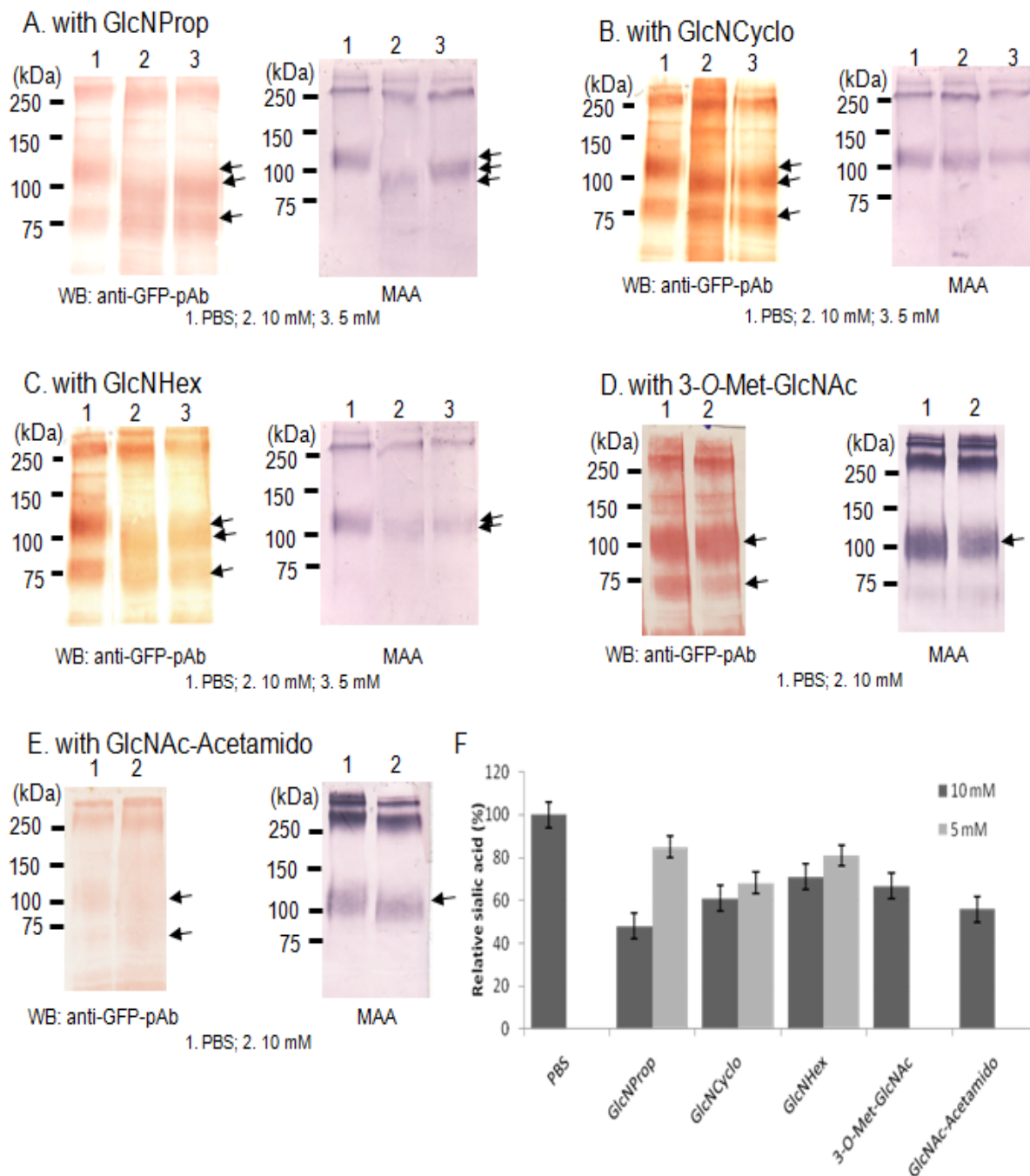


**Figure 3.17 Quantitative analysis of influence of hexosamines on GAT1/GFP protein in Hek293 cells.**

(A)-(E) Hek293 stable transfectants were treated with GlcNProp (10 and 5 mM), GlcNPent (10 and 5 mM), GlcNCyclo (10 and 5 mM), 3-O-Met-GlcNAc (10 mM) and GlcNAc-Acetamido (10 mM) for 72 h. After immunoprecipitation, aliquots were analyzed by SDS/PAGE (7.5%) with western blotting and lectin staining. GAT1/GFP fusion protein was indicated with arrows. (F) Quantification of sialic acid concentrations of GAT1/GFP in Hek293 cells with Quantity One software (Bio-rad). The sialic acid concentration values were normalized to the amount of total GAT1 protein. And the value in Hek293/GAT1 cells treated with PBS was set at 100%. All other values were expressed relative to these values.

### 3.2.2 Effect of naturally occurring compounds on GABA uptake activity

LZ acid, LZ-2 and LZ-3 are the fractions isolated from crude extract of fruit bodies of *Ganoderma lucidum*. Resveratrol is one of the active compounds isolated from *Polygonum cuspidatum*. In order to search potent inhibitors of GAT1 protein, the effect of the fungal crude extracts (LZ acid, LZ-2 and LZ-3) and resveratrol on GABA transport activities of CHO/GAT1 cells were measured. The GABA uptake assay was performed by incubating the GAT1/GFP transfectants with flux buffer containing the testing samples. It was found (Fig. 3.18) that LZ acid (100 µg/ml) activated the GABA uptake activity of GAT1/ GFP by 50% and LZ-2 (200 µg/ml) also increased the GABA uptake activity of GAT1/GFP to 128%. While GABA transport activity of GAT1/GFP protein was inhibited to 70% in the presence of resveratrol (40 µM).

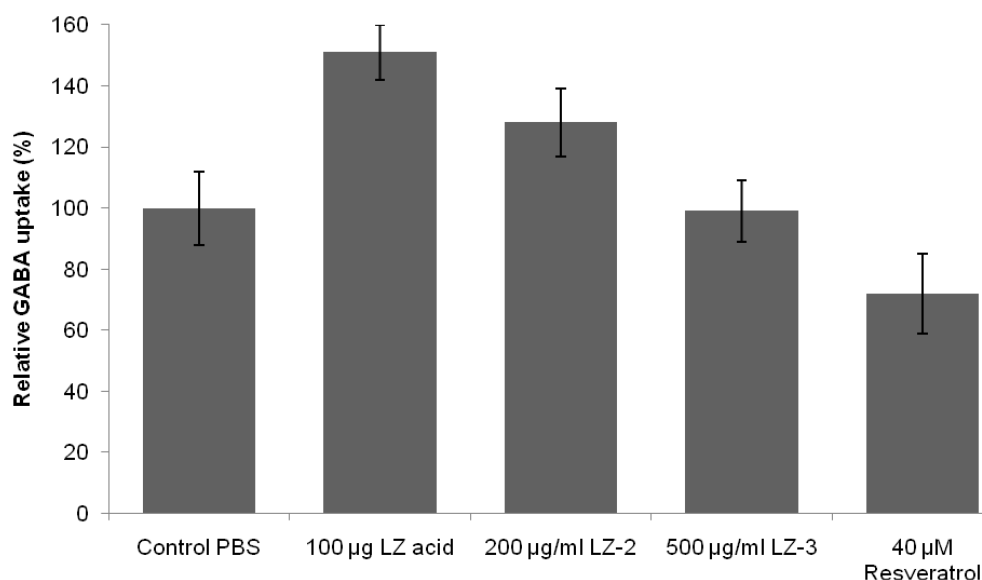


**Figure 3.18. Effect of *G. Lucidum* fractions and resveratrol on GABA uptake of GAT1.** The GABA transport activities of CHO/GAT1 cells were determined in the presence of *G. Lucidum* fractions (LZ acid, LZ-2 and LZ-3) and resveratrol. The value of CHO/GAT1 cells with PBS was set at 100%. All other values were expressed relative to this value. The values represent the mean  $\pm$  SD of at least three separate experiments.

Furthermore, the inhibition of resveratrol on GABA uptake activity of GAT1/GFP protein was measured with different concentrations resveratrol. As shown in Fig. 3.19, the relative GABA uptake rate of GAT1/GFP in CHO cells was inhibited by resveratrol in a dose-dependent manner. In the presence of 0.05, 0.1, 0.5 and 1 mM resveratrol, the

GABA uptake activities of GAT1 were reduced to 61%, 54%, 38% and 20%, respectively. The  $IC_{50}$  of resveratrol is about 100  $\mu$ M.

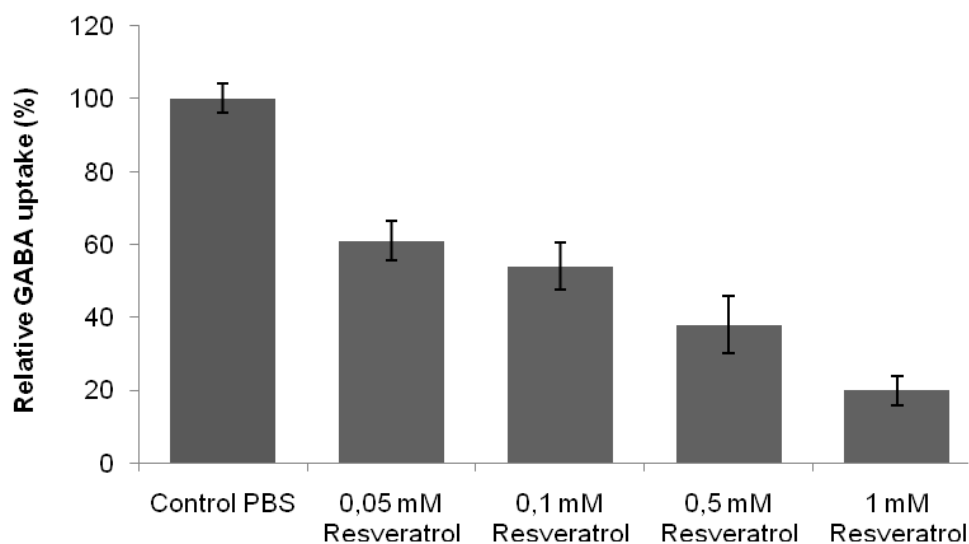


**Figure 3.19 Inhibition by resveratrol of GABA uptake by the GAT1/GFP protein.** The GABA transport activities of CHO/GAT1 cells were determined in the presence of 0.05, 0.1, 0.5 and 1 mM resveratrol by GABA uptake assay. The value of CHO/GAT1 cells measured with PBS was set at 100%. All other values were expressed relative to this value. The values represent the mean  $\pm$  SD of at least three separate experiments.

In order to provide an insight into the mechanism of inhibition of GABA transport by resveratrol, kinetic parameters of GABA transport were determined for the CHO/GAT1 cells with PBS (as control) and resveratrol (100  $\mu$ M in PBS). The kinetic constants were calculated from the initial rates of uptake using the double reciprocal plot analysis (Fig. 3.20). It can be seen that incubation with resveratrol decreased the  $V_{max}$ GABA values without affecting the  $K_m$ GABA value. The  $K_m$ GABA value of CHO/GAT1 cells incubated with PBS (4.6  $\mu$ M) showed in the same range as that of cells incubated with 100  $\mu$ M resveratrol (4.8  $\mu$ M). These suggest that resveratrol inhibits the GABA uptake of GAT1 in a non-competitive manner.

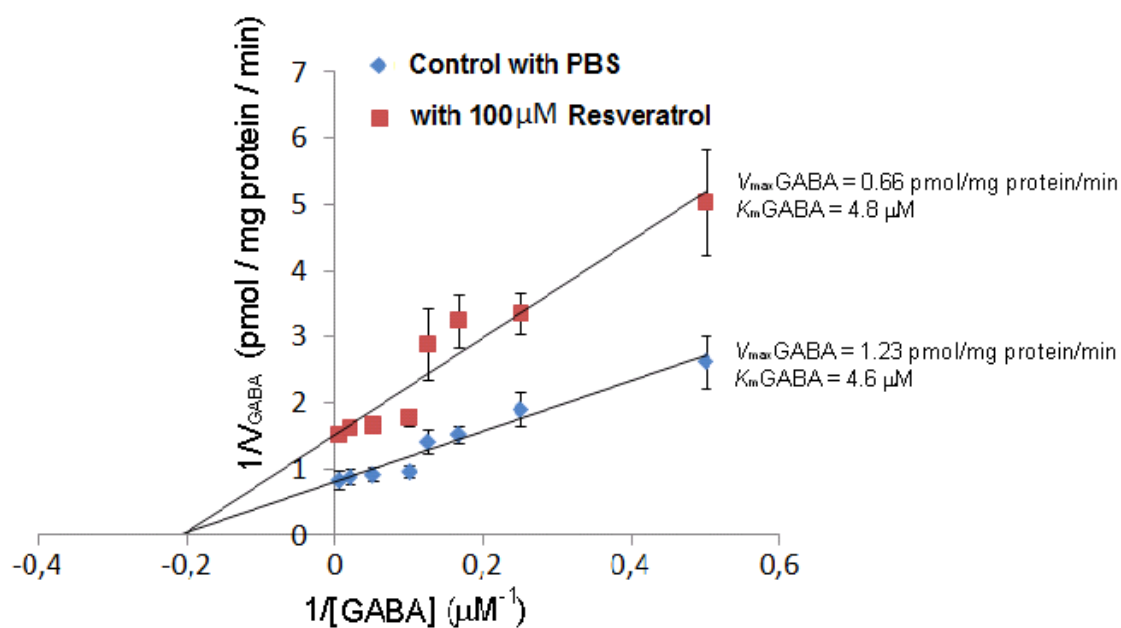


**Figure 3.20 Kinetic study of effect of resveratrol on GABA uptake of GAT1/GFP protein in CHO transfectants.** The uptake measurements were performed with CHO/GAT1 cells in the presence of PBS and resveratrol (100  $\mu\text{M}$ ). And different GABA concentrations 200, 50, 20, 10, 8, 6, 4 and 2 mM were utilized. The results are presented as double-reciprocal plots of the initial rates of uptake versus the GABA concentration. Kinetic constants were as follows:  $K_{\text{m GABA}}$  4.6 and 4.8  $\mu\text{M}$ ;  $V_{\text{max GABA}}$  1.23 and 0,66 pmol/mg protein/min for CHO/GAT1 cells in the presence of PBS and resveratrol (100  $\mu\text{M}$ ), respectively. The values represent the mean  $\pm$  SD of at least three separate experiments.

### **3.3. Purification of GAT1/GFP fusion protein**

In order to clarify the three-dimensional structure of proteins, high amount of the purified protein are needed for general methods such as nuclear magnetic resonance (NMR) and crystallography. The natural abundance of most membrane proteins is usually too low to isolate sufficient material for functional and structural studies. In this work the GAT1/GFP fusion protein was over-expressed in different expression systems for purification and thus for further structural analysis.

#### **3.3.1 Purification of GAT1/GFP fusion protein in Hek293 cells**

The overexpression of GAT1/GFP fusion protein in Hek293 cells are indicated in section 3.1.1. To obtain homogenous GAT1/GFP fusion protein, 15-20 dishes (150 mm) of Hek293 cells were cultured and lysed in solubilization buffer containing detergent 2% *n*-dodecyl- $\beta$ -D-maltoside for isolation.

##### **3.3.1.1 Isolation of GAT1/GFP fusion protein in Hek293 cells by ion exchange chromatography**

One isolation method of the GAT1/GFP fusion protein in Hek293 was ion exchange chromatography. Separation is obtained since different substances have different extents of interaction with the ion exchanger due to differences in their charges, charge densities and distribution of charge on their surfaces. The pI value of GAT1/GFP fusion protein was calculated as 6.8. The pH value of start buffer was adjusted to 7.8 to make GAT1/GFP fusion protein carrying negative charge for the anion column. All buffers contained detergent *n*-octyl- $\beta$ -D-glucopyranoside to prevent aggregation of target protein. After equilibration with start buffer, the cell lysate was loaded onto the HiTrap QFF anion exchange column (5 ml). Followed by wash again with start buffer, the column was eluted with a continuous salt gradient from 0 to 500 mM of NaCl and the bound proteins were eluted from the point of 350 mM NaCl and formed two peaks as elution profile showed (Fig. 3.21 A). The fractions were analysed by SDS/PAGE (7.5%) with western blotting (Fig. 3.21 B). Certain amount of GAT1/GFP fusion protein was detected mainly in peak 1 but not in peak 2 by western blotting as shown in Fig. 3.21 B. The fractions collected from the wash stage also contained GAT1/GFP protein since there was still GAT1/GFP protein did not combine with the column. However, the purity of these fractions checked by silver staining (results not shown) was very low. This method could not be suitable for the primary purification of GAT1/GFP from cell lysate.



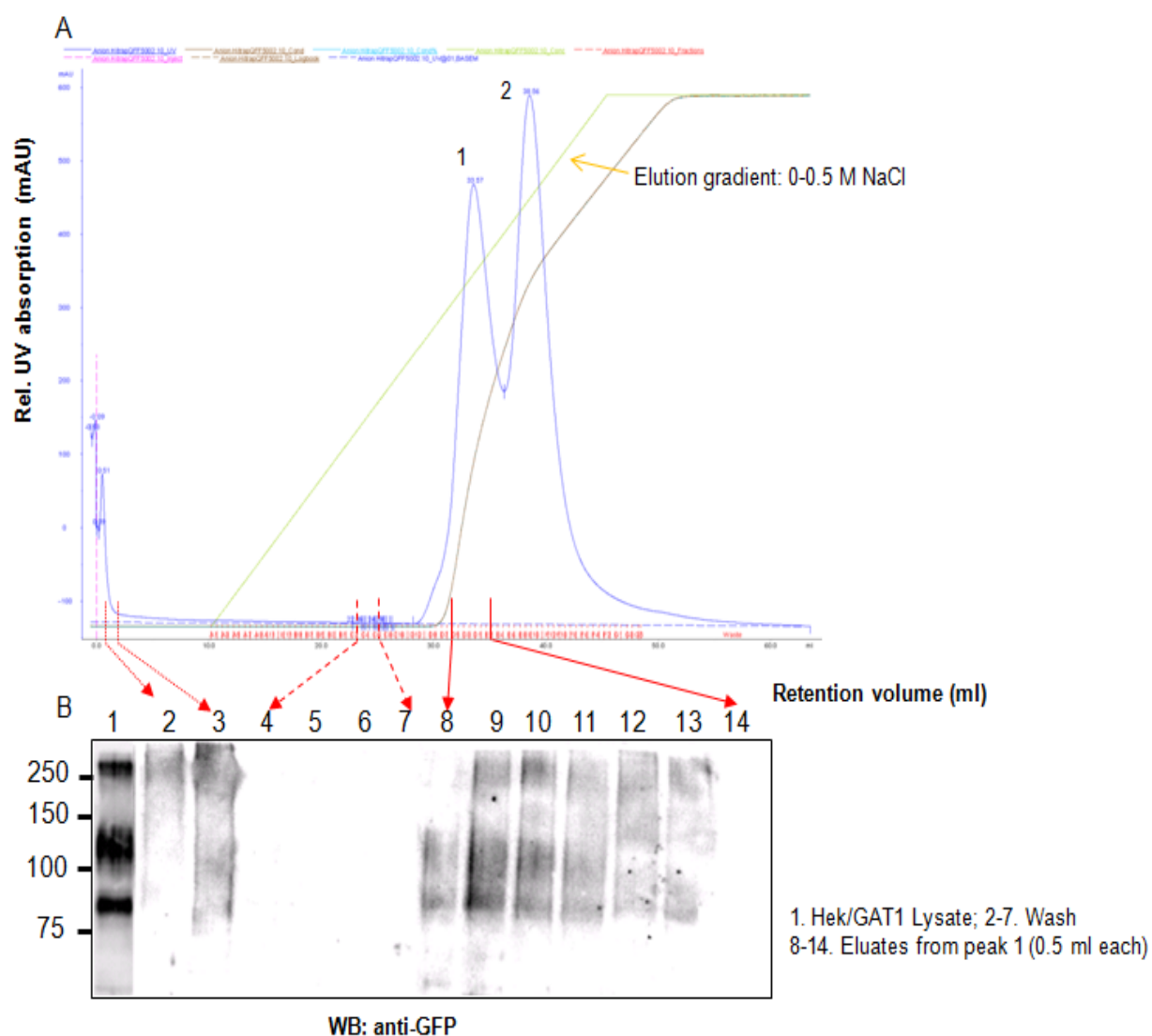


**Figure 3.21 Isolation of GAT1/GFP fusion protein by ion exchange chromatography.** (A) Elution profile of GAT1/GFP fusion protein from HiTrap QFF anion exchange column. Most proteins were eluted from the salt concentration reached 350 mM and formed two main peaks. (B) Analysis of fractions after ion exchange column by SDS/PAGE (7.5%) with western blotting.

### 3.3.1.2 Isolation of GAT1/GFP fusion protein in Hek293 cells by lectin-affinity chromatography

Another method to isolate GAT1/GFP fusion protein in Hek293 cells was lectin-affinity chromatography. GAT1/GFP is a glycoprotein with three conserved *N*-glycosylation sites and the terminal residues were determined as sialic acids. The wheat germ agglutinin (originated from *Triticum vulgare*) conjugated agarose was utilized for the column since this lectin selectively binds to *N*-acetyl glucosamine (GlcNAc) groups and to sialic acid.

The eluates were analyzed by SDS/PAGE (7.5%) with Western blotting as shown in Fig. 3.22. It can be seen only GAT1/GFP fusion protein with matured *N*-glycosylation but not the protein with *N*-glycans of mannosidic type could bind to WGA-agarose. And GAT1/GFP fusion protein with matured *N*-glycosylation could be detected mainly in the first several eluted fractions. But there were also a significant loss of target protein and the purity of these fractions checked by silver staining (results are not shown) was not high. It showed that this method was suitable for the relatively pure and large amount of samples.

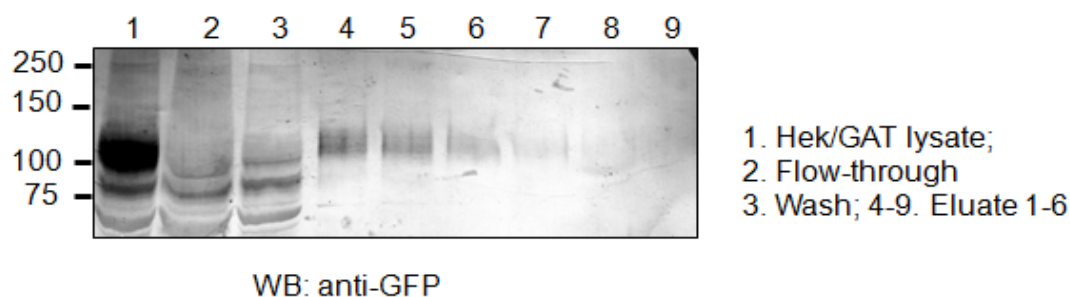


**Figure 3.22 Isolation of GAT1/GFP fusion protein by lectin affinity chromatography.** SDS/PAGE (7.5%) with western blotting of eluted fractions from WGA-agarose column.

### 3.3.1.3 Purification of GAT1/GFP fusion protein in Hek293 cells by immuno-affinity chromatography and Size-exclusion fast protein liquid chromatography (SE-FPLC)

The interaction of antigen-antibody complexes is stronger than that of lectin-carbohydrate complexes. Thus GAT1 recombinant protein with C-terminal green fluorescent protein (GFP)-tag was purified by immuno-affinity chromatography with specific anti-GFP monoclonal antibody. The eluted fractions were pooled and concentrated by vivaspin concentrators. And then a further purification was performed by SE-FPLC (also called gel filtration) but resulted in low yield of the protein.

#### 3.3.1.3.1 Purification of monoclonal and polyclonal GFP antibody

The polyclonal antibody against GFP was collected from serum of rabbits immunized with GFP protein and monoclonal antibody against GFP was purified from cell culture supernatants of monoclonal anti-GFP of hybridoma cells. Affi-Gel<sup>®</sup> Protein A MAPS<sup>®</sup> II Kit was used to purify IgG. For further purification SE-FPLC was performed. Coomassie blue-stained SDS/PAGE (7.5%) (Fig. 3.23 A and B) showed two main bands of around 50 and 25 kDa (indicated with arrows), which corresponded to heavy chains and light chains of IgGs, respectively. The elution profiles of both polyclonal and monoclonal

antibodies from SE-FPLC were shown in Fig. 3.23 C and D. The main peaks appearing at 14.9 - 15.3 ml corresponded to polyclonal and monoclonal GFP antibodies of 105 – 150 kDa. The purified monoclonal GFP antibody was then used for the immuno-affinity column to purify GAT1/GFP fusion protein by being immobilized onto Affi-gel 10 protein-A-sepharose.

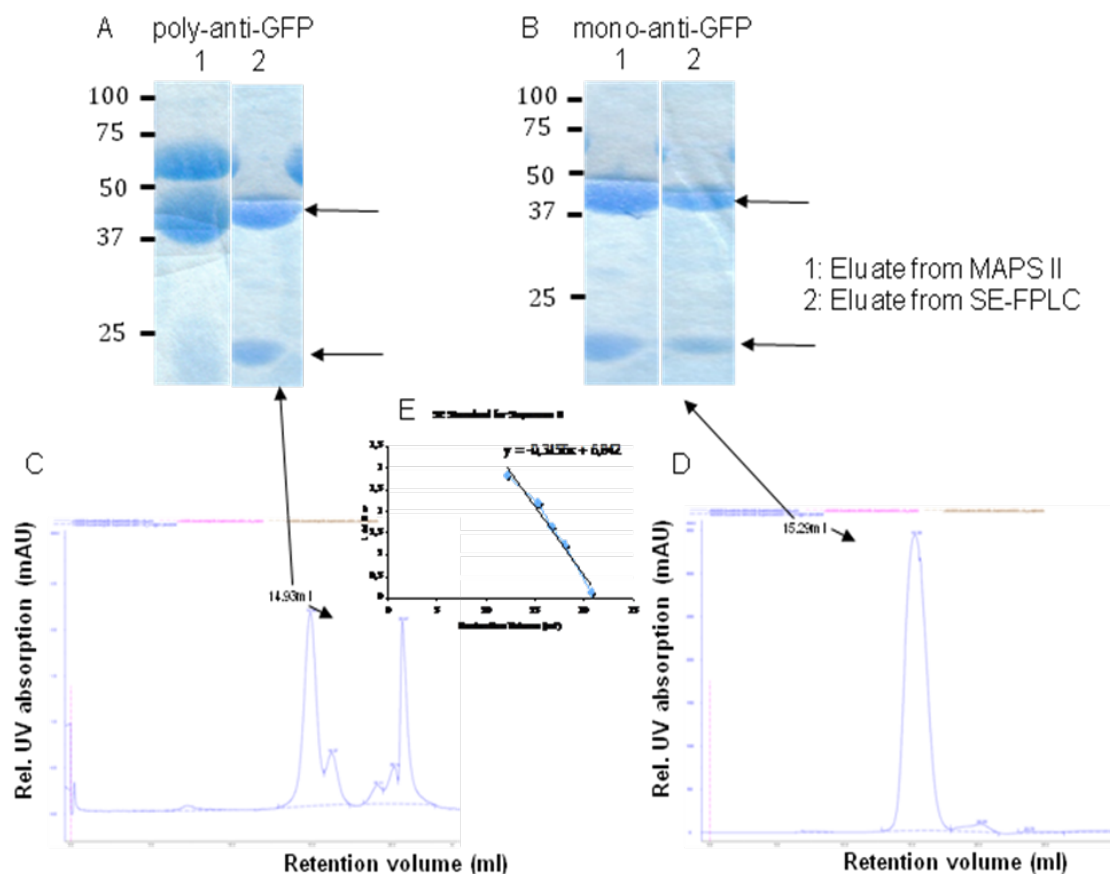


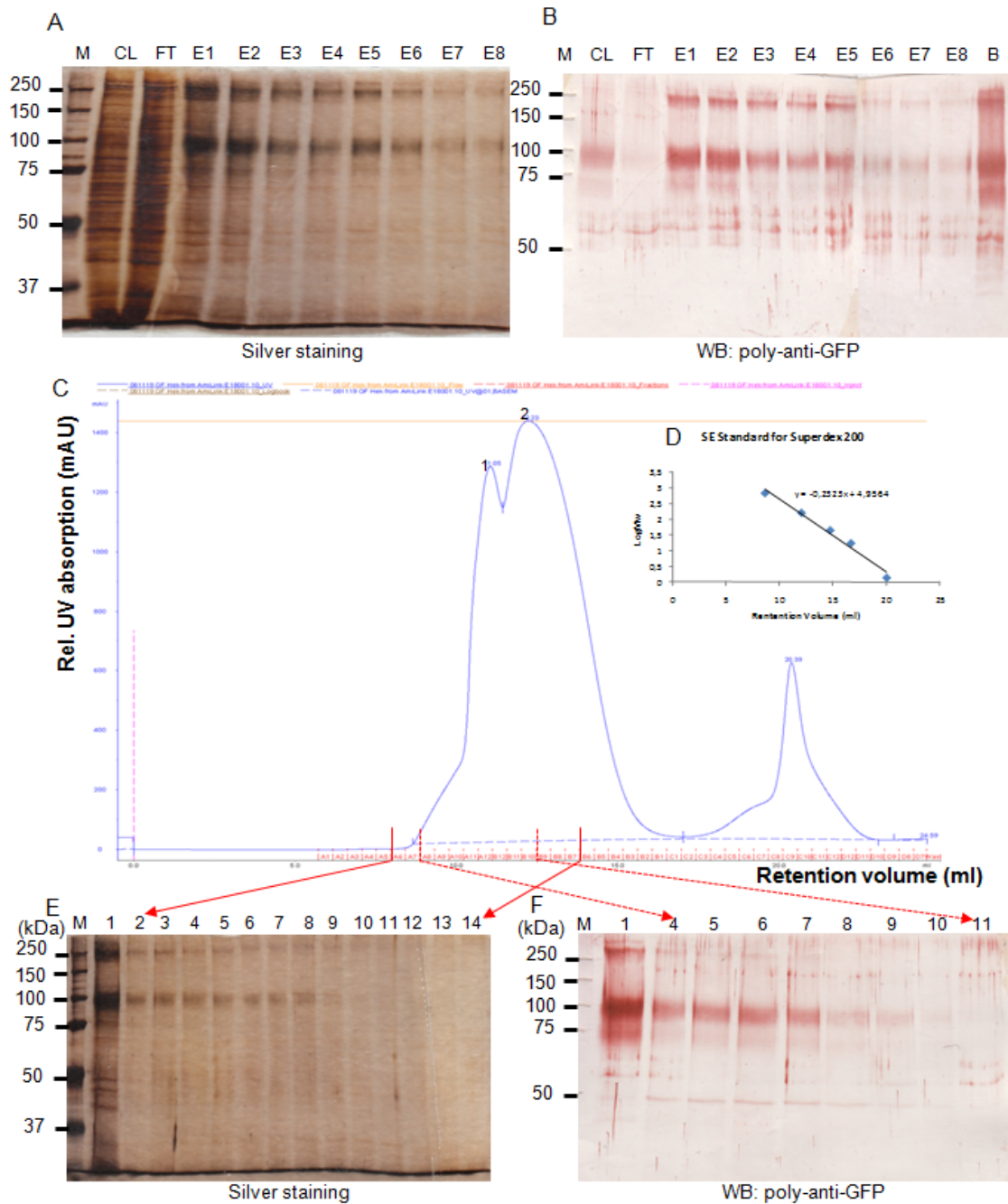
**Figure 3.23 Purity check of fractions of GFP antibodies separated by Affi-Gel Protein A MAPS system and SE-FPLC.** (A) (B) Coomassie blue-stained SDS/PAGE (7.5%) of IgGs from polyclonal and monoclonal GFP antibodies. The heavy chains and light chains of IgG were indicated with arrows. (C) (D) Elution profile of polyclonal and monoclonal GFP antibodies after SE-FPLC. (E) The standard linear regression curve of Superose 6<sup>TM</sup> column was generated by plotting the log of the molecular mass of different calibration proteins against their elution volume. Standard proteins are thyroglobulin (670 kDa), aldolase (158 kDa), ovalbumin (44 kDa), cytochrome c (17 kDa) and cobalamin (1.35 kDa), respectively.

### 3.3.1.3.2 Purification of GAT1/GFP fusion protein in Hek293 cells by immuno-affinity chromatography and SE-FPLC

After immuno-affinity chromatography the eluates were analyzed by SDS/PAGE (7.5%) with silver staining and Western blotting (Fig. 3.24 A and B). We can see that GAT1/GFP

protein could be eluted with 50 mM diethylamine (pH11.0) but not completely and certain amount of GAT1/GFP protein was still on the column beads. The eluates were neutralized with 1/10 (v/v) 0.5 M NaH<sub>2</sub>PO<sub>4</sub> and then 0.5% (w/v) *n*-dodecyl-β-D-maltoside was added to keep the protein from forming aggregates. The eluates containing GAT1/GFP proteins were pooled and concentrated on Vivaspin concentrators.

A further isolation of GAT1/GFP was performed by size exclusion chromatography on a Superdex 200 column with 0.7% (w/v) *n*-octyl-β-D-glucopyranoside. The elution profile of GAT1/GFP in Hek293 cells was shown in Fig. 3.24 C. In comparison with the standard proteins (Fig. 3.24 D), two main peaks (1 and 2) corresponded to 245 kDa and 130 kDa, respectively. The fractions (400 μl per fraction) from 9.3 to 13.8 ml after SE-FPLC were further analyzed by SDS-PAGE (20 μl per fraction) and western blotting (Fig. 3.24 E and F). It is indicated that peak 1, which should correspond to a dimeric GAT1/GFP with a molecular weight of 245 kDa, appeared at 9-12 ml (Lane 2-9). Peak 2 contains no clear protein bands, which might be due to a low concentration of GAT1/GFP protein in these fractions. However, fractions corresponding to the GAT1/GFP protein after SE-FPLC were not for further structural analysis since the proteins with different *N*-glycosylation were still mixed and could not be separated completely.



M: Standard Marker; CL: Cell Lysate; FT: Flow through; E1-E8: Eluates1-8; B: Beads  
 1: Concentrated sample of eluates from immuno-affinity column;  
 2-14: SE-FPLC fractions from 9.3 to 13.8 ml

**Figure 3.24 Purification of GAT1/GFP fusion protein in Hek293 cells by immuno-affinity column and SE-FPLC.** (A) (B) Silver-staining and Western blotting of SDS/PAGE (7.5%) of eluted fractions after immuno-affinity column. (C) Elution profile of GAT1/GFP after SE-FPLC on Superdex 200<sup>TM</sup> column. (D) The standard linear regression curve of Superdex 200<sup>TM</sup> column was generated by plotting the log of the molecular mass of different calibration proteins against their elution volume. (E) (F) Silver-staining and Western blotting analysis of SDS/PAGE (7.5%) of eluted fractions (peak 1 and 2) after SE-FPLC.

### 3.3.2 Expression, characterization and purification of GAT1/GFP fusion protein in *Sf9* cells with BAC-TO-BAC<sup>®</sup>-Baculovirus expression system

#### 3.3.2.1 Cloning, Preparation and analysis of GAT1/GFP recombinant baculovirus

The GAT1/GFP recombinant cDNA was cloned in the pFastBac1 and pFastBacHTa vectors (Fig. 3.25 A).

After transfection of these bacmids, the primary recombinant baculovirus stock was harvested and used for viral amplification. In order to verify the constructs, the Bacmid DNA content of the virus was purified with the “Zymoclean DNA clean and concentration kit” and used as template for PCR with the M13 amplification primers. Bacmid transposed with GAT1/GFP in pFastBac1 vector contains about 5000 bp and in pFastBacHTa vector contains about 5130 bp. As could be detected on agarose gel electrophoresis (Fig. 3. 25 B), the GAT1/GFP and GAT1/GFP/6xHis DNA constructs were stable and correct for use in expression of the fusion protein in insect cells.

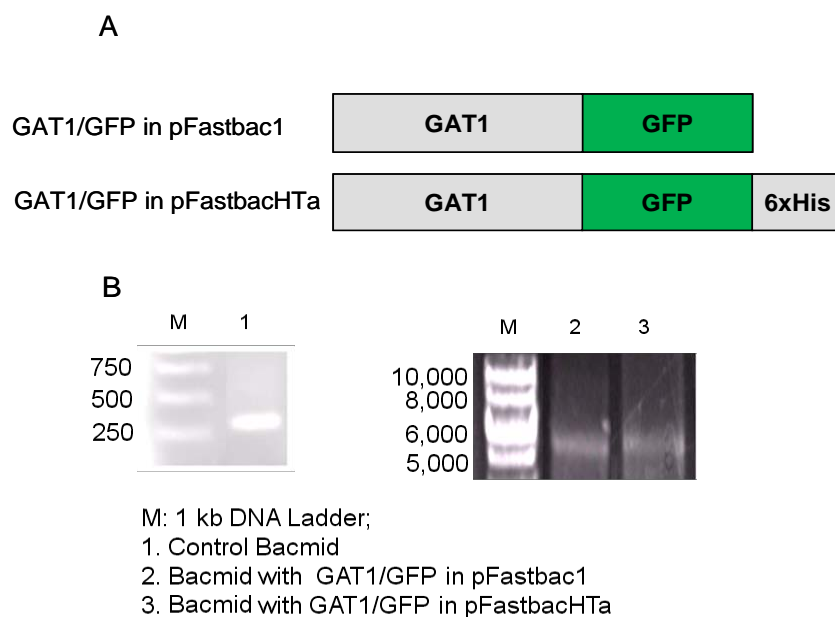


**Figure 3.25 Analysis of GAT1/GFP recombinant baculovirus.** (A) Schematic representation of the GAT1/GFP fusion protein constructs cloned into the pFastBac1 and pFastBacHTa vectors. (B) PCR-analysis of recombinant baculovirus. Recombinant baculoviruses for the two constructs were verified by PCR for the presence of the GAT1/GFP cDNA with M13 amplification primers.

#### 3.3.2.2 Expression and characterization of GAT1/GFP fusion protein in insect cells

GAT1/GFP and GAT1/GFP/6x His recombinant protein was expressed in *Sf9* cells by viral infection for 72 h. However, GAT1/GFP/6x His could not be detected with anti-His

antibody (result not shown). Then only GAT1/GFP fusion protein was further characterized and thus expressed for purification. After 72 h post-infection, *Sf9* cells with green fluorescence were controlled by flow cytometry (Fig. 3.26 A) as well as fluorescence microscopy (Fig. 3.26 B). The expressions of GAT1/GFP in insect cells were further determined by SDS/PAGE followed with Western blotting with either anti-GFP pAb (Fig. 3.26 C) or anti-GAT1 pAb (Fig. 3.26 D) and silver staining (Fig. 3.26 E) after immunoprecipitation with anti-GFP mAb. In infected *Sf9* cells, the the GAT1/GFP fusion protein showed two main bands in SDS/PAGE (7.5%), as indicated with arrows, the monomeric form running as a main band of about 75 kDa. This band can only bind strongly with *Galanthus nivalis* Agglutinin (GNA, digoxigenin-conjugated lectin) (Fig. 3.26 F) indicating the predominance of the pausi-mannose structure in insect cells. The band of about 250 kDa may represent an oligomer form or a protein aggregate which was then further identified.

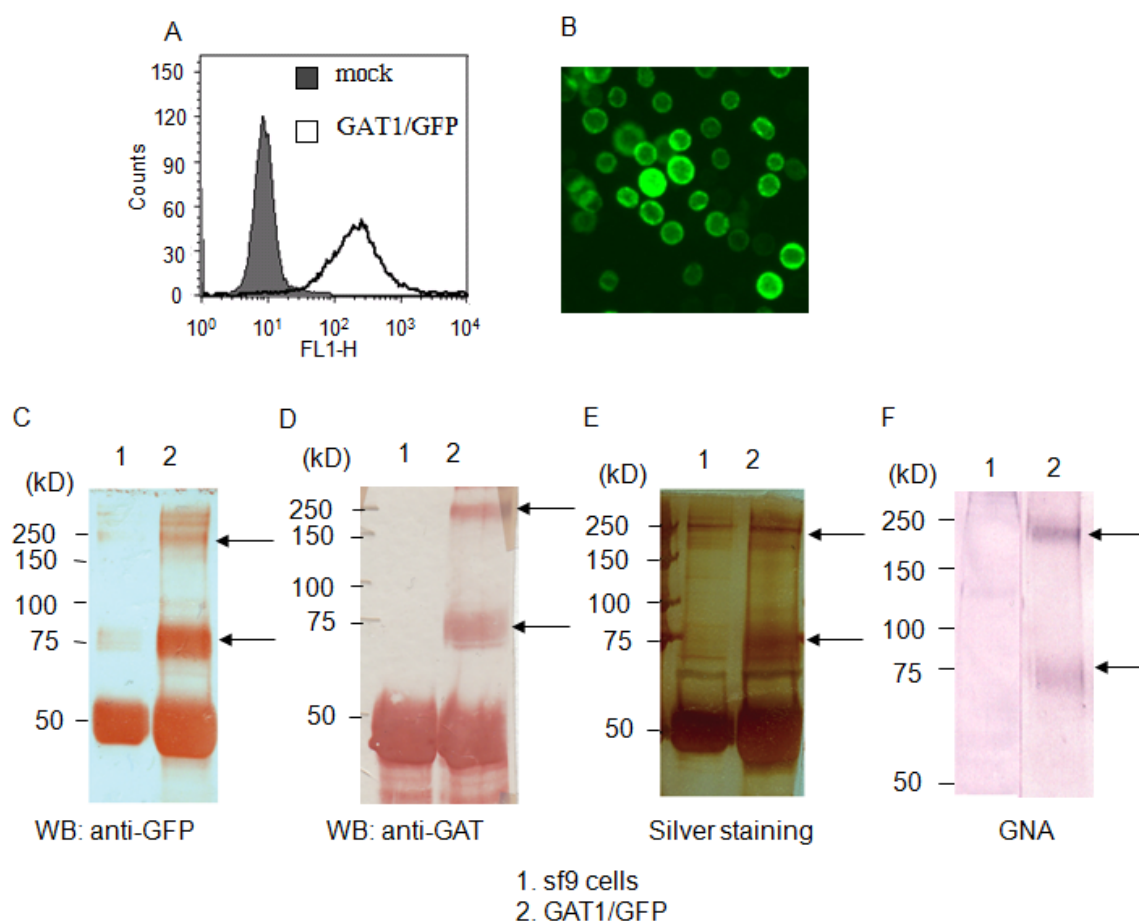


**Figure 3.26 Expression of GFP-tagged GAT1 in infected insect cells.** (A) Flow cytometry analysis of GAT1/GFP in *Sf9* cells. (B) Fluorescence microscopy of infected *Sf9* cells. The fluorescence of GFP in GAT1/GFP-fusion protein was detected. The solubilized protein of infected *Sf9* cells were subjected to immunoprecipitation with anti-GFP mAb IgG and then analyzed by SDS/PAGE (7.5%) and

immunoblotting. (C) and (D) Western blotting analysis of GAT1/GFP from un-infected and infected *Sf9* cells with anti-GFP pAb or anti-GAT1 pAb. (E) Silver staining of GAT1/GFP from infected *Sf9* cells. (F) GNA staining of GAT1/GFP from infected *Sf9* cells. The main bands which represented GAT1/GFP fusion protein were indicated with arrows. *Sf9* cells (lane 1); GAT1/GFP infected *Sf9* cells (lane 2).

After 72 h post-infection, GABA uptake activity of *Sf9* cells were measured to determine whether GAT1/GFP fusion protein was functionally expressed in Baculovirus system. Fig.3.27 shows that infected *Sf9* cells ( $0.15 \text{ pmol}/10^6 \text{ cells}$ ) had only a little higher GABA uptake activity than that of mock cells ( $0.1 \text{ pmol}/10^6 \text{ cells}$ ). The low GABA uptake activity of GAT1/GFP fusion protein in insect cells should be resulted from the terminal mannose structure on *N*-glycans, which is in agreement with the finding of role of the terminal sialic acid in GABA uptake as described above.

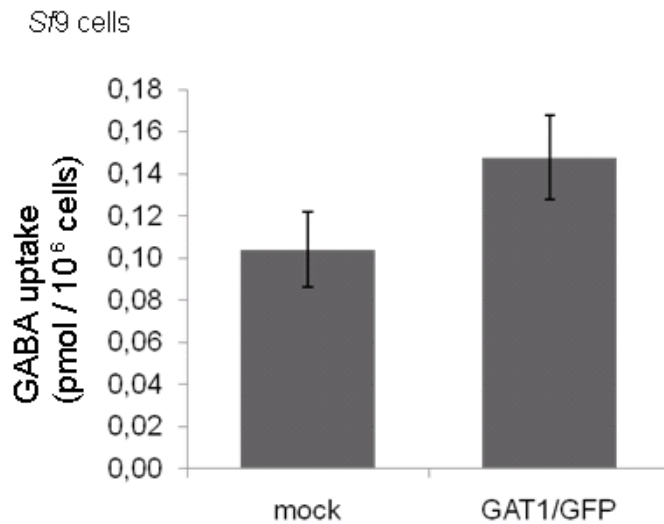


**Figure 3.27 Functional determination of GFP-tagged GAT1 in *Sf9* cells by GABA uptake assay.** The GABA uptake activities were normalized to the total cell number. The values represent the mean  $\pm$  SD of at least three separate experiments.

Since the GABA uptake activity of infected *Sf9* cells was little differentiated with non-infected cells, the characterization of GAT1/GFP fusion protein in *Sf9* cells was necessary. After immunoprecipitation and SDS-PAGE with commassie blue staining, proteins of two bands (a and b indicated in Fig. 3.27 A) were extracted for protein fingerprinting analysis. The proteins were denatured, reduced, alkylated and digested with trypsin and tryptic peptides were either analyzed directly by Matrix-assisted laser desorption/ionization –



Time-of-flight Mass-Spectrometry (MALDI-TOF MS) or guanidinated or then analyzed by MALDI. The labeled peptide peaks (Fig. 3.27 B) showed in mass spectrum were identified as either GAT or GFP by matching the peptides from primary sequence databases with Mascot (<http://www.matrixscience.com/>). And other high peaks were either from keratin (e.g. m/z 1179, 1791, 2383) or trypsin (m/z 2163).

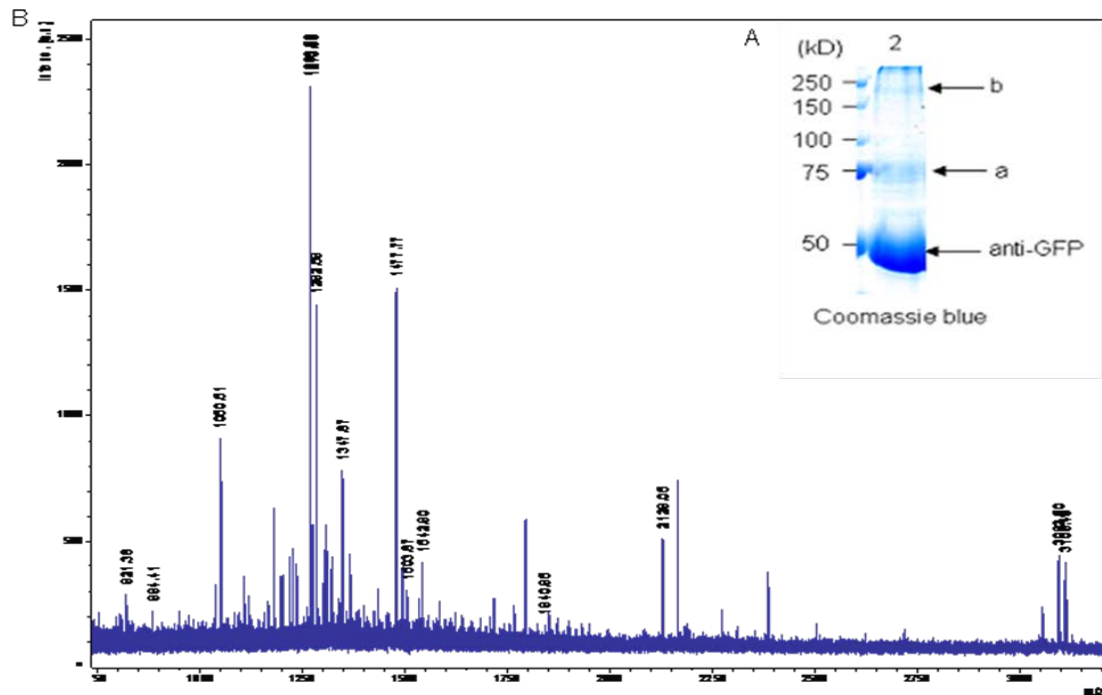


**Figure 3.28 Protein finger printing.** (A) Coomassie blue staining of GAT1/GFP protein from infected *Sf9* cells after immunoprecipitation. Bands a and b (indicated by arrows) were extracted for MALDI-TOF analysis. (B) Mass spectrum of trypsin digest of band a. The peaks labelled were assigned to either GAT or GFP.

After comparison between spectra for bands a and b, both spectra contain the same signals for GAT and GFP for selected peptides, m/z 1266/1282 for GFP (Fig. 3.28 A) and m/z 2128 for GAT (Fig. 3.28 B). The results identified that band b contains GAT1/GFP protein in an oligomeric or aggregated form.

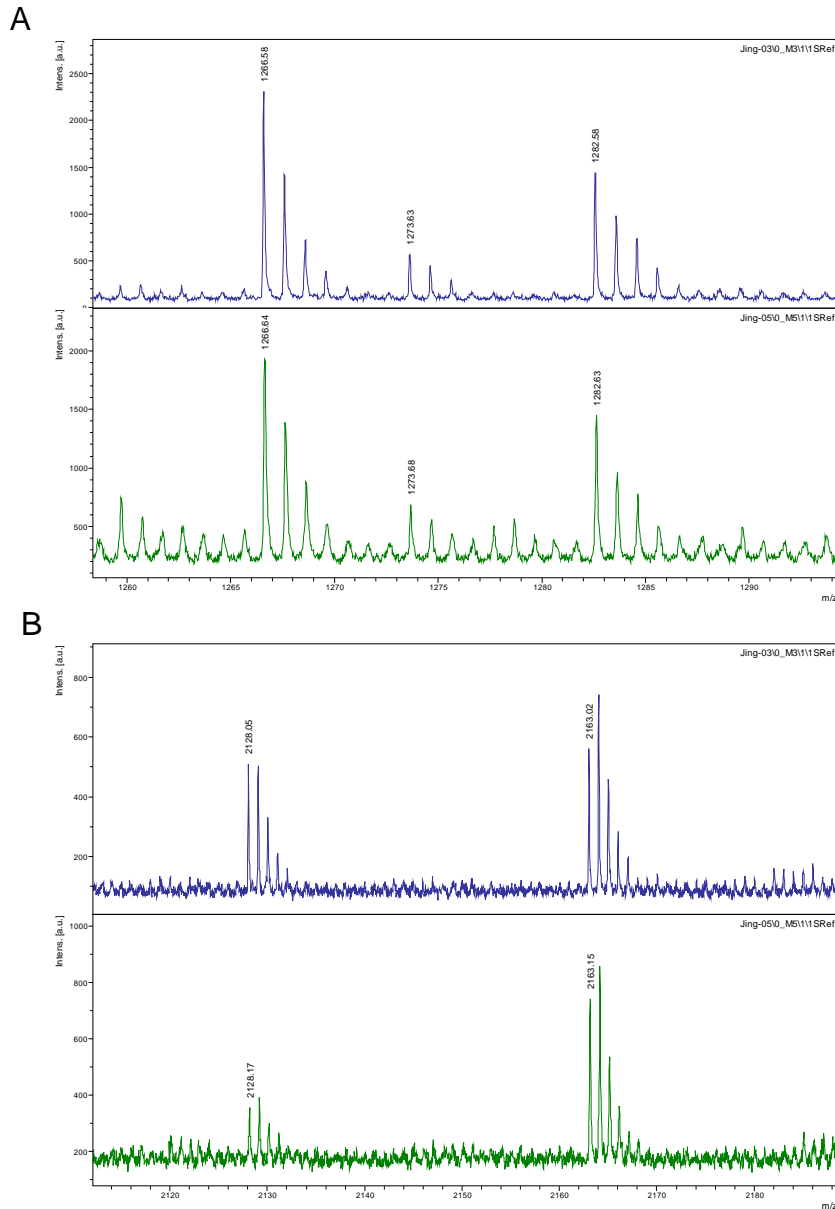


**Figure 3.29** Comparison of mass spectrum of bands a and b. (A) The typical peaks (m/z 1266/1282) for GFP. (B) The typical peak (m/z 2128) for GAT. Blue spectrum: from band a; green spectrum: from band b.

### 3.3.2.3 Isolation of GAT1/GFP fusion protein in insect cells by ion exchange chromatography

Ion exchange chromatography was also tested for the isolation of GAT1/GFP fusion protein in *Sf9* cells. The pH value of start buffer was increased from 7.8 to 8.5 to increase the affinity between GAT1/GFP fusion proteins with the anion column, which may also increase the unspecific protein on the column. And the elution was performed with a continuous salt gradient from 0 to 1 M of NaCl. The bound proteins were eluted from the

point of 680 mM NaCl and formed two peaks as elution profile showed (Fig. 3.29 A). The fractions were analysed by SDS/PAGE with western blotting (Fig. 3.30 B). It is showed that similar results as the isolation of GAT1/GFP in Hek293 cells. Only peak 1 contained certain amount of GAT1/GFP fusion protein after western blotting analysis as showed in Fig. 3.30 B. Similarly, the purity of these fractions checked by silver staining (results not shown) was still low. This method could be used to isolate the relatively pure GAT1/GFP.

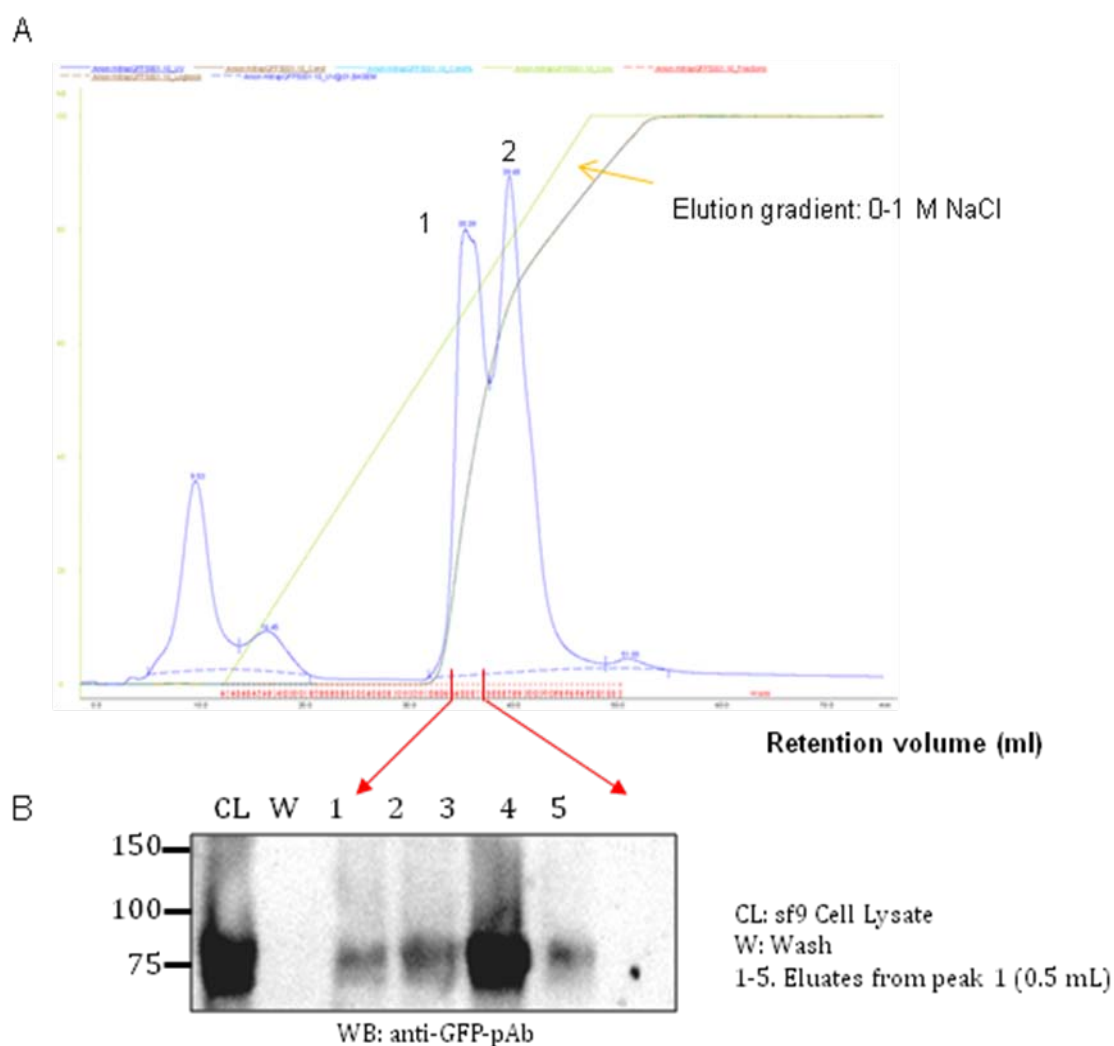


**Figure 3.30 Isolation of GAT1/GFP fusion protein from *Sf9* cells by ion exchange chromatography.** (A) Elution profile of GAT1/GFP fusion protein from *Sf9* cells from HiTrap QFF anion exchange column. Most proteins were eluted from the salt concentration reached 650 mM and formed two main peaks. (B) Analysis of fractions after ion exchange column by SDS/PAGE with western blotting.

### 3.3.2.4 Purification of GAT1/GFP fusion protein in insect cells by immuno-affinity chromatography and SE-FPLC

A two-step purification procedure for GAT1/GFP fusion protein in *Sf9* cells was established as shown in Fig. 3.31. The GAT1/GFP was expressed in *Sf9* cells by viral infection and then was isolated from mAb-GFP conjugated affinity chromatography. Subsequently, partially pure eluted fractions containing GAT1/GFP were pooled and subjected to SE-FPLC with Superdex 200<sup>TM</sup> column to purify homogeneous GAT1/GFP fusion protein.

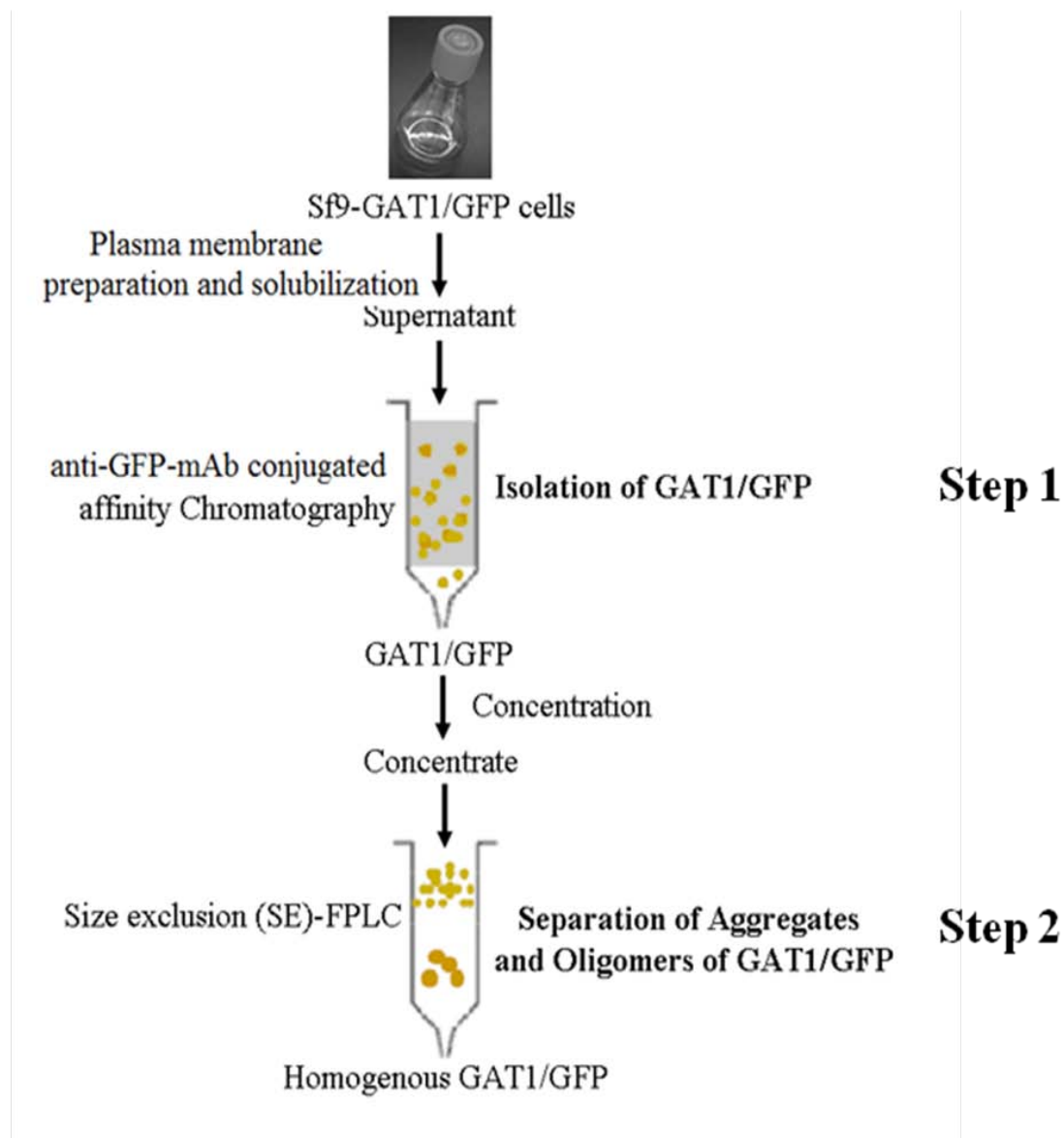
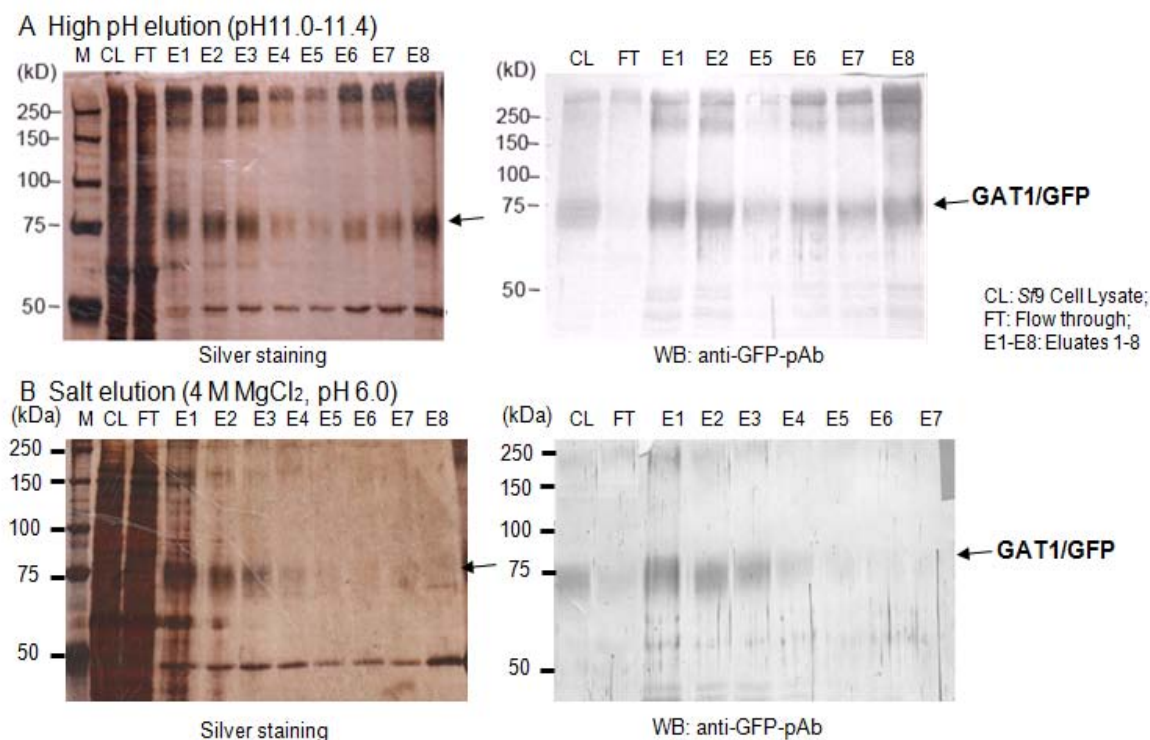


Figure 3.31 Schematic diagram of isolation and purification of homogeneous GAT1/GFP from insect cells.

To isolate GAT1/GFP from mAb-GFP conjugated affinity column, two elution conditions (pH value and ionic strength) were used to obtain an effective and appropriate elution buffer for GAT1/GFP protein without irreversibly denaturing or inactivating them.

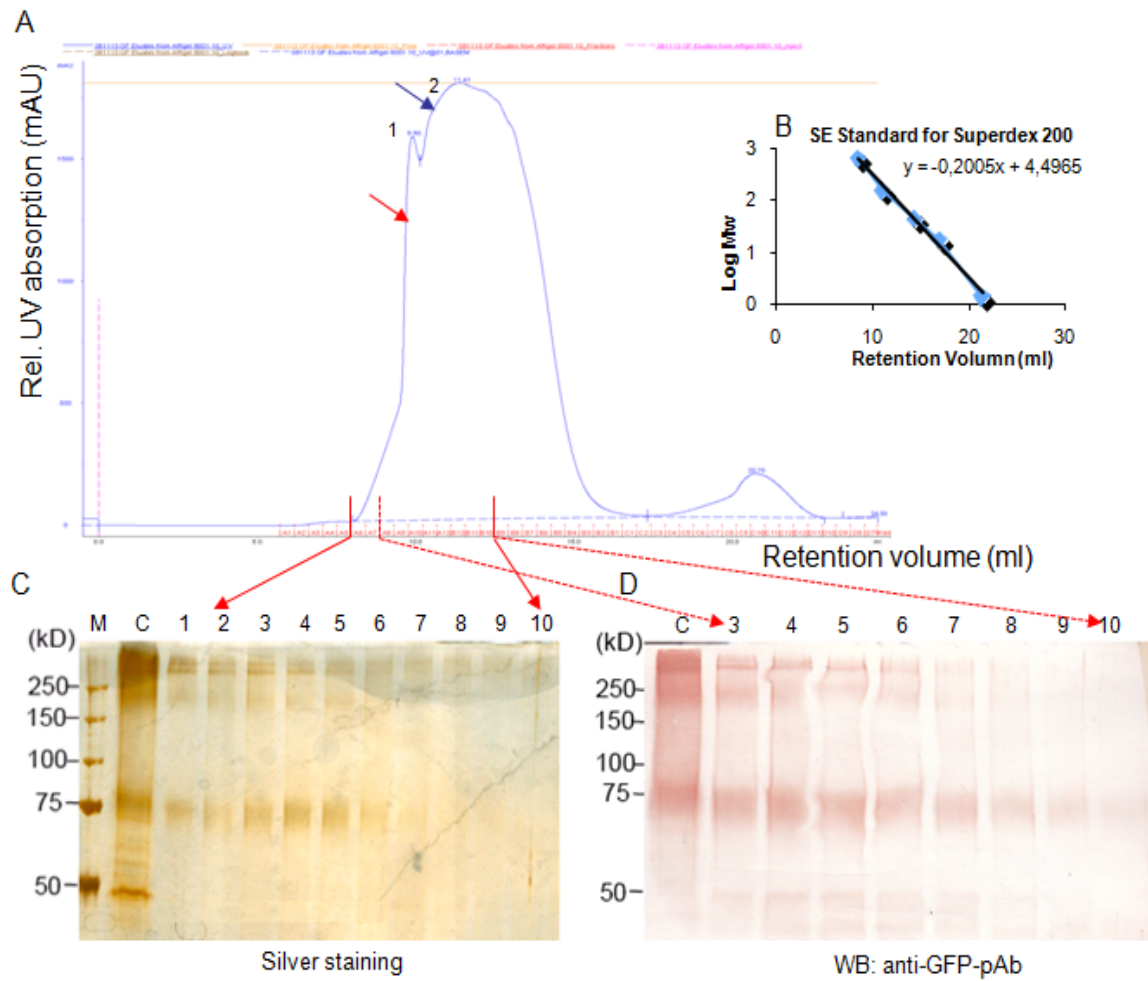
Firstly, we tried the most widely used elution buffer (0.1 M glycine•HCl, pH 2.5-3.0) for purification of proteins. Analysis of SDS/PAGE with silver staining and western blotting (results not shown) indicated that the low pH buffer did not elute GAT1/GFP effectively. Then a high pH buffer (50 mM diethylamine, pH 11.0-11.4) was used. Immediately following elution, eluted fractions were neutralized by addition of 1/10th volume of alkaline buffer (0.5 M Na<sub>2</sub>HPO<sub>4</sub>) in case the target protein was damaged by high pH. Meanwhile, a detergent stock solution was also added to prevent GAT1/GFP protein forming aggregates. Fig. 3.32 A showed that certain amount of GAT1/GFP protein can be eluted at pH11.0, while more GAT1/GFP protein can be eluted by increased pH till 11.4. However, high pH buffer is more effective for elution of GAT/GFP fusion protein than low pH buffer.

Since there is no easy and effective method to measure the activity of purified GAT1/GFP protein, an ionic strength buffer 4M MgCl<sub>2</sub> (pH 6) was also tried to avoid irreversible functional damage of GAT1, which may be caused by high pH value. As seen in Fig. 3.32 B, GAT1/GFP fusion protein can be eluted by a near-neutral high-salt buffer, but not effective as efficient as high pH buffer. The eluted fractions were pooled and dialysed against equilibrium buffer for SE-FPLC for the further purification by SE-FPLC.



**Figure 3.32 Isolation of GAT1/GFP fusion protein in *Sf9* cells by mAb-GFP conjugated affinity column.** (A) Analysis of eluted fractions from mAb-GFP conjugated affinity column with high pH buffer by SDS/PAGE (7.5%) with silver staining and Western blotting. E1-E4: pH 11.0; E5-E7: pH 11.2; E8: pH 11.4. (B) Analysis of eluted fractions from mAb-GFP conjugated affinity column with 4 M MgCl<sub>2</sub> (pH 6) by SDS/PAGE with silver staining and Western blotting. The arrow points out the fragment of mAb-GFP.

A second purification step with SE-FPLC was performed to remove the antibody fragments (Fig. 3.33) from the eluates after immuno-affinity column. The elution profile of GAT1/GFP in *Sf9* cells (3.33 A) was similar as that in Hek293 cells. In comparison with the standard proteins (Fig. 3.33 B), two main peaks (1 and 2) corresponded to Mr 320 kDa and 162 kDa, respectively. The fractions (300 µl per fraction) from 8.8 to 11.8 ml after SE-FPLC were further analyzed by SDS-PAGE (7.5%) (20 µl per fraction) followed with silver staining and Western blotting (Fig. 3.33 C and D). The results indicated that peak 1, which should correspond to a tetrameric GAT1/GFP with molecular weight of 320 kDa, appeared at 8.8-10.6 ml (Lane 2-8). Peak 2 contains only a few amount of GAT1/GFP protein, which should correspond to a dimeric form with molecular weight of 162 kDa. After FPLC, the protein concentrations of the fractions containing GAT1/GFP were determined by BCA and a yield of around 200-300 µg of GAT1/GFP protein per 400-600 ml of infected *Sf9* cells was obtained.



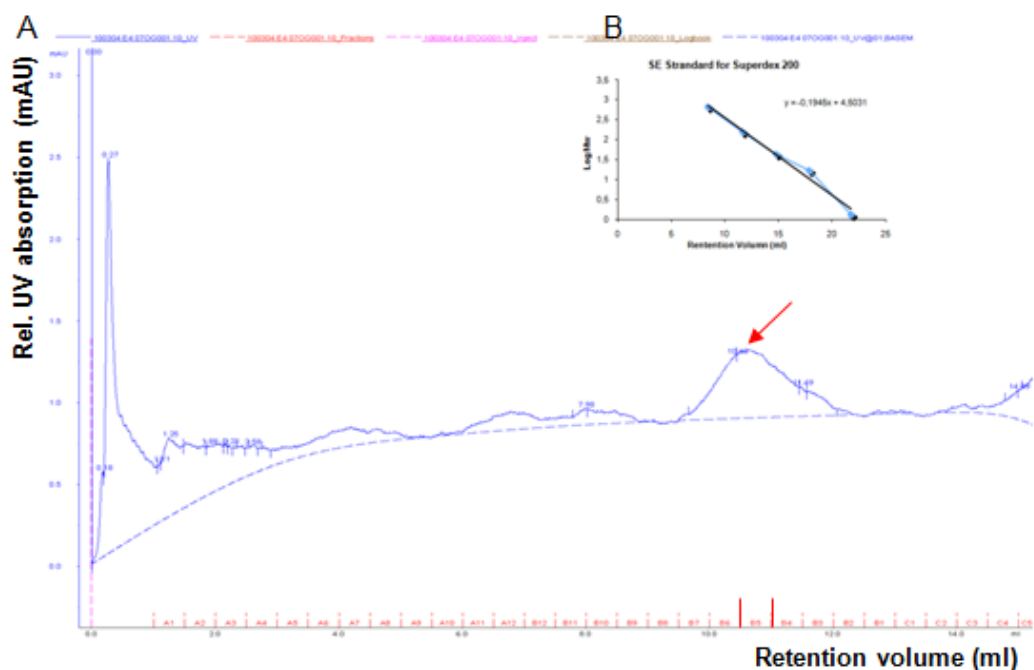
M: Standard Marker; C: Concentrated sample of eluates from immunoaffinity column;  
 1-10: SE-FPLC fractions from 8.8 to 10.8 ml

**Figure 3.33 Purification of GAT1/GFP fusion protein in Hek293 cells by SE-FPLC.** (A) Elution profile of GAT1/GFP after SE-FPLC on Superdex 200<sup>TM</sup> column. (B) The standard linear regression curve of Superdex 200<sup>TM</sup> column was generated by plotting the log of the molecular mass of different calibration proteins against their elution volume. (C) (D) Silver-staining and Western blotting of SDS/PAGE (7.5%) of eluted fractions (from 8.8 to 11.8 ml) after SE-FPLC.

### 3.3.2.5 Transmission electron microscopy (TEM) analysis

In order to obtain homogenous GAT1/GFP fusion protein for a sound structure analysis, different concentrations of detergents (*n*-dodecyl- $\beta$ -D-maltoside (DDM) and *n*-octyl- $\beta$ -D-glucopyranoside ( $\beta$ -OG)) were used in the context of immuno-affinity column and SE-FPLC, respectively. Fresh SE-FPLC fractions were promptly analyzed by TEM.

0.7% (w/v)  $\beta$ -OG was added to the high-pH-eluted GAT1/GFP fusion protein fractions obtained from the immuno-affinity column to prevent protein aggregation. The fractions were subsequently pooled and concentrated in TBS buffer (0.7%  $\beta$ -OG). A typical elution profile of GAT1/GFP (high pH-eluted) from SE-FPLC with TBS buffer (0.7%  $\beta$ -OG) is shown in Fig. 3.34 A. Compared to the standard proteins (Fig. 3.34 B), the main peak 1 (at 10.4-10.8 ml) corresponds to an oligomeric form of GAT1/GFP with a molecular weight of 300 kDa. The fraction of peak 1 (indicated with arrow in Fig. 3.34 A) was analyzed by negative staining TEM. As shown in Fig. 3.34 C, the particles (white arrows) have a diameter around 25 nm (a value that can approximately be expected for a 300kDa protein) and were designated as the oligomeric aggregates of the protein.





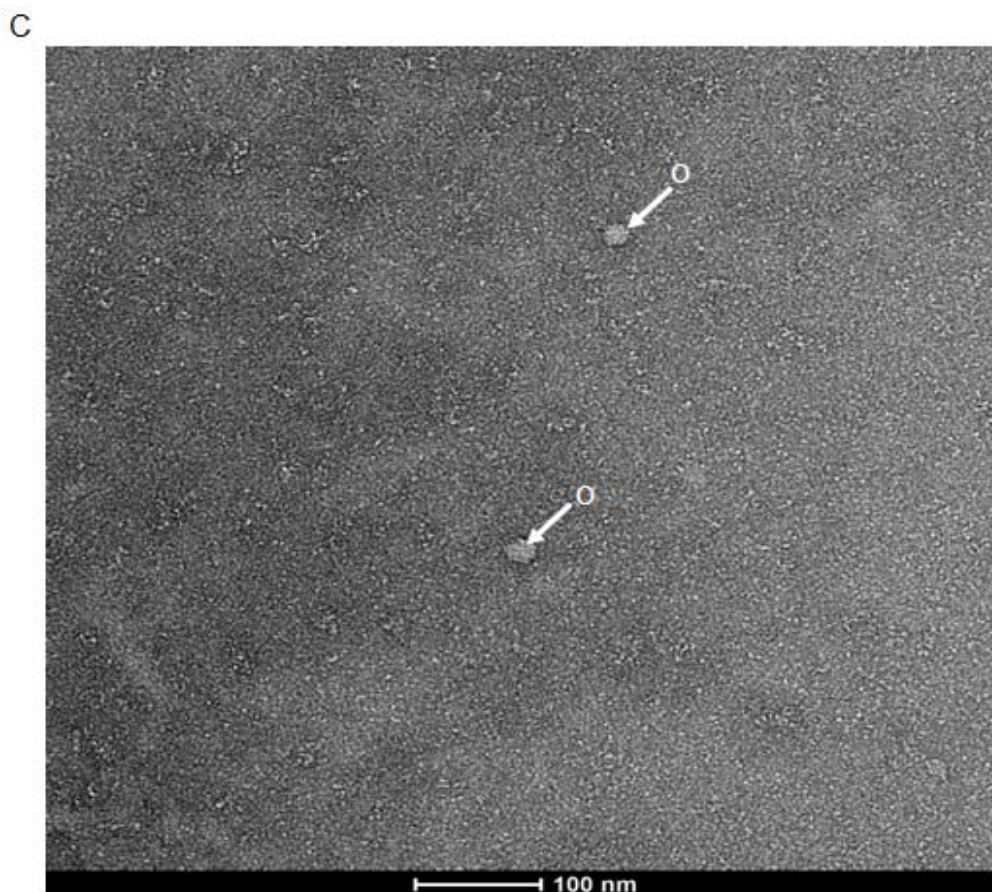
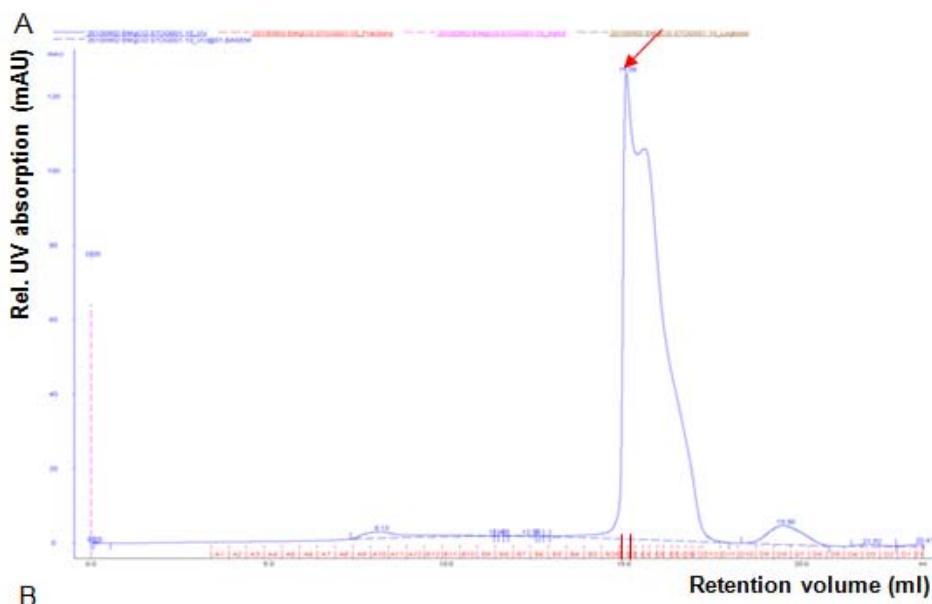


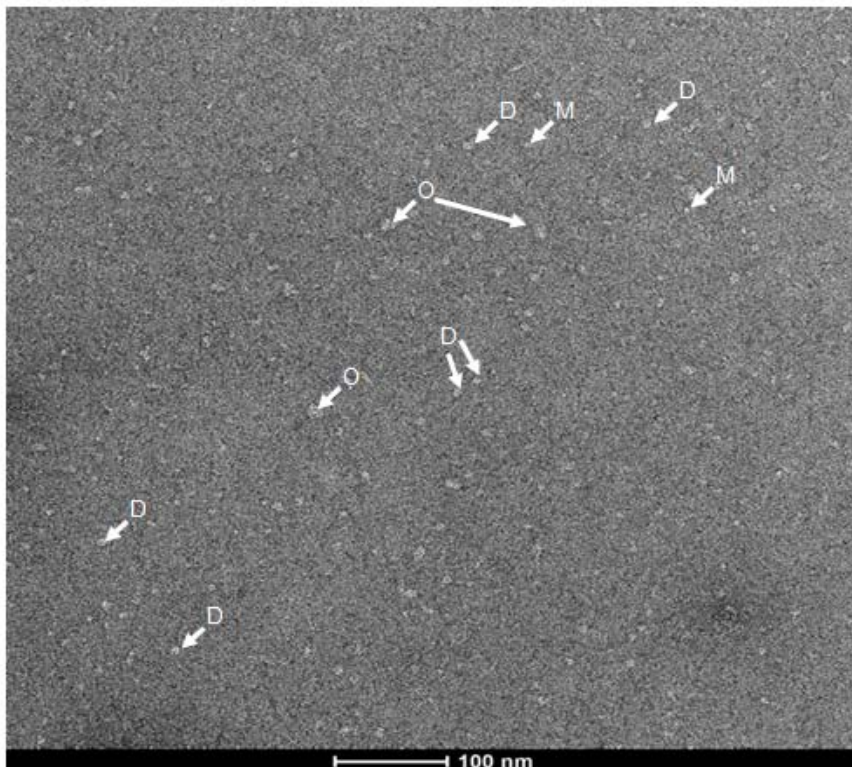
**Figure 3.34 Analysis of GAT1/GFP fusion protein after SE-FPLC.** (A) Elution profile of GAT1/GFP fusion protein (with 0.7%  $\beta$ -OG, high-pH-eluted) after SE-FPLC on a Superdex 200 column with 0.7%  $\beta$ -OG. (B) The standard linear regression curve of Superdex 200<sup>TM</sup> column (TBS, 0.7%  $\beta$ -OG). (C) TEM image (negative stain preparation using 1% uranyl acetate) of oligomeric aggregates (diameter = 25 nm) of GAT1/GFP fusion protein indicated with white arrows. O: oligomer

The same detergent condition was also used for the salt-eluted GAT1/GFP fusion protein fractions from immuno-affinity column. The salt-eluted fractions were pooled and then desalting in TBS buffer (0.7%  $\beta$ -OG). The elution profile of GAT1/GFP (salt-eluted) from SE-FPLC with TBS buffer (0.7%  $\beta$ -OG) was shown in Fig. 3.35 A. The main peak appeared in the range between 15.0-17.0 ml, corresponding to a molecular weight of around 40 kDa, if compared to the standard proteins (Fig. 3.34 B). However, the fractions analyzed by SDS-PAGE and Western blotting (data not shown) indicated that the protein contained in the peak was intact GAT1/GFP and was not fragments. Electron micrograph of the peak fraction (indicated with arrow in Fig. 3.35 A) however shows a mixture of assemblies varying in size (Fig. 3.35 B).

The staining preparation produced smaller particles (M) with a diameter of around 5 nm thought to represent monomers of the GAT1/GFP protein and also larger particles (D) with a diameter of around 8-9 nm, which can be attributed to dimeric protein aggregates. Larger oligomers (O) with a diameter in the range of 16-22 nm can also be found. Here, the molecular weight calculated from SE-FPLC fractions do not fully correlate with the size obtained by TEM. Since after high-pH elution most protein were thought to aggregate, high-salt buffer were tested to prevent oligomerization.



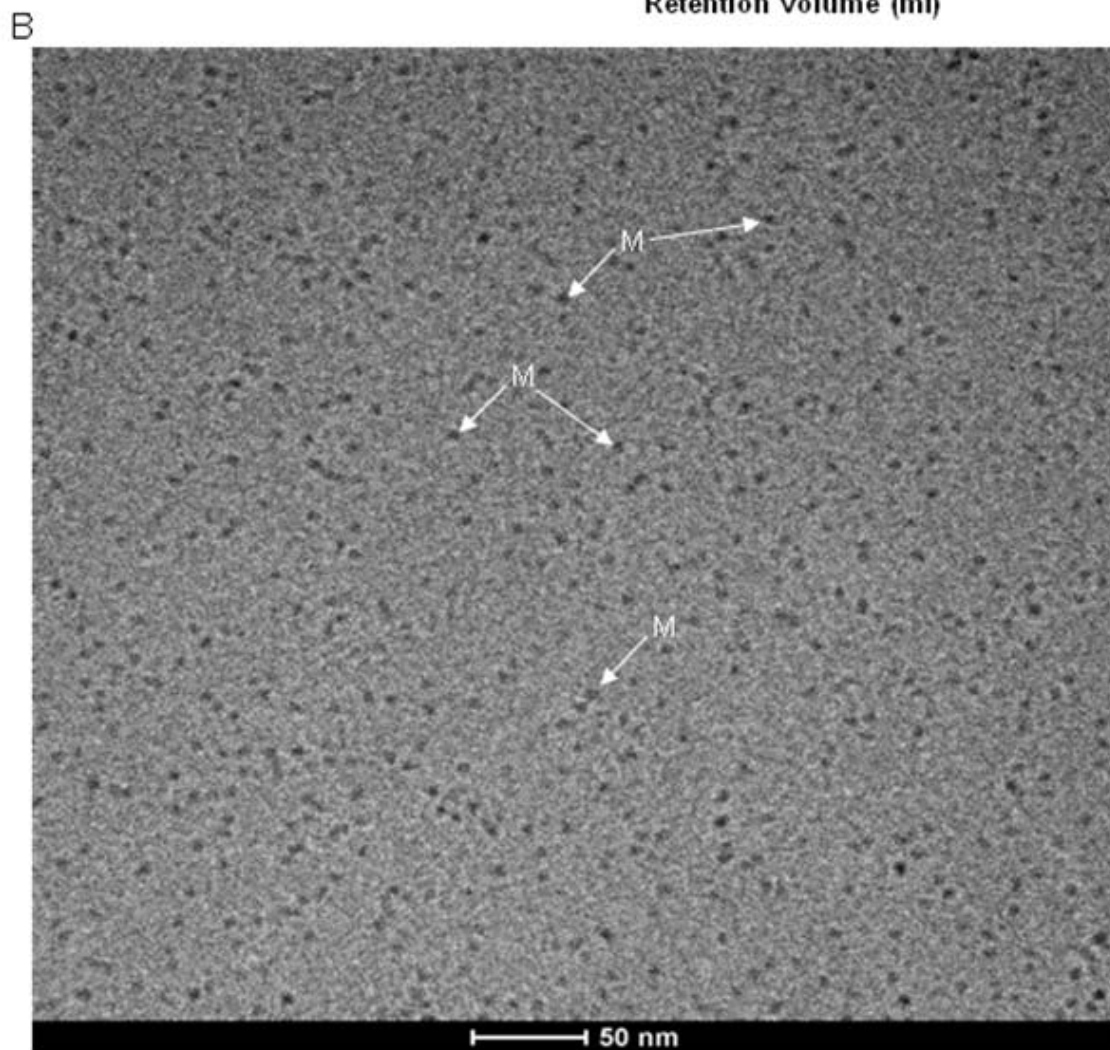
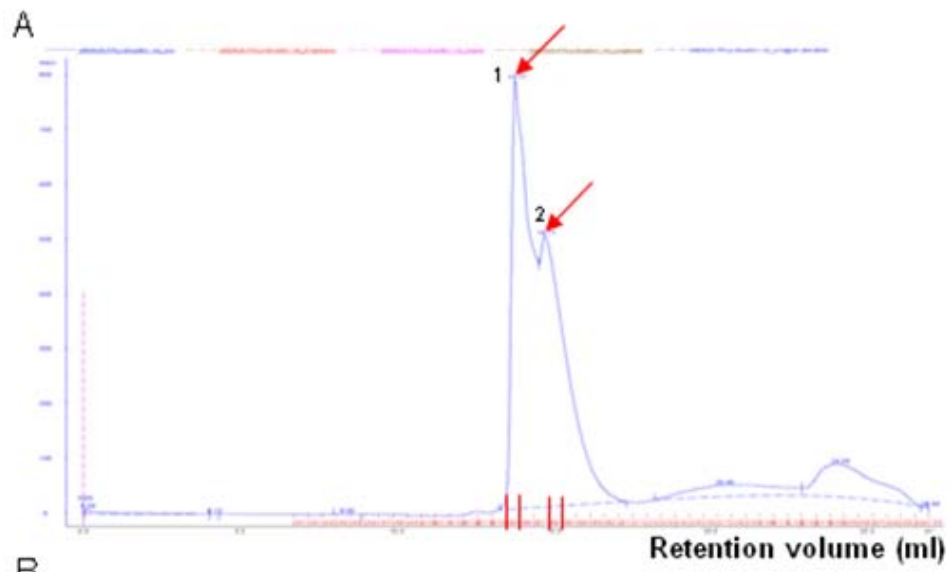
B



**Figure 3.35 Analysis of GAT1/GFP protein preparation after SE-FPLC.** (A) Elution profile of GAT1/GFP protein (with 0.7%  $\beta$ -OG, salt-eluted) after SE-FPLC on a Superdex 200 column with 0.7%  $\beta$ -OG. (B) TEM micrograph (negative staining preparation with 1% uranyl acetate) representing monomers (M, diameter = 5 nm), dimer (D, diameter = 8-9 nm) and oligomers (O, diameter = 16-22 nm) of GAT1/GFP fusion protein indicated with white arrows accordingly.

In order to prevent the protein forming oligomers after elution from immuno-affinity column, the more stabilizing detergent DDM (0.05%) was used. The eluted fractions were then pooled and dialyzed against TBS buffer (0.7%  $\beta$ -OG) in order to remove excess micelles of DDM. The elution profile of GAT1/GFP fusion protein (salt-eluted) from SE-FPLC with TBS buffer (0.7%  $\beta$ -OG) was shown in Fig. 3.36 A. Two overlapping peaks appeared from 13.5 – 15.8 ml. Peak 1 appearing at 13.5-14 ml corresponded to a molecular weight of around 70 kDa, and peak 2 (14.7 ml) corresponded to molecular weight of 45 kDa, comparing to the standard proteins (Fig. 3.34 B). After SDS-PAGE and western blotting analysis (data not shown), GAT1/GFP fusion protein was found mainly in peak 1 but very less in peak 2. Both fractions from these two peaks were then analyzed by TEM.

As aggregation observed by TEM in the above cases might also be due to the preparation conditions including drying of the sample on the support grid which is known to create artifacts cryogenic electron microscopy (cryo-TEM) was employed in order to avoid putative influences of sample drying and staining salts. The cryofixation by sample vitrification is known to preserve the sample in the native state of the buffer environment and correspondingly the cryo-microscopy allows a direct visualization of the protein in the fully hydrated state. The fraction of peak 2 was characterized by cryo-TEM and showed a very monodispers distribution of particles (Fig. 3.36 B) with a diameter in the 5-6 nm range, which might correlate with protein monomers. However, the high contrast of the relatively small particles is noticeable. Since the radius of DDM micelles was reported to be around 2.6-3.5 nm (Lipfert *et al.* 2007) it was not quite clear if the particles could simply be attributed to spherical micelles although the high contrast is not very typical for detergent micelles. As micellar DDM solutions give low UV signals, it can be speculated that peak 2 may contain both monomer of GAT1/GFP protein as well as DDM micelles which were not removed completely by dialysis. The fraction of peak 1 was analyzed by negative staining preparation with TEM. The electron micrograph shows a mixture of different forms, namely small particles of 5 nm diameter as before but also a considerable fraction of fiber-like aggregates of unknown origin (Fig. 3.36 C).



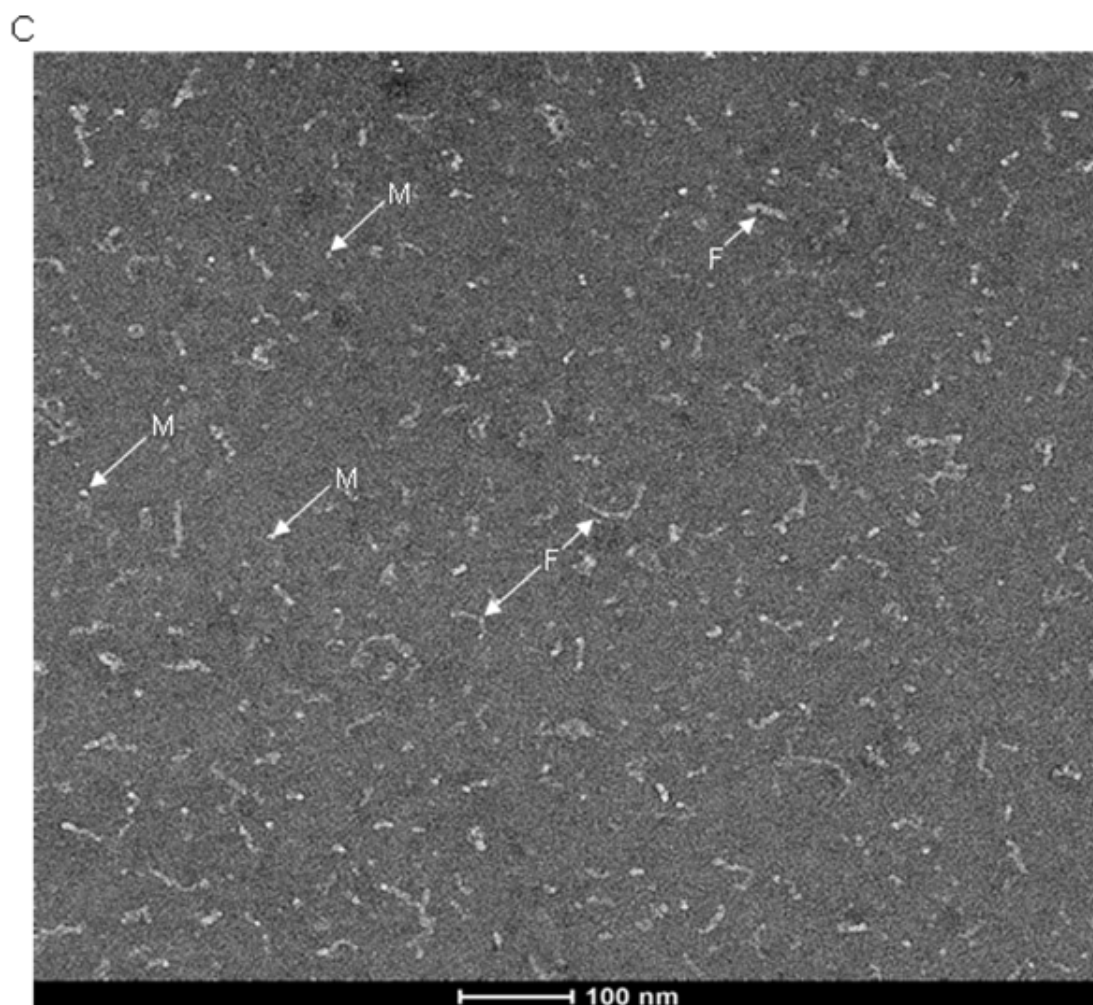


**Figure 3.36 Characterization of salt-eluted GAT1/GFP fusion protein after SE-FPLC.** (A) Elution profile of GAT1/GFP protein (with 0.05% DDM, salt-eluted) after SE-FPLC on a Superdex 200 column with 0.7%  $\beta$ -OG. (B) Cryo-TEM preparation of fraction peak 2 (cf. A). Assumed monomeric GAT1/GFP fusion protein (M, diameter = 5-6 nm) are indicated with white arrows. (C) Electron micrograph (negative staining preparation with 1% uranyl acetate) of fraction peak 1. M: Assumed monomers of GAT1/GFP fusion protein (M, diameter = 5-6 nm) and fiber-like aggregates of unknown origin (F) are indicated.

Therefore control experiments by cryo-TEM were performed of the TBS buffer solution in the presence of 0.05% DDM. However, at this DDM concentration (which is above the CMC (0.009% or 0.18 mM) of DDM) no significant population of micelles could be found (Fig. 3.37). This is a known effect that micelles of classic detergents are difficult to prove in the concentration range only slightly above the CMC. This fortunate control experiment however suggests that the observed particles of Fig. 3.36 B most probably correspond to a monodispers preparation of GAT1/GFP. A later experiment will strengthen this argument which was performed below the CMC of the detergent.

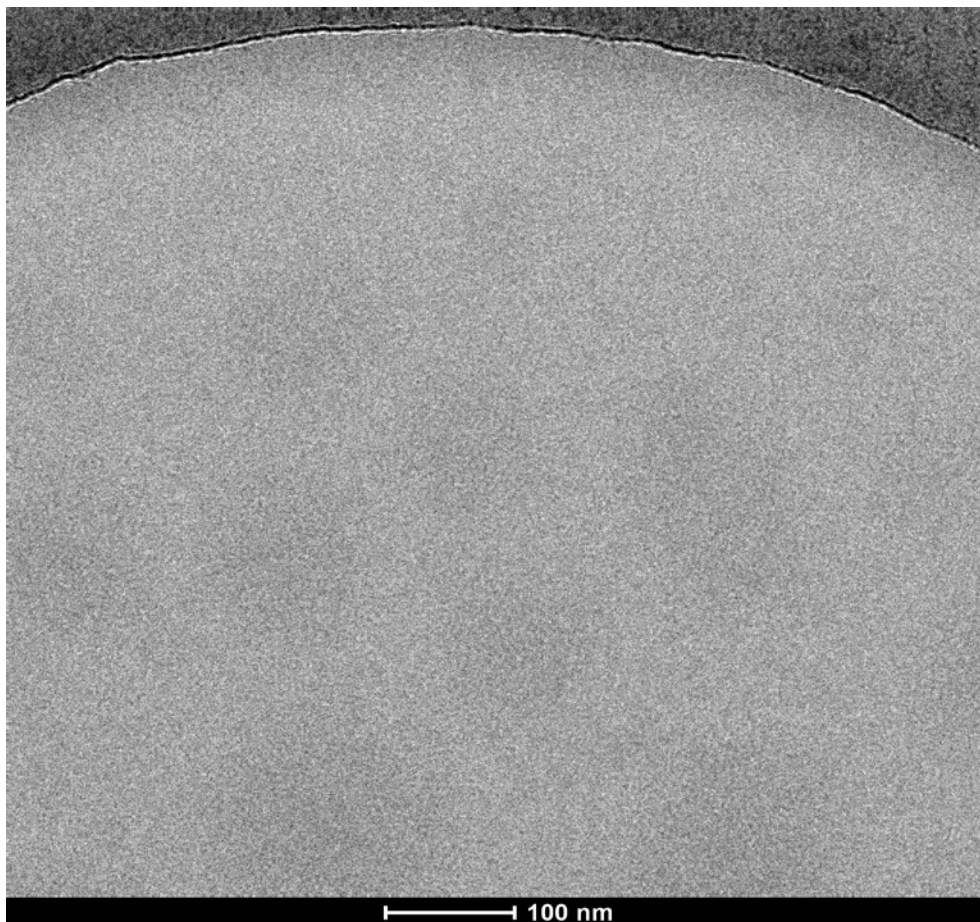


**Figure 3.37** Cryo-TEM image of TBS buffer in the presence of 0.05% DDM. The control experiment shows no significant population of spherical micelles, some isolated individual particles of low contrast are rarely detectable.

In order to exclude a possible structural contribution of the detergents in the electron micrographs and to determine the state of aggregation of the eluted GAT1/GFP fusion protein, a preparation with 0.085% DDM below its CMC was performed. Fig. 3.38 A shows a similar elution profile of GAT1/GFP fusion protein with two overlapping peaks as Fig. 3.36 A. The fraction of peak 1 which appeared at 11.5 ml corresponds to a molecular weight of 220 kDa and was again analyzed by cryo-TEM. The electron micrograph (Fig. 3.38 C) shows a mixture of individual particles (diameter 5 nm) and fiber-like aggregates (diameter 5 nm and length varying between 30 and 150 nm). The single particles can again be attributed to the monomer of GAT1/GFP fusion protein as we can exclude micelle formation for DDM below the CMC. This has also additionally proven by a cryo-TEM control experiment where the pure buffer in the presence of 0.0085% DDM did not show the formation of spherical or fiber-like assemblies at all (data not shown).

The peak 2 fraction was analyzed by negative staining and the electron micrograph (data not shown) also shows similar fiber-like aggregates. All these results indicated that the type and concentration of detergent are crucial for the isolation of homogenous GAT1/GFP fusion protein.

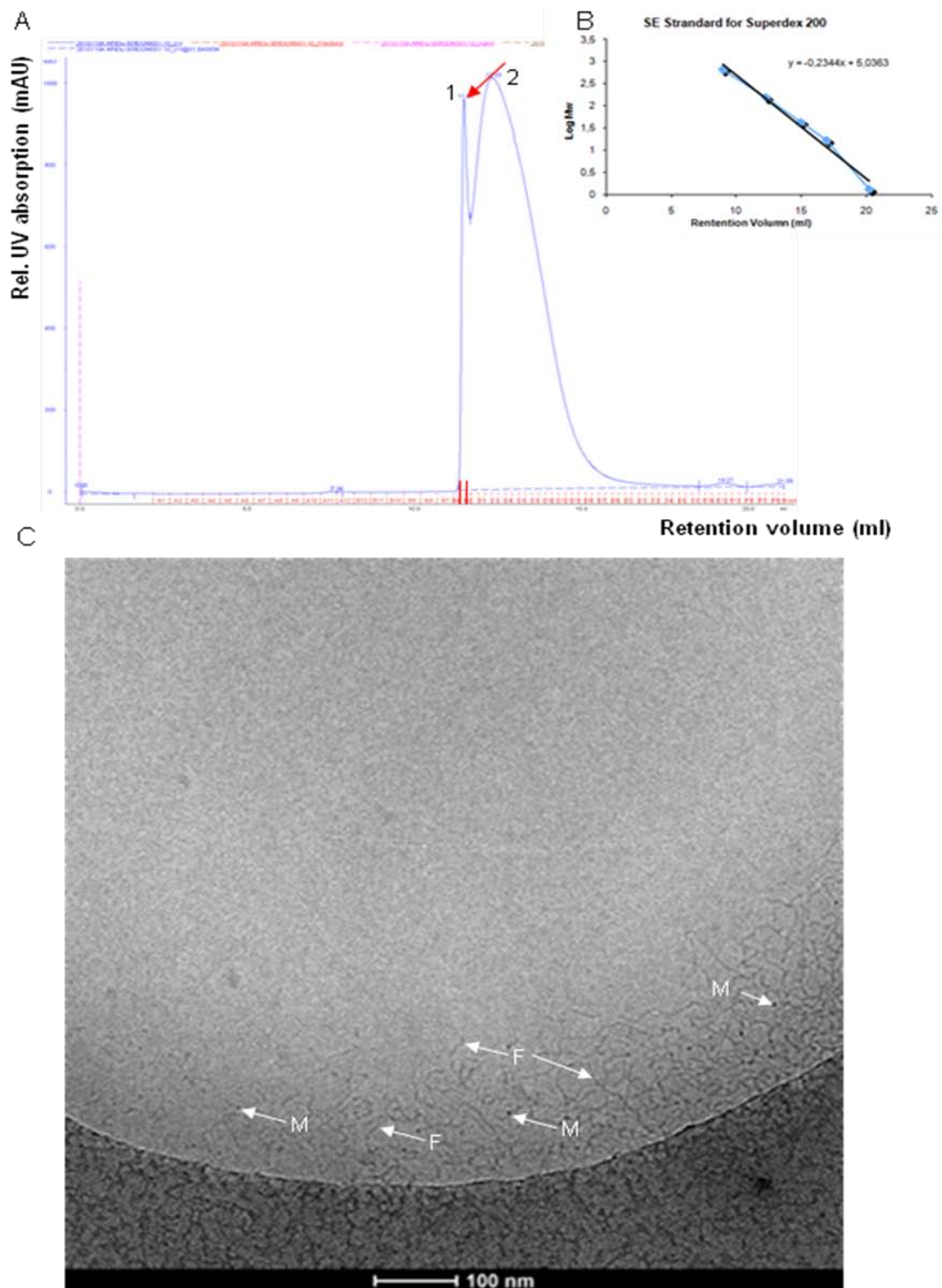


**Figure 3.38** Characterization of a salt-eluted GAT1/GFP protein preparation after SE-FPLC in the presence of 0.085% DDM. (A) Elution profile of GAT1/GFP protein (with 0.085% DDM, salt-eluted)

## *Results*

---

after SE-FPLC on a Superdex 200 column with 0.085% DDM. (B) The standard linear regression curve of Superdex 200<sup>TM</sup> column. (C) Cryo-electron micrograph of fraction peak 1. M: Assumed monomers of GAT1/GFP fusion protein (M, diameter = 5-6 nm) as well as fiber-like structures (F, diameter = 5-6 nm and length = 30 – 150 nm)



## 4 Discussion

### 4.1 Role of terminal sialic acid in the GABA uptake activity of GAT1

In this study we demonstrated for the first time that the terminal sialic acids of GAT1 are crucial for GABA uptake. Deficiency, removal or oxidation of surface sialic acid residues on *N*-glycans of GAT1/GFP respectively resulted in a strong reduction of GAT1 activity. Kinetic analysis revealed that the negative charge of terminal sialic acids of GAT1 is responsible for the GABA uptake activity by the apparent affinity for extracellular Na<sup>+</sup>. Meanwhile, the disruption of structure of sialic acids also strongly reduced  $V_{\max}$  without affecting both affinities of GAT1 to GABA and Na<sup>+</sup>.

In this work, all quantitative and kinetic analysis of GABA transporter expression and activity was performed using stable CHO, CHO Lec3 and Hek293 transfectants. GFP tagged GAT1 protein and anti-GFP antibody was used since both our own and commercially available anti-GAT1 antibodies were not suitable due to their weak and unstable binding activity to the protein. Meanwhile, GFP tag has been reported to not influence the intracellular distribution and characteristic function of GAT1 (Chiu *et al.* 2002). In order to exclude the possibility that the reduction of GAT1 activity results from a decrease in the number of GABA transporters per cell, a quantitative determination of the expression of GAT1/GFP fusion protein was performed, and both terminal sialic acid concentration and GABA transport activity was normalized to the amount of plasma membrane GAT1/GFP protein. For the quantitative analysis, the cell surface expression of GAT1 in different cell lines was determined by western blotting following cell surface biotinylation and the resulting values were used for normalization. This is a well established method for the quantitative analysis of cell surface proteins since the biotinylation reagent does not penetrate the cell membrane (Law *et al.* 2000).

#### 4.1.1 Terminal sialic acid is crucial for GABA uptake activity of GAT1

Previously, our group have shown the need of *N*-glycans for the biological activity of GAT1 and demonstrated a deficiency of *N*-glycosylation brought about by site-directed mutagenesis results in a reduction of protein stability and intracellular trafficking (Cai *et al.* 2005). However, inhibition of *N*-glycosylation processing by 1-deoxymannojirimycin (dMM) resulting in a mannose rich type of *N*-glycans does not affect either the protein stability or intracellular trafficking. This suggests that the co-translational *N*-glycosylation,

but not the terminal trimming of *N*-glycans is involved in the regulation of the correct folding of membrane glycoproteins. However, the GAT1 mutants containing mutations in any two of three *N*-glycosylation positions showed a significantly reduced GABA uptake activity, while GABA uptake activity could be hardly detected after all three *N*-glycosylation sites of GAT1 were mutated. These data suggest that the *N*-glycans of GAT1 play a crucial role in the GABA transport function of GAT1 (Cai et al. 2005). It has been demonstrated that purified GAT proteins can be reconstructed into liposomes with function which indicates that no other proteins are needed for GABA uptake activity (Radian and Kanner 1985). Taken together, we suggest that the reduced GAT1 activity resulted from deficiency of its own *N*-glycosylation, but not due to other cell surface glycoconjugates. Nevertheless, dMM reduced markedly the GABA uptake activity of GAT1 suggesting an involvement of the terminal *N*-glycan structures in the regulation of the GABA transport activity of GAT1. Kinetic analysis demonstrated that deficient *N*-glycan trimming decreased the  $V_{\max}$  values of GABA uptake by GAT1, while the  $K_m$  GABA values were not affected (Cai et al. 2005). It is indicated that the turnover rate of the transporter is affected, but not the substrate binding process. Voltage-clamp experiments revealed that the deficiency of *N*-glycans leads to the reduction of the affinity of GAT1 to  $\text{Na}^+$  (Liu et al. 1998; Cai et al. 2005). In this event the oligosaccharides of GAT1 play a pivotal role in the regulation of GABA uptake activity by affecting the affinity with sodium ions.

The molecular mechanism of the oligosaccharides in GABA uptake of GAT1 has remained unclear. It is widely known that the oligosaccharides turn into hybrid or complex forms after *N*-glycan trimming. Sialylation, which occurs on glycolipids and *N*- and *O*-glycans, stands out among the terminal positions of the glycan chains. Sialic acids are negatively charged, and are usually the terminal sugar residues on the oligosaccharide chains of cell surface or serum glycoconjugates, where they play an important role in key cellular and molecular interactions (Schauer 2009). It was reported that sialic acid is directly involved in the synaptosomal transport of amino acid transmitters (Zaleska and Erecinska 1987). The role of sialic acids terminated *N*-glycans in the GABA transport by GAT1 was here further investigated.

Firstly, quantitative analysis was performed in stably transfected CHO and CHO Lec3 cells with GAT1/GFP fusion protein. CHO Lec3 cells are deficient in sialic acid residues on cell surface glycoproteins due to mutations in the *gne* gene, which abolished UDP-GlcNAc 2-epimerase activity (Hinderlich et al. 2001; Hong and Stanley 2003). These cells

were cultured in serum-free medium to prevent sialic acid incorporation on glycoproteins during experiments. The expression of GAT1 protein and the sialic acid, as well as GABA uptake activity of GAT1 were quantified in both transfectants. We found that GAT1/GFP expressed on the cell surface in CHO Lec3 was in the same range as in CHO cells, however, after normalization the GABA uptake activity of GAT1 in CHO Lec3 cells decreased strongly with a reduced amount of cell surface sialic acid (Fig. 2). These results suggest that the reduced sialic acid concentrations on GAT1 resulted in the decrease of GABA uptake activity by GAT1 in CHO Lec3 cells.

As shown in Fig. 4.1, ManNAc is the specific sialic acid precursor. After supplementation with cells, ManNAc can be taken up and thus lead to an increased intracellular concentration of sialic acids as well as cell surface sialylation. ManNProp is an efficient unphysiological precursor which can introduce *N*-propanoyl-modified sialic acids into living cells (Kayser et al. 1992; Keppler et al. 2001). It was reported that treatment of ManNAc and ManNProp with UDP-GlcNAc 2-epimerase-deficient myeloid leukemia HL60 and B-cell lymphoma BJA-B increased cell surface sialylation significantly (Mantey *et al.* 2001). It suggests that CHO Lec3 cells, which cannot synthesize ManNAc and sialic acid *de novo*, can take up and metabolize ManNAc or ManNProp to natural or modified sialic acid after cultivation with these two precursors, respectively. After treatment of ManNAc or ManNProp, the GABA uptake activity of stable CHO transfectants was not affected which indicates a pre-existing saturation of all acceptor sites for sialic acid in this cell line. Whereas the GAT1 activity of stable CHO Lec3 transfectants was increased significantly, most likely resulting from the increased cell surface sialylation. The results provide additional evidence for the essential role of sialic acid in GABA uptake.

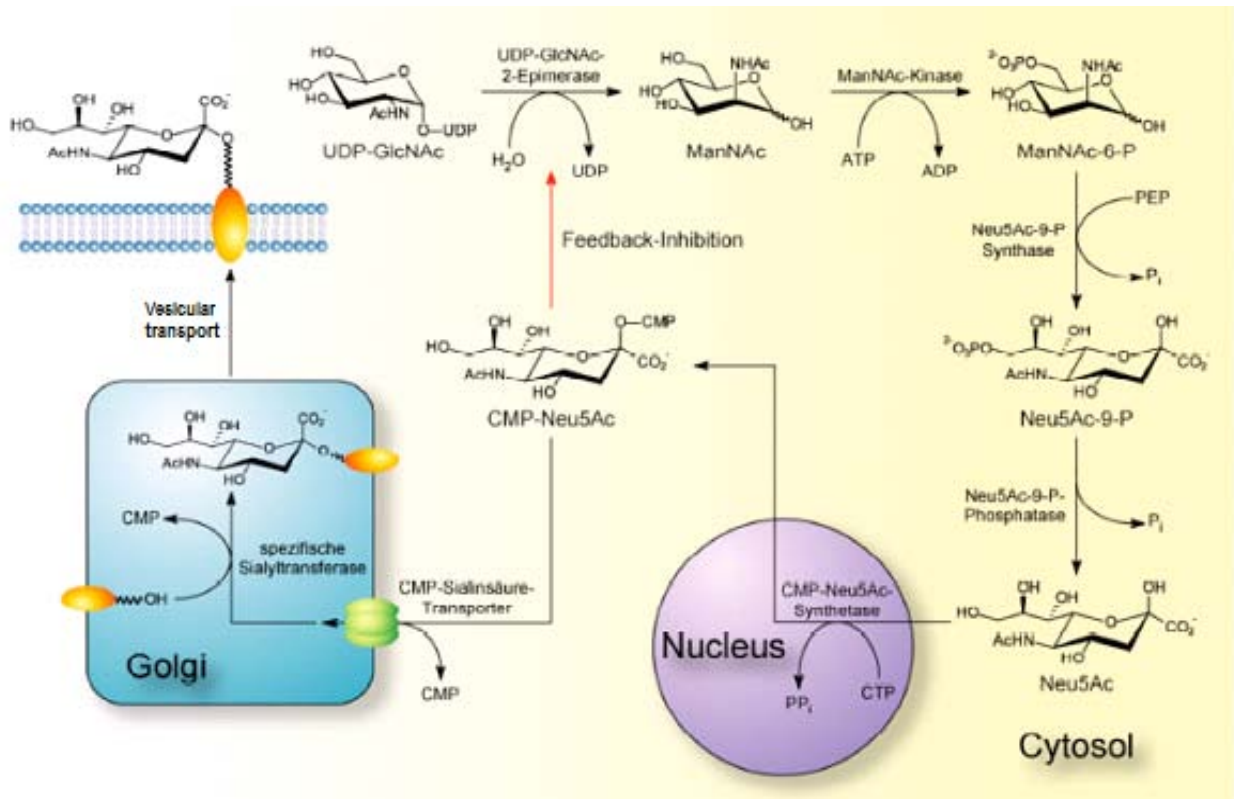


**Figure 4.1** Biosynthesis of sialic acid in mammalian cells.

It is not clear whether the reduction of GAT1 activity in CHO Lec3 cells is resulted from the change in the biochemical properties or other interference of the mutation. In order to exclude this possibility, further experiments were performed with sialidase to simply remove the sialic acids from cell surface glycoconjugates, including GAT1 protein. Our results showed that GAT1 expressed both in CHO and Hek293 cells displayed a significant reduction of GABA uptake activity after sialidase treatment in a dose dependent manner (Fig. 3.8). In order to quantitatively analyse the sialic acids of GAT1 and total and plasma membrane GAT1 protein, a certain amount of GAT1 is necessary for immunoprecipitation, immuno-blotting and lectin staining. The higher expression of GAT1 on the cell surface requires fewer cells to be used and thus, less sialidase for the analysis. Therefore, Hek293 transfectants were used for further quantification analysis due to their high expression levels of GAT1/GFP protein on the surface. Fig. 3.9 showed that after treatment of the Hek293/GAT1 cells with 1U/ml sialidase for 4 h, almost 80% of sialic acid was removed, and the GABA uptake activity was correlatively reduced to about 22% (Fig. 3.9). This result indicates directly that the reduced GABA uptake activity is directly attributed to the reduction of sialic acid on the *N*-glycans.

#### 4.1.2 Terminal sialic acid affects kinetics of transport cycle

It has been demonstrated that the GABA transport process is driven by the gradient of  $\text{Na}^+$  and  $\text{Cl}^-$  with a stoichiometry that results in an electrogenic substrate transport. The affinity of GAT1 to  $\text{Na}^+$  determines the turnover rate of GABA transport (Nelson 1998). Furthermore, voltage-clamp experiments revealed that a deficiency in the terminal part of the *N*-glycans of GAT1 by mutations did not affect the affinity of GAT1 to GABA, while reduced significantly the affinity of GAT to extracellular sodium ions (Cai et al. 2005). Our kinetic analysis with different GABA concentrations shows that deficiency, removal or oxidation of sialic acids on *N*-glycans decreased the  $V_{\text{max}}$  values of GABA uptake by GAT1, while the  $K_m$  GABA values were not affected. This result is consistent with former findings with deficient *N*-glycosylation and dMM treatment (Cai et al. 2005). It is clear that the deficient cell surface sialic acids reduces GABA uptake turnover rate, however, has no influence on the GABA binding.

It is well known that sialic acids are bulky hydrophilic and electronegatively charged monosaccharides on animal cells, which favour the affinity to inorganic cations. In addition to their negative charge, sialic acids also make a contribution to recognition of variety of ligands, such as hormones, lectins, antibodies and microorganisms (Schauer 2009). In order to clarify whether sialic acids are involved in the GAT1 activity based on only their negative charge, we determined the influence of oxidation of surface sialic acids on the GABA uptake activity by sodium periodate ( $\text{NaIO}_4$ ). As shown in Fig. 4.2,  $\text{NaIO}_4$  treatment of GAT1/GFP stable transfected Hek293 cells led to the oxidation of the cell surface sialic acid residues with formation of 7- or 8-aldehydic derivative that remains acidic groups (Perez et al. 1985). Thus the electronegative charge of GAT1 was not impaired. However, the GABA uptake activity of GAT1 was inhibited as a consequence of a direct effect of the removal of the two terminal exocyclic carbon atoms from membrane sialic acid with  $\text{NaIO}_4$ . After oxidation, it is possible that the free aldehyde form schiff base with available amino groups which thus cause inactivation of GAT1. In order to exclude this possibility, sodium borohydride ( $\text{NaBH}_4$ ) treatment was further performed to convert aldehyde to alcohol so that the shift base structure could not be formed. The GABA uptake activity of GAT1 was still inactivated. It suggests that the unique structure of sialic acid may be the essential component of GAT1 in GABA uptake process.

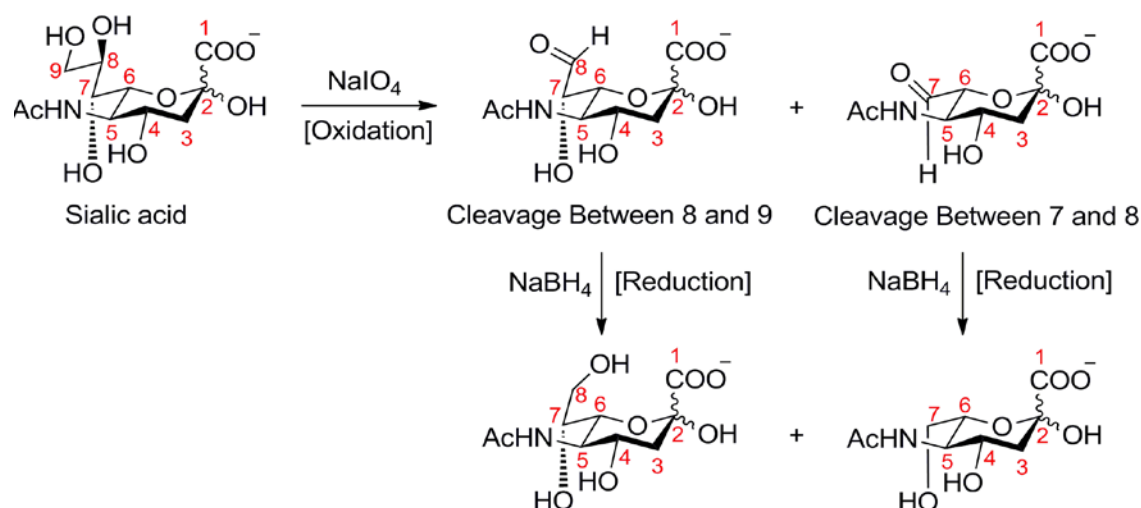


**Figure 4.2** Oxidation of sialic acid by  $\text{NaIO}_4$  followed by  $\text{NaBH}_4$  reduction.

To further clarify the molecular mechanism of the sialic acid in the GABA uptake by GAT1, the affinity of GAT1 for sodium ion was measured. The CHO Lec3 cells and sialidase- or  $\text{NaIO}_4$ -treated Hek293 cells are too fragile for the patch-clamp methods. Since the GAT1-dependent  $\text{Na}^+$  transport is proportional to GABA transport in ratio 2:1, sodium-dependent GABA uptake was kinetic analyzed with different sodium ions concentrations. Sodium ions were replaced with potassium ions in the buffer to compensate the loss of osmotic pressure and the GABA uptake activities were normalized to the plasma membrane expressed GAT1 amounts. We found that both deficiency (CHO Lec3) and removal of sialic acids (by sialidase) reduced the affinity of GAT1 for sodium ions significantly, which is in agreement with our former results of patch-clamp experiments with deficient *N*-glycosylation of GAT1. It is reported that removal of the surface sialic acids affected only the  $\text{Na}^+$ -dependent transport of amino acids but not the uptake of leucine, which is  $\text{Na}^+$  independent (Zaleska and Erecinska 1987). Our kinetic data provide strong evidence that absence of sialic acids reduces the affinity of GAT1 for  $\text{Na}^+$ ; consequently, GABA transport activity of GAT1 is reduced. However, the oxidation of sialic acid by  $\text{NaIO}_4$  does not affect the affinity of sodium ion for GAT1, while the oxidized residues still carry negative charge after structural disruption of sialic acids. It suggests that negative charge of sialic acids is not the only factor involved in the GABA transport by GAT1. The structure of sialic acids on *N*-glycans of GAT1 protein itself is required for the GABA uptake activity of GAT1.

### 4.1.3 Terminal sialic acid in altering access transport model

The involvement of sialic acid can be further explained with a widely accepted theory of GAT1-mediated GABA transport, an alternating access mechanism, in which conformational changes alternately expose a central binding site for one or more substrates to either side of the membrane (Jardetzky 1966). An alternating access transport model was developed in *Xenopus* oocyte membranes. The model assumes two predominantly states of GAT-1,  $E_{in}$  and  $E_{out}$  (Hilgemann and Lu 1999), and the complete transport cycle is proposed in four steps (Kanner and Zomot 2008) or six steps (Fig. 1.5) (Abramson and Wright 2009), mainly including binding/dissociating of substrate and coupled ions and conformational change of GAT1. Our results can be well-interpreted within this model. We assumed that the negative charge of sialic acid influences the binding of GABA and  $Na^+$  with GAT1, while the structure of sialic acid is involved in the conformational changes of GAT1 during the translocation cycle. The impaired structure of sialic acids could disturb the correct conformational changes of GAT1, which results in a blocked GABA translocation.

In conclusion, deficiency in sialic acid biosynthesis leading to a decreased sialic acid concentration, enzymatic removal or chemical oxidation of sialic acids results in reduction of GABA uptake activity of GAT1. In consideration of the previous results of GAT1 *N*-glycosylation mutants (Cai et al. 2005) and functional reconstruction of purified GAT1 protein (Radian and Kanner 1985), we conclude that the reduction of GAT1 activity specifically due to the deficiency/removal/oxidation of terminal sialic acids in the *N*-glycans of GAT1, but not the lack/oxidation of sialic acid of other surface glycoconjugates. Reduced GABA transport activity caused by defective sialic acids can be partially attributed to a reduced affinity of GAT1 to  $Na^+$  and slowed kinetics of the transport cycle. Furthermore, not only is the negative charge involved, but also the unique structure of sialic acid itself is crucial for the GABA uptake process. It also brings out the possibility that terminal sialic acid of GAT1 is involved in two main steps of the GABA transport mechanism: substrate and  $Na^+$  binding and translocation.

## 4.2 Influence of synthetic *N*-acyl hexosamines on GABA uptake activity of GAT1

In this work, several synthetic *N*-acyl hexosamines were found to have inhibitory effect on GABA uptake activity of GAT1 as potent inhibitors of *N*-glycan trimming or sialic acid biosynthesis. Our results described above demonstrate a correlation between the reduction of the GABA uptake activity and the reduction of the terminal sialic acid concentration of GAT1/GFP. Furthermore, it could also be applied for searching potent GAT1 inhibitors from these synthetic *N*-acyl hexosamines that may regulate *N*-glycan trimming or sialic acid biosynthesis of cell surface glycoconjugates using GAT1 transfectants.

In view of the great biological importance of sialic acid, especially with respect to its high concentration on the plasma membrane of cancer cells, more attention has been focused upon the inhibitors of the biosynthesis of sialic acid. As shown in Fig.4.1, the biosynthesis of sialic acid in eukaryotic cells is a multistep process. The key enzyme of this pathway is the bifunctional UDP-*N*-acetylglucosamine 2-epimerase/*N*-acetylmannosamine kinase (GNE) (Hinderlich *et al.* 1997), which catalyzes the conversion of UDP-GlcNAc to ManNAc and the phosphorylation of ManNAc to ManNAc-6-phosphate. The synthesis pathway of sialic acid can be blocked by effective inhibitors of this enzyme. In this work, treatment with 3-*O*-Met-GlcNAc only reduced the concentration of terminal sialic acid of GAT1 but did not change the size and amount of GAT1/GFP protein. It suggest 3-*O*-Met-GlcNAc possesses a strong inhibition on sialic acid biosynthesis which is consistent with the previous findings that it was a potent inhibitor of *N*-acetylglucosamine kinase and *N*-acetylmannosamine kinase *in vitro* (Zeitler *et al.* 1992). However, when the *N*-acetyl group was replaced by *N*-propionyl or *N*-cyclopropylcarbox group, the 3-*O*-Met-D-glucosamine derivatives exhibited no apparent inhibitory effect on sialylation of GAT1/GFP. Our results suggested that longer or bulky aliphatic side chain alongside much more electrodonating properties led to lower inhibitor activities. GlcNProp was also known as an inhibitor of *N*-acetylmannosamine kinase *in vitro* (Grunholz *et al.* 1981). In this study, we found that GlcNProp, GlcNHex, GlcNCyclo and GlcNAc-Acetamido inhibited GABA uptake activity to a certain extent by their influence on *N*-glycosylation, especially terminal trimming of *N*-glycans of GAT1/GFP. In comparison with GlcNProp, the hexanoyl and cyclopropylcarbox substituted glucosamines hold less inhibitory effects on GABA uptake and terminal trimming of *N*-glycans including sialylation, whereas the



acetamidoacetyl group remained the inhibitory effect indicating an unknown interaction between this structure and its substrate. The inhibition by GlcNProp and its derivatives leads to the formation of GAT1/GFP with less terminal trimming of *N*-glycans, which suggests a similar effect of 1-deoxymannojirimycin (dMM) (Cai et al. 2005) or kifunensine as inhibitors of mannosidase I. The molecular mechanisms of these compounds in the *N*-glycan trimming are still unclear and should be further investigated.

### **4.3 Potent inhibitors on GABA uptake activity of GAT1 from naturally occurring compounds**

Several central nervous system (CNS) disorders have been linked to hypoactivity in inhibitory neurotransmission elicited by GABA (Lloyd and Morselli, 1987). The GABA transporters have been recognized as therapeutic targets since inhibition of GABA transporters would prolong the GABAergic signal thereby compensating for GABA hypoactivity (Schousboe *et al.* 2004). A class of heterocyclic GABA uptake inhibitors has been developed using muscimol as a lead structure. Muscimol, is a naturally occurring GABA analogue from the fly agaric mushroom *Amanita muscaria*. Muscimol is a potent GABA<sub>A</sub> receptor agonist with weak inhibitory effect on GAT and is a substrate for the GABA transaminase (Krogsgaard-Larsen *et al.*, 1975).

Although many GABA uptake inhibitors possess antiepileptic properties only one compound (i.e. Tiagabine) with this mechanism has been approved so far for the treatment of epileptic disorders (Schousboe *et al.* 2004). Our work is to search more potent GABA uptake inhibitors from two specific traditional Chinese medicines *Polygonum cuspidatum* and *Ganoderma lucidum*. *Polygonum cuspidatum*, commonly called Japanese knotweed, is a member of the buckwheat family (Polygonaceae) and is therapeutically used in several different ways. Extracts from *P. cuspidatum* appeared to have antipyretic and analgesic activities, as studied in intact mice and rats, while it also depressed the activity of the central nervous system in mice (Lin & Hsu, 1987). As the centrally active constituent, resveratrol was found in this work to have an inhibitory effect ( $IC_{50} = 100 \mu\text{M}$ ) on GABA uptake activity of GAT1 (Fig 3.20). The further kinetic analysis with  $100 \mu\text{M}$  resveratrol suggests a noncompetitive inhibition. It decreased the  $V_{\text{max}}\text{GABA}$  values without changing the apparent binding affinity of GABA for GAT1. It may be that resveratrol reversibly binds to an allosteric site on GAT1 protein, thus preventing GABA from binding to the

active site. *Ganoderma lucidum*, also called “Linzhi” in China, is a basidiomycete, lamellaless fungus belonging to the family of polyporaceae. This medicinal mushroom has been widely used for the treatment of various diseases, including Parkinson's disease (Zhang *et al.* 2009). There are many studies to date on the biological and medicinal functions of the extracts or the components of *Ganoderma lucidum*. LZ acid, LZ-2 and LZ-3 are fractions isolated from crude extract from its fruiting body using successive chromatographic steps. From these fractions, no potential GAT1 inhibitors could be found, while LZ acid and LZ-2 contain certain components which may be GAT1 antagonists.

The role of natural products as a source for remedies has been recognized since ancient times (de Pasquale, 1984, Harvey, 1999). Natural products have been an attractive and economical source for new therapeutic candidate compounds for modern drug discovery due to their tremendous structural diversity. In addition, natural products that are biologically active in assays are generally small molecules which are capable of being absorbed and metabolized easily by the body. A research on the number of chemotherapeutic agents and their sources indicates that over 60% of approved drugs are derived from natural compounds (Cragg *et al.*, 1997). However, only less than 10% of the world's biodiversity has been tested for biological activity, many more useful natural leading compounds are awaiting discovery.

#### **4.4 Expression, characterization and purification of GAT1/GFP recombinant protein**

Purification of GAT1/GFP recombinant protein is quite difficult. In our work, the mouse GAT1 was expressed with GFP tag at C-terminus, which does not affect the relevant functions of GAT1 (Chiu *et al.* 2002). Therefore, GAT1 protein with GFP tag could be purified in a functional form. Besides, the crystal structure of GFP was solved in 1996 (Ormo *et al.* 1996; Yang *et al.* 1996), which should not interfere the further structural studies of GAT1/GFP fusion protein. The GFP tag provides an easy way to control the expression of the protein of interest due to the green fluorescence. Meanwhile, we produced specific monoclonal and polyclonal antibodies for GFP which can be used for further characterization and purification, such as construction of specific immuno-affinity column and immunostaining.

The natural abundance of most membrane proteins is usually too low to isolate sufficient material for functional and structural studies. A prerequisite of purification of the protein

of interest for structural studies is an abundant source of the protein from heterogeneous overexpression. Some simpler mammalian membrane proteins can be produced in bacteria and it is now possible to produce some G protein-coupled receptors (GPCRs) in a functional form at mg/L levels in *E. coli* for crystallisation trials (Petrovskaya *et al.*; White and Grisshammer 2007). However, the expression of mGAT1/GFP fusion protein in bacteria is quite problematic due to its twelve transmembrane domains and its *N*-glycosylation. The folding of membrane proteins is not a trivial process, and it is therefore best to express complex membrane proteins in cells closely related to their native source (Grisshammer and Tate 1995). In this work mammalian and insect cell expression systems were used for the over-expression of the protein of interest. The approach to protein extraction is to first prepare a highly enriched membrane fraction by ultracentrifugation with Percoll and an aqueous two-phase extraction as reported by Park *et al.* (2008). This removes most of the contaminating soluble proteins and is a significant purification step. Following the solubilization of membrane proteins several purification strategies were tried, including the purification by lectin-affinity chromatography, by ion exchange chromatography (using HiTrap QFF anion exchange column) and by immuno-affinity chromatography with subsequent size exclusion chromatography (Fig. 3.31). The former two methods could be applied only for the relatively pure samples but not for the primary purification step. The latter one is proved to be the most successful for the purification of GAT1/GFP fusion protein from the baculovirus expression system. This is mainly due to the comparably high affinity of the GFP tag for the anti-GFP antibodies. In mammalian cells, the latter purification is not sufficient because the *N*-glycan structures of GAT1/GFP are not homogenous. The possible solution is to combine the immuno-affinity chromatography with lectin-affinity chromatography or ion exchange chromatography, which can isolate the GAT1/GFP with only mature *N*-glycans from high mannose structure. Unfortunately, purifications by both chromatography methods result in a quite large amount loss of the target protein while the expression level of GAT1/GFP in mammalian cells is relatively low.

The purified protein should be in their active form in order to elucidate the functional three-dimensional structure. In mammalian cells, GAT1/GFP fusion protein was functionally expressed by determination of the GABA uptake activity. While in insect cells, GABA uptake activity was determined at a very low level, for which a possible explanation is that the terminal trimming including sialylation of *N*-glycans of GAT1/GFP

cannot take place in insect cells. It has been determined previously that the co-translational *N*-glycosylation, but not the terminal trimming of *N*-glycans is involved in the regulation of the correct folding of membrane glycoproteins, since the inhibition of *N*-glycosylation processing by 1-deoxymannojirimycin (dMM) resulting in a mannose rich type of *N*-glycans does not affect either the protein stability or intracellular trafficking (Cai et al. 2005). So the correct folding of GAT1/GFP protein in insect cells should not be affected without terminal trimming including sialylation of *N*-glycans. Therefore, the baculovirus expression system could be used for the purification of GAT1/GFP protein. During the purification procedure, the structural and functional status of GAT1/GFP fusion protein cannot be readily measured in the solubilised state, which is problematic for transporters and simple channels since passage a ligand across a membrane cannot be measured without an intact membrane. In this work, SE-FPLC, cryo-TEM and SDS-PAGE were used to assess the protein stability of GAT1/GFP protein under different buffer conditions.

The elution condition for immuno-affinity chromatography was optimized to prevent denaturation of GAT1/GFP. Different pH was first utilized and only high-pH buffer can effectively elute GAT1/GFP fusion protein. Alternatively, an ionic strength buffer 4M MgCl<sub>2</sub> (pH 6) was also tried to avoid the protein of interest to be denatured by high pH value. The eluted fractions were further purified by size exclusion chromatography and the eluted GAT1/GFP proteins under different elution conditions showed a similar elution profile after SE-FPLC on Superdex 200<sup>TM</sup> column. After TEM analysis, high-salt buffer is thought to be more suitable for the elution of immuno-affinity column since the high-pH elution resulted in an aggregation of most proteins.

Several studies have been shown that GAT1 expressed in an oligomeric formation in the plasma membrane. Gonzales *et al* examined GAT1-expressed *Xenopus laevis* oocytes by freeze-fracture and electron microscopy and GAT1 expression in the plasma membrane led to the appearance of a distinct population of 9-nm freeze-fracture particles which represented GAT1 dimers. The monomer is found to be the functional unit since each monomer functions independently (Soragna *et al.* 2005; Gonzales *et al.* 2007). The example is that the bacteria homologue LeuT was also crystallized as a dimer (Yamashita et al. 2005), but each monomer has its own binding pocket in each monomer indicative of the functional unit. It suggests that monomer of GAT1/GFP fusion protein could be used for further structural analysis. Full-length GAT1 protein comprises 12 highly hydrophobic

transmembrane domains which promotes a strong aggregation behavior of the protein if isolated from the membrane. Hence, purification and monodisperse isolation of GAT1/GFP fusion protein in the absence of detergents which are ubiquitous and necessary reagents to maintain the structural stability of the protein is essentially not possible.

The biochemical study of a membrane protein almost always involves the use of one or more detergents, and the careful consideration of the unique properties of a purifying, stabilizing or crystallizing detergent can sometimes make the difference between success and failure. The central step in this work is the identification of a favorable detergent (or detergents) for GAT1/GFP protein. *n*-Octyl- $\beta$ -D-glucopyranoside ( $\beta$ -OG) is a widely used detergent. It forms fairly compact micelles, and is one of the most successful detergents for membrane protein crystallization. However, it is not suitable for preparation of homogenous GAT1/GFP protein, since the purified protein still tended to form oligomers or higher aggregates if  $\beta$ -OG was used alone for purification.

In order to optimize the stabilization of GAT1/GFP fusion protein, the purification was performed with *n*-Dodecyl- $\beta$ -D-maltoside (DDM) for immuno-affinity column and  $\beta$ -OG for SE-FPLC as used by Yamashita *et al.* (2005). DDM is one of the gentler detergents, and has very favorable properties for maintaining the functionality of more aggregation-prone membrane proteins in solution. Interestingly, below the CMC of DDM isolated GAT1/GFP fusion protein was found to form larger fiber-like structures which may be protein-detergent complexes. When the combination of detergents were used for the purification, certain amount of monodisperse, as well as a mixture of monomers and smaller fiber-like structures were obtained, which was most likely due to the dissociation of the large protein-detergent complexes by the relatively “harsh” detergent  $\beta$ -OG. The behaviors of GAT1/GFP-DDM complexes under different detergent conditions suggest that the detergent's contribution dominates the behavior of protein-detergent complexes. It provides the possibility that the peak fraction containing the monomers of GAT1/GFP fusion protein can be used for a further structural analysis. Meanwhile, an improved detergent condition is still needed to be searched to increase the monodisperse of GAT1/GFP fusion protein after purification.

## 5 Future perspectives

The experiments presented in this work suggest a crucial role of terminal sialic acid in GABA uptake activity of GAT1. A correlation between the reduced GABA uptake activity and the reduced concentration of the terminal sialic acid of GAT1/GFP was revealed. It suggests that the GAT1 activity could be regulated by modification of the *N*-glycosylation or sialylation. Based on this finding, a primary screening model using GAT1 transfected cell culture was established for the selection of the inhibitors of GAT1, as well as inhibitors of *N*-glycan processing or sialic acid biosynthesis. The influence of the candidate compounds on GAT1 activity can quickly determined by performing GABA uptake assay in GAT1/GFP stable trasfected Hek293 cells. Thus the compounds which have inhibitory effect on GAT1 activity could be selected. Combined with Western blotting analysis followed with immunoblotting and lectin staining, we can find whether they have influence on *N*-glycan processing or sialic acid biosynthesis of GAT1 protein. A further study should be performed with the potential targets (such as mannosidase or GNE) of candidate compounds involved in the *N*-glycan trmming or sialic acid biosynthesis process.

Future purification of GAT1 protein should focus on three topics. First of all, a fine condition to obtain high homogeneity and solubility of GAT1/GFP protein is needed to be further modified for the structural studies. Second, a specific antibody of GAT1 protein should be prepared in order to characterize and purify GAT1 without GFP tag by immunostaining and immune-affinity chromatography. Finally, GAT1 protein with other purifications tags could be evaluated.

## 6 Summary

GABA ( $\gamma$ -aminobutyric acid) is the major inhibitory neurotransmitter in the central nervous system (CNS). GABA re-uptake by GABA transporters from the synaptic cleft is one important mechanism in the regulation of GABA concentration in the synaptic cleft. GABAergic dysfunction is involved in a lot of diseases such as Parkinson's disease, epilepsy, chorea Huntingtone and schizophrenia. The GABA transporter 1 (GAT1) belongs to the family of  $\text{Na}^+$  and  $\text{Cl}^-$ -coupled transport proteins and possesses 12 putative transmembrane domains and three *N*-glycosylation sites in the extracellular loop between the transmembrane domain 3 and 4.

Previous work showed that *N*-glycosylation, but not terminal trimming of the *N*-glycan is involved in the attainment of a correctly folded and stable conformation of GAT1, which influences on the protein stability and trafficking to the plasma membrane. It also demonstrated that *N*-linked oligosaccharides side chains of GAT1, in particular their terminal structures, are involved in the GABA transport process of GAT1. Sialic acids are negatively charged terminal sugar residues on the oligosaccharide chains of cell surface or serum glycoconjugates, which are involved in a broad range of biological and pathological processes. In this work, we examined the effect of deficiency, removal or oxidation of surface sialic acid residues on GABA uptake activity to investigate their role in the GABA uptake of GAT1. We found that the reduced concentration of terminal sialic acid on *N*-glycans was paralleled by a decreased GABA uptake activity of GAT1 in CHO Lec3 cells (mutant defective in sialic acid biosynthesis) in comparison to CHO cells. Likewise, either enzymatic removal or chemical oxidation of terminal sialic acids using sialidase or sodium periodate ( $\text{NaIO}_4$ ), respectively, resulted in a strong reduction of GAT1 activity. Kinetic analysis revealed that deficiency, removal or oxidation of terminal sialic acids did not affect the  $K_m$ GABA values. However, deficiency and removal of terminal sialic acids of GAT1 reduced the  $V_{\max}$ GABA values with a reduced apparent affinity for extracellular  $\text{Na}^+$ , suggesting a reduced affinity of GAT1 for  $\text{Na}^+$  and slowed kinetics of the transport cycle. Oxidation of cell surface sialic acids also strongly reduced  $V_{\max}$ GABA without affecting both affinities of GAT1 to GABA and  $\text{Na}^+$ , respectively, indicating further that not only is the negative charge involved, but also the unique structure of sialic acid itself is crucial for the GABA uptake process. These results demonstrated for the first time that the terminal sialic acid of *N*-linked oligosaccharides of GAT1 is directly involved in regulation of GABA uptake process of GAT1.

Based on the correlation between the reduction of the GABA uptake activity and the reduction of the terminal sialic acid concentration of GAT1/GFP, a primary screening model using GAT1 transfected cell culture was established for the selection of potent inhibitors of

GAT1 activity by regulating *N*-glycan trimming or sialic acid biosynthesis. The influence of the candidate compounds on GAT1 activity can quickly determined by performing GABA uptake assay in GAT1/GFP stable trasfected Hek293 cells. Thus the compounds which have inhibitory effect on GAT1 activity could be selected. In this work, several synthetic *N*-acyl hexosamines, such as GlcNProp, GlcNCyclo, GlcNHex, GlcNAc-Acetamido and 3-*O*-Met-GlcNAc was found to have inhibitory effect on GABA uptake activity of GAT1 as inhibitors of *N*-glycan trimming or sialic acid biosynthesis. Besides, several naturally occurring compounds were used for selection of potent inhibitors on GABA uptake activity of GAT1. Resveratrol was found to exhibit a typical non-competitive inhibition on GABA uptake of GAT1.

In order to perform structural analysis of GAT1 protein, GAT1/GFP fusion protein was functionally expressed in mammalian (Hek293) cells, as well as in insect *Sf9* cells by BAC-TO-BAC<sup>TM</sup>-Baculovirus expression system. Different chromatography methods including affinity chromatography, ion-exchange chromatography and size exclusion chromatography were tested for the purification of this protein. A two-step purification procedure for GAT1/GFP fusion protein from insect *Sf9* cells was established containing immuno-affinity chromatography using self-prepared anti-GFP and size exclusion-FPLC. Certain amount (200-300 µg per 400-600 mL culture) GAT1/GFP protein can be purified, which was analysed by transmission electron microscopy (TEM) analysis. Different buffer conditions were tested to obtain homogenous GAT1/GFP fusion protein. TEM results showed different formations of purified GAT1/GFP fusion protein with different detergents and certain amount of the monomers of GAT1/GFP fusion protein has been isolated.



## 7 Zusammenfassung

GABA ( $\gamma$ -Aminobuttersäure) ist der wichtigste inhibitorische Neurotransmitter des Zentralnervensystems (ZNS). Die Wiederaufnahme von GABA durch GABA-Transporter ist ein bedeutender Mechanismus zur Regulation der Konzentration dieser Substanz im synaptischen Spalt. Störungen in der GABA-Regulation werden mit vielen Krankheiten wie beispielsweise Parkinson, Epilepsie, Chorea Huntington oder Schizophrenie in Zusammenhang gebracht. Der GABA-Transporter 1 (GAT1) gehört zu der Familie der  $\text{Na}^+/\text{Cl}^-$  gekoppelten Transporter. Es besitzt 12 vermeintliche Transmembrandomänen (TMD) und drei N-Glykosylierungsstellen in der extrazellulären Schleife zwischen der dritten und vierten TMD.

Frühere Arbeiten haben gezeigt, dass N-Glykosylierungen und nicht das terminale Trimmen von N-Glykanen für die korrekte Faltung und stabile Konformation von GAT1 eine Rolle spielen; was wiederum die Proteinstabilität und den Transport an die Plasmamembran beeinflussen. Es wurde zudem gezeigt, dass N-Glykan Seitenketten von GAT1, insbesondere die terminalen Oligosaccharide, am GABA-Transportprozess von GAT1 beteiligt sind.

Sialinsäuren sind terminale negativ geladene Zuckerstrukturen an Oligosaccharideketten auf Zelloberflächen oder Serumglykokonjugate, die an vielfältigen biologischen und pathologischen Prozessen beteiligt sind. In der vorliegenden Arbeit untersuchten wir die Rolle von Sialinsäuren auf die GABA-Wiederaufnahmeaktivität von GAT1. Wir stellten fest, dass die Erniedrigung der Sialinsäurekonzentration auf Zelloberflächen mit der Abnahme der GABA-Wiederaufnahmeaktivität korreliert: In CHO Lec3-Zellen mit defekter Sialinsäurebiosynthese war diese Aktivität im Vergleich zu normalen CHO Zellen erniedrigt. Auch den enzymatischen Verdau durch Sialidase sowie chemische Oxidation von terminalen Sialinsäuren durch Natriumperiodat ( $\text{NaIO}_4$ ) führte zur Reduktion der GAT1-Aktivität. Kinetische Analysen ergaben, dass das Fehlen von terminalen Sialinsäuren - sei es durch Verdau oder Oxidation - keinen Einfluss auf den  $K_m$ -Wert für GABA hat. Vielmehr wurde dadurch der  $V_{\max}$  für GABA reduziert; einhergehend mit einer offensichtlichen Reduktion der Affinität für extrazelluläres Natrium. Das Fehlen von terminalen Sialinsäuren führt demnach zu einer reduzierten Affinität von GAT1 zu  $\text{Na}^+$  und einer verlangsamten Kinetik des Transportzyklus. Die Oxidation von Oberflächensialinsäuren reduzierte den  $V_{\max}$  von GAT1 stark, ohne dabei die Affinität für GABA und  $\text{Na}^+$  zu beeinflussen. Diese Tatsache weist darauf hin, dass nicht nur die negative Ladung von Sialinsäuren, sondern auch ihre Struktur eine bedeutende Rolle beim GABA-Wiederaufnahmeprozess spielt. Mit dieser Arbeit konnte zum ersten Mal gezeigt werden, dass terminale Sialinsäuren auf N-Glykanen am GABA-Wiederaufnahmeprozess von GAT1 direkt beteiligt sind.

Aufgrund der Korrelation zwischen der Reduktion der terminalen Sialinsäuren auf GAT1 und dessen GABA-Wiederaufnahmeaktivität wurden erste Screenings hinsichtlich der Wirkung von mutmaßlichen Sialinsäurebiosyntheseinhibitoren auf die GAT1-Aktivität in GAT1-transfizierten HEK293-Zellen durchgeführt. In dieser Arbeit wurden einige synthetische *N*-Acylhexoamine auf ihre inhibitorische Wirkung hinsichtlich der GABA-Wiederaufnahme hin überprüft. Verbindungen wie GlcNProp, GlcNCyclo, GlcHex, GlcNAc-Acetamido und 3-*O*-Met-GlcNAc wurden als Inhibitor der Sialinsäurebiosynthese und GABA-Aktivität von GAT1 identifiziert. Neben vielen natürlichen Substanzen, die hier ebenfalls untersucht wurden, zeigte Resveratrol eine typische nicht-kompetitive Inhibition der GAT1-Aktivität.

Um strukturelle Analysen des GAT1-Proteins durchzuführen, wurde GAT1/GFP als funktionelles Fusionsprotein sowohl in die Säugerzelllinie HEK293 als auch die Insektenzelllinie Sf9 über das BAC-TO-BAC™-Baculovirus-System exprimiert. Unterschiedliche Chromatographiemethoden einschließlich Affinitätschromatographie, Ionaustauschchromatographie und Gelfiltration wurden für die Reinigung dieses Proteins getestet. Eine zweistufige Reinigungsprozedur mit GFP-Immunoaffinitätschromatographie und Gelfiltration konnte für das GAT1/GFP Fusionsprotein von Sf9 Zellen erfolgreich etabliert, und das so aufgereinigte GAT1/GFP unter dem Transmissionselektronenmikroskop (TEM) analysiert werden. Unterschiedliche Pufferbedingungen wurden getestet, um homogenes GAT1-GFP Fusionsprotein zu erhalten. TEM Ergebnisse zeigten unterschiedliche Formationen von gereinigtem GAT1-GFP in unterschiedlichen Detergenzien und eine bestimmte Menge von monomerem GAT1-GFP Fusionsprotein konnten isoliert werden.

## 8 Materials and methods

### 8.1 Materials

#### 8.1.1 Chemicals

Salts and buffer reagents were purchased in analytical quality from AppliChem (Germany), Calbiochem (Germany), ICN (Germany), Merck Eurolab (Germany), Roche (Germany), Roth (Germany) or Sigma (Germany).

Special agents were purchased as listed below:

Amino acids	Sigma (Germany)
N, N'-Bisacrylamide	Serva (Germany)
BSA Standard	Pierce (USA)
CHAPSO	Calbiochem (Germany)
Dextran T500	Sigma (Germany)
<i>n</i> -Dodecyl- $\beta$ -D-maltoside	Alexis Biochemicals (Switzerland)
4-Hydroxycinamic acid	Sigma (Germany)
Luminol	Sigma (Germany)
3-Mercapto-1,2-propandiol	Merck (Germany)
Nitrocellulose-Membrane	Schleicher and Schüll, Dassel
Nonidet-P40 (NP40)	USBiological (USA)
<i>n</i> -Octyl- $\beta$ -D-glucopyranoside	BACHEM (Switzerland)
Percoll	GE Healthcare (Germany)
PEG 3350	Sigma (Germany)
PEG 400	Sigma (Germany)
PMSF	Sigma (Germany)
Silver nitrate	Sigma (Germany)
Triton x-100	Sigma (Germany)

Sources of other reagents and materials were stated in the text of Methods.

#### 8.1.2 Cells and bacteria

##### Mammalian cells

CHO cell line (Chinese Hamster Ovary cell line)	ATCC (USA)
CHO Lec3 cell line (Chinese Hamster Ovary Mutants)	Stanley <i>et al.</i> , 1981
Hek293 cell line (Human Embryonic Kidney 293 cells)	ATCC (USA)

### **Insect cells**

Sf9/Sf900 Invitrogen (USA)

### ***E. coli* Bacteria strains**

TOP10 competent cells Invitrogen (Netherlands)

DH10BAC™ competent cells Invitrogen (Netherlands)

### **8.1.3 Cell culture materials and mediums**

Sterile disposable materials were purchased from Corning (Netherland), Falcon (Germany) or Sarstedt (Germany).

#### Mediums and regents for cell culture

Alpha medium	Lonza (Belgium)
DMEM medium	Biochrom (Germany)
EDTA (VERSEN) 1% ig in PBS	PAN Biotech (Germany)
Fetal calf serum	Perbio (Germany)
G418 Sulphate	PAA (Austria)
L-Glutamine	PAN Biotech (Germany)
Penicillin/streptomycin	PAN Biotech (Germany)
Sodium pyruvate	PAN Biotech (Germany)
Trypsin/EDTA 0.05/0.02% ig in PBS	PAN Biotech (Germany)
Adenosin	Sigma (Deutschland)
Guanosin	Sigma (Deutschland)
Uridin	Sigma (Deutschland)
Cytidin	Sigma (Deutschland)
Thymidin	Sigma (Deutschland)
Ampicillin/Kanamycin	Boehringer (Germany)
Yeast extract	Roth (Germany)
Peptone	Roth (Germany).
Agar	Roth (Germany).
Sf9 II medium	Invitrogen (USA)
Fetal calf serum	Invitrogen (USA)

### 8.1.4 Vectors

pEGFP-N1 Reporter vector	BD Bioscience (Germany)
pFASTBAC1 Baculovirus expression vector	Invitrogen (USA)
pFASTBACHTa Baculovirus expression vector	Invitrogen (USA)

### 8.1.5 Primers

All primers were synthesized by MWG Biotech (Ebersberg, Germany)

M13 For	5'-GTA AAA CGA CGG CCA GT-3'	5' IRD 800
M13 Rev	5'-CAG GAA ACA GCT ATG ACC ATG -3'	5' IRD 700
GFP-N-R	5'-CGG ACA CGC TGA ACT TGT -3'	5' IRD 800
GFP-870R	5'-CTG AAG CAC TGC ACG CCG TAG -3'	5' IRD 800
BArc	5'-AAA GCA AGT AAA ACC TCT AC-3'	5' IRD 700
GAT-1-c	5'-CTG TAC AAC TCC TTC ACC AC -3'	5' IRD 700
GAT-2-c	5'-CTT CGA CTT CCT CAT GTC CT -3'	5' IRD 800
GAT-1910C	5'-CAT GTT CCT CAC CCT GAA GG -3'	5' IRD 700
pFastBac1-For	5'-TGG CTA CGT ATA CTC CGG AA-3'	5' IRD 800
pFASTBAC-Rev	5' -TTT CAG GTT CAG GGG GAG GT-3'	5' IRD 700

### 8.1.6 Markers and Enzymes

Precision Plus Protein™ standard

All Blue/Dual Color/Unstained Standard Bio-rad (USA)

Gel filtration standard Bio-rad (USA)

GeneRuler™ 1 Kb DNA Ladder Fermentas (Germany)

Neuraminidase (Sialidase)

from *Arhrobacter ureafaciens* Roche (Germany)

Restriction endonucleases

including buffers Fermentas (Germany)

### 8.1.7 Antibodies

Rabbit polyclonal anti-GABA Transporter (GAT1) IgG Abcam (UK)

Rabbit polyclonal anti-Rat GAT1 IgG Alpha Diagnostic (Germany)

Monoclonal anti-GFP (Mouse) AG Fan/Reutter, Charité

Polyclonal anti-GFP (Rabbit) AG Fan/Reutter, Charité

HRP $\alpha$ -Rabbit EnVision+®	Dako Cytomation (USA)
HRP $\alpha$ -Mouse EnVision +®	Dako Cytomation (USA)
Peroxidase conjugated Goat anti rabbit	Sigma (Germany)
Peroxidase conjugated Rabbit anti mouse	Sigma (Germany)

### **8.1.8 Lectins**

FITC-Labeled Lectin	EY Laboratories (USA)
Texas Red-Labeled Lectin	EY Laboratories (USA)

### **8.1.9 Kits**

Accuprime pfxSupermix kit	Invitrogen (USA)
AEC substrate kit	Calbiochem (Germany)
NucleoSpin® Plasmid kit	Macherey-Nagel (Germany)
QIAprep® Spin Midi-kit	QIAGEN (Germany)
QIAprep® Spin Maxi-kit	QIAGEN (Germany)
SilverSNAP® Stain Kit II	Pierce (USA)
Glycan Differentiation Kit	Roche (Germany)

### **8.1.10 Laboratory equipments and instruments**

#### Centrifuges:

Centrifuge Megafuge 1.0	Heraeus
Centrifuge 3-18K	Sigma Laborzentrifugen GmbH
Cold Centrifuge RC-5B	Sorvall
Desk Centrifuge Biofuge 13	Heraeus
Desk Centrifuge Biofuge fresco	Heraeus
Mini centrifuge	National Labnet
Multifuge 1 L-R	Heraeus
Ultracentrifuge	Beckmann

#### Incubators:

Incubator BK6160	Heraeus
Shaking Incubator Novotron	Infors
Shaking Incubator IH50	Incutec GmbH

Shaking Incubator Multitron

Infors

STERI-CULT 200 Incubator

Forma Scientific

Other equipments:

Autoclave Varioklav

Sauter-Schubert

ÄKTA purifier

GE Healthcare

Axio observer fluorescence microscope

Carl Zeiss

Clean bench Faster 1

BioFlow-Technik

FACS Vantage cell-sorter

Becton Dickinson

HERA safe

Thermo Electron Corporation

Inverted microscope DIAVERT

Leitz

Laminar Airflow clean bench 1.8

Holten LaminAir

Liquid Scintillation Counter Tri-Carb 1900 CA

Packard

Molecular Imager ChemiDoc XRS + System

Bio-rad

Mastercycler ep gradient S

Eppendorf

Microplate reader Spectra Rainbow

TECAN

Microwaveoven RZV2G,

Sharp

pH-Meter pH 211

Hanna Instruments

Pipettes

Eppendorf

Power-Supply Power-Pac 1000

Bio-rad

SDS-PAGE-System Mini-Protean III

Bio-rad

Sonicator Labsonic

Braun Biotech GmbH

Spectral photometer Ultrospec 500 *pro*

Amersham Biosciences

Thermoblock Thermomixer Compact

Eppendorf

Water bath M16

Harry Gestigkeit GmbH

Weigh handy/1602 MP

Sartorius

## 8.2 Methods

### 8.2.1 Molecular biological methods

#### 8.2.1.1 Generation of competent *E.coli* cells

Competent cells have the ability to take up foreign ("naked") DNA from its environment. Normally bacteria cells are treated with CaCl<sub>2</sub> to make them transiently permeable to DNA (Dagert and Ehrlich, 1979).

Briefly, 2 ml overnight culture of TOP10 cells was inoculated with 100 ml fresh SOC medium and grown at 37°C and 225 rpm to an OD<sub>600</sub> between 0.3 to 0.5. The cells were harvested by centrifugation at 5000 rpm for 10 min. The cell pellets were then resuspended in 20 ml ice-cold CaCl<sub>2</sub> (100 mM) and incubated on ice for 30 min. After centrifugation, the supernatants were removed. 1 ml cold CaCl<sub>2</sub> (100 mM) was added to cell pellets, mixed gently and incubated on ice for 1 h. The cells were either used immediately for transformation or stored with 20% glycerol (v/v) at -80°C in aliquots of 100 µl each.

DH10 BAC<sup>TM</sup> competent cells were prepared for the transposition of bacmid-DNA with pFASTBAC<sup>TM</sup> 1-Vektor and Roti<sup>®</sup>-Transform according to the manufacturer's instructions.

SOC medium	20 g/l Peptone
	5 g/l Yeast extract
	4 g/l MgCl <sub>2</sub>
	0.5 g/l NaCl
	186 mg/l KCl
	3.6 g/l Glucose

#### 8.2.1.2 Transformation of *E.coli* competent cells

The incorporation of foreign DNA by *E.coli* leads to the modification of their total genetical material, thereby to their transformation.

##### Method 1

For the transformation of 100 µl competent cells, 100 ng plasmid-DNA or 10-20 µl ligation products were added to the cells on ice and incubated for 30 min. After heat shocking the cells at 42°C for 45 sec and regeneration on ice for 2 min. 250 µl SOC medium was added and mixed briefly. The cells were incubated for 1 h at 37°C in a thermomixer with mixing at 500 rpm. 100 µl aliquots were plated on solid LB-agar medium supplemented with respective antibiotics and the plates incubated over night at 37°C.



## Method 2

In brief, dilute some fresh overnight culture with LB medium 1 to 100 times. Allow the bacteria grow under shaking at 37°C to an optimum OD<sub>600</sub> between 0.4 and 0.5. 1.9ml of competent cells are collected and resuspended in 190µl of LB liquid medium. Add 90µl ice-cold Roti<sup>®</sup>-Transform 1 and 10 µl Roti<sup>®</sup>-Transform 2, and mix by vortexing gently for each step. After incubate the transformation mixture for 5 min on ice, add 1-5 ng plasmid DNA or half a ligation preparation (5-10 µl volume) and mix by gentle pipetting. Incubate the transformation preparations on ice for 30 min. Bacteria are incubated at 37°C for 1 h before being plated on LB-agar plates containing the suitable antibiotic to select the transformed bacteria. Agar plates are incubated at 37°C overnight to allow for the growth of bacterial colonies.

LB liquid medium	1% Pepton 0.5% Yeast extract 1% NaCl, in H <sub>2</sub> O
LB-agar	15 g Agar in 1 l LB liquid medium 12 g Agar in 1 l LB liquid medium for DH10BAC <sup>TM</sup> -cell
Antibiotic stock solutions	50 mg/ml Ampicillin 25 mg/ml Chloramphenicol 50 mg/ml Kanamycin 10 mg/ml Tetracyclin 7 mg/ml Gentamycin
For blue-white selection	40 mg/ml Isopropyl-1-thio-β-D-galactosid (IPTG) in H <sub>2</sub> O  1:1000 200 mg/ml Bluo-Gal in DMSO 1:2000

### **8.2.1.3 Preparation of plasmid-DNA from *E.coli***

After preparation of *E.coli* overnight cultures, 2 ml were aliquoted in tubes and centrifuged at 5,000 rpm for 5 min. The bacteria pellets were then homogeneously resuspended in 200 µl Buffer 1. Then 200 µl of Buffer 2 was added and mixed carefully. Incubation was done at RT for 5 min and 200 µl cold Buffer 3 was added. The suspensions were mixed carefully and incubation done on ice for 10 min. Following this, the samples were centrifuged for 10 min at 13,000 rpm and 4°C to pellet cellular proteins and DNA, the supernatants decanted in clean tubes and the centrifugation step was

repeated. Supernatants from this centrifugation were put in clean tubes, mixed thoroughly with 1 ml isopropanol and incubated at 4°C for 10 min to precipitate the plasmid DNA.

The precipitated DNA was pelleted by a 15 min centrifugation at 13,000 rpm at 4°C and the DNA pellet washed with 500 µl of 80% ice cold ethanol. The plasmid DNA was then air dried, resuspended in 50 µl sterile ddH<sub>2</sub>O or TE buffer and the concentration determined. Storage was done at -20°C.

For the small scale plasmid preparation, 500 -1,000 µg total plasmid-DNA/ml bacteria culture was extracted. For the extraction of large amounts of plasmid DNA, 50-200 ml overnight cultures were used and the extraction done with the Qiagen Maxi-preparation kit (Qiagen) according to the user manual.

Buffer 1 (pH 8.0)    25 mM Tris-HCl  
                          10 mM EDTA  
                          100 µg/ml RNase A

Buffer 2            0.2 M NaOH,  
                          1% SDS (w/v)

Buffer 3            3 M Na-acetate, pH 4.8

TE buffer           10 mM Tris-HCl, pH 8  
                          1 mM EDTA

#### **8.2.1.4 Determination of DNA concentration**

The amount of DNA in aqueous solution can be quantified by measuring the absorbance at 260 nm. At this wavelength, an extinction of 1.0 corresponds to the concentration of 50 µg/ml of double-stranded DNA.

The purity of a DNA preparation can be assessed by measuring the absorbance at  $\lambda= 280$  nm at the same time: For pure samples, the ratio  $OD_{260}/OD_{280}$  should amount between 1.8 and 2.0. Lower values indicate a contamination with protein or phenol. To analyze the integrity of isolated nucleic acid, an aliquot of the DNA or RNA solution was loaded on an agarose gel parallel with a DNA ladder with defined masses.

#### **8.2.1.5 Digestion with restriction endonucleases**

Restriction endonucleases are enzymes that catalyze the hydrolysis of the DNA

phosphodiester bond. They are frequently used in molecular biology to prepare DNA fragments for ligation or to analyze DNA plasmids. Restriction endonucleases recognize specific DNA sequences (4-8 bp) that are oftentimes palindromic. Digestion of double-stranded DNA with restriction endonucleases either produces blunt ends or sticky ends, depending on the nature of the enzyme.

1 unit (1U) of a restriction enzyme is defined as the amount of enzyme that catalyzes the cleavage of 1 µg DNA in 1 h. 1-50 µg DNA was digested for 1 to 4 h at 37°C with 0.1-1 U of appropriate restriction enzymes from Fermentas (Germany) or Invitrogen (Germany) in their respective buffer. The digested DNA was then analysed by agarose-gel electrophoresis.

#### **8.2.1.6 Agarose gel electrophoresis**

Linearized DNA fragments can be separated by agarose gel electrophoresis according to their sizes. The DNA is detected by the means of ethidium bromide, a dye that intercalates into the DNA double helix.

Agarose is resuspended in TAE buffer at the appropriate concentration (0.5-2% agarose). The suspension is heated until the agarose is completely dissolved. The solution is cooled to 50-60°C and poured into a horizontal gel chamber that is stuffed with a comb. Once the gel has become solid, it can be loaded with DNA.

DNA samples are mixed with dye solution (6x). Samples are electrophoresed at ~100 V for 1 h using TAE buffer as the running buffer. Then the gel was incubated in TAE-Buffer with ethidium bromide (0.5 µg/ml) for 10-15 min. DNA is detected by the means of UV irradiation (366nm).

TAE buffer	40 mM Tris/HCl, pH 8 5 mM Sodium acetate 1 mM EDTA
------------	--

Dye solution (6x)	50 % (v/v) Glycerin 50 mM EDTA 0,05 ‰ (w/v) Bromophenol blue
-------------------	--

#### **8.2.1.7 DNA sequencing**

DNA sequencing is based on the method of chain termination that was originally developed by Sanger (Sanger et al., 1977). It relies on the polymerase chain reaction as described in 7.2.1.8. However, in addition to the deoxynucleotides, 2',

3'-dideoxynucleotides are added. Whenever the dideoxynucleotides are incorporated into the growing DNA strand, chain termination occurs because the dideoxynucleotides do not possess a free 3' hydroxyl group. As a consequence, the PCR products constitute a heterogeneous mixture of DNA fragments with each fragment having incorporated exactly one dideoxynucleotide at the 3' end. Dideoxynucleotides are coupled to different fluorescent dyes. Once the PCR is complete, the fragments can be separated by gel electrophoresis or capillary electrophoresis. The DNA sequence is determined by measuring the fluorescence signal that corresponds to each fragment.

All sequencings of DNA were performed with fluorescence-labelled sequencing primers by using the Thermo Sequenase<sup>TM</sup> Primer Cycle Sequencing Kit (Amersham Biosciences) according to manufacturer's instructions.

1.3 µg template DNA and 2 pmol sequencing primers labelled with infrared fluorescent dye (IRD700 and IRD800) dissolved in ddH<sub>2</sub>O with final volume 13 µl. 3 µl of this mixture was transferred to four tubes containing 3 µl of one of the sequencing reagents A, C, G or T. Besides the dNTPs (Deoxynucleoside triphosphate) each of the reagents contains an excess of one of the ddNTPs (Dideoxynucleoside triphosphate) which leads to the interruption of the polymerisation reaction. The reaction was run with the following program: 2 min 94°C, 25× (20 sec 94°C / 20 sec 45-60°C / 20 sec 72°C), 72°C 3 min, + 5 µl stop solution

The reaction mixtures were run on polyacrylamide-gels (6%) and analysed in an automated sequencing facility (LI-COR 4200, MWG-Biotech, Germany).

### **8.2.1.8 Polymerase Chain Reaction (PCR)**

Polymerase chain reaction (PCR) is a method that allows the amplification of specific DNA fragments *in vitro*. It capitalizes on the property of the DNA polymerase to extend a short piece of double-stranded DNA. Specificity is determined by two oligodeoxynucleotides that hybridize to the 5' and the 3' end of the fragment to be amplified. A single reaction cycle begins with denaturation of the DNA into single strands then the binding (annealing) of the primer to the single strands at primer suitable temperatures, followed by amplification of the DNA matrix by the polymerase.

Since the bacmid DNA is >135 kb, it is better to use PCR to confirm the insertion of the gene of interest in bacmid than using classical restriction endonuclease digestion analysis. For analytical purpose, PCR was done with the Accuprime pfx Supermix kit (Invitrogen) according to the manufacturers instructions. PCR was performed in a standard reaction

sample of 25  $\mu$ l total volume composed of the following:

Template DNA: 10 - 200 ng

M13 primers (forward and reverse): 200 nM each

Accuprime pfx Supermix: 22  $\mu$ l

The PCR was performed under the following condition:

Step 1	Initial denaturation	95°C, 2 min
Step 2	Denaturation	95°C, 1 min
Step 3	Annealing	55-60°C, 1 min
Step 4	Elongation	72°C, 2 min/1kb DNA
Step 5	Proofreading	72°C, 10 min

Steps 2-4 were repeated 24-30 times.

#### **8.2.1.9 Expression of recombinant proteins in Baculovirus system**

In this work, the BAC-TO-BAC<sup>TM</sup>- Baculovirus expression system was utilized for the expression of recombinant protein in Sf9 insect cells. The system is based on site-specific transposition of a gene of interest from a pFastBac<sup>TM</sup> donor plasmid into a baculovirus shuttle vector (bacmid) propagated in *E. coli* which is then inserted into insect cells with the help of Baculovirus particles.

Recombinant bacmids are constructed by transposing a mini-Tn7 from a donor plasmid (pFASTBAC<sup>TM</sup>1) to the mini-attTn7 attachment site on the bacmid with Tn7 transposition functions provided in *trans* by a helper plasmid. Positive clones carrying the gene of interest, in which a *lacZ* deletion is completed, remain white in the presence of Bluo-gal and the inducer IPTG.

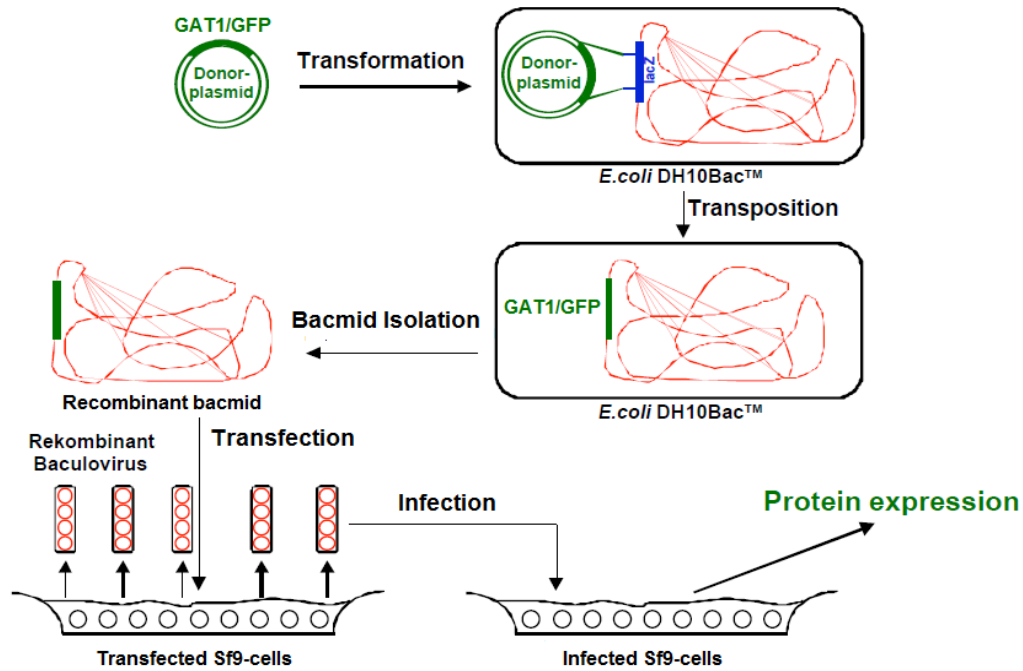


**Figure 8.1 BAC-TO-BAC®-Baculovirus-Expressionssystem.** Generation of recombinant Baculovirus and protein expression in insect cells.

### 8.2.1.9.1 Cultivation of insect cells

Sf9 cells were cultured at 27°C either as suspension cultures in shakers (Multitron; HAT-Infors, Switzerland) at 115 rpm or as monolayer cultures in culture incubators (Heraeus, Germany). As soon as the cells reached a density of  $1 \times 10^7$  cells/ml, they were diluted 1:10 with fresh medium (usually twice a week).

For long term storage of insect cells, cells were cultured in suspension pelleted and resuspended at a density of  $2 \times 10^8$  cells /ml in 90% FCS (v/v) and 10% (v/v) DMSO. Cryotubes were filled with aliquots of 1.5 ml, frozen gradually in - 80°C and then stored in liquid nitrogen. When needed frozen cells were thawed at RT and cultured in fresh media on plates for 24 h. Dying non-adhering cells were then removed by aspiration and viable adhering cells cultured in fresh media in suspension.

**Sf9-cells:** Sf900 II medium  
2mM Glutamine  
10% FCS

**Sf900-cells:** Sf900 II medium  
2mM Glutamine

#### **8.2.1.9.2 Generation of recombinant Bacmid DNA**

In this work the preparation of GAT1/His and GAT1/GFP recombinant Bacmid DNAs were done by first cloning the cDNA into the MCS of the pFASTBAC1 donor vector then using the plasmids to transform the *E. coli* cell line DH10Bac as stated above.

1 µg plasmid-DNA was added to 100 µl competent DH10 Bac cells and incubated on ice for 30 min. After heat shocking at 42°C for 45 sec, the cells were incubated on ice for 2 min. 900 µl SOC medium was added and mixed briefly. The cells were incubated for 4 h at 37°C in a thermomixer with mixing at 500 rpm. 100 µl aliquots were plated on solid LB-agar selection medium containing the antibiotics kanamycin, tetracycline and the substrates blueo-gal and IPTG. Positive clones remained white and were selected with blue-white selection after the plates were incubated for 48 h at 37°C.

Overnight cultures of the white clones were prepared in LB-Medium containing kanamycin and tetracycline and the recombinant Bacmids were purified with the Plasmid purification kit (Qiagen).

#### **8.2.1.9.3 Analysis of Bacmid DNA**

After determining the bacmid DNA concentration, 1 µg DNA was loaded on 0.5% agarose gels and electrophoresed at a constant voltage of 20v overnight (16-19 h). The DNA bands were detected under UV after staining in ethidium bromide.

A second analysis of the recombinant Bacmid DNA was done by PCR with specific primers for the gene of interest in order to confirm that the gene of interest has transposed to the bacmid.

#### **8.2.1.9.4 Generation of recombinant virus**

Recombinant baculoviruses were generated using the CellFECTIN® Reagent according to the manufacturer's instructions. In brief, for each transfection,  $9 \times 10^5$  Sf9 insect cells per well (6 well plate) were seeded in 2 ml Sf900 II medium and allow cells to adhere to the plate for at least 1 h at 27°C. Meanwhile, two solutions were prepared. 5 µl of Bacmid-DNA sample was diluted in 100 µl Sf900-II medium without serum and antibiotics. 6 µl Cellfectin reagents was diluted in 100 µl Sf900-II medium without additives and mixed thoroughly. Both solutions were combined and mixed carefully, and

then incubated for 45 min at RT enables the formation of a DNA-lipid complex. After the incubation, 800  $\mu$ l Sf900-II medium without additives was added to transfection mixture and mixed lightly. The cells were washed once with 2 ml Sf900-II medium without additives and were incubated with the diluted lipid-DNA complexes for at least 5 h at 27°C. Then the transfection mixture was aspirated carefully and 2 ml/well Sf900-II medium containing glutamine and serum was added to the cells. The cells were then incubated for 5 days at 27°C to generate the recombinant virus. The supernatant containing the recombinant virus was harvested 5 days post transfection. The initial viral stock (passage 1) was stored at 4°C.

#### **8.2.1.9.5 Amplification of virus**

In order to produce high virus titer for high expression of recombinant protein in insect cells, 30 ml  $0.5 \times 10^6$  cells /ml Sf9 insect cell suspension is infected with 0.5 ml of the initial virus stock and incubated for 5 days at 27°C with shaking at 115 rpm. The supernatant containing recombinant virus (passage 2) was harvested by centrifugation for 5 min at 2,000 rpm. The second amplification was repeated.

Virus titers were analyzed by a plaque assay (see 4.1.9.6).

#### **8.2.1.9.6 Plaque Assay**

$1.5 \times 10^6$  Sf9 cells per well were transferred to a 6 well plate and incubated for 1 h at 27°C for the cells to adhere to the plate. Cells were infected with serial dilutions ( $10^{-3}$  to  $10^{-7}$ ) of 500  $\mu$ l the recombinant baculovirus (5 dilutions per virus and 1 negative control medium without virus) for 2 h at RT. Meanwhile, 14 ml Sf900-II medium was warmed at 45°C and 7 ml solution of a 3% sterile sea-plaque agarose (Biozym) was boiled to melt the agarose and then kept at 45°C in the water bath. Once the infection was completed, the pre-warmed medium and agarose solution were then mixed thoroughly. The virus was aspirated from the 6-well plates and the cells were overlaid with 3 ml diluted agarose solution per well. Once the agarose had become solid at RT, it was overlaid with 1ml of Sf900-II medium per well to prevent the overlay from drying out. The plates were then incubated for 5 days at 27°C for plaque formation.

To score for production of viral, the medium was aspirated from the wells and 200  $\mu$ l of a sterile 5 mg/ml MTT (tetrasodium thiazolal blue bromide) solution was added per well. The MTT assay is a viability assay that allows the discrimination between alive



(uninfected) and dead (infected cells). Infected cell colonies were counted to calculate the viral titer after the incubation for 2 h at 27°C.

Based on the fomular:

$$\text{Virus titre} = \frac{\text{Number of plaques counted}}{\text{Dilution coefficient} \times (\text{infection volume per well in ml})}$$

the virus titer in pfu (number of virus particles per cell) was deduced and the multiplicity of infection (MOI), given as pfu/ml was calculated.

### 8.2.1.9.7 Expression of recombinant protein in insect cells

Sf9 cells were infected in 100 ml suspension cultures at a density of  $2 \times 10^6$  cells/ml. For infection, cells were infected with the recombinant virus to final MOI rate 1, then incubated at 27°C and shaking at 115 rpm for 3 days. Infected cells were harvested by centrifugation (2000 rpm for 5 min.).

## 8.2.2 Cell biological methods

### 8.2.2.1 General cultivation conditions

All mammalian cells were cultured in a cell culture chamber (Heraeus 6000, Kendro Laboratory Products) at 37°C in the respective medium with 5% CO<sub>2</sub> and >90% humidity.

The cell lines and their culture mediums are stated as following:

For CHO cell line

$\alpha$ -MEM -Medium (500 ml)	Ribonucleoside (2,5 mg G, 5 mg A, C, T each) 2 mM L-Glutamine 50.000 U Penicillin/streptomycin-Lsg. 10 % v/v inactive FKS
--------------------------------	--

$\alpha$ -MEM -Selection-Medium	600 or 400 mg/l G418 (Geneticin) in $\alpha$ -MEM -Medium
---------------------------------	---

For Hek293 cell line

DMEM -Medium (500 ml) w 4,5 g/l D-Glucose	1 mM Na-Pyruvat 2 mM L-Glutamine 50.000 U Penicillin/streptomycin-Lsg. 10 % v/v inactive FKS
--	---

DMEM -Selection-Medium	400 mg/l G418 (Geneticin) in DMEM -Medium
------------------------	---

For CHO Lec3 cells, serum free growth was accomplished by gradually reducing the fetal calf serum concentration to zero. As soon as the cells reached 80-90% confluency, they were washed with PBS and detached by addition of 0.05% EDTA. Cells were seeded in fresh medium on new culture plates at different dilutions in order to ascertain optimal growth.

PBS (10×), pH 7,4      140 mM NaCl  
                                  3 mM KCl  
                                  10 mM Na<sub>2</sub>HPO<sub>4</sub>  
                                  1,5 mM KH<sub>2</sub>PO<sub>4</sub>

**Cell storage and reculture:** For long term storage, mammalian cells are frozen and maintained at -175°C in liquid nitrogen to keep the viability. The cells were pelleted and then diluted in FCS containing 10% DMSO (against cryogenic injuries) and transferred in 1 ml aliquots to cryogenic vials. The vials were frozen at -20°C for at least 2 h, at -80°C for 24 h then finally kept in a liquid nitrogen storage tank.

To reculture the cells, vials were removed from the nitrogen and thawed immediately at 37°C. After centrifugation, the cell pellets were then transferred to prewarmed culture media and were cultured as above.

#### **8.2.2.2 Stable transfection of GAT1/GFP in CHO and CHO Lec3 cells**

CHO cells ( $2 \times 10^5$ ) were seeded in a 60 mm dish and grown overnight to reach 40-50% confluent, then transfected with 5-10  $\mu$ g GAT1/GFP plasmid DNA with the Superfect transfection reagent (Qiagen) according to the user's manual. Briefly, cells were washed then the transfection complex added and kept at RT for 10 min. Culture medium (w/o serum and antibiotics) was added and the cells cultured for 5 h. Subsequently, medium was replaced with alpha MEM medium containing 10% FCS and 1% penicillin and streptomycin and grown for 48 hrs. The cells then grown in selection medium containing 600  $\text{mg}\cdot\text{l}^{-1}$  G418 for 1–3 weeks. For stable clones, the concentration of G418 can be decreased to 400  $\text{mg}\cdot\text{l}^{-1}$ .

#### **8.2.2.3 Stable transfection of GAT1/GFP in Hek293 cells**

Hek293 cells were transfected with GAT1/GFP plasmid same as indicated for the CHO cells with higher cell densities. Selection of stable clones was achieved with 400  $\text{mg}\cdot\text{l}^{-1}$  G418.

#### **8.2.2.4 Selection of stable transfected cells by cloning**

To select stable clones, the cells were diluted to 10-30 cells/ml and then 100 µl cells per well were seeded into 96-well plates. Those wells only containing single were marked and observed under fluorescence microscope. Positive clones could be selected after cell growing.

#### **8.2.2.5 FACS and fluorescence microscopy analysis**

Flow cytometry is a means of measuring certain physical and chemical characteristics of cells, such as cell size, shape and internal complexity. It utilizes color-differentiated fluorescence and light scatter measurements to analyze cells. As the cells in suspension one by one pass through the laser beam, they will scatter light and/or fluoresce, due to either auto fluorescence or to the presence of fluorescent stains which have been selectively absorbed or bound by the cell. The scatter and fluorescence emissions are collected by detectors (photo diodes and photomultiplier tubes) which convert the signals to voltage pulses that are proportional to the amount of light scattered and/or to the intensity of the fluorescence. These pulses are then amplified and converted to a digital form which can be displayed in numeric and/or histogram formats.

For optimal expression of GAT1/GFP fusion protein, selected clones were further selected and analysed by flow cytometry on a Beckton Dickinson FACScan using Cellquest II software.

All GAT1/GFP expression in mammalian cells and Sf9 cells was evaluated under the Axio observer fluorescence microscope and images made with the Axio Cam.

#### **8.2.2.6 Cell counting**

Cells were diluted with trypan blue and counted in a Neubauer-chamber or with a Coulter Z series equipment (Coulter electronics, USA).

### **8.2.3 Protein biochemical and immunological methods**

#### **8.2.3.1 Immunoprecipitation**

Anti-GFP Igs (5µg) were mixed with PBS and immobilized on 40 µl protein-G-sepharose/10 mg protein-A-sepharose per test overnight at 4°C. Unbound antibody was removed by washing twice with 1 ml PBS. Cell lysates or the intracellular fractions after biotinylation (see 4.3.2) were added and incubated for 10-16 hours at 4°C.

Unbound protein was removed and samples were washed with RIPA buffer, Prewash buffer and PBS. The pellets were boiled in SDS sample for 4 min at 99°C and analyzed by western blot.

RIPA                    50 mM Tris-HCl, pH 7.2  
                          150 mM NaCl  
                          1% Triton-x-100  
                          1% Na-deoxycholate  
                          0.1% SDS

Prewash                10 mM Tris-HCl, pH 7.2  
                          1 M NaCl  
                          0.1% Triton-x-100

### **8.2.3.2 Biotinylation**

Cell-surface biotinylation is an important tool for studying the expression and regulation of receptors and transporters, differentiation of plasma membrane proteins from those localized to organelle membranes, and distribution of membrane proteins in polarized epithelial cells. The biotinylation reagents can be applied for specific labeling of cell surface protein since they are both water-soluble and membrane impermeable.

Briefly, at least  $5 \times 10^6$  cells were collected and washed twice with cold PBS (pH 8.0) to remove amine-containing media and proteins. Then the cells were suspended in a freshly prepared solution of Sulfo-NHS-LC-Biotin (Pierce, USA) ( $1.5 \text{ mg} \cdot \text{ml}^{-1}$  in 10 mM Hepes buffer pH 9.0, 2 mM  $\text{CaCl}_2$ , 150 mM NaCl) for 30 min at RT. The cells were washed three times with 100 mM glycine to quench the reaction. After cells were solubilized, the supernatant was incubated with 60  $\mu\text{l}$  streptavidin beads (Pierce, USA) at 4°C overnight. The beads were washed twice with RIPA and once with Prewash and PBS, the membrane proteins attached to beads were boiled for 4 min in SDS sample buffer, and then subjected to western blotting analysis.

### **8.2.3.3 Sialidase treatment**

Transfected CHO and Hek293 cells were incubated with different concentrations of sialidase in alpha-modified Eagle's medium ( $\alpha$ -MEM) (pH 5.5) and Dulbecco's modified Eagle's medium (DMEM) (pH 5.5) for 4 h at 37 °C, respectively. Then aliquots of cells were used for measurement of [ $^3\text{H}$ ]GABA uptake and the rest of cells were solubilized for immunoprecipitation, western blotting and glycan differentiation analysis.

#### **8.2.3.4 Sodium periodate treatment**

Transfected Hek293 cells ( $2 \times 10^6$  cells/ml) suspended in PBS, were incubated with Sodium periodate ( $\text{NaIO}_4$ , 1mM) on ice for 15 min. Then aliquots of cells were used for measurement of [ $^3\text{H}$ ]GABA uptake and the rest of cells were solubilized for immunoprecipitation, western blotting and glycan differentiation analysis.

#### **8.2.3.5 Mild sodium borohydride reduction**

Following periodate oxidation, aliquots of cells were subjected to treatment by sodium borohydride to reduce the aldehydes generated by periodate. A fresh stock of 2 M sodium borohydride was prepared for each experiment. After two washes in cold PBS, periodate-treated cells were resuspended in PBS with 10 mM sodium borohydride at RT for 20 min, washed in cold PBS, and then subjected to GABA uptake assay.

#### **8.2.3.6 Alamar Blue Assay**

Cell suspension (180  $\mu\text{l}$ ) with a suitable concentration was cultured in each well of a 96-well microplate, meanwhile 20  $\mu\text{l}$  of various test agents were added in triplicate. After incubation at  $37^\circ\text{C}$  in a 5%  $\text{CO}_2$  atmosphere for a defined time, 20  $\mu\text{l}$  Alamar Blue Assay (AbD Serotec, Germany) was added to each well. After incubation for another 6 h, the extinction was measured using a micro ELISA autoreader at 570 and 600 nm, respectively. The proliferation rate was calculated according to the Biosource protocol.

#### **8.2.3.7 Determination of protein concentration**

Several methods are commonly used for determination of protein concentration. Bradford and BCA assay methods are routinely used during protein purification and screening.

##### **8.2.3.7.1 Bradford assay**

The Coomassie Brilliant Blue G-250 reacts with arginine and aromatic residues of proteins, leading to the formation of a complex which has an absorption maximum at 595 nm.

To determine the concentration of a protein solution, 5  $\mu\text{l}$  of the solution was added to 995  $\mu\text{l}$  Bradford reagent (10% (v/v) ethanol, 5% (v/v) phosphoric acid, 0.1% (w/v) Coomassie G-250) and mixed thoroughly. After 1 min incubation at RT, the extinctions of

the samples were measured at 595 nm. Purified bovine serum albumin (Pierce, USA) of known concentration was used as standards.

#### **8.2.3.7.2 BCA protein assay**

The BCA method is a detergent-compatible formulation based on bicinchoninic acid (BCA) for the colorimetric detection and quantitation of total protein. The method combines the reduction of  $\text{Cu}^{2+}$  to  $\text{Cu}^{1+}$  by protein in an alkaline medium with the colorimetric detection of the cuprous cation ( $\text{Cu}^{1+}$ ) using a reagent containing bicinchoninic acid. This complex is formed by the chelation of two BCA molecules with one  $\text{Cu}^{1+}$  which can be measured at the wavelengths 562 nm or 570 nm.

In this work, the BCA protein assay kit (Pierce, USA) was used and the procedures were according to the manufacturer's instructions.

Briefly, a fresh protein standard was prepared by diluting the 2 mg/ml Bovine Serum Albumin (BSA) stock standard in serial dilutions. PBS was used as diluent. 8 points of standard were applied (500, 400, 300, 200, 150, 100, 50, 0  $\mu\text{g/ml}$ ). 20  $\mu\text{l}$  of each standard, sample or blank was added to each well of a 96-well plate. 200  $\mu\text{l}$  of reagent's mixture (Reagent A and B at a ratio 50:1) was added to each standard, sample or blank and the plate was incubated for 30 min at 37°C. The absorptions were read at 570 nm on a microplate reader (TECAN, Austria). The protein concentrations were calculated with reference to a standard curve.

#### **Materials**

BCA Protein Assay Reagent (Pierce, USA) contains:

- Reagent A, consists of sodium carbonate, sodium bicarbonate, bicinchoninic acid and sodium tartrate in 0.1 M sodium hydroxide.
- Reagent B, consists of 4% cupric sulfate.
- Albumin Standard, Bovine Serum Albumin (BSA).

#### **8.2.3.8 Endoglycosidase H treatment**

The enzyme Endoglycosidase H (Endo- $\beta$ -N-acetylglucosaminidase H) is a highly specific endoglycosidase which cleaves asparagine-linked mannose rich oligosaccharides, but not highly processed complex oligosaccharides from glycoproteins. Endoglycosidase H cleaves the bond between two *N*-acetylglucosamine (GlcNAc) subunits directly proximal to the asparagine residue.

After immunoprecipitation, probes were eluted by boiling for 4 min in denaturate buffer. Endoglycosidase H (Endo H, Boehringer Mannheim) treatment was performed with Endo H (0.02 U/ 80  $\mu$ l) at 37 °C for 16 h in 50 mM sodium acetate containing 0.5  $\mu$ l protease inhibitor cocktail (Sigma) at pH 5.5.

Denaturate buffer      0.4% SDS  
                                 1% 2-Mercaptoethanol  
                                 40 mM EDTA

### **8.2.3.9 SDS-polyacrylamide gel electrophoresis (SDS-PAGE)**

In this work the SDS-PAGE method was performed according to Laemmli (1970). The Biorad Mini-Protean II system was used. The electrophoretic separation was done at a constant flow rate at 150 V. For size determination of the protein molecules, high molecular weight standards (Bio-rad) were used.

Protein samples were prepared for electrophoresis by addition of SDS sample buffer (5 X). Samples were heated to 99°C for 3-5 min. In a protein solution denatured with the detergent SDS, the protein molecules are bound on their hydrophobic moieties by the anionic SDS molecules which make them anionic. Denatured protein samples migrate quickly through the large pores of the stacking gel (4% acrylamide) before entering the narrow pores of the resolving gel (6-15% acrylamide). An additional focusing effect is obtained by shifting the pH from 6.8 in the stacking gel to 8.8 in the resolving gel: glycine, which is the main constituent of the running buffer, has an isoelectric point of ~6.0. This means that, once glycine enters the stacking gel, it assumes its zwitterionic form and is essentially uncharged. The resulting deficiency of charge carriers is synonymous with an increased electrical resistance R and, according to Ohm's law ( $E=RI$ ), and an increased electric field E in the stacking gel. In response to this increased field, proteins are accelerated in the stacking gel relative to the resolving gel. The concentration of acrylamide in the gels determines the pore size of the gels. The composition of the gels is summarized in the following table. The movements of the protein molecules are inversely proportional to the logarithm of their molecular weights. For non-denaturing gels the preparation was done with ddH<sub>2</sub>O instead of SDS in the buffers and the electrophoresis ran at 4°C at 100 V constantly.

Table 8.1 Composition of the stacking gel 4% gel (volumes are for 4 gels)

dd H <sub>2</sub> O	5 ml
Stacking gel buffer (4 X)	2.5 ml
30% Acrylamide/Bis	1.3 ml
1% SDS	1 ml
TEMED	10 µl
Ammonium peroxy disulfate (10%) in H <sub>2</sub> O	100 µl

Table 8.2 Composition of the running gel 10% gel (volumes are for 2 gels)

concentration (%)	7.5	10	12	15
dd H <sub>2</sub> O	4.7	3.9	3.2	2.2
Resolving gel buffer (6 X)	1.7	1.7	1.7	1.7
30% Acrylamide/Bis	2.5	3.3	4	5
1% SDS	1	1	1	1
TEMED	10	10	10	10
Ammonium peroxy disulfate (10%) in H <sub>2</sub> O	100	100	100	100

SDS sample buffer (5 X)                    0.25 M Tris/HCl, pH 6.8  
     50% Glycerin  
     8% SDS  
     0.5 M DTT  
     0.5% Bromophenol blue

Stacking gel buffer (4 X)                    0.5 M Tris/HCl, pH 6.8

Resolving gel buffer (6 X)                    1.5 M Tris/HCl, pH 8.8

Electrophoresis buffer (10 X)                250 mM Tris  
     1.92 M Glycine  
     1 % SDS

### 8.2.3.10 Silver staining

Silver staining of SDS-polyacrylamide gels is a very sensitive method that allows the detection of proteins in lower nanogram range (~10 ng). Under the buffer conditions used, Ag<sup>+</sup> ions bind with Glu-, Asp- and Cys- residues of proteins. Reduction of Ag<sup>+</sup> with formaldehyde forms insoluble brown precipitate of metallic silver, which is then



visualised by addition of the developer. Unfortunately, nucleic acids, lipopolysaccharides, lipids and glycolipids on the gel are stained, making silver staining of protein unspecific. The method used here was modified according to Heukeshoven and Dernick (1985). Once the electrophoresis is completed, the gel was soaked in fixation solution for at least 1 h at RT or overnight (4°C). Then the gel was washed 3 x 10 min with 50% ethanol. Incubation for 1 min in sensitising solution followed, after which the gel was washed 3 x 20 sec with ddH<sub>2</sub>O. The gel was then incubated for 10-15 min in silver solution and washed again with ddH<sub>2</sub>O. The gel was soaked in developing solution. Once protein bands were visibly brown, the reaction was then stopped with stop solution and the gel washed with water.

Fixation solution:	50% Ethanol 12% Acetic acid
Sensitising solution:	0.02% Sodium thiosulphate (Na <sub>2</sub> S <sub>2</sub> O <sub>3</sub> )
Silver solution:	0.2% AgNO <sub>3</sub> 0.02% Formaldehyde
Developing solution:	3% Sodium carbonate 0.05% Formaldehyde 0.0005% Sodium thiosulphate
Stop solution:	1% Glycine

#### **8.2.3.11 Coomassie blue staining**

The same as in the Bradford test, proteins in gels react with coomassie G250 to a blue complex. This method is less sensitive than silver staining and bands containing >100 ng of proteins are can be visualized. The Biosafe coomassie (Bio-rad) was used in this work. It is easy to use and fast to develop.

After electrophoresis, the gel was removed and washed 3 x 5 min with distilled water.

After washing, gel was immersed in 25 ml Bio-safe Coomassie solution and incubated on a shaker at RT for 1 h. The staining solution was then discarded and the gel washed with water till the bands were seen clearly and no background was left.

#### **8.2.3.12 Analysis and identification of protein by MALDI-TOF MS**

With the aid of MALDI-TOF MS (Matrix-Assisted Laser-Desorption-Ionization

Time-Of-Flight Mass Spectrometry) protein fragments with blocked n-termini or which are available only in limited concentrations can be easily analysed. In this work the GAT1/GFP fusion protein expressed and purified from insect cells were analysed by Mass-fingerprinting.

All solutions and buffers used were prepared with sterile pure HPLC grade water (Milli-Q® Water filter apparatus, Millipore, Germany) in order to avoid contaminations.

**In-gel tryptic digestion of proteins:**

The Coomassie stained spots were excised from the gels with a scalpel. They were cut into very tiny fragments (1x1 mm) and transferred to clean Eppendorf tubes before the digestion.

The gel fragments were rinsed once with 100 µl sterile dd H<sub>2</sub>O and then incubated in 20 µl (for small bands) and 100 µl (for big bands) of a 1:1 mixture of acetonitrile and 100 mM NH<sub>4</sub>HCO<sub>3</sub> for 15 min at RT with shaking. After centrifugation, the supernatant was discarded and the fragments were incubated in 20 µl /100µl acetonitrile till they became milky white. The supernatant were removed again and the gel fragments were lyophilised for 10 min. Then the gel pieces were incubated in 20 µl /100 µl of a 1:1 100 mM DTT and 100 mM NH<sub>4</sub>HCO<sub>3</sub> for 30 min at 56°C. The fragments were shrunk with 20 µl/100 µl acetonitrile again and the supernatants were removed. The milky white gel cubes were then incubated in 20 µl or 100 µl iodoacetamide solutions (55 mM iodoacetamide/100 mM NH<sub>4</sub>HCO<sub>3</sub>) for 20 min at RT in the dark. And then the gel fragments were washed with 20 µl or 100 µl 100 mM NH<sub>4</sub>HCO<sub>3</sub> for 15 min at RT. Then the fragments were shrunk again with acetonitrile for 5 min at RT. After removing all the dye from the gel pieces, the fragments were lyophilized and exact volumes (as those of the supernatants noted earlier + 3 µl) of trypsin solutions (12.5 ng/µl bovine trypsin, in 100 mM NH<sub>4</sub>HCO<sub>3</sub>) were added to digest the protein samples. The tubes were then incubated on ice for 30 min then overnight at 37°C with light shaking.

The next day the tubes were centrifuged and checked if enough supernatant for analysis was present. If there was no supernatant, pure milliQ water was added and tubes were incubated at RT for 30 min. Then the extractions of trypsin digested protein fragments were collected. To make sure that the protein fragments were isolated totally from the tubes, 10 µl 40% acetonitrile/0.1% TFA was added to the gel pellets and the tubes incubated for several hours at RT with shaking. The supernatants were then also collected to clean eppendorf tubes and 1 µl used for MALDI-Mass fingerprinting analysis. Unused rest were lyophilised and stored at -20°C.

### **MALDI-TOF-MS analysis:**

The MALDI Mass Fingerprinting was performed by Dr. Chris Weise (FU Berlin) with a Bruker-Biflex Reflex Mass spectrometer (Bruker Daltonics, Germany) in reflector-mode with alpha-cyano-4-hydroxycinnamic acid as matrix. Ionisation was enhanced with a 337 nm-ray of a Nitrogen-Laser. The peptide masses were determined by calibration with the PACpeptide calibrant standard.

Evaluation and identification of the mass spectra were performed with help of the internet search software Mascot (Perkins et al., 1999).

### **8.2.3.13 Western blot**

Proteins were electrophoresed on an SDS-polyacrylamide gel and transferred to nitrocellulose membrane by Western blotting. After SSD-PAGE, the proteins were transferred onto a nitrocellulose membrane under wet conditions in a Bio-rad blot apparatus at 150 V/250 mA in ice-cold transfer buffer for 60 min. Due to negativity of the protein molecules post SDS-PAGE, they therefore move from the gel (cathode end) towards the membrane (anode end) of the blot system.

Proteins on nitrocellulose membrane can be detected by their specific antibodies. The nitrocellulose membrane was firstly incubated in blocking buffer at RT for 1- 2 h or at 4°C overnight to block unspecific binding sites. After washed for 3 x 5 min with PBS-T, the membrane was hybridized in primary antibodies (1:500-2000) in PBS-T at 4°C overnight. The membrane was then washed for 3 times with PBS-T and hybridized with the second antibody (horseradish peroxidase conjugated secondary antibody in PBS-T, 1:5000) at RT for at least 1 h. Before detection, the membrane was washed for 3 times with PBS-T. For detection, the membrane was in the luminol reaction mix (1 ml luminol solution B, 10 µl luminol solution A and 3 µl luminol solution C). Visualisation and documentation of the chemiluminescence was performed with the digital Fujifilm LAS-1000 Imaging-System and captured on a CCD-camera. To quantify protein band densities, images were then analyzed through Quantity One Software (Bio-rad).

Transfer buffer	20 mM Tris-HCl, pH 8.3 150 mM Glycine 10% Ethanol
PBS-T	0.1% Tween-20 in PBS
Blocking buffer	5% (w/v) Non fat milk powder in PBS-T

luminol solution A	6.8 mM Plovinuric acid in DMSO
luminol solution B	0.1 M Tris-HCl, pH 8.5 1.25 mM Luminol
luminol solution C	3% H <sub>2</sub> O <sub>2</sub>

#### 8.2.3.14 Glycan staining

The aliquots from immunoprecipitation with anti-GFP IgG were divided in half and subjected separately to SDS-PAGE and then transferred to nitrocellulose membrane as described in 7.2.3.13. One membrane was used for immunostaining of GAT1 protein. Another membrane was stained with MAA (DIG Glycan Differentiation Kit, Roche) to detect sialic acids 2, 3-linked to galactose of GAT1/GFP. This method is based on the specific binding of lectins conjugated with the steroid hapten digoxigenin to carbohydrate moieties, which enables immunological detection of the bound lectins.

The stain procedure was done as suggested by the manufacturer. In brief, the membrane was soaked in blocking solution at RT for at least 30 min or at 4 °C overnight. After washed for 2 x 10 min with TBS and once with Buffer 1, the membrane was incubated in lectin solution (for MAA (*maackia amurensis agglutinin*) 50 µl to 10 ml Buffer 1) at RT for 1 h. Then the membrane was washed 3x 10 min with TBS and incubated with anti-Digoxigenin-AP solution (10 µl to 10 ml TBS) at RT for 1 h. The blot was washed again and then stained in the freshly prepared staining solution (200 µl NBT/BCIP to 10 ml Buffer 1) till the development was completed. The blot was rinsed several times with dd H<sub>2</sub>O to stop the reaction. To quantify sialic acid expression, the membrane was scanned and the image was then analyzed through Quantity One Software (Bio-rad).

TBS (pH7.5)	50 mM Tris-HCl 150 mM NaCl
Buffer 1 (pH7.5)	TBS 1 mM MgCl <sub>2</sub> 1 mM MnCl <sub>2</sub> 1 mM CaCl <sub>2</sub>
Buffer 2 (pH7.5)	100 mM Tris-HCl 100 mM NaCl 50 mM MgCl <sub>2</sub>

DIG Glycan Differentiation Kit, (Roche, Germany) contains:

- Digoxigenin-labeled lectins (GNA, SNA, MAA, PNA, DSA)
- Anti-Digoxigenin-AP
- NBT/BCIP
- Control glycoproteins (carboxypeptidase Y, for GNA; transferrin, for SNA; fetuin, for SNA, MAA and DSA; asialofetuin, for PNA and DSA)
- Blocking Reagent (10 ×, diluted with TBS before use)
- Ponceau S solution

### 8.2.3.15 GABA uptake assay

To determine the transport activity of GAT1 Protein, [<sup>3</sup>H] GABA uptake assays were performed. Cells were washed three times with wash buffer and then incubated with 200 μl Flux buffer (wash buffer containing 3.7 × 10<sup>4</sup> Bq [<sup>3</sup>H] GABA (Perkin Elmer), 10 μM cold GABA, 3.7 × 10<sup>4</sup> Bq [<sup>14</sup>C] sucrose (Perkin Elmer) and 100 μM cold sucrose) for 15 min at RT. The uptake was stopped by washing cells three times with cold wash buffer, followed by solubilization of the cells with 100 μl of 0.5% SDS (w/v) solution for 1 h at 4°C.

Aliquots were used for measurement of the remaining [<sup>3</sup>H] GABA and [<sup>14</sup>C] sucrose. The protein concentration in the supernatant was determined using the BCA protein assay as indicated in 4.3.5.2. Unspecific uptake was determined in mock transfected cells. The GABA uptake activity was measured as pM·μg protein<sup>-1</sup>·min<sup>-1</sup>.

Wash buffer (pH7.4)	128 mM NaCl
	5.2 mM KCl
	2.1 mM CaCl <sub>2</sub>
	2.9 mM MgSO <sub>4</sub>
	5 mM Dextrose
	10 mM Hepes

### 8.2.3.16 Sialic acid concentration assay

In this work a periodate-resorcinol method (Jourdian *et al.*, 1971) was used to determine the total and bound sialic acid concentration. The glycosides produced chromogens stable to periodate oxidation at 37 °C, whereas free sialic acid produced chromogens that were destroyed at this temperature, but were stable at 0 °C.

Cells (2 × 10<sup>6</sup>) were washed with PBS and then suspended in 250 μl PBS. The cell suspension was then frozen at -80 °C and defrozen at 37 °C several times to lysis the cells. 6 points of sialic acid standard were applied (200, 100, 50, 20, 10, 0 μg/ml) and 250 μl of them were added in the tubes. 5 μl periodic acid solution (0.4 M) was added in each

sample and standard and mixed well. The mixtures were incubated on ice for 10-20 min and followed by incubation for 60 min at 4 °C for total sialic acid measurement, or for 60-90 min at 37 °C for bound sialic acid measurement. Then 500 µl freshly prepared Resorcinol/CuSO<sub>4</sub> solution was added to each tube and mixed shortly. The samples and standards were boiled for 15 min. After cooling for a few minutes, 500 µl *tert*-butyl alcohol were added, the samples were vortexed and centrifuged for 5 min to precipitate cell debris. Immediately after spinning, the supernatants were poured into microtiter plates and read at 630 nm. Sialic acid concentrations were calculated by comparison with a standard curve.

Resorcinol/CuSO <sub>4</sub> solution	6% Resorcinol
	2.5 mM CuSO <sub>4</sub>
	44% HCl

#### **8.2.3.17 Cell surface sialic acid analysis by flow cytometry**

Cells ( $2 \times 10^6$ ) were washed twice with PBS and then incubated in 100 µl PBS containing 20 µg/ml FITC-labeled *Limax flavus* agglutinin (LFA) for 1 h on ice in the dark. After washing with PBS cells were suspended in 500 µl PBS and analyzed by flow cytometry on a Beckton Dickinson FACScan using Cellquest II software.

#### **8.2.3.18 Membrane preparation and solubilization**

The membrane preparation was done through a ultracentrifugation method combined with a two-phase extraction procedure (Park *et al.* 2008).

The harvested cells were homogenized with an ultra sonic machine and centrifuged for 10 min at 1000 g. After the pellet containing the nuclei was removed, the post-nuclear supernatant (PNS) was obtained. The collected PNS was then loaded into 30% Percoll (w/v) and centrifuged at 84,000 g for 35 min (Beckman Ti45 rotor), and the visible band of the crude PM fraction was collected.

For aqueous two-phase extraction, two sets of a Dextran 500 (6.6%, w/w)/polyethylene glycol (PEG) 3350 (6.6%, w/w) were prepared via the addition of stock solutions of 20% (w/w) Dextran 500 (GE Health Care, Uppsala, Sweden) and 40% (w/w) PEG 3350 (Sigma–Aldrich, Steinheim, Germany). The crude PM sample prepared was then added into a set of two-phase mixtures. The potassium phosphate buffer (0.2 M, pH 7.2) was added to the other set of two-phase mixtures. After 40 inversions at 4 °C, the two phase mixtures were centrifuged for 5 min at 750 g at 4 °C. The two-phase mixtures were then phase-separated via centrifugation (upper phase: PEG, lower phase: Dextran). The two

upper phases of the two-phase systems were exchanged. The mixtures were inverted 40 times at 4 °C and subjected to 5 min of centrifugation at 750 *g* at 4 °C. Two upper phases were recovered and pooled together. The pooled samples were centrifuged for 1 h at 100,000 *g* with 1 mM sodium bicarbonate. The purified PM proteins were then recovered as a pellet and for solubilization or stored at -80 °C.

For solubilization, pure PM pellets were washed once with PBS and resuspended in solubilisation buffer containing Trasylol (Bayer, Germany) (1:1000), 1 mM EDTA, 1 mM DTT and protease inhibitor cocktail (1:500) (Merck, USA). After a 4 x 30 s sonication step the cells were incubated overnight at 4°C with agitation. The solubilised protein was fractionated by 45 min centrifugation at 18,000 rpm.

Solubilization buffer            10 mM Tris, pH 7.8  
    150 mM NaCl  
    1mM CaCl<sub>2</sub>  
    2% (w/v) *n*-Dodecyl β-D-maltoside

### **8.2.3.19 Ion exchange chromatography**

Ion Exchange Chromatography relies on the reversible adsorption of charged solute molecules to immobilized ion exchange groups of opposite charge on the resin. After equilibration, the solute molecules carrying the appropriate charge displace counter-ions and bind reversibly to the beads with certain pH and ionic strength. And then the substances are eluted by increasing the ionic strength of the eluting buffer or changing its pH. It can be subdivided into cation and anion exchange chromatography according to the charge on resin. Generally used as a batch step in initial purification or a selective step in the latter stages of a purification scheme.

In this work HiTrap QFF anion exchange column (GE Healthcare) was used for isolation of GAT1/GFP protein from Hek293 cells or insect cells. Cells were harvested and solubilized in 50 mM Diethylamine (pH7.8 for Hek 293 cells; pH8.5 for insect cells) containing 2% *n*-dodecyl β-D-maltoside, Trasylol (1:1000) and protease inhibitor cocktail (1:500) (Merck, USA). After the column was equilibrated with 5-10 column volumes of start buffer at a flow rate of 5 ml/min, cell lysate was loaded and the column then washed again with 2-5 column volumes of start buffer. Then the column was eluted with 30 ml of a continuous salt gradient of start buffer to elute buffer at a flow rate of 5 ml/min. 1 ml per fraction was collected and the effluent at  $\lambda = 280$  nm.

Start buffer            50 mM Diethylamine, pH8.5 (for insect cells); pH7.8 (for Hek 293 cells)  
    0.7% (w/v) *n*-Octyl-β-D-glucopyranoside

Elute buffer      20 mM Tris-HCl, pH6.8  
                      0.7% (w/v) *n*-Octyl- $\beta$ -D-glucopyranoside  
                      1 M NaCl (for insect cells); 0.5 M NaCl (for Hek 293 cells)

### **8.2.3.20 Lectin affinity chromatography**

Affinity chromatography is an effective method for the purification of biomolecules based on a highly specific biological interaction such as that between antigen and antibody, enzyme and substrate, or receptor and ligand. Lectin affinity chromatography is a form of affinity chromatography where lectins are used to separate specific carbohydrate (sugar) molecules within the sample. Lectins in general are oligomeric proteins composed of subunits with at least one carbohydrate binding site per subunit. They are able to form reversible complexes with mono- or oligosaccharide structures.

For Hek293 cell line, 3 ml concentrated cell lysate was loaded onto 300  $\mu$ l wheat germ agglutinin (WGA)-agarose (Vector Laboratories, USA) column. After extensive wash with TBS and 200 mM *N*-acetyl glucosamine (GlcNAc)/TBS, the column was eluted with 10  $\times$  600  $\mu$ l 800 mM GlcNAc/TBS.

### **8.2.3.21 Immunoaffinity chromatography**

#### **8.2.3.21.1 Purification of the GFP-specific antiserum**

The polyclonal antibody against GFP was collected from rabbits immunized with GFP protein every one to two weeks. Blood was centrifuged for one hour at 3000 rpm and the supernatant was used directly or stored at -20°C. Monoclonal antibody against GFP was purified from cell culture supernatants of hybridoma cells.

The purification procedure was performed with the Affi-Gel<sup>®</sup> Protein A MAPS<sup>®</sup> II Kit (Biorad) according to manufacturer's instructions. 1 ml of the Affi-Gel protein-A-agarose was packed equivalent to bind 6-8 mg/ml IgG<sub>1</sub>. The resin was washed with dd H<sub>2</sub>O and then equilibrated with 5x 1 ml pH 9 binding buffer. 2 ml cell culture medium from the hybridoma cells (or 1 ml rabbit serum) were diluted with 2 ml of binding buffer then transferred to the columns and incubated for 15 min at RT with agitation. Unbound components were washed away with 6 times 2 ml binding buffer and the respective antibodies eluted with 7x 750  $\mu$ l elution buffer (pH 3.0). Eluates were neutralized immediately by adding 100  $\mu$ l of a 1M Tris HCl, pH 9.0 in each tube in which eluates were collected. After elution the column was washed with 5x 1 ml regeneration buffer and stored in PBS containing 0.05% (w/v) sodium azide. A further purification was



performed by size exclusion chromatography with Superose 6<sup>TM</sup> 10/300 GL column and TBS buffer.

The eluates were concentrated as well as changing buffer with 0.1 M MOPS (pH7.5) in a Vivaspin column (Vivasciences) at 4°C and 3,000 g and the concentrations and purity determined by BCA and SDS PAGE respectively.

Affi-Gel<sup>®</sup> Protein A MAPS<sup>®</sup> II Kit contains:

Affi-Gel protein-A-agarose

Binding buffer

Elution buffer

Regeneration buffer

#### **8.2.3.21.2 Preparation of immunoaffinity column**

200 µl Affi-gel 10 protein-A-sepharose (Amersham Pharmacia, Sweden) was loaded on a 10 ml disposable chromatography column and washed twice with 1 ml ice cold dd H<sub>2</sub>O. About 6-8 mg purified antibody in 0.1 M MOPS buffer pH 7.5 was put on the resin and the columns incubated overnight at 4°C for covalent binding to take place. Subsequently, unbound antibodies were collected as flow through and the sepharose washed once with 1 ml 1 M ethanolamine pH 8.0. Blocking of the sepharose is performed with 3 ml 1M ethanolamine pH 8.0 for 2 h at RT. Finally the sepharose coupled with antibody was washed three times with 15 mM sodium phosphate buffer pH 8.0. For later use of the affinity columns, 1 ml PBS with 0.02% NaN<sub>3</sub> was added to the sepharose and stored at 4°C.

#### **8.2.3.21.3 Isolation of GAT1/GFP by immunoaffinity column**

Cell lysate (prepared as indicated as in 4.3.16) were added directly to immunoaffinity chromatography. Protein was coupled on the column by agitation overnight at 4°C. Unbound protein was collected as flow through and the resin washed three times with RIPA and twice with Prewash. Elution of GAT1/GFP was done with 8 x 250 µl elution buffer (50 mM diethylamine pH 11.4). Eluates were neutralized immediately by adding 100 µl of a 0.5 M NaH<sub>2</sub>PO<sub>4</sub> in each tube in which eluates were collected.

### **8.2.3.22 Size exclusion chromatography**

Size exclusion chromatography is also called gel filtration or gel exclusion chromatography. It separates molecules on the basis of molecular weight, size and shape by the porous beads with a well-defined range of pore sizes.

The immuno-purified GAT1/GFP isolated from affinitycolumn was concentrated to 250-300  $\mu$ l with Vivaspin column (Vivasciences) at 4°C and 3,000 g. The concentrate was further purified by SE-FPLC on a Superdex 200 column (GE Healthcare) which had been equilibrated with equilibrium buffer (TBS containing different concentrations of detergent). Elution of the protein was performed with equilibrium buffer at a flow rate of 0.3 ml/min. The molecular weight of the obtained protein was determined based on the elution profile of standard proteins under same buffer condition.

TBS                                    10 mM Tris, pH 7.8  
    150 mM NaCl

### **8.2.3.23 Transmission electron microscopy (TEM) analysis**

#### **8.2.3.23.1 Negative staining preparation**

Droplets (5 $\mu$ l) of the sample were placed onto hydrophilised (glow discharged for 60s at 8W in a BALTEC MED 020 device (Baltec, Liechtenstein) carbon covered microscopical copper grids (400 mesh) and the supernatant fluid was removed with a filter paper to create an ultrathin layer of the sample. A droplet of contrasting material (1% uranyl acetate, 2% phosphotungstic acid or 2% ammonium molybdate in the presence of 0.1% trehalose) was added, blotted again and air-dried. Imaging was performed using a Tecnai F20 FEG (FEI Company, Oregon) at 160 kV accelerating voltage under low-dose conditions. Micrographs were recorded following the low-dose protocol of the microscope at a primary magnification of 62,000x. The defocus value was chosen to correspond to a first zero of the contrast transfer function (CTF) at  $\sim 15$  Å.

#### **8.2.3.23.2 Cryo-TEM preparation**

Droplets of the sample solution (5  $\mu$ l) were applied to perforated (1  $\mu$ m hole diameter) carbon film covered 200 mesh grids (R1/4batch of Quantifoil Micro Tools GmbH, Jena, Germany), which had been hydrophilized prior to use by 60 s plasma treatment at 8 W in a BALTEC MED 020 device. The supernatant fluid was removed with a filter paper until an ultra-thin layer was obtained spanning the holes of the carbon film. The specimen were immediately vitrified by propelling the grids into liquid ethane at its freezing point (90 K)

operating a guillotine-like plunging device (Dubochet and McDowell, 1981; Dubochet (a), 1982; Dubochet (b), 1982)

#### **8.2.3.23.3 Cryo-TEM**

Vitrified samples were transferred into a Tecnai F20 FEG using a Gatan cryoholder and –stage (Model 626). Samples were constantly cooled by LN2 during imaging to maintain a sample temperature of  $T = 93$  K. Imaging was performed at 160 kV accelerating voltage at a defocus value of 600 nm, which corresponds to a first zero of the contrast transfer function at  $13 \text{ \AA}$  ( $C_s = 2.0$  mm). Micrographs were recorded following the low-dose protocol of the microscope at a primary magnification of 62, 000x.

## 9. References

- Abramson, J. and Wright, E.M. (2009) Structure and function of Na(+)-symporters with inverted repeats. *Curr Opin Struct Biol*, 19, 425-432.
- Accardi, A. and Miller, C. (2004) Secondary active transport mediated by a prokaryotic homologue of Cl<sup>-</sup> channels. *Nature*, 427, 803-807.
- Ahrens, P.B. and Ankel, H. (1987) The role of asparagine-linked carbohydrate in natural killer cell-mediated cytotoxicity. *J Biol Chem*, 262, 7575-7579.
- Ali, F.E., Bondinell, W.E., Dandridge, P.A., Frazee, J.S., Garvey, E., Girard, G.R., Kaiser, C., Ku, T.W., Lafferty, J.J., Moonsammy, G.I. and et al. (1985) Orally active and potent inhibitors of gamma-aminobutyric acid uptake. *J Med Chem*, 28, 653-660.
- Amara, S.G. (2007) Chloride finds its place in the transport cycle. *Nat Struct Mol Biol*, 14, 792-794.
- Amara, S.G. and Kuhar, M.J. (1993) Neurotransmitter transporters: recent progress. *Annu Rev Neurosci*, 16, 73-93.
- Angata, T. and Varki, A. (2002) Chemical diversity in the sialic acids and related alpha-keto acids: an evolutionary perspective. *Chem Rev*, 102, 439-469.
- Ashwell, G. and Harford, J. (1982) Carbohydrate-specific receptors of the liver. *Annu Rev Biochem*, 51, 531-554.
- Basu, S., Basu, M., Basu, S. S. (1995) Biological specificity of sialyltransferases. In: *Biology of the sialic acids* (Rosenberg, A.; Plenum Press, New York), 69-93
- Bennett, E.R. and Kanner, B.I. (1997) The membrane topology of GAT-1, a (Na<sup>+</sup> + Cl<sup>-</sup>)-coupled gamma-aminobutyric acid transporter from rat brain. *J Biol Chem*, 272, 1203-1210.
- Bennett, E.R., Su, H. and Kanner, B.I. (2000) Mutation of arginine 44 of GAT-1, a (Na<sup>+</sup> + Cl<sup>-</sup>)-coupled gamma-aminobutyric acid transporter from rat brain, impairs net flux but not exchange. *J Biol Chem*, 275, 34106-34113.
- Bhavanandan, V.P. (1991) Cancer-associated mucins and mucin-type glycoproteins. *Glycobiology*, 1, 493-503.
- Bismuth, Y., Kavanaugh, M.P. and Kanner, B.I. (1997) Tyrosine 140 of the gamma-aminobutyric acid transporter GAT-1 plays a critical role in neurotransmitter recognition. *J Biol Chem*, 272, 16096-16102.
- Blakely, R.D., Clark, J.A., Pacholczyk, T. and Amara, S.G. (1991) Distinct, developmentally regulated brain mRNAs direct the synthesis of neurotransmitter transporters. *J Neurochem*, 56, 860-871.
- Blatow, M., Rozov, A., Katona, I., Hormuzdi, S.G., Meyer, A.H., Whittington, M.A., Caputi, A. and Monyer, H. (2003) A novel network of multipolar bursting interneurons generates theta frequency oscillations in neocortex. *Neuron*, 38, 805-817.
- Blix, G., (1936). "Über die Kohlenhydratgruppen des Submaxillarismucins." *Hoppe-Seylers Z* 240: 43-54.

- Bolvig, T., Larsson, O.M., Pickering, D.S., Nelson, N., Falch, E., Krogsgaard-Larsen, P. and Schousboe, A. (1999) Action of bicyclic isoxazole GABA analogues on GABA transporters and its relation to anticonvulsant activity. *Eur J Pharmacol*, 375, 367-374.
- Borden, L.A. (1996) GABA transporter heterogeneity: pharmacology and cellular localization. *Neurochem Int*, 29, 335-356.
- Borden, L.A., Dhar, T.G., Smith, K.E., Branchek, T.A., Gluchowski, C. and Weinshank, R.L. (1994) Cloning of the human homologue of the GABA transporter GAT-3 and identification of a novel inhibitor with selectivity for this site. *Receptors Channels*, 2, 207-213.
- Borden, L.A., Murali Dhar, T.G., Smith, K.E., Weinshank, R.L., Branchek, T.A. and Gluchowski, C. (1994) Tiagabine, SK&F 89976-A, CI-966, and NNC-711 are selective for the cloned GABA transporter GAT-1. *Eur J Pharmacol*, 269, 219-224.
- Borden, L.A., Smith, K.E., Gustafson, E.L., Branchek, T.A. and Weinshank, R.L. (1995) Cloning and expression of a betaine/GABA transporter from human brain. *J Neurochem*, 64, 977-984.
- Borden, L.A., Smith, K.E., Hartig, P.R., Branchek, T.A. and Weinshank, R.L. (1992) Molecular heterogeneity of the gamma-aminobutyric acid (GABA) transport system. Cloning of two novel high affinity GABA transporters from rat brain. *J Biol Chem*, 267, 21098-21104.
- Borden, L.A., Smith, K.E., Vaysse, P.J., Gustafson, E.L., Weinshank, R.L. and Branchek, T.A. (1995) Re-evaluation of GABA transport in neuronal and glial cell cultures: correlation of pharmacology and mRNA localization. *Receptors Channels*, 3, 129-146.
- Bremer, E.G., Schlessinger, J. and Hakomori, S. (1986) Ganglioside-mediated modulation of cell growth. Specific effects of GM3 on tyrosine phosphorylation of the epidermal growth factor receptor. *J Biol Chem*, 261, 2434-2440.
- Bresalier, R.S., Rockwell, R.W., Dahiya, R., Duh, Q.Y. and Kim, Y.S. (1990) Cell surface sialoprotein alterations in metastatic murine colon cancer cell lines selected in an animal model for colon cancer metastasis. *Cancer Res*, 50, 1299-1307.
- Brockhausen, I. (2006) Mucin-type O-glycans in human colon and breast cancer: glycodynamics and functions. *EMBO Rep*, 7, 599-604.
- Burnham, C.E., Buerk, B., Schmidt, C. and Bucuvalas, J.C. (1996) A liver-specific isoform of the betaine/GABA transporter in the rat: cDNA sequence and organ distribution. *Biochim Biophys Acta*, 1284, 4-8.
- Cai, G., Salonikidis, P.S., Fei, J., Schwarz, W., Schulein, R., Reutter, W. and Fan, H. (2005) The role of N-glycosylation in the stability, trafficking and GABA-uptake of GABA-transporter 1. Terminal N-glycans facilitate efficient GABA-uptake activity of the GABA transporter. *Febs J*, 272, 1625-1638.
- Chen, J.G., Liu-Chen, S. and Rudnick, G. (1998) Determination of external loop topology in the serotonin transporter by site-directed chemical labeling. *J Biol Chem*, 273, 12675-12681.
- Chen, J.G., Sachpatzidis, A. and Rudnick, G. (1997) The third transmembrane domain of the serotonin transporter contains residues associated with substrate and cocaine binding. *J Biol Chem*, 272, 28321-28327.

- Chen, N.H., Reith, M.E. and Quick, M.W. (2004) Synaptic uptake and beyond: the sodium- and chloride-dependent neurotransmitter transporter family SLC6. *Pflugers Arch*, 447, 519-531.
- Chiu, C.S., Jensen, K., Sokolova, I., Wang, D., Li, M., Deshpande, P., Davidson, N., Mody, I., Quick, M.W., Quake, S.R. and Lester, H.A. (2002) Number, density, and surface/cytoplasmic distribution of GABA transporters at presynaptic structures of knock-in mice carrying GABA transporter subtype 1-green fluorescent protein fusions. *J Neurosci*, 22, 10251-10266.
- Christiansen, B., Meinild, A.K., Jensen, A.A. and Brauner-Osborne, H. (2007) Cloning and characterization of a functional human gamma-aminobutyric acid (GABA) transporter, human GAT-2. *J Biol Chem*, 282, 19331-19341.
- Clark, J.A. (1997) Analysis of the transmembrane topology and membrane assembly of the GAT-1 gamma-aminobutyric acid transporter. *J Biol Chem*, 272, 14695-14704.
- Clausen, R.P., Madsen, K., Larsson, O.M., Frolund, B., Krosgaard-Larsen, P. and Schousboe, A. (2006) Structure-activity relationship and pharmacology of gamma-aminobutyric acid (GABA) transport inhibitors. *Adv Pharmacol*, 54, 265-284.
- Clausen, R.P., Moltzen, E.K., Perregaard, J., Lenz, S.M., Sanchez, C., Falch, E., Frolund, B., Bolvig, T., Sarup, A., Larsson, O.M., Schousboe, A. and Krosgaard-Larsen, P. (2005) Selective inhibitors of GABA uptake: synthesis and molecular pharmacology of 4-N-methylamino-4,5,6,7-tetrahydrobenzo[d]isoxazol-3-ol analogues. *Bioorg Med Chem*, 13, 895-908.
- Colli, W. (1993) Trans-sialidase: a unique enzyme activity discovered in the protozoan *Trypanosoma cruzi*. *Faseb J*, 7, 1257-1264.
- Conti, F., Melone, M., De Biasi, S., Minelli, A., Brecha, N.C. and Ducati, A. (1998) Neuronal and glial localization of GAT-1, a high-affinity gamma-aminobutyric acid plasma membrane transporter, in human cerebral cortex: with a note on its distribution in monkey cortex. *J Comp Neurol*, 396, 51-63.
- Conti, F., Minelli, A. and Melone, M. (2004) GABA transporters in the mammalian cerebral cortex: localization, development and pathological implications. *Brain Res Brain Res Rev*, 45, 196-212.
- Conti, F., Zuccarello, L.V., Barbaresi, P., Minelli, A., Brecha, N.C. and Melone, M. (1999) Neuronal, glial, and epithelial localization of gamma-aminobutyric acid transporter 2, a high-affinity gamma-aminobutyric acid plasma membrane transporter, in the cerebral cortex and neighboring structures. *J Comp Neurol*, 409, 482-494.
- Cope, D.W., Di Giovanni, G., Fyson, S.J., Orban, G., Errington, A.C., Lorincz, M.L., Gould, T.M., Carter, D.A. and Crunelli, V. (2009) Enhanced tonic GABA inhibition in typical absence epilepsy. *Nat Med*, 15, 1392-1398.
- Corfield, A. P., Schauer, R. (1982) Occurrence of sialic acids. In: *Sialic acids* (Schauer, R.; Springer, Wien, New York), 5-50
- Coyle, J.T. and Enna, S.J. (1976) Neurochemical aspects of the ontogenesis of GABAergic neurons in the rat brain. *Brain Res*, 111, 119-133.
- Cremer, H., Lange, R., Christoph, A., Plomann, M., Vopper, G., Roes, J., Brown, R., Baldwin, S., Kraemer, P., Scheff, S. and et al. (1994) Inactivation of the N-CAM gene in mice results in size reduction of the olfactory bulb and deficits in spatial learning. *Nature*, 367, 455-459.

- Crocker, P.R., Paulson, J.C. and Varki, A. (2007) Siglecs and their roles in the immune system. *Nat Rev Immunol*, 7, 255-266.
- Crocker, P.R. and Varki, A. (2001) Siglecs, sialic acids and innate immunity. *Trends Immunol*, 22, 337-342.
- David, L., Nesland, J.M., Funderud, S. and Sobrinho-Simoes, M. (1993) CDw75 antigen expression in human gastric carcinoma and adjacent mucosa. *Cancer*, 72, 1522-1527.
- Deken, S.L., Wang, D. and Quick, M.W. (2003) Plasma membrane GABA transporters reside on distinct vesicles and undergo rapid regulated recycling. *J Neurosci*, 23, 1563-1568.
- Dennis, J.W. and Laferte, S. (1985) Recognition of asparagine-linked oligosaccharides on murine tumor cells by natural killer cells. *Cancer Res*, 45, 6034-6040.
- Dhar, T.G., Borden, L.A., Tyagarajan, S., Smith, K.E., Branchek, T.A., Weinshank, R.L. and Gluchowski, C. (1994) Design, synthesis and evaluation of substituted triaryl nipecotinic acid derivatives as GABA uptake inhibitors: identification of a ligand with moderate affinity and selectivity for the cloned human GABA transporter GAT-3. *J Med Chem*, 37, 2334-2342.
- Docherty, M., Bradford, H.F., Wu, J.Y., Joh, T.H. and Reis, D.J. (1985) Evidence for specific immunolysis of nerve terminals using antisera against choline acetyltransferase, glutamate decarboxylase and tyrosine hydroxylase. *Brain Res*, 339, 105-113.
- Dreyfuss, A.I., Clark, J.R. and Andersen, J.W. (1992) Lipid-associated sialic acid, squamous cell carcinoma antigen, carcinoembryonic antigen, and lactic dehydrogenase levels as tumor markers in squamous cell carcinoma of the head and neck. *Cancer*, 70, 2499-2503.
- Dubochet, J. and McDowell, A.W. (1981) Vitification of pure water for electron microscopy. *J. Microsc.* 124,RP3-RP4.
- Dubochet, J., Lepault, J., Freeman, R., Berriman, J.A. and Homo J.C. (1982) Electron microscopy of frozen water and aqueous solutions. (a) *J. Microsc.* 128, 219-237.
- Dubochet, J.; Chang, J.J.; Freeman, R.; Lepault, J.; McDowell, A.W. (1982) Frozen Aqueous suspensions. (b) *Ultramicroscopy*. 10( 1-2), 55-61.
- Dupuy, C., Auvray, X. and Petipas C., (1997) Anomeric Effects on the Structure of Micelles of Alkyl Maltosides in Water. *Langmuir*, 13 (15), 3965–3967
- Durkin, M.M., Smith, K.E., Borden, L.A., Weinshank, R.L., Branchek, T.A. and Gustafson, E.L. (1995) Localization of messenger RNAs encoding three GABA transporters in rat brain: an in situ hybridization study. *Brain Res Mol Brain Res*, 33, 7-21.
- Dutzler, R., Campbell, E.B., Cadene, M., Chait, B.T. and MacKinnon, R. (2002) X-ray structure of a Cl<sup>-</sup> channel at 3.0 Å reveals the molecular basis of anion selectivity. *Nature*, 415, 287-294.
- Dutzler, R., Campbell, E.B. and MacKinnon, R. (2003) Gating the selectivity filter in Cl<sup>-</sup> channels. *Science*, 300, 108-112.

- Edelman, G.M. and Crossin, K.L. (1991) Cell adhesion molecules: implications for a molecular histology. *Annu Rev Biochem*, 60, 155-190.
- Egrie, J.C. and Browne, J.K. (2001) Development and characterization of novel erythropoiesis stimulating protein (NESP). *Br J Cancer*, 84 Suppl 1, 3-10.
- Emig, S., Schmalz, D., Shakibaei, M. and Buchner, K. (1995) The nuclear pore complex protein p62 is one of several sialic acid-containing proteins of the nuclear envelope. *J Biol Chem*, 270, 13787-13793.
- Faham, S., Watanabe, A., Besserer, G.M., Cascio, D., Specht, A., Hirayama, B.A., Wright, E.M. and Abramson, J. (2008) The crystal structure of a sodium galactose transporter reveals mechanistic insights into Na<sup>+</sup>/sugar symport. *Science*, 321, 810-814.
- Fahr, C. and Schauer, R. (2001) Detection of sialic acids and gangliosides with special reference to 9-O-acetylated species in basalioomas and normal human skin. *J Invest Dermatol*, 116, 254-260.
- Falch, E., Perregaard, J., FrLlund, B., B, S.L., Buur, A., Hansen, L.M., Frydenvang, K., Brehm, L., Bolvig, T., Larsson, O.M., Sanchez, C., White, H.S., Schousboe, A. and Krogsgaard-Larsen, P. (1999) Selective inhibitors of glial GABA uptake: synthesis, absolute stereochemistry, and pharmacology of the enantiomers of 3-hydroxy-4-amino-4,5,6,7-tetrahydro-1,2-benzisoxazole (exo-THPO) and analogues. *J Med Chem*, 42, 5402-5414.
- Fogel, M., Altevogt, P. and Schirmacher, V. (1983) Metastatic potential severely altered by changes in tumor cell adhesiveness and cell-surface sialylation. *J Exp Med*, 157, 371-376.
- Forrest, L.R., Tavoulari, S., Zhang, Y.W., Rudnick, G. and Honig, B. (2007) Identification of a chloride ion binding site in Na<sup>+</sup>/Cl<sup>-</sup>-dependent transporters. *Proc Natl Acad Sci U S A*, 104, 12761-12766.
- Forrest, L.R., Zhang, Y.W., Jacobs, M.T., Gesmonde, J., Xie, L., Honig, B.H. and Rudnick, G. (2008) Mechanism for alternating access in neurotransmitter transporters. *Proc Natl Acad Sci U S A*, 105, 10338-10343.
- Gagneux, P., Moore, J.J. and Varki, A. (2005) The ethics of research on great apes. *Nature*, 437, 27-29.
- Garcia-Alloza, M., Tsang, S.W., Gil-Bea, F.J., Francis, P.T., Lai, M.K., Marcos, B., Chen, C.P. and Ramirez, M.J. (2006) Involvement of the GABAergic system in depressive symptoms of Alzheimer's disease. *Neurobiol Aging*, 27, 1110-1117.
- Golovanevsky, V. and Kanner, B.I. (1999) The reactivity of the gamma-aminobutyric acid transporter GAT-1 toward sulfhydryl reagents is conformationally sensitive. Identification of a major target residue. *J Biol Chem*, 274, 23020-23026.
- Gonzales, A.L., Lee, W., Spencer, S.R., Oropeza, R.A., Chapman, J.V., Ku, J.Y. and Eskandari, S. (2007) Turnover rate of the gamma-aminobutyric acid transporter GAT1. *J Membr Biol*, 220, 33-51.
- Grisshammer, R. and Tate, C.G. (1995) Overexpression of integral membrane proteins for structural studies. *Q Rev Biophys*, 28, 315-422.
- Grossman, T.R. and Nelson, N. (2002) Differential effect of pH on sodium binding by the various GABA transporters expressed in *Xenopus* oocytes. *FEBS Lett*, 527, 125-132.



- Grossman, T.R. and Nelson, N. (2003) Effect of sodium lithium and proton concentrations on the electrophysiological properties of the four mouse GABA transporters expressed in *Xenopus* oocytes. *Neurochem Int*, 43, 431-443.
- Grunholz, H.J., Harms, E., Opetz, M., Reutter, W. and Cerny, M. (1981) Inhibition of in vitro biosynthesis of N-acetylneuraminic acid by N-acyl- and N-alkyl-2-amino-2-deoxyhexoses. *Carbohydr Res*, 96, 259-270.
- Guastella, J., Nelson, N., Nelson, H., Czyzyk, L., Keynan, S., Miedel, M.C., Davidson, N., Lester, H.A. and Kanner, B.I. (1990) Cloning and expression of a rat brain GABA transporter. *Science*, 249, 1303-1306.
- Hachiya, Y. and Takashima, S. (2001) Development of GABAergic neurons and their transporter in human temporal cortex. *Pediatr Neurol*, 25, 390-396.
- Hakomori, S. (1989) Aberrant glycosylation in tumors and tumor-associated carbohydrate antigens. *Adv Cancer Res*, 52, 257-331.
- Hanai, N., Dohi, T., Nores, G.A. and Hakomori, S. (1988) A novel ganglioside, de-N-acetyl-GM3 (II3NeuNH2LacCer), acting as a strong promoter for epidermal growth factor receptor kinase and as a stimulator for cell growth. *J Biol Chem*, 263, 6296-6301.
- Hartnell, A., Steel, J., Turley, H., Jones, M., Jackson, D.G. and Crocker, P.R. (2001) Characterization of human sialoadhesin, a sialic acid binding receptor expressed by resident and inflammatory macrophage populations. *Blood*, 97, 288-296.
- Hedlund, M., Ng, E., Varki, A. and Varki, N.M. (2008) alpha 2-6-Linked sialic acids on N-glycans modulate carcinoma differentiation in vivo. *Cancer Res*, 68, 388-394.
- Herbison, A.E., Augood, S.J., Simonian, S.X. and Chapman, C. (1995) Regulation of GABA transporter activity and mRNA expression by estrogen in rat preoptic area. *J Neurosci*, 15, 8302-8309.
- Herrler, G., Rott, R., Klenk, H.D., Muller, H.P., Shukla, A.K. and Schauer, R. (1985) The receptor-destroying enzyme of influenza C virus is neuraminidase-O-acetyltransferase. *Embo J*, 4, 1503-1506.
- Hanganutziu-Deicher antigen. *Trends Glycosci. Glycotechnol.* 2, 7-15
- Higashi, H. (1990) N-glycoylneuraminic acid-containing glycoconjugate as a tumor associated antigen.
- Hildebrandt, H., Muhlenhoff, M., Weinhold, B. and Gerardy-Schahn, R. (2007) Dissecting polysialic acid and NCAM functions in brain development. *J Neurochem*, 103 Suppl 1, 56-64.
- Hilgemann, D.W. and Lu, C.C. (1999) GAT1 (GABA:Na<sup>+</sup>:Cl<sup>-</sup>) cotransport function. Database reconstruction with an alternating access model. *J Gen Physiol*, 114, 459-475.
- Hinderlich, S., Berger, M., Keppler, O.T., Pawlita, M. and Reutter, W. (2001) Biosynthesis of N-acetylneuraminic acid in cells lacking UDP-N-acetylglucosamine 2-epimerase/N-acetylmannosamine kinase. *Biol Chem*, 382, 291-297.
- Hinderlich, S., Stasche, R., Zeitler, R. and Reutter, W. (1997) A bifunctional enzyme catalyzes the first two steps in N-acetylneuraminic acid biosynthesis of rat liver. Purification and characterization of UDP-N-acetylglucosamine 2-epimerase/N-acetylmannosamine kinase. *J Biol Chem*, 272, 24313-24318.

- Hong, Y. and Stanley, P. (2003) Lec3 Chinese hamster ovary mutants lack UDP-N-acetylglucosamine 2-epimerase activity because of mutations in the epimerase domain of the Gne gene. *J Biol Chem*, 278, 53045-53054.
- Hynes, R.O. and Lander, A.D. (1992) Contact and adhesive specificities in the associations, migrations, and targeting of cells and axons. *Cell*, 68, 303-322.
- Ikegaki, N., Saito, N., Hashima, M. and Tanaka, C. (1994) Production of specific antibodies against GABA transporter subtypes (GAT1, GAT2, GAT3) and their application to immunocytochemistry. *Brain Res Mol Brain Res*, 26, 47-54.
- Irie, A., Koyama, S., Kozutsumi, Y., Kawasaki, T. and Suzuki, A. (1998) The molecular basis for the absence of N-glycolylneuraminic acid in humans. *J Biol Chem*, 273, 15866-15871.
- Ito, T., Couceiro, J.N., Kelm, S., Baum, L.G., Krauss, S., Castrucci, M.R., Donatelli, I., Kida, H., Paulson, J.C., Webster, R.G. and Kawakita, Y. (1998) Molecular basis for the generation in pigs of influenza A viruses with pandemic potential. *J Virol*, 72, 7367-7373.
- Iversen, L.L. and Kelly, J.S. (1975) Uptake and metabolism of gamma-aminobutyric acid by neurones and glial cells. *Biochem Pharmacol*, 24, 933-938.
- Iversen, L.L. and Neal, M.J. (1968) The uptake of [3H]GABA by slices of rat cerebral cortex. *J Neurochem*, 15, 1141-1149.
- Jardetzky, O. (1966) Simple allosteric model for membrane pumps. *Nature*, 211, 969-970.
- Jasmin, L., Wu, M.V. and Ohara, P.T. (2004) GABA puts a stop to pain. *Curr Drug Targets CNS Neurol Disord*, 3, 487-505.
- Jiang, Y., Lee, A., Chen, J., Cadene, M., Chait, B.T. and MacKinnon, R. (2002) The open pore conformation of potassium channels. *Nature*, 417, 523-526.
- Jin, Y., Jorgensen, E., Hartweg, E. and Horvitz, H.R. (1999) The *Caenorhabditis elegans* gene *unc-25* encodes glutamic acid decarboxylase and is required for synaptic transmission but not synaptic development. *J Neurosci*, 19, 539-548.
- Jursky, F. and Nelson, N. (1999) Developmental expression of the neurotransmitter transporter GAT3. *J Neurosci Res*, 55, 394-399.
- Jursky, F., Tamura, S., Tamura, A., Mandiyan, S., Nelson, H. and Nelson, N. (1994) Structure, function and brain localization of neurotransmitter transporters. *J Exp Biol*, 196, 283-295.
- Kanner, B.I. (1994) Sodium-coupled neurotransmitter transport: structure, function and regulation. *J Exp Biol*, 196, 237-249.
- Kanner, B.I. (2003) Transmembrane domain I of the gamma-aminobutyric acid transporter GAT-1 plays a crucial role in the transition between cation leak and transport modes. *J Biol Chem*, 278, 3705-3712.

- Kanner, B.I. and Bendahan, A. (1990) Two pharmacologically distinct sodium- and chloride-coupled high-affinity gamma-aminobutyric acid transporters are present in plasma membrane vesicles and reconstituted preparations from rat brain. *Proc Natl Acad Sci U S A*, 87, 2550-2554.
- Kanner, B.I., Keynan, S. and Radian, R. (1989) Structural and functional studies on the sodium- and chloride-coupled gamma-aminobutyric acid transporter: deglycosylation and limited proteolysis. *Biochemistry*, 28, 3722-3728.
- Kanner, B.I. and Sharon, I. (1978) Active transport of L-glutamate by membrane vesicles isolated from rat brain. *Biochemistry*, 17, 3949-3953.
- Kanner, B.I. and Zomot, E. (2008) Sodium-coupled neurotransmitter transporters. *Chem Rev*, 108, 1654-1668.
- Kavanaugh, M.P., Arriza, J.L., North, R.A. and Amara, S.G. (1992) Electrogenic uptake of gamma-aminobutyric acid by a cloned transporter expressed in *Xenopus* oocytes. *J Biol Chem*, 267, 22007-22009.
- Kayser, H., Geilen, C.C., Paul, C., Zeitler, R. and Reutter, W. (1992) Incorporation of N-acyl-2-amino-2-deoxy-hexoses into glycosphingolipids of the pheochromocytoma cell line PC 12. *FEBS Lett*, 301, 137-140.
- Kelm, S. and Schauer, R. (1997) Sialic acids in molecular and cellular interactions. *Int Rev Cytol*, 175, 137-240.
- Keppler, O.T., Herrmann, M., von der Lieth, C.W., Stehling, P., Reutter, W. and Pawlita, M. (1998) Elongation of the N-acyl side chain of sialic acids in MDCK II cells inhibits influenza A virus infection. *Biochem Biophys Res Commun*, 253, 437-442.
- Keppler, O.T., Horstkorte, R., Pawlita, M., Schmidt, C. and Reutter, W. (2001) Biochemical engineering of the N-acyl side chain of sialic acid: biological implications. *Glycobiology*, 11, 11R-18R.
- Keshet, G.I., Bendahan, A., Su, H., Mager, S., Lester, H.A. and Kanner, B.I. (1995) Glutamate-101 is critical for the function of the sodium and chloride-coupled GABA transporter GAT-1. *FEBS Lett*, 371, 39-42.
- Keynan, S. and Kanner, B.I. (1988) gamma-Aminobutyric acid transport in reconstituted preparations from rat brain: coupled sodium and chloride fluxes. *Biochemistry*, 27, 12-17.
- Keynan, S., Suh, Y.J., Kanner, B.I. and Rudnick, G. (1992) Expression of a cloned gamma-aminobutyric acid transporter in mammalian cells. *Biochemistry*, 31, 1974-1979.
- Kircheis, R., Kircheis, L., Oshima, H., Kohchi, C., Soma, G. and Mizuno, D. (1996) Selective lysis of early embryonic cells by the alternative pathway of complement--a possible mechanism for programmed cell death in embryogenesis. *In Vivo*, 10, 389-403.
- Klenk, E. (1935). "Über die Natur der Phosphatide und anderer Lipide des Gehirns und der Leber in Niemann-Pickscher Krankheit." *Hoppe-Seylers Z* 235: 24-36.
- Kluge, A., Reuter, G., Lee, H., Ruch-Heeger, B. and Schauer, R. (1992) Interaction of rat peritoneal macrophages with homologous sialidase-treated thrombocytes in vitro: biochemical and morphological studies. Detection of N-(O-acetyl)glycolylneuraminic acid. *Eur J Cell Biol*, 59, 12-20.
- Kolter, T. and Sandhoff, K. (1997) Sialic acids--why always alpha-linked? *Glycobiology*, 7, vii-ix.

- Krause, S. and Schwarz, W. (2005) Identification and selective inhibition of the channel mode of the neuronal GABA transporter 1. *Mol Pharmacol*, 68, 1728-1735.
- Krogsgaard-Larsen, P., Falch, E., Larsson, O.M. and Schousboe, A. (1987) GABA uptake inhibitors: relevance to antiepileptic drug research. *Epilepsy Res*, 1, 77-93.
- Krogsgaard-Larsen, P., Frolund, B. and Frydenvang, K. (2000) GABA uptake inhibitors. Design, molecular pharmacology and therapeutic aspects. *Curr Pharm Des*, 6, 1193-1209.
- Krogsgaard-Larsen, P., Johnston, G.A., Curtis, D.R., Game, C.J. and McCulloch, R.M. (1975) Structure and biological activity of a series of conformationally restricted analogues of GABA. *J Neurochem*, 25, 803-809.
- Krystal, J.H., Sanacora, G., Blumberg, H., Anand, A., Charney, D.S., Marek, G., Epperson, C.N., Goddard, A. and Mason, G.F. (2002) Glutamate and GABA systems as targets for novel antidepressant and mood-stabilizing treatments. *Mol Psychiatry*, 7 Suppl 1, S71-80.
- Lanctot, K.L., Herrmann, N., Mazzotta, P., Khan, L.R. and Ingber, N. (2004) GABAergic function in Alzheimer's disease: evidence for dysfunction and potential as a therapeutic target for the treatment of behavioural and psychological symptoms of dementia. *Can J Psychiatry*, 49, 439-453.
- Larsson, O.M., Falch, E., Krogsgaard-Larsen, P. and Schousboe, A. (1988) Kinetic characterization of inhibition of gamma-aminobutyric acid uptake into cultured neurons and astrocytes by 4,4-diphenyl-3-butenyl derivatives of nipecotic acid and guvacine. *J Neurochem*, 50, 818-823.
- Larsson, O.M., Johnston, G.A. and Schousboe, A. (1983) Differences in uptake kinetics of cis-3-aminocyclohexane carboxylic acid into neurons and astrocytes in primary cultures. *Brain Res*, 260, 279-285.
- Lasky, L.A. (1995) Selectin-carbohydrate interactions and the initiation of the inflammatory response. *Annu Rev Biochem*, 64, 113-139.
- Law, R.M., Stafford, A. and Quick, M.W. (2000) Functional regulation of gamma-aminobutyric acid transporters by direct tyrosine phosphorylation. *J Biol Chem*, 275, 23986-23991.
- Lin, M.H. & S.Y. Hsu. (1987) Studies on pharmacological effects of various extracts of *Polygonum cuspidatum* S. et Z. *Tai-wan Yao Hsueh Tsa Chih* 39(1): 42-53.
- Lipfert, J., Columbus, L., Chu, V.B., Lesley, S.A. and Doniach, S. (2007) Size and shape of detergent micelles determined by small-angle X-ray scattering. *J Phys Chem B*, 111, 12427- 12438.
- Liu, G.X., Liu, S., Cai, G.Q., Sheng, Z.J., Cai, Y.Q., Jiang, J., Sun, X., Ma, S.K., Wang, L., Wang, Z.G. and Fei, J. (2007) Reduced aggression in mice lacking GABA transporter subtype 1. *J Neurosci Res*, 85, 649-655.
- Liu, Q.R., Lopez-Corcuera, B., Mandiyan, S., Nelson, H. and Nelson, N. (1993) Molecular characterization of four pharmacologically distinct gamma-aminobutyric acid transporters in mouse brain [corrected]. *J Biol Chem*, 268, 2106-2112.
- Liu, Q.R., Mandiyan, S., Nelson, H. and Nelson, N. (1992) A family of genes encoding neurotransmitter transporters. *Proc Natl Acad Sci U S A*, 89, 6639-6643.

- Liu, Y., Eckstein-Ludwig, U., Fei, J. and Schwarz, W. (1998) Effect of mutation of glycosylation sites on the Na<sup>+</sup> dependence of steady-state and transient currents generated by the neuronal GABA transporter. *Biochim Biophys Acta*, 1415, 246-254.
- Lloyd, K.G., Morselli, P.L., 1987. Psychopharmacology of GABAergic drugs. In: Meltzer, H.Y. (Ed.), *Psychopharmacology: The Third Generation of Progress*. Raven Press, New York, pp. 183–195.
- Loo, D.D., Eskandari, S., Boorer, K.J., Sarkar, H.K. and Wright, E.M. (2000) Role of Cl<sup>-</sup> in electrogenic Na<sup>+</sup>-coupled cotransporters GAT1 and SGLT1. *J Biol Chem*, 275, 37414-37422.
- Lopez-Corcuera, B., Liu, Q.R., Mandiyan, S., Nelson, H. and Nelson, N. (1992) Expression of a mouse brain cDNA encoding novel gamma-aminobutyric acid transporter. *J Biol Chem*, 267, 17491-17493.
- Lu, C.C. and Hilgemann, D.W. (1999) GAT1 (GABA:Na<sup>+</sup>:Cl<sup>-</sup>) cotransport function. Kinetic studies in giant *Xenopus* oocyte membrane patches. *J Gen Physiol*, 114, 445-457.
- Mabjeesh, N.J. and Kanner, B.I. (1993) The substrates of a sodium- and chloride-coupled gamma-aminobutyric acid transporter protect multiple sites throughout the protein against proteolytic cleavage. *Biochemistry*, 32, 8540-8546.
- MacAulay, N., Bendahan, A., Loland, C.J., Zeuthen, T., Kanner, B.I. and Gether, U. (2001) Engineered Zn(2+) switches in the gamma-aminobutyric acid (GABA) transporter-1. Differential effects on GABA uptake and currents. *J Biol Chem*, 276, 40476-40485.
- MacAulay, N., Zeuthen, T. and Gether, U. (2002) Conformational basis for the Li(+)-induced leak current in the rat gamma-aminobutyric acid (GABA) transporter-1. *J Physiol*, 544, 447-458.
- Madsen, K.K., Clausen, R.P., Larsson, O.M., Krogsgaard-Larsen, P., Schousboe, A. and White, H.S. (2009) Synaptic and extrasynaptic GABA transporters as targets for anti-epileptic drugs. *J Neurochem*, 109 Suppl 1, 139-144.
- Madsen, K.K., White, H.S. and Schousboe, A. Neuronal and non-neuronal GABA transporters as targets for antiepileptic drugs. *Pharmacol Ther*, 125, 394-401.
- Madsen, K.K., White, H.S. and Schousboe, A. (2009) Neuronal and non-neuronal GABA transporters as targets for antiepileptic drugs. *Pharmacol Ther*.
- Mager, S., Kleinberger-Doron, N., Keshet, G.I., Davidson, N., Kanner, B.I. and Lester, H.A. (1996) Ion binding and permeation at the GABA transporter GAT1. *J Neurosci*, 16, 5405-5414.
- Mager, S., Naeve, J., Quick, M., Labarca, C., Davidson, N. and Lester, H.A. (1993) Steady states, charge movements, and rates for a cloned GABA transporter expressed in *Xenopus* oocytes. *Neuron*, 10, 177-188.
- Mantey, L.R., Keppler, O.T., Pawlita, M., Reutter, W. and Hinderlich, S. (2001) Efficient biochemical engineering of cellular sialic acids using an unphysiological sialic acid precursor in cells lacking UDP-N-acetylglucosamine 2-epimerase. *FEBS Lett*, 503, 80-84.
- Manzi, A.E., Dell, A., Azadi, P. and Varki, A. (1990) Studies of naturally occurring modifications of sialic acids by fast-atom bombardment-mass spectrometry. Analysis of positional isomers by periodate cleavage. *J Biol Chem*, 265, 8094-8107.

- Mari, S.A., Soragna, A., Castagna, M., Bossi, E., Peres, A. and Sacchi, V.F. (2004) Aspartate 338 contributes to the cationic specificity and to driver-amino acid coupling in the insect cotransporter KAAT1. *Cell Mol Life Sci*, 61, 243-256.
- McIntire, S.L., Jorgensen, E. and Horvitz, H.R. (1993) Genes required for GABA function in *Caenorhabditis elegans*. *Nature*, 364, 334-337.
- Melone, M., Cozzi, A., Pellegrini-Giampietro, D.E. and Conti, F. (2003) Transient focal ischemia triggers neuronal expression of GAT-3 in the rat perilesional cortex. *Neurobiol Dis*, 14, 120-132.
- Miller-Podraza, H., Bergstrom, J., Milh, M.A. and Karlsson, K.A. (1997) Recognition of glycoconjugates by *Helicobacter pylori*. Comparison of two sialic acid-dependent specificities based on haemagglutination and binding to human erythrocyte glycoconjugates. *Glycoconj J*, 14, 467-471.
- Minelli, A., Alonso-Nanclares, L., Edwards, R.H., DeFelipe, J. and Conti, F. (2003) Postnatal development of the vesicular GABA transporter in rat cerebral cortex. *Neuroscience*, 117, 337-346.
- Minelli, A., Barbaresi, P. and Conti, F. (2003) Postnatal development of high-affinity plasma membrane GABA transporters GAT-2 and GAT-3 in the rat cerebral cortex. *Brain Res Dev Brain Res*, 142, 7-18.
- Minelli, A., Brecha, N.C., Karschin, C., DeBiasi, S. and Conti, F. (1995) GAT-1, a high-affinity GABA plasma membrane transporter, is localized to neurons and astroglia in the cerebral cortex. *J Neurosci*, 15, 7734-7746.
- Minelli, A., DeBiasi, S., Brecha, N.C., Zuccarello, L.V. and Conti, F. (1996) GAT-3, a high-affinity GABA plasma membrane transporter, is localized to astrocytic processes, and it is not confined to the vicinity of GABAergic synapses in the cerebral cortex. *J Neurosci*, 16, 6255-6264.
- Neal, M.J. and Bowery, N.G. (1977) Cis-3-aminocyclohexanecarboxylic acid: a substrate for the neuronal GABA transport system. *Brain Res*, 138, 169-174.
- Nelson, H., Mandiyan, S. and Nelson, N. (1990) Cloning of the human brain GABA transporter. *FEBS Lett*, 269, 181-184.
- Nelson, N. (1998) The family of Na<sup>+</sup>/Cl<sup>-</sup> neurotransmitter transporters. *J Neurochem*, 71, 1785-1803.
- Ofek, I. and Sharon, N. (1990) Adhesins as lectins: specificity and role in infection. *Curr Top Microbiol Immunol*, 151, 91-113.
- Oland, L.A., Gibson, N.J. and Tolbert, L.P. Localization of a GABA transporter to glial cells in the developing and adult olfactory pathway of the moth *Manduca sexta*. *J Comp Neurol*, 518, 815-838.
- Olden, K., Parent, J.B. and White, S.L. (1982) Carbohydrate moieties of glycoproteins. A re-evaluation of their function. *Biochim Biophys Acta*, 650, 209-232.
- Olesen, C., Picard, M., Winther, A.M., Gyrop, C., Morth, J.P., Oxvig, C., Moller, J.V. and Nissen, P. (2007) The structural basis of calcium transport by the calcium pump. *Nature*, 450, 1036-1042.
- Ormo, M., Cubitt, A.B., Kallio, K., Gross, L.A., Tsien, R.Y. and Remington, S.J. (1996) Crystal structure of the *Aequorea victoria* green fluorescent protein. *Science*, 273, 1392-1395.

- Otsuka, M. and Yanagisawa, M. (1990) Pain and neurotransmitters. *Cell Mol Neurobiol*, 10, 293-302.
- Pacholczyk, T., Blakely, R.D. and Amara, S.G. (1991) Expression cloning of a cocaine- and antidepressant-sensitive human noradrenaline transporter. *Nature*, 350, 350-354.
- Pantanowitz, S., Bendahan, A. and Kanner, B.I. (1993) Only one of the charged amino acids located in the transmembrane alpha-helices of the gamma-aminobutyric acid transporter (subtype A) is essential for its activity. *J Biol Chem*, 268, 3222-3225.
- Park, E.I., Mi, Y., Unverzagt, C., Gabius, H.J. and Baenziger, J.U. (2005) The asialoglycoprotein receptor clears glycoconjugates terminating with sialic acid alpha 2,6GalNAc. *Proc Natl Acad Sci U S A*, 102, 17125-17129.
- Park, S.A., Kim, M.R., Kim, P.K., Cho, H.D., Han, G.Y. and Kim, C.W. (2008) Sample preparation method for plasma membrane proteome analysis. *J Chromatogr B Analyt Technol Biomed Life Sci*, 872, 177-180.
- Paulson, J.C., Weinstein, J. and Schauer, A. (1989) Tissue-specific expression of sialyltransferases. *J Biol Chem*, 264, 10931-10934.
- Perez, H.D., Ong, R.R. and Elfman, F. (1985) Removal or oxidation of surface membrane sialic acid inhibits formyl-peptide-induced polymorphonuclear leukocyte chemotaxis. *J Immunol*, 134, 1902-1908.
- Petrovskaya, L.E., Shulga, A.A., Bocharova, O.V., Ermolyuk, Y.S., Kryukova, E.A., Chupin, V.V., Blommers, M.J., Arseniev, A.S. and Kirpichnikov, M.P. Expression of G-protein coupled receptors in *Escherichia coli* for structural studies. *Biochemistry (Mosc)*, 75, 881-891.
- Pilatte, Y., Bignon, J. and Lambre, C.R. (1993) Sialic acids as important molecules in the regulation of the immune system: pathophysiological implications of sialidases in immunity. *Glycobiology*, 3, 201-218.
- Ponce, J., Biton, B., Benavides, J., Avenet, P. and Aragon, C. (2000) Transmembrane domain III plays an important role in ion binding and permeation in the glycine transporter GLYT2. *J Biol Chem*, 275, 13856-13862.
- Quick, M.W., Corey, J.L., Davidson, N. and Lester, H.A. (1997) Second messengers, trafficking-related proteins, and amino acid residues that contribute to the functional regulation of the rat brain GABA transporter GAT1. *J Neurosci*, 17, 2967-2979.
- Radian, R., Bendahan, A. and Kanner, B.I. (1986) Purification and identification of the functional sodium- and chloride-coupled gamma-aminobutyric acid transport glycoprotein from rat brain. *J Biol Chem*, 261, 15437-15441.
- Radian, R. and Kanner, B.I. (1983) Stoichiometry of sodium- and chloride-coupled gamma-aminobutyric acid transport by synaptic plasma membrane vesicles isolated from rat brain. *Biochemistry*, 22, 1236-1241.
- Radian, R. and Kanner, B.I. (1985) Reconstitution and purification of the sodium- and chloride-coupled gamma-aminobutyric acid transporter from rat brain. *J Biol Chem*, 260, 11859-11865.
- Ramsay, P.B., Krigman, M.R. and Morell, P. (1980) Developmental studies of the uptake of choline, GABA and dopamine by crude synaptosomal preparations after in vivo or in vitro lead treatment. *Brain Res*, 187, 383-402.
- Rasola, A., Galiotta, L.J., Barone, V., Romeo, G. and Bagnasco, S. (1995) Molecular cloning and functional characterization of a GABA/betaine transporter from human kidney. *FEBS Lett*, 373, 229-233.

- Rens-Domiano, S. and Reisine, T. (1991) Structural analysis and functional role of the carbohydrate component of somatostatin receptors. *J Biol Chem*, 266, 20094-20102.
- Ressl, S., Terwisscha van Scheltinga, A.C., Vonrhein, C., Ott, V. and Ziegler, C. (2009) Molecular basis of transport and regulation in the Na(+)/betaine symporter BetP. *Nature*, 458, 47-52.
- Reuter, G., Pfeil, R., Stoll, S., Schauer, R., Kamerling, J.P., Versluis, C. and Vliegthart, J.F. (1983) Identification of new sialic acids derived from glycoprotein of bovine submandibular gland. *Eur J Biochem*, 134, 139-143.
- Reutter, W. and Bauer, C. (1985) Inhibitors of glycoprotein biosynthesis. *Adv Enzyme Regul*, 24, 405-416.
- Richards, R.L., Moss, J., Alving, C.R., Fishman, P.H. and Brady, R.O. (1979) Cholera toxin (cholera toxin): a bacterial lectin. *Proc Natl Acad Sci U S A*, 76, 1673-1676.
- Roux, M.J. and Supplisson, S. (2000) Neuronal and glial glycine transporters have different stoichiometries. *Neuron*, 25, 373-383.
- Sawada, R., Tsuboi, S. and Fukuda, M. (1994) Differential E-selectin-dependent adhesion efficiency in sublines of a human colon cancer exhibiting distinct metastatic potentials. *J Biol Chem*, 269, 1425-1431.
- Schachner, M. and Bartsch, U. (2000) Multiple functions of the myelin-associated glycoprotein MAG (siglec-4a) in formation and maintenance of myelin. *Glia*, 29, 154-165.
- Schauer, R. (1985) Sialic acids and their role as biological masks. *Trends Biochem. Sci.* **10**, 357-360
- Schauer, R., Kelm, S., Reuter, G., Roggentin, P., Shaw, L. (1995) Biochemistry and role of sialic acids. In: *Biology of sialic acids* (Rosenberg, A.; Plenum Press, New York), 7-67
- Schauer, R. (2000) Achievements and challenges of sialic acid research. *Glycoconj J*, 17, 485-499.
- Schauer, R. (2009) Sialic acids as regulators of molecular and cellular interactions. *Curr Opin Struct Biol*, 19, 507-514.
- Schengrund, C.L., DasGupta, B.R. and Ringler, N.J. (1991) Binding of botulinum and tetanus neurotoxins to ganglioside GT1b and derivatives thereof. *J Neurochem*, 57, 1024-1032.
- Schlepper-Schafer, J., Kolb-Bachofen, V. and Kolb, H. (1980) Analysis of lectin-dependent recognition of desialylated erythrocytes by Kupffer cells. *Biochem J*, 186, 827-831.
- Schousboe, A. (1979) Effects of GABA-analogues on the high-affinity uptake of GABA in astrocytes in primary cultures. *Adv Exp Med Biol*, 123, 219-237.
- Schousboe, A. (2000) Pharmacological and functional characterization of astrocytic GABA transport: a short review. *Neurochem Res*, 25, 1241-1244.
- Schousboe, A., Larsson, O.M., Sarup, A. and White, H.S. (2004) Role of the betaine/GABA transporter (BGT-1/GAT2) for the control of epilepsy. *Eur J Pharmacol*, 500, 281-287.



## References

---

- Schousboe, A., Sarup, A., Bak, L.K., Waagepetersen, H.S. and Larsson, O.M. (2004) Role of astrocytic transport processes in glutamatergic and GABAergic neurotransmission. *Neurochem Int*, 45, 521-527.
- Schuske, K., Beg, A.A. and Jorgensen, E.M. (2004) The GABA nervous system in *C. elegans*. *Trends Neurosci*, 27, 407-414.
- Sillanauke, P., Ponnio, M. and Jaaskelainen, I.P. (1999) Occurrence of sialic acids in healthy humans and different disorders. *Eur J Clin Invest*, 29, 413-425.
- Singh, S.K., Yamashita, A. and Gouaux, E. (2007) Antidepressant binding site in a bacterial homologue of neurotransmitter transporters. *Nature*, 448, 952-956.
- Sjoberg, E.R., Manzi, A.E., Khoo, K.H., Dell, A. and Varki, A. (1992) Structural and immunological characterization of O-acetylated GD2. Evidence that GD2 is an acceptor for ganglioside O-acetyltransferase in human melanoma cells. *J Biol Chem*, 267, 16200-16211.
- Soragna, A., Bossi, E., Giovannardi, S., Pisani, R. and Peres, A. (2005) Functionally independent subunits in the oligomeric structure of the GABA cotransporter rGAT1. *Cell Mol Life Sci*, 62, 2877-2885.
- Stasche, R., Hinderlich, S., Weise, C., Effertz, K., Lucka, L., Moormann, P. and Reutter, W. (1997) A bifunctional enzyme catalyzes the first two steps in N-acetylneuraminic acid biosynthesis of rat liver. Molecular cloning and functional expression of UDP-N-acetyl-glucosamine 2-epimerase/N-acetylmannosamine kinase. *J Biol Chem*, 272, 24319-24324.
- Sur, M. and Leamey, C.A. (2001) Development and plasticity of cortical areas and networks. *Nat Rev Neurosci*, 2, 251-262.
- Suzdak, P.D., Frederiksen, K., Andersen, K.E., Sorensen, P.O., Knutsen, L.J. and Nielsen, E.B. (1992) NNC-711, a novel potent and selective gamma-aminobutyric acid uptake inhibitor: pharmacological characterization. *Eur J Pharmacol*, 224, 189-198.
- Tedder, T.F., Tuscano, J., Sato, S. and Kehrl, J.H. (1997) CD22, a B lymphocyte-specific adhesion molecule that regulates antigen receptor signaling. *Annu Rev Immunol*, 15, 481-504.
- Thoeringer, C.K., Ripke, S., Unschuld, P.G., Lucae, S., Ising, M., Bettecken, T., Uhr, M., Keck, M.E., Mueller-Myhsok, B., Holsboer, F., Binder, E.B. and Erhardt, A. (2009) The GABA transporter 1 (SLC6A1): a novel candidate gene for anxiety disorders. *J Neural Transm*, 116, 649-657.
- Thomsen, C., Sorensen, P.O. and Egebjerg, J. (1997) 1-(3-(9H-carbazol-9-yl)-1-propyl)-4-(2-methoxyphenyl)-4-piperidinol, a novel subtype selective inhibitor of the mouse type II GABA-transporter. *Br J Pharmacol*, 120, 983-985.
- Thurin, J., Herlyn, M., Hindsgaul, O., Stromberg, N., Karlsson, K.A., Elder, D., Steplewski, Z. and Koprowski, H. (1985) Proton NMR and fast-atom bombardment mass spectrometry analysis of the melanoma-associated ganglioside 9-O-acetyl-GD3. *J Biol Chem*, 260, 14556-14563.
- Tomlinson, S., Pontes de Carvalho, L.C., Vandekerckhove, F. and Nussenzweig, V. (1994) Role of sialic acid in the resistance of *Trypanosoma cruzi* trypomastigotes to complement. *J Immunol*, 153, 3141-3147.

- Torres, G.E., Gainetdinov, R.R. and Caron, M.G. (2003) Plasma membrane monoamine transporters: structure, regulation and function. *Nat Rev Neurosci*, 4, 13-25.
- Toyoshima, C., Nakasako, M., Nomura, H. and Ogawa, H. (2000) Crystal structure of the calcium pump of sarcoplasmic reticulum at 2.6 Å resolution. *Nature*, 405, 647-655.
- Treiman, D.M. (2001) GABAergic mechanisms in epilepsy. *Epilepsia*, 42 Suppl 3, 8-12.
- Uhl, G.R. (1992) Neurotransmitter transporters (plus): a promising new gene family. *Trends Neurosci*, 15, 265-268.
- Varki, A. (1992) Diversity in the sialic acids. *Glycobiology*, 2, 25-40.
- Varki, A. (1993) Biological roles of oligosaccharides: all of the theories are correct. *Glycobiology*, 3, 97-130.
- Varki, A. (2007) Glycan-based interactions involving vertebrate sialic-acid-recognizing proteins. *Nature*, 446, 1023-1029.
- Varki, N.M. and Varki, A. (2007) Diversity in cell surface sialic acid presentations: implications for biology and disease. *Lab Invest*, 87, 851-857.
- Waagepetersen, H.S., Sonnewald, U. and Schousboe, A. (2003) Compartmentation of glutamine, glutamate, and GABA metabolism in neurons and astrocytes: functional implications. *Neuroscientist*, 9, 398-403.
- Wafford, K.A. and Ebert, B. (2006) Gaboxadol--a new awakening in sleep. *Curr Opin Pharmacol*, 6, 30-36.
- Wasley, L.C., Timony, G., Murtha, P., Stoudemire, J., Dorner, A.J., Caro, J., Krieger, M. and Kaufman, R.J. (1991) The importance of N- and O-linked oligosaccharides for the biosynthesis and in vitro and in vivo biologic activities of erythropoietin. *Blood*, 77, 2624-2632.
- Weinglass, A.B., Smirnova, I.N. and Kaback, H.R. (2001) Engineering conformational flexibility in the lactose permease of *Escherichia coli*: use of glycine-scanning mutagenesis to rescue mutant Glu325-->Asp. *Biochemistry*, 40, 769-776.
- Weyand, S., Shimamura, T., Yajima, S., Suzuki, S., Mirza, O., Krusong, K., Carpenter, E.P., Rutherford, N.G., Hadden, J.M., O'Reilly, J., Ma, P., Saidijam, M., Patching, S.G., Hope, R.J., Norbertczak, H.T., Roach, P.C., Iwata, S., Henderson, P.J. and Cameron, A.D. (2008) Structure and molecular mechanism of a nucleobase-cation-symport-1 family transporter. *Science*, 322, 709-713.
- White, H.S., Sarup, A., Bolvig, T., Kristensen, A.S., Petersen, G., Nelson, N., Pickering, D.S., Larsson, O.M., Frolund, B., Krosgaard-Larsen, P. and Schousboe, A. (2002) Correlation between anticonvulsant activity and inhibitory action on glial gamma-aminobutyric acid uptake of the highly selective mouse gamma-aminobutyric acid transporter 1 inhibitor 3-hydroxy-4-amino-4,5,6,7-tetrahydro-1,2-benzisoxazole and its N-alkylated analogs. *J Pharmacol Exp Ther*, 302, 636-644.
- White, H.S., Watson, W.P., Hansen, S.L., Slough, S., Perregaard, J., Sarup, A., Bolvig, T., Petersen, G., Larsson, O.M., Clausen, R.P., Frolund, B., Falch, E., Krosgaard-Larsen, P. and Schousboe, A. (2005) First demonstration of a functional role for central nervous system betaine/gamma-aminobutyric acid transporter (mGAT2) based on synergistic anticonvulsant action among inhibitors of mGAT1 and mGAT2. *J Pharmacol Exp Ther*, 312, 866-874.

- White, J.F. and Grisshammer, R. (2007) Automated large-scale purification of a recombinant g-protein-coupled neurotensin receptor. *Curr Protoc Protein Sci*, Chapter 6, Unit 6 8.
- Wilson, F.A., O'Scalaidhe, S.P. and Goldman-Rakic, P.S. (1994) Functional synergism between putative gamma-aminobutyrate-containing neurons and pyramidal neurons in prefrontal cortex. *Proc Natl Acad Sci U S A*, 91, 4009-4013.
- Yamashita, A., Singh, S.K., Kawate, T., Jin, Y. and Gouaux, E. (2005) Crystal structure of a bacterial homologue of Na<sup>+</sup>/Cl<sup>-</sup>-dependent neurotransmitter transporters. *Nature*, 437, 215-223.
- Yamashita, K., Fukushima, K., Sakiyama, T., Murata, F., Kuroki, M. and Matsuoka, Y. (1995) Expression of Sia alpha 2-->6Gal beta 1-->4GlcNAc residues on sugar chains of glycoproteins including carcinoembryonic antigens in human colon adenocarcinoma: applications of *Trichosanthes japonica* agglutinin I for early diagnosis. *Cancer Res*, 55, 1675-1679.
- Yamauchi, A., Uchida, S., Kwon, H.M., Preston, A.S., Robey, R.B., Garcia-Perez, A., Burg, M.B. and Handler, J.S. (1992) Cloning of a Na<sup>(+)</sup>- and Cl<sup>(-)</sup>-dependent betaine transporter that is regulated by hypertonicity. *J Biol Chem*, 267, 649-652.
- Yang, C.Y., Brecha, N.C. and Tsao, E. (1997) Immunocytochemical localization of gamma-aminobutyric acid plasma membrane transporters in the tiger salamander retina. *J Comp Neurol*, 389, 117-126.
- Yang, F., Moss, L.G. and Phillips, G.N., Jr. (1996) The molecular structure of green fluorescent protein. *Nat Biotechnol*, 14, 1246-1251.
- Yunger, L.M., Fowler, P.J., Zarevics, P. and Setler, P.E. (1984) Novel inhibitors of gamma-aminobutyric acid (GABA) uptake: anticonvulsant actions in rats and mice. *J Pharmacol Exp Ther*, 228, 109-115.
- Yuyama, Y., Yoshimatsu, K., Ono, E., Saito, M. and Naiki, M. (1993) Postnatal change of pig intestinal ganglioside bound by *Escherichia coli* with K99 fimbriae. *J Biochem*, 113, 488-492.
- Zaleska, M.M. and Erecinska, M. (1987) Role of sialic acid in synaptosomal transport of amino acid transmitters. *Proc Natl Acad Sci U S A*, 84, 1709-1712.
- Zeitler, R., Giannis, A., Danneschewski, S., Henk, E., Henk, T., Bauer, C., Reutter, W. and Sandhoff, K. (1992) Inhibition of N-acetylglucosamine kinase and N-acetylmannosamine kinase by 3-O-methyl-N-acetyl-D-glucosamine in vitro. *Eur J Biochem*, 204, 1165-1168.
- Zhang, R., Xu, S., Cai, Y., Zhou, M., Zuo, X. and Chan, P. (2009) *Ganoderma lucidum* Protects Dopaminergic Neuron Degeneration Through Inhibition of Microglial Activation. *Evid Based Complement Alternat Med*.
- Zhao, Y., Terry, D., Shi, L., Weinstein, H., Blanchard, S.C. and Javitch, J.A. (2010) Single-molecule dynamics of gating in a neurotransmitter transporter homologue. *Nature*, 465, 188-193.
- Zhou, Y., Bennett, E.R. and Kanner, B.I. (2004) The aqueous accessibility in the external half of transmembrane domain I of the GABA transporter GAT-1 is modulated by its ligands. *J Biol Chem*, 279, 13800-13808.
- Zhou, Y. and Kanner, B.I. (2005) Transporter-associated currents in the gamma-aminobutyric acid transporter GAT-1 are conditionally impaired by mutations of a conserved glycine residue. *J Biol Chem*, 280, 20316-20324.

## References

---

Zhou, Y., Zomot, E. and Kanner, B.I. (2006) Identification of a lithium interaction site in the gamma-aminobutyric acid (GABA) transporter GAT-1. *J Biol Chem*, 281, 22092-22099.

Zhou, Z., Zhen, J., Karpowich, N.K., Goetz, R.M., Law, C.J., Reith, M.E. and Wang, D.N. (2007) LeuT-desipramine structure reveals how antidepressants block neurotransmitter reuptake. *Science*, 317, 1390-1393.

Zimmer, G., Suguri, T., Reuter, G., Yu, R.K., Schauer, R. and Herrler, G. (1994) Modification of sialic acids by 9-O-acetylation is detected in human leucocytes using the lectin property of influenza C virus. *Glycobiology*, 4, 343-349.

Zomot, E., Bendahan, A., Quick, M., Zhao, Y., Javitch, J.A. and Kanner, B.I. (2007) Mechanism of chloride interaction with neurotransmitter:sodium symporters. *Nature*, 449, 726-730.

Zomot, E. and Kanner, B.I. (2003) The interaction of the gamma-aminobutyric acid transporter GAT-1 with the neurotransmitter is selectively impaired by sulfhydryl modification of a conformationally sensitive cysteine residue engineered into extracellular loop IV. *J Biol Chem*, 278, 42950-42958.

**Appendix****Abbreviations**

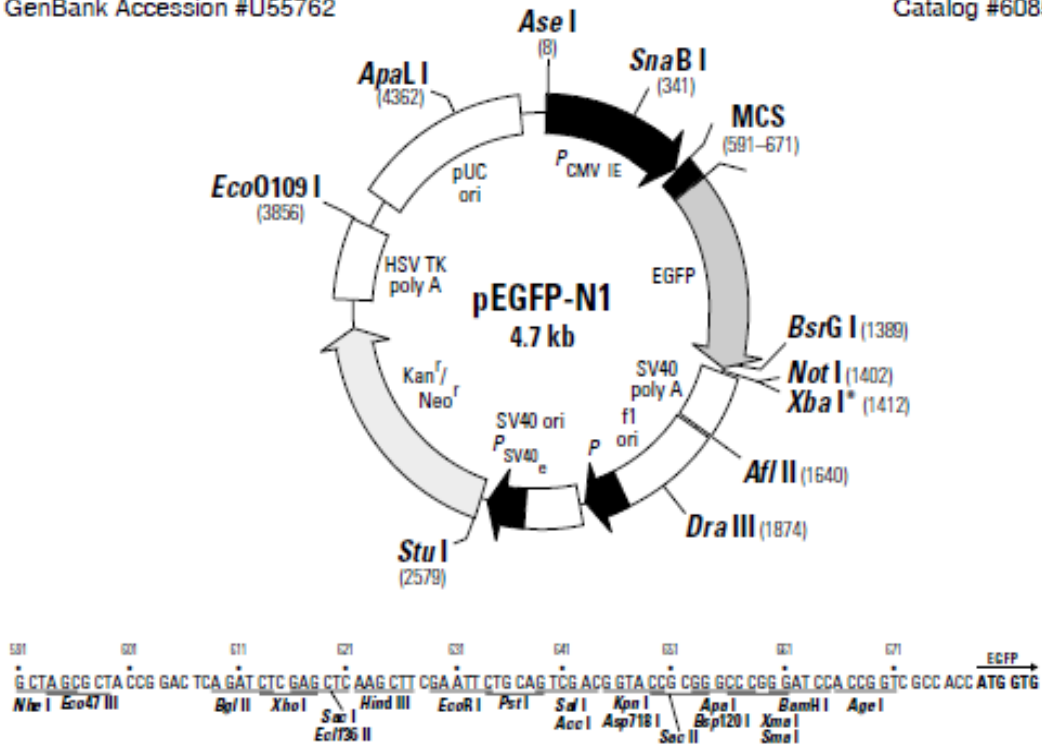
Ac	Acetyl
Ac-Acetamido	Acetamidoacetyl
Ac-Formamido	Formamidoacetyl
Ala	Alanine
Amp	Ampicillin
Arg	Arginine
Asn	Asparagine
Asp	Aspartic acid
ATP	Adenosine triphosphate
bp	Base pair
But	Butanoyl
BSA	Bovine Serumalbumin
<i>C. elegans</i>	<i>Caenorhabditis elegans</i>
CHO	<i>Chinese Hamster Ovary</i>
CMP	Cytidinmonophosphat
Cyclo	Cyclopropylcarbox
Da	Dalton
dMM	1-Deoxymannojirimycin
DMSO	Dimethylsulfoxid
DTT	Dithiothreitol
EDTA	Ethylendiamintetraessigsäure
EGF	Epidermal Growth Factor
ES cells	Embryonic stem cells
FACS	<i>Fluorescence Activated Cell Sorting</i>
FCS	Fetal calf serum
GABA	$\gamma$ -amino butyric acid
GAD	Glutamic acid decarboxylase
Gal	Galactose
GAT	GABA transporter
GlcNAc	<i>N</i> -Acetylglucosamine
GlcNGc	<i>N</i> -Glycolylglucosamine
GlcNProp	<i>N</i> -Propionylglucosamine
Glu	Glutamic acid
Gln	Glutamine
Gly	Glycine
GNE	UDP-GlcNAc-2-Epimerase/ManNAc-Kinase
Hex	Hexanoyl
6x His tag	6x Histidine tag
Ile	Isoleucine
IPTG	Isopropyl-1-thio- $\beta$ -D-galactosid
LB	Lauria Bertani

Leu	Leucine
LeuT <sub>Aa</sub>	Leucine transporter from <i>Aquifex aeolicus</i>
LFA	<i>Limax flavus</i>
M	Molar
MAA	<i>Maackia amurensis</i>
MALDI	Matrixunterstützte Laserdesorption/-ionisierung
ManNAc	<i>N</i> -Acetylmannosamine
ManNProp	<i>N</i> -Propionylmannosamine
Me	Methyl
MOI	<i>Multiplicity of infection</i>
MS	Mass spectrometry
NCAM	Neural cell adhesion molecules
Neu5,9Ac2	9-O-Acetylated Neu5Ac
Neu5Ac	<i>N</i> -Acetylneuraminic acid
Neu5Gc	<i>N</i> -Glycolylneuraminic acid
Ni-NTA	Nickel-nitrilotriacetic acid
NSS	Neurotransmitter: sodium symporters
PAGE	Polyacrylamide gel electrophoresis
PBS	Phosphate buffered saline
PCR	Polymerase chain reaction
PFU	<i>Plaque-forming units</i>
Phe	Phenylalanine
PMSF	Phenylmethylsulfonylfluorid
PSA	Polysialic acid
Prop	Propionyl
rpm	<i>Rounds per minute</i>
SDS	Sodium dodecyl sulfate
Ser	Serine
SERT	Serotonin transporter
SLC	Solute carrier
SNA	<i>Sambucus nigra agglutinin</i>
TAE	Tris Acetate-EDTA-Buffer
Taq	<i>Thermus aquaticus</i>
Thr	Threonine
Tris	Tris(hydroxymethyl)aminomethane
TM	Transmembrane domain
Tyr	Tyrosine
U	<i>Unit</i>
UDP	Uridine diphosphate

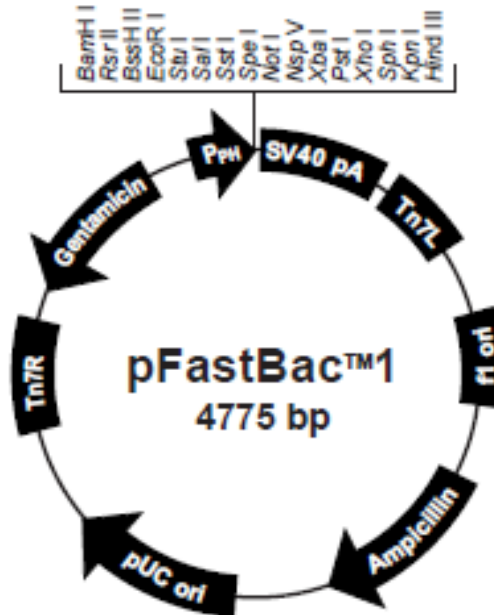
Restriction Map and Multiple Cloning Site (MCS) of pEGFP-N1 Vector.

pEGFP-N1 Vector Information  
 GenBank Accession #U55762

PT3027-5  
 Catalog #6085-1



## Restriction Map and Multiple Cloning Site (MCS) of pFASTBAC™ 1-Vector.



Comments for pFastBac™1  
4775 nucleotides

f1 origin: bases 2-457  
Ampicillin resistance gene: bases 589-1449  
pUC origin: bases 1594-2267  
Tn7R: bases 2511-2735  
Gentamicin resistance gene: bases 2802-3335 (complementary strand)  
Polyhedrin promoter (P<sub>PH</sub>): bases 3904-4032  
Multiple cloning site: bases 4037-4142  
SV40 polyadenylation signal: bases 4160-4400  
Tn7L: bases 4429-4594





## **Curriculum Vitae**

**For reasons of data protection,  
the curriculum vitae is not included in the online version**

## Publications

### Patent

“Aprepitant an antineoplastic drug”

Kuhn M., Campillos M., Jensen L. J., Bork P., Gavin A. C., Luciani R., Fan H., Hossbach J., Hu J., Ahmed J. and Preissner R.

US patent application 61/043299. **2008**

### Research articles

1. “Molecular mechanism and structural basis of interactions of dipeptidyl peptidase IV with adenosine deaminase or human immunodeficiency virus type-1 transcripition transactivator”  
Fan H, Tansi F, Hu J., Christoph B, Reutter W and Sanger W.  
*Eur J Cell Biol* , **2011**, In press.
2. “Involvement of Sialic Acid in the Regulation of GABA Uptake Activity of GABA Transporter 1”  
Hu J., Fei J, Fan H and Reutter W.  
*Glycobiology*, **2010**, In press.
3. “Studies on Structure-Activity Relationship of Influenza Neuraminidase Inhibitors”  
Hu J. and Wang EH.  
*Progress in Pharmaceutical Sciences*, **2004**, 28, 204-208.
4. “Progress in Study and Application of Hematoporphyrin Compounds using in Diagnosis and Therapy of Tumour”  
Li DP, and Hu J.  
*Chinese Journal of Biochemical Pharmaceutics*, **2003**, 24, 162-163.

### Conferences abstracts and posters

1. “Role of Terminal Sialic acids of GABA Transporter 1 in GABA Uptake & Expression, Characterization and Purification of GABA Transporter 1”  
Hu J., Bottcher C, Reutter W and Fan H.  
*SFB449 2010*, Dec. 21-26, **2010**, Berlin, Germany.
2. “Role of Terminal Sialic Acids of GABA Transporter 1 in the GABA Uptake Process”  
Hu J., Fei J, Reutter W and Fan H.  
*SIALOGLYCO 2010*, Aug. 21-26, **2010**, Potsdam, Germany.
3. “Involvement of N-Acetylneuraminic Acid in the Regulation of GABA-uptake Activity of GABA Transporter 1”  
Fan H, Hu J., Fei J, Stanley P and Reutter W.  
*The 20<sup>th</sup> International Symposium on Glycoconjugates*, Nov. 29-Dec. 4, **2009**, San Juan, USA.

4. *“Terminal Sialic acid of GABA-Transporter 1 plays a Key Role in the GABA-Uptake Activity”*  
Hu J, Fei J, Stanley P, Reutter W and Fan H.  
2009 Annual Meeting of the Society for Glycobiology, Nov. 12-16, **2009**, San Diego, USA.
5. *“Biological Implications of the Biochemical Modification of the N-Acyl Side Chain of Hexosamines”*  
Fan H, Kontou M, Hu J and Reutter W.  
2009 Annual Meeting of the Society for Glycobiology, Nov. 12-16, 2009, San Diego, USA.
6. *“Investigation on the Role of N-Acetylneuraminic acid in the Regulation of GABA Transport of GABA Transporter 1 (GAT1)”*  
Hu J, Fei J, Reutter W and Fan H.  
*The 4<sup>th</sup> Glycan Forum in Berlin*, May 23-24, **2008**, Berlin, Germany.
7. *“Role of N-glycosylation and N-glycan Trimming of GABA Transporter 1”*  
Fan H, Cai G, Hu J, Salonikidis P, Fei J, Reutter W and Schwarz W.  
*The 48<sup>th</sup> Annual Meeting of the American Society for Cell Biology*, Dec. 13-17, **2008**, San Francisco, USA.
8. *“The agonists and antagonists of GABA-uptake of GABA-transporter 1”*  
Hu J, Zhang J, Fei J, Zimmermann-Kordmann M, Reutter W and Fan H.  
*The 3<sup>rd</sup> Glycan Forum in Berlin*, Feb. 22-23, **2007**, Berlin, Germany.
9. *“Inhibition of Proliferation of Tumour Cells by a Bioactive Compound from Ploygonum Cuspidatum Identification as Resveratrol”*  
Hu J, Tang Q, Da Silva L, Jia W, Reutter W and Fan H.  
*ELSO meeting*, Sept. 3-6, **2005**, Dresden, Germany.